

# World Journal of *Clinical Cases*

*World J Clin Cases* 2024 August 16; 12(23): 5283-5447



## Contents

Thrice Monthly Volume 12 Number 23 August 16, 2024

## EDITORIAL

- 5283 Gastrointestinal tuberculosis: Diagnostic approaches for this uncommon pathology  
*Brown L, Colwill M, Poullis A*
- 5288 Pay attention to the application of indocyanine green fluorescence imaging technology in laparoscopic liver cancer resection  
*Kang LM, Zhang FW, Yu FK, Xu L*
- 5294 Impact of parenting styles on preschoolers' behaviors  
*Sarac E*
- 5299 Essential role of postoperative follow-up in the management of clear cell sarcoma  
*Zhang ZH, Guo JT, Xie Y, Sun SY*
- 5304 Application of artificial intelligence in the diagnosis and treatment of Kawasaki disease  
*Pan Y, Jiao FY*
- 5308 Understanding the etiology of mental health problems in post-rehabilitation COVID-19 patients: Insights and strategies for effective intervention  
*Hu HS, Sun BQ*

## MINIREVIEWS

- 5313 Discharging patients home from the intensive care unit: A new trend  
*Hassan EM, Jama AB, Sharaf A, Shaikh A, El Labban M, Surani S, Khan SA*

## ORIGINAL ARTICLE

## Case Control Study

- 5320 Correlation and predictive value of pathological complete response and ultrasound characteristic parameters in neoadjuvant chemotherapy for breast  
*Zheng L, Yang LX, Liu JY, Jiang Z, Li XW, Pu PP*

## Retrospective Study

- 5329 Hounsfield units in assessing bone mineral density in ankylosing spondylitis patients with cervical fracture-dislocation  
*Gao ZY, Peng WL, Li Y, Lu XH*
- 5338 Establishment and performance analysis of a new multiplex detection method for influenza A and B virus antigen  
*Xia CJ, Li BH, Guo YN, Zhou XH, Zhang RL, Niu YN*

- 5346** Evaluating the role of interleukin-2 and interleukin-12 in pediatric patients with concurrent *Mycoplasma pneumoniae* and Epstein-Barr virus infections

Hao YP

### Observational Study

- 5354** Perception of dental appearance and aesthetic analysis among patients, laypersons and dentists

Aldegheishem A, Alfayadh HM, AlDossary M, Asaad S, Eldwakhly E, AL Refaei NAH, Alsenan D, Soliman M

- 5366** Effects of pulmonary surfactant combined with noninvasive positive pressure ventilation in neonates with respiratory distress syndrome

Shi ZN, Zhang X, Du CY, Zhao B, Liu SG

- 5374** Impact of interleukin 6 levels on acute lung injury risk and disease severity in critically ill sepsis patients

Liu Y, Chen L

### SCIENTOMETRICS

- 5382** Knowledge domain and emerging trends in the rupture risk of intracranial aneurysms research from 2004 to 2023

Chen JC, Luo C, Li Y, Tan DH

### CASE REPORT

- 5404** Necrolytic migratory erythema caused by pancreatic hyperglycemia with emphasis on therapeutic and prognosis: A case report

Zhan SP

- 5410** Small cell lung carcinoma with *KIF5B-RET* fusion partially responded to the 4<sup>th</sup>-line therapy with anlotinib: A case report

Zhang R, He YT, Liu YS, Li H, Zhao F

- 5416** Endobronchial metastasis secondary to renal clear cell carcinoma: A case report

Xie TH, Fu Y, Ha SN, Meng QX, Sun Q, Wang P

- 5422** Fatal multiple acyl-CoA dehydrogenase deficiency caused by *ETFDH* gene mutation: A case report

Li XX, Yang XN, Pan HD, Liu L

- 5431** Cushing's syndrome caused by giant Ewing's sarcoma of the kidney: A case report and review of literature

Dong GF, Hou YK, Ma Q, Ma SY, Wang YJ, Rexiati M, Wang WG

- 5441** Rare extraintestinal manifestations of ulcerative colitis treated with dual biologic therapy: A case report

Filipiuk A, Gonciarz M

**ABOUT COVER**

Peer Reviewer of *World Journal of Clinical Cases*, Flavia Feier, MD, PhD, Professor, Surgeon, Pediatric Liver Transplantation, Hospital de Clínicas de Porto Alegre, Porto Alegre 90810230, Brazil. flavia.feier@gmail.com

**AIMS AND SCOPE**

The primary aim of *World Journal of Clinical Cases* (WJCC, *World J Clin Cases*) is to provide scholars and readers from various fields of clinical medicine with a platform to publish high-quality clinical research articles and communicate their research findings online.

WJCC mainly publishes articles reporting research results and findings obtained in the field of clinical medicine and covering a wide range of topics, including case control studies, retrospective cohort studies, retrospective studies, clinical trials studies, observational studies, prospective studies, randomized controlled trials, randomized clinical trials, systematic reviews, meta-analysis, and case reports.

**INDEXING/ABSTRACTING**

The WJCC is now abstracted and indexed in Science Citation Index Expanded (SCIE, also known as SciSearch®), Journal Citation Reports/Science Edition, Current Contents®/Clinical Medicine, PubMed, PubMed Central, Reference Citation Analysis, China Science and Technology Journal Database, and Superstar Journals Database. The 2024 Edition of Journal Citation Reports® cites the 2023 journal impact factor (JIF) for WJCC as 1.0; JIF without journal self cites: 0.9; 5-year JIF: 1.1; JIF Rank: 168/325 in medicine, general and internal; JIF Quartile: Q3; and 5-year JIF Quartile: Q3.

**RESPONSIBLE EDITORS FOR THIS ISSUE**

Production Editor: Xiang-Di Zhang; Production Department Director: Xiang Li; Cover Editor: Jin-Lei Wang.

**NAME OF JOURNAL**

*World Journal of Clinical Cases*

**ISSN**

ISSN 2307-8960 (online)

**LAUNCH DATE**

April 16, 2013

**FREQUENCY**

Thrice Monthly

**EDITORS-IN-CHIEF**

Bao-Gan Peng, Salim Surani, Jerzy Tadeusz Chudek, George Kontogeorgos, Maurizio Serati

**EDITORIAL BOARD MEMBERS**

<https://www.wjgnet.com/2307-8960/editorialboard.htm>

**PUBLICATION DATE**

August 16, 2024

**COPYRIGHT**

© 2024 Baishideng Publishing Group Inc

**INSTRUCTIONS TO AUTHORS**

<https://www.wjgnet.com/bpg/gerinfo/204>

**GUIDELINES FOR ETHICS DOCUMENTS**

<https://www.wjgnet.com/bpg/GerInfo/287>

**GUIDELINES FOR NON-NATIVE SPEAKERS OF ENGLISH**

<https://www.wjgnet.com/bpg/gerinfo/240>

**PUBLICATION ETHICS**

<https://www.wjgnet.com/bpg/GerInfo/288>

**PUBLICATION MISCONDUCT**

<https://www.wjgnet.com/bpg/gerinfo/208>

**ARTICLE PROCESSING CHARGE**

<https://www.wjgnet.com/bpg/gerinfo/242>

**STEPS FOR SUBMITTING MANUSCRIPTS**

<https://www.wjgnet.com/bpg/GerInfo/239>

**ONLINE SUBMISSION**

<https://www.f6publishing.com>



## Gastrointestinal tuberculosis: Diagnostic approaches for this uncommon pathology

Lottie Brown, Michael Colwill, Andrew Poullis

**Specialty type:** Medicine, research and experimental

**Provenance and peer review:** Invited article; Externally peer reviewed.

**Peer-review model:** Single blind

**Peer-review report's classification**

**Scientific Quality:** Grade B

**Novelty:** Grade B

**Creativity or Innovation:** Grade C

**Scientific Significance:** Grade B

**P-Reviewer:** Iizuka M, Japan

**Received:** February 29, 2024

**Revised:** May 6, 2024

**Accepted:** June 17, 2024

**Published online:** August 16, 2024

**Processing time:** 126 Days and 16.4 Hours



**Lottie Brown, Michael Colwill, Andrew Poullis**, Department of Gastroenterology, St George's University Hospital NHS Foundation Trust, London SW17 0QT, United Kingdom

**Corresponding author:** Michael Colwill, BSc, MBBS, MRCP, Doctor, Research Fellow, Department of Gastroenterology, St George's University Hospital NHS Foundation Trust, Blackshaw Road, London SW17 0QT, United Kingdom. [michael.colwill@nhs.net](mailto:michael.colwill@nhs.net)

### Abstract

A case report entitled "Primary gastroduodenal tuberculosis presenting as gastric outlet obstruction" recently published in the *World Journal of Clinical Cases* presented a rare cause of gastric outlet obstruction and highlighted the atypical manner in which gastrointestinal tuberculosis (TB) can present. The literature with regards to this rare pathology is limited to case reports and case series with the largest being published using data from between 2003 and 2013. However, since then the diagnostic tools available have significantly changed with more modern and increasingly accurate tests now available. This editorial reviews the current state of the art with regards to diagnosis in gastrointestinal TB.

**Key Words:** Gastrointestinal tuberculosis; Diagnostic approach; Microbiology; Serology; Molecular diagnosis; Infectious disease

©The Author(s) 2024. Published by Baishideng Publishing Group Inc. All rights reserved.

**Core Tip:** Gastrointestinal tuberculosis is a rare pathology that can present in many atypical ways. This pathology is relatively rare and can be a significant challenge to diagnose. This editorial, in response to a recently published case report, aims to provide an update on diagnostic tests and approaches available.

**Citation:** Brown L, Colwill M, Poullis A. Gastrointestinal tuberculosis: Diagnostic approaches for this uncommon pathology. *World J Clin Cases* 2024; 12(23): 5283-5287

**URL:** <https://www.wjgnet.com/2307-8960/full/v12/i23/5283.htm>

**DOI:** <https://dx.doi.org/10.12998/wjcc.v12.i23.5283>

## INTRODUCTION

The case report “Primary gastroduodenal tuberculosis presenting as gastric outlet obstruction” presented in this edition by Ali *et al*[1] highlights the difficulties in diagnosing gastrointestinal tuberculosis (TB). TB is an infectious disease caused by the bacteria *Mycobacterium tuberculosis* (*M. tuberculosis*) which affects an estimated 10.6 million people and causes over 1.3 million deaths each year. Though primarily a respiratory disease, extrapulmonary disease is found in around 20% of patients with TB and occurs both in isolation or conjunction with pulmonary TB[2]. Abdominal TB, affecting the gastrointestinal tract, visceral organs, peritoneum and/or lymph nodes is thought to represent between 3%-21% of cases of extrapulmonary TB[3]. Abdominal TB may develop through ingestion of infected lung secretions, direct invasion from adjacent infected tissues and through haematogenous or lymphatic spread[4]. Our previously published case series reported on all the cases of abdominal TB seen at St George’s Hospital, London between 2003 and 2013, 65 cases in total. Since the report of this series there have been a number of advances in TB diagnostics but it’s variable and non-specific clinical presentation mean that abdominal TB remains a challenge to diagnose (see Table 1)[5].

## DIAGNOSING ABDOMINAL TUBERCULOSIS

Abdominal TB often mimics other gastrointestinal conditions such as inflammatory bowel disease, peptic ulcer disease, lymphoma and other malignancies[6,7]. Delays in diagnosis contribute to the poor prognosis of abdominal TB and progression to severe and potentially life-threatening complications including acute gastrointestinal haemorrhage, obstruction or perforation[8,9].

Establishing a diagnosis of abdominal TB begins with clinical signs and symptoms. As in pulmonary TB, features of systemic infection including low-grade fever, night sweats and weight loss may be present[5,9]. Abdominal symptoms vary according to site of infection and may only become apparent late in the disease course[4]. Gastrointestinal (or luminal) TB typically presents with chronic, colicky abdominal pain, vomiting, loss of appetite, chronic diarrhoea and/or constipation. Weight loss, accompanied with iron deficiency anaemia, are often predominant features of gastrointestinal TB due to impaired absorption, decreased food intake and a chronic inflammatory process[8]. Complications of gastrointestinal TB include ulceration, haemorrhage, stricture and fistula formation, obstruction and perforation. In India, abdominal TB is the second most common cause of bowel perforation, after typhoid, usually proximal to a TB-related stricture[4]. Organ-specific signs (such as jaundice, elevated blood liver enzymes or amylase) may aid differential diagnosis of visceral TB, a less common type of abdominal TB which affects the liver, spleen, gallbladder, pancreas, biliary or genitourinary tract[10]. Peritoneal TB may present insidiously, with sub-acute abdominal pain, distension and eventually, peritonitis. Depending on the site of infection, examination may reveal an abdominal mass, ascites, organomegaly or lymphadenopathy[10].

Imaging should be performed in all patients with a suspicion of abdominal TB. Ultrasound is useful as an initial and non-invasive tool able to detect features of abdominal TB, without the use of ionising radiation, including ascites, peritoneal thickening, lymphadenopathy and hepatic or splenic lesions. However, in confirmed TB infection, ultrasound has a relatively low sensitivity of 63% and specificity of 68% for diagnosing abdominal disease[11]. Ultrasound-guided fine needle aspiration also offers the option to obtain tissue for histopathology and microbiological evaluation and is particularly useful for the diagnosis of visceral TB; whereas paracentesis or laparoscopy or may be required for definitive diagnosis of peritoneal disease[7,12,13]. Computed tomography (CT) findings are similarly non-specific but useful for evaluating the extent and type of abdominal TB and identifying any complications[7,14]. CT appearances of abdominal TB may mimic other infections, inflammatory disorders or malignancies including lymphoma[6,7].

In cases of gastrointestinal TB, alongside cross-sectional imaging, endoscopy is crucial to investigate the extent and severity of disease and provide an opportunity for tissue biopsy. The endoscopic findings in gastrointestinal TB are variable and may include a loss of vascular pattern, erythema, superficial to deep ulcerations, nodularity, polyps, inflammatory masses, strictures or colitis (see Figure 1)[5,15]. Endoscopic and histological appearance of gastrointestinal TB may be mistaken for Crohn’s, since both diseases have a predilection for the small bowel and cause chronic granulomatous inflammation[16].

Histopathological examination of biopsy samples may demonstrate typical (though non-specific) features of abdominal TB including granulomas with caseating necrosis, Langerhans giant cells, chronic ulcers lined by conglomerate epithelioid histiocytes and disproportionate submucosal inflammation[8]. Although the sensitivity of histopathology is relatively low, diagnostic accuracy can be improved through increasing the number, volume and depth of biopsy specimens[17]. Analysis of ascitic fluid obtained through paracentesis usually reveals leucocytosis, low glucose and a low serum ascites albumin gradient[18]. Raised adenosine deaminase levels in ascitic fluid is suggestive of peritoneal TB, but is not useful in HIV populations[19].

For many years, conventional microbiology techniques including Ziehl Nelsen staining of acid-fast bacilli (AFB) and culture were the mainstay of TB diagnostics. For the diagnosis of abdominal TB, culture and Ziehl Nelsen staining have very high specificity (reaching 100%) but their value is limited by very low sensitivity (17.3%-31.0% and 9.3%, respectively)[8]. Sensitivity is reduced further in peritoneal TB, where the bacterial load in ascitic fluid is typically very low[20]. Due to the slow growth rate of *M. tuberculosis*, it may require 6-8 weeks to obtain a culture result. As with histopathology, diagnostic yield of culture and AFB staining, also known as Ziehl-Neelsen staining, can be significantly improved by increasing the number of samples sent for microbiological examination[21]. Combining histopathology and culture findings increases diagnostic accuracy[8].

**Table 1 Summary of diagnostic tools useful in abdominal tuberculosis**

Diagnostic tools	
Clinical signs	Vary according to site of infection (luminal, visceral, peritoneal) Non-specific and may only be present in late stage of disease
Imaging	Ultrasound is useful as a non-invasive imaging modality and can guide fine needle aspiration to obtain tissue for diagnosis of visceral TB, but has low sensitivity and specificity Cross-sectional abdominal imaging is non-specific but recommended to assess extent of TB infection and identify complications
Endoscopy	Gross endoscopic appearance may mimic other diseases such as Crohn's (Figure 1) Facilitates targeted tissue biopsy for histological and microbiological examination
Histopathology	Characteristic tissue features include granulomas with caseating necrosis, Langerhans giant cells, chronic ulcers lined by conglomerate epithelioid histiocytes and disproportionate submucosal inflammation
Conventional microbiology	Ziehl Nelsen staining of acid-fast bacilli provides rapid diagnosis with high specificity Both staining and culture have low sensitivity Due to slow growth rate of <i>M. tuberculosis</i> , culture may require 6-8 weeks
Molecular	PCR provides very high specificity across all specimen types PCR sensitivity is superior in tissue compared to ascitic fluid or paraffin-embedded specimens Stool PCR and cell-free DNA have potential as alternative, non-invasive tests but require further evaluation to confirm diagnostic performance
Serology	T-cell based IGRA, including QuantiFERON® and T-SPOT® on blood or ascitic fluid cannot differentiate between latent and active infection but can complement other diagnostic modalities Poor sensitivity in patients who are immunocompromised or who have disseminated disease

TB: Tuberculosis; IGRA: Interferon-gamma release assays; *M. tuberculosis*: *Mycobacterium tuberculosis*.

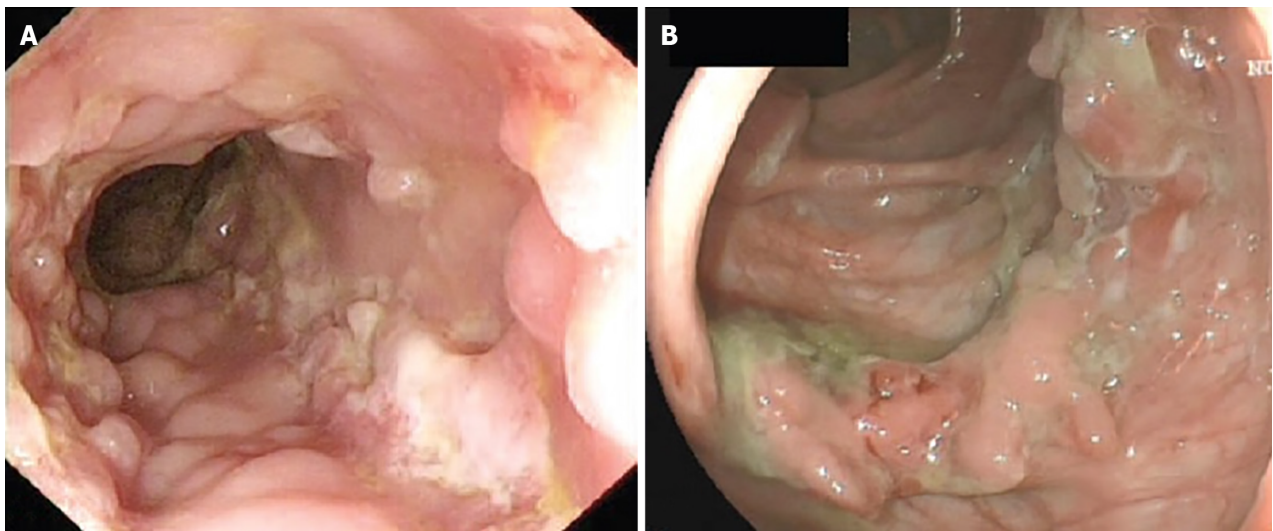


**Figure 1 The endoscopic findings of intestinal Crohn's compared to intestinal Tuberculosis.** A: Longitudinal ulcers and cobblestone appearance seen in Crohn's disease; B: Circumferential ulceration seen in intestinal Tuberculosis. Citation: Ye Z, Lin Y, Cao Q, He Y, Xue L. Granulomas as the Most Useful Histopathological Feature in Distinguishing between Crohn's Disease and Intestinal Tuberculosis in Endoscopic Biopsy Specimens. *Medicine (Baltimore)* 2015; 94(49): e2157 Copyright ©The Author(s) 2015. All rights reserved. Published by Wolters Kluwer Health, Inc[27] (Supplementary material).

In recent years, molecular diagnostics such as PCR have emerged as promising new tools for the diagnosis of abdominal TB. The main advantage of PCR over conventional culture or microscopy is the rapid detection of even very low bacterial burdens directly from clinical specimens. Certain assays, such as Gene-Xpert®, offer simultaneous detection of mutations conferring antimicrobial resistance, which can guide treatment regimens[8]. In a recent meta-analysis, the pooled sensitivity of PCR for the diagnosis of abdominal TB was low (58%, 95%CI 51%–64%) and specificity was high (99%, 95%CI 97%–99%) compared to a composite reference standard of clinical, radiological and histopathological evidence[22]. Though specificity remained consistently very high, there was significant variability in the sensitivity of

PCR according to assay specifics. The sensitivity of multiplex PCR, which amplifies multiple DNA targets in a single reaction, was superior to simple PCR and Gene-Xpert<sup>®</sup> (82%, *vs* 56% and 45%, respectively). PCR assays targeting the *IS6110* gene were more sensitive than those targeting the *rpoB* gene (60% *vs* 45%). Other PCR assays including single-tube loop-mediated isothermal amplification and fluorescent quantitative PCR (qPCR) have been used for the diagnosis of abdominal PCR but data is limited. The sensitivity of PCR was superior in evaluation of tissue specimens over ascitic fluid (62% *vs* 51%), likely due to higher bacterial burdens found in the gastrointestinal tract. Sensitivity of PCR dropped significantly when using paraffin-embedded specimens, secondary to DNA degradation and introduction of PCR inhibitors (sensitivity 34% compared to 58% and 72% for fresh and frozen tissue specimens, respectively).

PCR analysis of stool samples provides a non-invasive diagnostic tool to aid in the diagnosis of gastrointestinal TB. Stool PCR has demonstrated a moderate sensitivity of 64%, though data is limited and larger, multicentre cohort studies are needed before widespread implementation is recommended[22]. Detection of circulating cell-free DNA (cfDNA) within easily-accessible blood, urine or ascitic fluid samples provides another potential non-invasive diagnostic test for abdominal TB[23]. A recent meta-analysis identified only a single study evaluating qPCR of cfDNA in ascitic fluid, with low sensitivity of 40% and specificity of 90% against a composite reference standard[24,25].

T-cell based interferon-gamma release assays (IGRA), including QuantiFERON<sup>®</sup> and T-SPOT<sup>®</sup> on blood or ascitic fluid, have largely replaced tuberculin skin test (TST) for diagnosis of active and latent TB[8]. Unlike TST, specificity of IGRA is not affected by prior BCG vaccination. For peritoneal TB, sensitivity and specificity of IRGA on peripheral blood was found to be high at 91% and 78%, respectively[26]. The utility of IGRA is limited by poor sensitivity in patients who are immunocompromised or have disseminated disease[8].

## CONCLUSION

Abdominal TB continues to pose a major diagnostic challenge for clinicians. There exists no single test that has proved to be adequate in both sensitivity and specificity for the diagnosis of abdominal TB. In recent years, non-invasive diagnostic tools including stool or cfDNA PCR and serological tests have emerged with some promising results, though larger, prospective trials are needed before widespread implementation is recommended. Until then, combining results of multiple diagnostic modalities (including clinical, radiological, histopathological, microbiological, molecular and serological evidence) remains necessary in order to diagnose this clinical conundrum.

## FOOTNOTES

**Author contributions:** Brown L, Colwill M and Poullis A all contributed to manuscript inception, writing, reviewing and editing.

**Conflict-of-interest statement:** Dr. Colwill has nothing to disclose.

**Open-Access:** This article is an open-access article that was selected by an in-house editor and fully peer-reviewed by external reviewers. It is distributed in accordance with the Creative Commons Attribution NonCommercial (CC BY-NC 4.0) license, which permits others to distribute, remix, adapt, build upon this work non-commercially, and license their derivative works on different terms, provided the original work is properly cited and the use is non-commercial. See: <https://creativecommons.org/licenses/by-nc/4.0/>

**Country of origin:** United Kingdom

**ORCID number:** Lottie Brown 0000-0001-9896-8682; Michael Colwill 0000-0001-6925-8358; Andrew Poullis 0000-0003-0703-0328.

**Corresponding Author's Membership in Professional Societies:** British Society of Gastroenterology, BSG60672.

**S-Editor:** Lin C

**L-Editor:** A

**P-Editor:** Che XX

## REFERENCES

- 1 Ali AM, Mohamed YG, Mohamud AA, Mohamed AN, Ahmed MR, Abdullahi IM, Saydam T. Primary gastroduodenal tuberculosis presenting as gastric outlet obstruction: A case report and review of literature. *World J Clin Cases* 2024; **12**: 1536-1543 [PMID: 38576818 DOI: 10.12998/wjcc.v12.i8.1536]
- 2 World Health Organization. Global tuberculosis report 2023. Nov 7, 2023. [cited 4 May 2022]. Available from: <https://www.who.int/publications/i/item/9789240083851>
- 3 Al-Zanbagi AB, Shariff MK. Gastrointestinal tuberculosis: A systematic review of epidemiology, presentation, diagnosis and treatment. *Saudi J Gastroenterol* 2021; **27**: 261-274 [PMID: 34213424 DOI: 10.4103/sjg.sjg\_148\_21]
- 4 Farrar J, Hotez PJ, Junghanss T, Kang G, Lalloo D, White NJ, Garcia PJ. Manson's Tropical Diseases. 24th ed. Cham: Elsevier health sciences, 2023
- 5 Nayagam JS, Mullender C, Cosgrove C, Poullis A. Abdominal tuberculosis: Diagnosis and demographics, a 10-year retrospective review from

- a single centre. *World J Clin Cases* 2016; **4**: 207-212 [PMID: 27574607 DOI: 10.12998/wjcc.v4.i8.207]
- 6 **Ladumor H**, Al-Mohannadi S, Ameerudeen FS, Ladumor S, Fadl S. TB or not TB: A comprehensive review of imaging manifestations of abdominal tuberculosis and its mimics. *Clin Imaging* 2021; **76**: 130-143 [PMID: 33596517 DOI: 10.1016/j.clinimag.2021.02.012]
  - 7 **Abu-Zidan FM**, Sheek-Hussein M. Diagnosis of abdominal tuberculosis: lessons learned over 30 years: pectoral assay. *World J Emerg Surg* 2019; **14**: 33 [PMID: 31338118 DOI: 10.1186/s13017-019-0252-3]
  - 8 **Maulahela H**, Simadibrata M, Nelwan EJ, Rahadiani N, Renesteen E, Suwarti SWT, Anggraini YW. Recent advances in the diagnosis of intestinal tuberculosis. *BMC Gastroenterol* 2022; **22**: 89 [PMID: 35227196 DOI: 10.1186/s12876-022-02171-7]
  - 9 **Cho JK**, Choi YM, Lee SS, Park HK, Cha RR, Kim WS, Kim JJ, Lee JM, Kim HJ, Ha CY, Kim HJ, Kim TH, Jung WT, Lee OJ. Clinical features and outcomes of abdominal tuberculosis in southeastern Korea: 12 years of experience. *BMC Infect Dis* 2018; **18**: 699 [PMID: 30587154 DOI: 10.1186/s12879-018-3635-2]
  - 10 **Das CJ**, Rednam N, Vora Z, Aggarwal A, Chandrashekhara SH, Kundra V. Abdominal visceral tuberculosis: a malignancy mimic. *Abdom Radiol (NY)* 2023; **48**: 2705-2715 [PMID: 37204509 DOI: 10.1007/s00261-023-03939-5]
  - 11 **Van Hoving DJ**, Griesel R, Meintjes G, Takwoingi Y, Maartens G, Ochodo EA. Abdominal ultrasound for diagnosing abdominal tuberculosis or disseminated tuberculosis with abdominal involvement in HIV-positive individuals. *Cochrane Database Syst Rev* 2019; **9**: CD012777 [PMID: 31565799 DOI: 10.1002/14651858.CD012777.pub2]
  - 12 **Islam J**, Clarke D, Thomson SR, Wilson D, Dawood H. A prospective audit of the use of diagnostic laparoscopy to establish the diagnosis of abdominal tuberculosis. *Surg Endosc* 2014; **28**: 1895-1901 [PMID: 24442683 DOI: 10.1007/s00464-013-3410-9]
  - 13 **Handa U**, Garg S, Mohan H. Fine needle aspiration cytology in the diagnosis of abdominal TB: a review of 92 cases. *Trop Doct* 2009; **39**: 30-32 [PMID: 19211420 DOI: 10.1258/td.2008.070477]
  - 14 **Lee WK**, Van Tonder F, Tartaglia CJ, Dagia C, Cazzato RL, Duddalwar VA, Chang SD. CT appearances of abdominal tuberculosis. *Clin Radiol* 2012; **67**: 596-604 [PMID: 22212637 DOI: 10.1016/j.crad.2011.11.003]
  - 15 **Gan H**, Mely M, Zhao J, Zhu L. An Analysis of the Clinical, Endoscopic, and Pathologic Features of Intestinal Tuberculosis. *J Clin Gastroenterol* 2016; **50**: 470-475 [PMID: 26974755 DOI: 10.1097/MCG.0000000000000514]
  - 16 **Choudhury A**, Dhillon J, Sekar A, Gupta P, Singh H, Sharma V. Differentiating gastrointestinal tuberculosis and Crohn's disease- a comprehensive review. *BMC Gastroenterol* 2023; **23**: 246 [PMID: 37468869 DOI: 10.1186/s12876-023-02887-0]
  - 17 **Mehta V**, Desai D, Abraham P, Rodrigues C. Making a Positive Diagnosis of Intestinal Tuberculosis with the Aid of New Biologic and Histologic Features: How Far Have We Reached? *Inflamm Intest Dis* 2019; **3**: 155-160 [PMID: 31111030 DOI: 10.1159/000496482]
  - 18 **Debi U**, Ravisankar V, Prasad KK, Sinha SK, Sharma AK. Abdominal tuberculosis of the gastrointestinal tract: revisited. *World J Gastroenterol* 2014; **20**: 14831-14840 [PMID: 25356043 DOI: 10.3748/wjg.v20.i40.14831]
  - 19 **Ntwari J**, Dusabejamba V, Page C. Use of adenosine deaminase (ADA) to diagnose suspected peritoneal tuberculosis in Rwanda: a cross-sectional study. *BMC Infect Dis* 2020; **20**: 239 [PMID: 32197582 DOI: 10.1186/s12879-020-04965-0]
  - 20 **Fitzgerald DW**, Sterling TR, Haas DW. 251 - Mycobacterium tuberculosis. *Mandell, Douglas, Bennett's Princ Pract Infect Dis* 2015 [DOI: 10.1016/B978-1-4557-4801-3.00251-4]
  - 21 **Lowbridge C**, Fadhil SAM, Krishnan GD, Schimann E, Karuppan RM, Sriram N, Rajahram GS, Menon J, Patel A, William T, Paul DC, Ralph AP. How can gastro-intestinal tuberculosis diagnosis be improved? A prospective cohort study. *BMC Infect Dis* 2020; **20**: 255 [PMID: 32228479 DOI: 10.1186/s12879-020-04983-y]
  - 22 **Shen Y**, Fang L, Ye B, Yu G. Meta-analysis of diagnostic accuracy of nucleic acid amplification tests for abdominal tuberculosis. *PLoS One* 2023; **18**: e0289336 [PMID: 38011098 DOI: 10.1371/journal.pone.0289336]
  - 23 **Fernández-Carballo BL**, Broger T, Wyss R, Banaei N, Denking CM. Toward the Development of a Circulating Free DNA-Based In Vitro Diagnostic Test for Infectious Diseases: a Review of Evidence for Tuberculosis. *J Clin Microbiol* 2019; **57** [PMID: 30404942 DOI: 10.1128/JCM.01234-18]
  - 24 **Sharma P**, Anthwal D, Kumari P, Gupta RK, Lavania S, Sharma N, Sharma LK, Rath D, Soraganvi PK, Sharma A, Gadpayle AK, Taneja RS, Tyagi JS, Haldar S. Utility of circulating cell-free Mycobacterium tuberculosis DNA for the improved diagnosis of abdominal tuberculosis. *PLoS One* 2020; **15**: e0238119 [PMID: 32845896 DOI: 10.1371/journal.pone.0238119]
  - 25 **Yu G**, Shen Y, Ye B, Shi Y. Diagnostic accuracy of Mycobacterium tuberculosis cell-free DNA for tuberculosis: A systematic review and meta-analysis. *PLoS One* 2021; **16**: e0253658 [PMID: 34161399 DOI: 10.1371/journal.pone.0253658]
  - 26 **Luo Y**, Xue Y, Mao L, Lin Q, Tang G, Song H, Wang F, Sun Z. Diagnostic Value of T-SPOT.TB Assay for Tuberculous Peritonitis: A Meta-Analysis. *Front Med (Lausanne)* 2020; **7**: 585180 [PMID: 33425937 DOI: 10.3389/fmed.2020.585180]
  - 27 **Ye Z**, Lin Y, Cao Q, He Y, Xue L. Granulomas as the Most Useful Histopathological Feature in Distinguishing between Crohn's Disease and Intestinal Tuberculosis in Endoscopic Biopsy Specimens. *Medicine (Baltimore)* 2015; **94**: e2157 [PMID: 26656343 DOI: 10.1097/MD.0000000000002157]



## Pay attention to the application of indocyanine green fluorescence imaging technology in laparoscopic liver cancer resection

Li-Min Kang, Fu-Wei Zhang, Fa-Kun Yu, Lei Xu

**Specialty type:** Medicine, research and experimental

**Provenance and peer review:** Invited article; Externally peer reviewed.

**Peer-review model:** Single blind

**Peer-review report's classification**

**Scientific Quality:** Grade C

**Novelty:** Grade C

**Creativity or Innovation:** Grade C

**Scientific Significance:** Grade C

**P-Reviewer:** Urade T, Japan

**Received:** March 10, 2024

**Revised:** May 27, 2024

**Accepted:** June 7, 2024

**Published online:** August 16, 2024

**Processing time:** 116 Days and 23.1 Hours



**Li-Min Kang, Fu-Wei Zhang, Fa-Kun Yu, Lei Xu**, Department of Hepatobiliary and Pancreatic Surgery, Puer People's Hospital, Puer 665000, Yunnan Province, China

**Corresponding author:** Li-Min Kang, PhD, Doctor, Surgeon, Department of Hepatobiliary and Pancreatic Surgery, Puer People's Hospital, No. 44 Zhenxing Street, Puer 665000, Yunnan Province, China. [kanglimin2010@163.com](mailto:kanglimin2010@163.com)

### Abstract

Traditional laparoscopic liver cancer resection faces challenges, such as difficulties in tumor localization and accurate marking of liver segments, as well as the inability to provide real-time intraoperative navigation. This approach falls short of meeting the demands for precise and anatomical liver resection. The introduction of fluorescence imaging technology, particularly indocyanine green, has demonstrated significant advantages in visualizing bile ducts, tumor localization, segment staining, microscopic lesion display, margin examination, and lymph node visualization. This technology addresses the inherent limitations of traditional laparoscopy, which lacks direct tactile feedback, and is increasingly becoming the standard in laparoscopic procedures. Guided by fluorescence imaging technology, laparoscopic liver cancer resection is poised to become the predominant technique for liver tumor removal, enhancing the accuracy, safety and efficiency of the procedure.

**Key Words:** Indocyanine green; Fluorescence imaging technology; Laparoscopy; Hepatectomy; Liver tumor

©The Author(s) 2024. Published by Baishideng Publishing Group Inc. All rights reserved.

**Core Tip:** Fluorescence laparoscopic liver cancer resection, such as indocyanine green (ICG) fluorescence imaging, offers various advantages including visualizing bile ducts, tumor localization, staining of liver segments, detection of microscopic lesions, assessment of resection margins, and visualization of lymph nodes. This technology addresses the lack of direct tactile feedback in traditional laparoscopy and is becoming the standard in laparoscopic procedures. Fluorescence imaging in guiding laparoscopic liver cancer resection is expected to enhance the accuracy, safety and efficiency of the procedure. However, caution is advised regarding potential drawbacks of ICG fluorescence imaging such as false-positive liver staining and limited tissue penetration.

**Citation:** Kang LM, Zhang FW, Yu FK, Xu L. Pay attention to the application of indocyanine green fluorescence imaging technology in laparoscopic liver cancer resection. *World J Clin Cases* 2024; 12(23): 5288-5293

**URL:** <https://www.wjgnet.com/2307-8960/full/v12/i23/5288.htm>

**DOI:** <https://dx.doi.org/10.12998/wjcc.v12.i23.5288>

## INTRODUCTION

The treatment model for primary liver cancer has evolved significantly with the advent of targeted therapy and immunotherapy. Some patients in intermediate and advanced stages now have the opportunity for radical surgical resection through conversion therapy, expanding the scope of liver cancer surgery indications[1]. This has made the conditions faced by surgeons more complex, requiring higher precision in surgical damage control and resection[2]. Traditional laparoscopic liver cancer resection has technical limitations, such as difficulty in tumor localization and segment marking, hindering real-time intraoperative navigation[3]. These inherent flaws may result in positive resection margins, preventing radical cure and contradicting the increasingly valued concept of precision liver resection[4].

The emergence of fluorescence laparoscopy technology, particularly indocyanine green (ICG) fluorescence imaging, has effectively addressed the limitations of traditional laparoscopic liver cancer resection[5]. Aoki *et al*[6] first reported on laparoscopic liver cancer resection guided by ICG fluorescence in 2008, sparking global interest in using fluorescence laparoscopy for laparoscopic liver cancer resection[7,8]. This technology combines functional imaging and laparoscopic surgery, offering significant benefits in tumor localization, liver segment marking, and intraoperative navigation[9]. Over the past decade, the application of fluorescence imaging in laparoscopic liver cancer resection has become increasingly refined[10]. Kokudo *et al*[11] suggest that fluorescence imaging represents one of the major technological advances in liver surgery over the last two decades.

## PRINCIPLES OF FLUORESCENCE IMAGING

When a substance is irradiated by incident light of a specific wavelength, it absorbs light energy and enters an excited state, immediately de-exciting and emitting emergent light. This emergent light, known as fluorescence, is generated with the incident light typically referred to as the excitation light source[12]. Common excitation light sources include ultraviolet light, visible light, infrared light, and x-ray micro-computed tomography (CT). Luminescent substances used as probe molecules include melatonin, histone deacetylase and glutathione[13]. ICG, a water-soluble molecule with fluorescent dye properties, binds to high-molecular-weight proteins like albumin and lipoproteins in plasma and bile without altering their structure, providing good intravascular stability. Intravenous injection of ICG does not elicit toxic reactions in the body, maintaining effective concentration levels even with low-dose administration[14]. Experimental studies have demonstrated that when excited by light of 750 nm–810 nm, ICG molecules emit fluorescence with a peak wavelength of 840 nm. This fluorescence falls within the window limit of the deep red and near-infrared spectrum, with a wavelength of approximately 10 mm. Utilizing an interference filter lens on a camera, the fluorescence emitted by ICG in deep tissues 10 mm from the surface can be captured, enabling the extraction of signals and the formation of a fluorescence image[15].

Studies have demonstrated that following intravenous injection of ICG into the systemic circulation, hepatocytes take up ICG molecules through their active transport system, leading to secretion into the biliary system and subsequent drainage into the intestines. Notably, there is no enterohepatic circulation. While normal liver tissue can effectively clear ICG within 12 hours–24 hours, patients with cirrhosis exhibit reduced clearance ability[16]. Research has indicated that hepatocellular carcinoma with differentiation retains the capacity to uptake ICG; however, the lack of normal bile duct structure in these cases results in ICG accumulation within the tumor tissue. In contrast, poorly differentiated or metastatic liver cancer cells may impede ICG secretion from adjacent liver tissue, leading to ICG retention in local tissues[17]. Consequently, tissues or fluids containing ICG often exhibit green fluorescence during fluorescence laparoscopy, creating a distinct visual contrast with the red color of normal liver tissue in laparoscopic fusion images.

## ICG FLUOROSCOPY IN LAPAROSCOPIC HEPATOCELLULAR CARCINOMA RESECTION

### ***Intraoperative display and examination of the biliary system***

The prevention of bile duct injury during laparoscopic liver resection and timely detection of bile leakage during surgery are crucial for preventing and treating complications of laparoscopic liver cancer resection[18]. ICG has a unique advantage in visualizing and examining the biliary system due to its excretion through the biliary tract[19]. The fluorescence produced when ICG-laden bile flows through the biliary system allows for clear visualization of the biliary system, reducing the risk of intraoperative bile duct damage by aiding in the identification of the biliary system and preventing inadvertent injuries[20]. Additionally, in cases of bile leakage during surgery, the fluorescence of leaked ICG can more sensitively pinpoint the location of the leakage compared to traditional bile staining[21]. Real-time ICG fluorescence imaging can assist in identifying variant bile ducts during surgery, offering a level of detail comparable to preoperative magnetic resonance imaging (MRI) and enhancing surgical safety[22]. In summary, the implementation of ICG fluorescence imaging can identify intraoperative biliary variations, thereby helping to prevent complications such as biliary injury and bile leakage[23,24].

### ***Tumor staining for primary liver cancer***

The accurate localization of tumor boundaries during laparoscopic liver cancer resection has long been a challenge. ICG fluorescence imaging capitalizes on the differential absorption and excretion of ICG between tumors and normal liver tissue to precisely stain liver tumors with fluorescence[25]. This technique aids in the precise positioning and navigation of tumor resection, enhancing surgical efficiency and minimizing the risk of positive resection margins. The application of fluorescence imaging is particularly prominent in laparoscopic liver resection[26]. Despite advances in imaging techniques such as CT and MRI, approximately 7% of liver tumors remain difficult to detect preoperatively. ICG fluorescence imaging demonstrates high sensitivity for small lesions, detecting lesions as small as 2 mm and addressing the issue of missed diagnoses associated with traditional imaging methods[27]. Research by Kose *et al*[28] showed that intraoperative ultrasound had a 89% recognition rate for superficial liver tumors, whereas ICG fluorescence imaging achieved a recognition rate of 95%. Furthermore, ICG fluorescence imaging can reveal lesions that are undetectable by preoperative MRI or intraoperative ultrasound. The staining patterns observed during ICG fluorescence imaging can provide initial insights into the nature of the tumor[29]. Different tumor properties manifest in distinct staining patterns, such as whole-tumor fluorescence for well-differentiated hepatocellular carcinoma, partial fluorescence for moderately differentiated hepatocellular carcinoma, and ring fluorescence for poorly differentiated hepatocellular carcinoma or metastatic tumor[30].

### ***Laparoscopic anatomical hepatectomy with staining of liver segments***

Anatomical liver resection is currently considered to offer a better clinical prognosis for treating malignant tumors that spread along the portal venous system[31]. In the past, liver segment marking relied on the surgeon's subjective estimation of liver segment boundaries based on experience and traditional imaging, rather than true anatomical resection[32]. ICG fluorescence can accurately visualize liver segments and subsegments, offering advantages over traditional labeling methods[33]. ICG is quickly absorbed by hepatocytes after entering the liver through peripheral or portal vein puncture, leading to a significant color difference between stained and unstained liver segments. This clear boundary formation enables real-time navigation of liver dissection boundaries even within the liver parenchyma[34].

### ***Other applications***

ICG can flow through lymphatic vessels and attach to proteins within these vessels, becoming concentrated in lymph nodes for identification, aiding in lymphatic dissection for tumors like cholangiocarcinoma[35]. Moreover, ICG fluorescence can also assist in determining the presence of any remaining tumor at the margin of liver resection, thus enhancing the rate of achieving R0 tumor resection[36]. Consequently, it is suggested that liver cancer patients undergoing ICG fluorescence laparoscopic resection may experience improved survival outcomes compared to those undergoing conventional laparoscopic surgery[37].

## DEFECTS IN ICG FLUOROSCOPY IN LAPAROSCOPIC HEPATOCELLULAR CARCINOMA RESECTION

### ***ICG fluorescence laparoscopy for cutting edge problems***

The staining of tumors with ICG is thought to be due to the tumor compressing the surrounding normal liver tissue, leading to decreased excretion of ICG and its accumulation around the tumor. The fluorescence boundary is expected to be larger than the tumor boundary[18], suggesting that resection beyond the fluorescence boundary is necessary for R0 resection[38]. However, a recent study[39] indicated that, in hepatocellular carcinoma, the pathological border closely aligned with the fluorescent border, requiring a resection margin of 1.5 cm–2.0 cm from the tumor edge for ideal resection. This study suggested resecting the tumor along the fluorescent border, acknowledging that absolute safety could not be guaranteed. We have only one chance to delineate fluorescence for the perfusion region because the liver absorbs ICG. Vigilance is essential when using ICG fluorescence imaging to guide laparoscopic liver cancer resection, and adjusting the resection margin in real-time with intraoperative ultrasound can help reduce the risk of tumor rupture and positive resection margins.

### The problem of false positives in ICG fluorescence laparoscopy

The sensitivity of ICG fluorescence to liver lesions can lead to false positives, where additional stained areas may appear during surgery that are later confirmed to be normal liver tissue[27]. Studies have shown that the median false-positive rate for detecting tumors with ICG fluorescence imaging can be as high as 10.5% [40], with even higher rates in patients with liver cirrhosis[29]. Therefore, it is important to carefully assess the timing and dosage of ICG based on the patient's liver condition before surgery, and to approach each stained lesion during surgery with caution using a combination of visual observation, palpation and other imaging techniques.

### Limited tissue penetration of ICG fluorescence

The tissue penetration of ICG fluorescence is usually only 8 mm–10 mm, although this depth of penetration already exceeds that of many other probe molecules. Densitometry of ICG fluorescence images is based on the assessment of fluorescent areas by adjusting the threshold of fluorescence intensity, which is insufficient for the penetration of deep tumors in the liver. Therefore, ICG fluorescence staining is still unfavorable for the exploration of deep tumors in the liver [41]. A systematic review[27] highlighted that the sensitivity of ICG fluorescence for tumors deeper than 8 mm ranges from 71% to 79%. Therefore, it is crucial to complement ICG fluorescence imaging with preoperative imaging or intraoperative ultrasound to prevent overlooking deep liver tumor lesions.

## CONCLUSION

The continuous advancement of fluorescence imaging technology is enabling the integration of high-end features such as ultra-high definition, large depth of field, high dynamics, wide color gamut, and intelligent adjustment in fluorescence laparoscopy. This progress is expected to drive significant growth in fluorescence laparoscopy. It is anticipated that the technical capabilities of fluorescence laparoscopy will soon match or even surpass those of the current predominant white light laparoscopy, positioning fluorescence laparoscopy as the future standard in laparoscopy. The benefits of fluorescent imaging in tumor staining, liver segment staining, and real-time intraoperative navigation, mean that laparoscopic liver cancer resection guided by fluorescent imaging is poised to become the leading technique for liver tumor resection. This advancement will enhance the precision, safety and efficiency of laparoscopic liver cancer resection.

## FOOTNOTES

**Author contributions:** Kang LM, Zhang FW, Yu FK and Xu L designed the study, performed the study, analyzed the data, and wrote the manuscript. Kang LM has read and approve the final manuscript.

**Conflict-of-interest statement:** All the authors report no relevant conflicts of interest for this article.

**Open-Access:** This article is an open-access article that was selected by an in-house editor and fully peer-reviewed by external reviewers. It is distributed in accordance with the Creative Commons Attribution NonCommercial (CC BY-NC 4.0) license, which permits others to distribute, remix, adapt, build upon this work non-commercially, and license their derivative works on different terms, provided the original work is properly cited and the use is non-commercial. See: <https://creativecommons.org/licenses/by-nc/4.0/>

**Country of origin:** China

**ORCID number:** Li-Min Kang 0000-0002-3062-897X; Fu-Wei Zhang 0009-0002-3737-0112; Fa-Kun Yu 0009-0007-1331-2432; Lei Xu 0009-0002-7732-7856.

**S-Editor:** Luo ML

**L-Editor:** A

**P-Editor:** Chen YX

## REFERENCES

- 1 Laface C, Ranieri G, Maselli FM, Ambrogio F, Foti C, Ammendola M, Laterza M, Cazzato G, Memeo R, Mastrandrea G, Lioce M, Fedele P. Immunotherapy and the Combination with Targeted Therapies for Advanced Hepatocellular Carcinoma. *Cancers (Basel)* 2023; **15**: 654 [PMID: 36765612 DOI: 10.3390/cancers15030654]
- 2 Jianxi W, Xiongfeng Z, Zehao Z, Zhen Z, Tianyi P, Ye L, Haosheng J, Zhixiang J, Huiling W. Indocyanine green fluorescence-guided laparoscopic hepatectomy versus conventional laparoscopic hepatectomy for hepatocellular carcinoma: A single-center propensity score matching study. *Front Oncol* 2022; **12**: 930065 [PMID: 35928871 DOI: 10.3389/fonc.2022.930065]
- 3 Liu F, Wang H, Ma W, Li J, Liu Y, Tang S, Li K, Jiang P, Yang Z, He Y, Liu Z, Zhang Z, Yuan Y. Short- and Long-Term Outcomes of Indocyanine Green Fluorescence Navigation- Versus Conventional-Laparoscopic Hepatectomy for Hepatocellular Carcinoma: A Propensity Score-Matched, Retrospective, Cohort Study. *Ann Surg Oncol* 2023; **30**: 1991-2002 [PMID: 36645540 DOI: 10.1245/s10434-022-13027-5]
- 4 Wang J, Xu Y, Zhang Y, Tian H. Safety and effectiveness of fluorescence laparoscopy in precise hepatectomy: A meta-analysis. *Photodiagnosis Photodyn Ther* 2023; **42**: 103599 [PMID: 37156455 DOI: 10.1016/j.pdpdt.2023.103599]

- 5 Liu Y, Wang Q, Du B, Wang XZ, Xue Q, Gao WF. Meta-analysis of indocyanine green fluorescence imaging-guided laparoscopic hepatectomy. *Photodiagnosis Photodyn Ther* 2021; **35**: 102354 [PMID: 34052422 DOI: 10.1016/j.pdpdt.2021.102354]
- 6 Aoki T, Yasuda D, Shimizu Y, Odaira M, Niiya T, Kusano T, Mitamura K, Hayashi K, Murai N, Koizumi T, Kato H, Enami Y, Miwa M, Kusano M. Image-guided liver mapping using fluorescence navigation system with indocyanine green for anatomical hepatic resection. *World J Surg* 2008; **32**: 1763-1767 [PMID: 18543027 DOI: 10.1007/s00268-008-9620-y]
- 7 Takemura N, Ito K, Inagaki F, Mihara F, Kokudo N. Added value of indocyanine green fluorescence imaging in liver surgery. *Hepatobiliary Pancreat Dis Int* 2022; **21**: 310-317 [PMID: 34953679 DOI: 10.1016/j.hbpd.2021.12.007]
- 8 Li J, Li X, Zhang X, Wang H, Li K, He Y, Liu Z, Zhang Z, Yuan Y. Indocyanine green fluorescence imaging-guided laparoscopic right posterior hepatectomy. *Surg Endosc* 2022; **36**: 1293-1301 [PMID: 33683434 DOI: 10.1007/s00464-021-08404-2]
- 9 Zhu W, Zeng X, Hu H, Xiang N, Zeng N, Wen S, Tian J, Yang J, Fang C. Perioperative and Disease-Free Survival Outcomes after Hepatectomy for Centrally Located Hepatocellular Carcinoma Guided by Augmented Reality and Indocyanine Green Fluorescence Imaging: A Single-Center Experience. *J Am Coll Surg* 2023; **236**: 328-337 [PMID: 36648260 DOI: 10.1097/XCS.0000000000000472]
- 10 Zhou K, Zhou S, Du L, Liu E, Dong H, Ma F, Sun Y, Li Y. Safety and effectiveness of indocyanine green fluorescence imaging-guided laparoscopic hepatectomy for hepatic tumor: a systematic review and meta-analysis. *Front Oncol* 2023; **13**: 1309593 [PMID: 38234399 DOI: 10.3389/fonc.2023.1309593]
- 11 Kokudo N, Takemura N, Ito K, Mihara F. The history of liver surgery: Achievements over the past 50 years. *Ann Gastroenterol Surg* 2020; **4**: 109-117 [PMID: 32258975 DOI: 10.1002/ags3.12322]
- 12 Li C, Chen G, Zhang Y, Wu F, Wang Q. Advanced Fluorescence Imaging Technology in the Near-Infrared-II Window for Biomedical Applications. *J Am Chem Soc* 2020; **142**: 14789-14804 [PMID: 32786771 DOI: 10.1021/jacs.0c07022]
- 13 Cosco ED, Spearman AL, Ramakrishnan S, Lingg JGP, Saccomano M, Pengshung M, Arús BA, Wong KCY, Glasl S, Ntziachristos V, Warmer M, McLaughlin RR, Bruns OT, Sletten EM. Shortwave infrared polymethine fluorophores matched to excitation lasers enable non-invasive, multicolour in vivo imaging in real time. *Nat Chem* 2020; **12**: 1123-1130 [PMID: 33077925 DOI: 10.1038/s41557-020-00554-5]
- 14 Lou JX, Wu Y, Huhe M, Zhang JJ, Jia DW, Jiang ZY. Diagnosis of poorly differentiated adenocarcinoma of the stomach by confocal laser endomicroscopy: A case report. *World J Clin Cases* 2024; **12**: 1481-1486 [PMID: 38576802 DOI: 10.12998/wjcc.v12.i8.1481]
- 15 Rossi G, Tarasconi A, Baiocchi G, De' Angelis GL, Gaiani F, Di Mario F, Catena F, Dalla Valle R. Fluorescence guided surgery in liver tumors: applications and advantages. *Acta Biomed* 2018; **89**: 135-140 [PMID: 30561406 DOI: 10.23750/abm.v89i9-S.7974]
- 16 Piccolo G, Barabino M, Lecchi F, Santambrogio R, Nava C, Opocher E, Bianchi PP. Laparoscopic Indocyanine Green Fluorescence Imaging for Intrahepatic Cholangiocarcinoma. *Am Surg* 2023; **89**: 2577-2582 [PMID: 35605160 DOI: 10.1177/00031348221103659]
- 17 Rompianesi G, Pegoraro F, Ramaci L, Ceresa CD, Montalti R, Troisi RI. Preoperative planning and intraoperative real-time navigation with indocyanine green fluorescence in robotic liver surgery. *Langenbecks Arch Surg* 2023; **408**: 292 [PMID: 37522938 DOI: 10.1007/s00423-023-03024-x]
- 18 Oldhafer KJ, Reese T, Fard-Aghaie M, Strohmaier A, Makridis G, Kantas A, Wagner KC. [Intraoperative fluorescence angiography and cholangiography with indocyanine green in hepatobiliary surgery]. *Chirurg* 2019; **90**: 880-886 [PMID: 31559461 DOI: 10.1007/s00104-019-01035-3]
- 19 Luo D, Liang W, Ma B, Xue D. Global trends of indocyanine green fluorescence navigation in laparoscopic cholecystectomy: bibliometrics and knowledge atlas analysis. *Surg Endosc* 2022; **36**: 6419-6431 [PMID: 35029767 DOI: 10.1007/s00464-021-08988-9]
- 20 Yoo D. Laparoscopic choledocholithotomy and transductal T-tube insertion with indocyanine green fluorescence imaging and laparoscopic ultrasound: A case report. *World J Clin Cases* 2023; **11**: 7193-7199 [PMID: 37946768 DOI: 10.12998/wjcc.v11.i29.7193]
- 21 Kaibori M, Ishizaki M, Matsui K, Kwon AH. Intraoperative indocyanine green fluorescent imaging for prevention of bile leakage after hepatic resection. *Surgery* 2011; **91**: 91-98 [PMID: 21514613 DOI: 10.1016/j.surg.2011.02.011]
- 22 Pesce A, La Greca G, Esposito Ultimo L, Basile A, Puleo S, Palmucci S. Effectiveness of near-infrared fluorescent cholangiography in the identification of cystic duct-common hepatic duct anatomy in comparison to magnetic resonance cholangio-pancreatography: a preliminary study. *Surg Endosc* 2020; **34**: 2715-2721 [PMID: 31598878 DOI: 10.1007/s00464-019-07158-2]
- 23 Pesce A, Fabbri N, Feo CV. Should Fluorescent Cholangiography Become a Gold Standard During All Cholecystectomies? *J Am Coll Surg* 2023; **237**: 169 [PMID: 36988208 DOI: 10.1097/XCS.0000000000000696]
- 24 Lehrskov LL, Westen M, Larsen SS, Jensen AB, Kristensen BB, Bisgaard T. Fluorescence or X-ray cholangiography in elective laparoscopic cholecystectomy: a randomized clinical trial. *Br J Surg* 2020; **107**: 655-661 [PMID: 32057103 DOI: 10.1002/bjs.11510]
- 25 Urade T, Sawa H, Iwatani Y, Abe T, Fujinaka R, Murata K, Mii Y, Man-I M, Oka S, Kuroda D. Laparoscopic anatomical liver resection using indocyanine green fluorescence imaging. *Asian J Surg* 2020; **43**: 362-368 [PMID: 31043331 DOI: 10.1016/j.asjsur.2019.04.008]
- 26 Zhu G, Qiu X, Zeng L, Zou Z, Yang L, Nie S, Wang Z, Zhang X, Tang J, Pan Y, Tang S, Wu T. Application of indocyanine green-mediated fluorescence molecular imaging technology in liver tumors resection: a systematic review and meta-analysis. *Front Oncol* 2023; **13**: 1167536 [PMID: 37384301 DOI: 10.3389/fonc.2023.1167536]
- 27 Purich K, Dang JT, Poonja A, Sun WYL, Bigam D, Birch D, Karmali S. Intraoperative fluorescence imaging with indocyanine green in hepatic resection for malignancy: a systematic review and meta-analysis of diagnostic test accuracy studies. *Surg Endosc* 2020; **34**: 2891-2903 [PMID: 32266547 DOI: 10.1007/s00464-020-07543-2]
- 28 Kose E, Kahramangil B, Aydin H, Donmez M, Takahashi H, Acevedo-Moreno LA, Sasaki K, Aucejo F, Berber E. A comparison of indocyanine green fluorescence and laparoscopic ultrasound for detection of liver tumors. *HPB (Oxford)* 2020; **22**: 764-769 [PMID: 31653594 DOI: 10.1016/j.hpb.2019.10.005]
- 29 Ishizawa T, Fukushima N, Shibahara J, Masuda K, Tamura S, Aoki T, Hasegawa K, Beck Y, Fukayama M, Kokudo N. Real-time identification of liver cancers by using indocyanine green fluorescent imaging. *Cancer* 2009; **115**: 2491-2504 [PMID: 19326450 DOI: 10.1002/cncr.24291]
- 30 Takemura N, Kokudo N. Do we need to shift from dye injection to fluorescence in respective liver surgery? *Surg Oncol* 2020; **33**: 207-209 [PMID: 31375295 DOI: 10.1016/j.suronc.2019.07.003]
- 31 Liao K, Yang K, Cao L, Lu Y, Zheng B, Li X, Wang X, Li J, Chen J, Zheng S. Laparoscopic Anatomical Versus Non-anatomical hepatectomy in the Treatment of Hepatocellular Carcinoma: A randomised controlled trial. *Int J Surg* 2022; **102**: 106652 [PMID: 35525414 DOI: 10.1016/j.ijsu.2022.106652]
- 32 Sato N, Marubashi S. What is the optimal surgical treatment for hepatocellular carcinoma beyond the debate between anatomical versus non-anatomical resection? *Surg Today* 2022; **52**: 871-880 [PMID: 34392420 DOI: 10.1007/s00595-021-02352-z]
- 33 Chen JY, Han J, Liu ZW, Xin XL, Wang PF, Cai SW. Combined hepatic segment color rendering technique improves the outcome of

- anatomical hepatectomy in patients with hepatocellular carcinoma. *Hepatobiliary Pancreat Dis Int* 2023; **22**: 528-531 [PMID: [35710483](#) DOI: [10.1016/j.hbpd.2022.05.014](#)]
- 34 **Tao H**, Wang Z, Zeng X, Hu H, Li J, Lin J, Lin W, Fang C, Yang J. Augmented Reality Navigation Plus Indocyanine Green Fluorescence Imaging Can Accurately Guide Laparoscopic Anatomical Segment 8 Resection. *Ann Surg Oncol* 2023; **30**: 7373-7383 [PMID: [37606841](#) DOI: [10.1245/s10434-023-14126-7](#)]
  - 35 **Zhang Y**, Zhang Y, Zhu J, Tao H, Liang H, Chen Y, Zhang Z, Zhao J, Zhang W. Clinical application of indocyanine green fluorescence imaging in laparoscopic lymph node dissection for intrahepatic cholangiocarcinoma: A pilot study (with video). *Surgery* 2022; **171**: 1589-1595 [PMID: [34857382](#) DOI: [10.1016/j.surg.2021.09.032](#)]
  - 36 **Tong M**, Zhang BC, Jia FY, Wang J, Liu JH. Hepatic inflammatory myofibroblastic tumor: A case report. *World J Clin Cases* 2023; **11**: 4318-4325 [PMID: [37449218](#) DOI: [10.12998/wjcc.v11.i18.4318](#)]
  - 37 **Zhou Y**, Zhang C, Wang Y, Yu J, Wang D, Ma J. Effects of indocyanine green fluorescence imaging of laparoscopic anatomic liver resection for HCC: a propensity score-matched study. *Langenbecks Arch Surg* 2023; **408**: 51 [PMID: [36662263](#) DOI: [10.1007/s00423-023-02781-z](#)]
  - 38 **Tashiro Y**, Aoki T, Hirai T, Koizumi T, Mansou DA, Kusano T, Matsuda K, Yamada K, Nogaki K, Hakoziaki T, Wada Y, Shibata H, Tomioka K, Yamazaki T, Saito K, Fujimori A, Enami Y, Hoffman RM, Murakami M. Pathological Validity of Using Near-infrared Fluorescence Imaging for Securing Surgical Margins During Liver Resection. *Anticancer Res* 2020; **40**: 3873-3882 [PMID: [32620627](#) DOI: [10.21873/anticancer.14377](#)]
  - 39 **Cai X**, Hong H, Pan W, Chen J, Jiang L, Du Q, Li G, Lin S, Chen Y. Does Using Indocyanine Green Fluorescence Imaging for Tumors Help in Determining the Safe Surgical Margin in Real-Time Navigation of Laparoscopic Hepatectomy? A Retrospective Study. *Ann Surg Oncol* 2023; **30**: 1981-1987 [PMID: [36484905](#) DOI: [10.1245/s10434-022-12893-3](#)]
  - 40 **Wakabayashi T**, Cacciaguerra AB, Abe Y, Bona ED, Nicolini D, Mocchegiani F, Kabeshima Y, Vivarelli M, Wakabayashi G, Kitagawa Y. Indocyanine Green Fluorescence Navigation in Liver Surgery: A Systematic Review on Dose and Timing of Administration. *Ann Surg* 2022; **275**: 1025-1034 [PMID: [35121701](#) DOI: [10.1097/SLA.0000000000005406](#)]
  - 41 **Lu H**, Gu J, Qian XF, Dai XZ. Indocyanine green fluorescence navigation in laparoscopic hepatectomy: a retrospective single-center study of 120 cases. *Surg Today* 2021; **51**: 695-702 [PMID: [33128594](#) DOI: [10.1007/s00595-020-02163-8](#)]



## Impact of parenting styles on preschoolers' behaviors

Elif Sarac

**Specialty type:** Psychology, social

**Provenance and peer review:**

Invited article; Externally peer reviewed.

**Peer-review model:** Single blind

**Peer-review report's classification**

**Scientific Quality:** Grade C

**Novelty:** Grade C

**Creativity or Innovation:** Grade C

**Scientific Significance:** Grade C

**P-Reviewer:** Setiawati Y, Indonesia

**Received:** March 27, 2024

**Revised:** May 11, 2024

**Accepted:** June 3, 2024

**Published online:** August 16, 2024

**Processing time:** 100 Days and 0.6 Hours



**Elif Sarac**, Ministry of National Defense, General Directorate of Management Services, Ankara 06000, Türkiye

**Corresponding author:** Elif Sarac, PhD, Researcher, Ministry of National Defense, General Directorate of Management Services, Bilkent/Ankara, Ankara 06000, Türkiye.  
[sarac.elf@gmail.com](mailto:sarac.elf@gmail.com)

### Abstract

In this editorial, I comment on the article "Association of preschool children behavior and emotional problems with the parenting behavior of both parents" which was published in the latest issue of "World Journal of Clinical Cases" that demonstrates the prevalence of behavioral disorders in preschool children. Therefore I am focused on parenting which is the most effective factor shown to affect the development and continuity of these behaviors. The management of child behavior problems is crucial. Children in early ages, especially preschoolers who are in the first 5 years of life, are influenced by dramatic changes in various aspects of development, such as social, emotional, and physical. Also, children experience many changes linked to different developmental tasks, such as discovering themselves, getting new friendships, and adapting to a new environment. In this period, parents have a critical role in supporting child development. If parents do not manage and overcome their child's misbehavior, it could be transformed into psychosocial problems in adulthood. Parenting is the most powerful predictor in the social development of preschool children. Several studies have shown that to reduce the child's emotional and behavioral problems, a warm relationship between parents and children is needed. In addition, recent studies have demonstrated significant relationships between family regulation factors and parenting, as well as with child behaviors.

**Key Words:** Behavioral problems; Children; Emotional problems; Parenting style; Preschool

©The Author(s) 2024. Published by Baishideng Publishing Group Inc. All rights reserved.

**Core Tip:** Positive supporting behavior of parents towards their children is associated with children's increased prosocial behaviors. Conversely authoritative, coercive and permissive behavior styles are shown to be related to increased hyperactivity, conduct problems and emotional maladjustment of preschoolers.

**Citation:** Sarac E. Impact of parenting styles on preschoolers' behaviors. *World J Clin Cases* 2024; 12(23): 5294-5298

**URL:** <https://www.wjgnet.com/2307-8960/full/v12/i23/5294.htm>

**DOI:** <https://dx.doi.org/10.12998/wjcc.v12.i23.5294>

## INTRODUCTION

Preschool children are in a critical period of their lives related to developing socio-emotional behaviors[1,2]. Parenting style is the first effective factor in physical, social, emotional, motor, and cognitive development[3-5]. There is great evidence that parenting behavior is a significant risk factor for children's functioning and has been linked with children's misbehaviors[6-8]. The vast majority of studies have focused on parental anxiety and lack of parental social support, which have been linked with children's functioning and development[4,5,6].

Parent psychopathology is also a predictive factor in children's behavioral and emotional problems[8]. For example, parents may have symptoms of psychopathology, may be less available or skilled at caretaking, may have difficulty facilitating children's activities, or may have difficulty in the relationship with their children. This situation may lead children to misbehave in their social life. The findings of many studies have linked the authoritarian behavior of the father to depression and emotional behavioral problems in children, while the authoritarian style of motherhood has been linked to anxiety, depression, as well as behavioral and emotional disorders[4,9]. In addition, having an authoritarian parenting style in relationships contributes to an antisocial, deviant, or delinquent personality in adolescence for children [10]. Although negative parental behavior negatively affects child development, positive parental support has such positive effects on and special importance for a child's social and emotional growth and has the potential to avoid emotional and behavioral difficulties[11]. For example, positive parenting behaviors and positive support in relationships and engagement in activities, such as play and learning with the child, are key elements for desired changes in child behaviors[12].

To prevent the development of behavioral disorders, modifiable factors and increased symptoms need to be identified at early ages. Also, permissive parenting style has been associated with problem behaviors, social skills, and school misconduct[13]. Furthermore, emotional and social misbehavior are found to predict anxiety, recurrent depression, and attempted suicide in adolescents[14].

Uninvolved, oppressive, and permissive maternal or paternal behaviors are one of the reasons for reduced positive interactions with children[15]. When these dysfunctional interactions are repeated, strengthened aversive behaviors and increased behavior problems often occur. Preschoolers are susceptible to the family environment to such an extent that they mirror their parents in their interactions. Studies have shown that systematic changes in parenting behaviors, such as close and warm communication, and requesting instead of ordering can lessen the frequency of a child's conduct disorder[14,16]. In addition, understanding and assessing the role of parenting style in children's development can also be further advanced by building a stronger knowledge base regarding the role of parents in preschoolers' development.

## CHARACTERISTICS AND OUTCOMES OF THE MOST COMMON BEHAVIORAL DISORDERS OF PRESCHOOLERS

### **Anxiety disorder**

Characterized by a lack of overcoming the fears and worries that are typical[17]. If this fear interferes with the activities or relationships at school, home, or in the social environment, an anxiety disorder can be diagnosed.

### **Depression**

Defined as feeling persistent sadness and hopelessness in daily life[18]. If the child has changes in sleeping or eating patterns or does not enjoy fun activities, depression disorder may be diagnosed.

### **Childhood oppositional defiant disorder**

Characterized by an angry or argumentative mood and/or vindictiveness[18]. Children with oppositional defiant disorder (ODD) often argue with their parents, refuse to comply with their requests, and intentionally annoy others. A high level of ODD symptoms in preschoolers has been examined[18,19].

### **Attention deficit/hyperactivity disorder**

Characterized by inattention and hyperactivity-impulsivity that interfere with functioning. It is one of the most common psychiatric disorders in preschoolers[18]. The typical symptom of attention deficit/hyperactivity disorder (ADHD) is having difficulty sustaining focus both at home/school or in the social environment. The child has excessive motor activity and/or talkativeness, in addition to having actions without forethought[19].

### **Conduct disorder**

Is a prevalent chronic developmental disorder of childhood that is characterized by iterative and persistent behaviors in which the rights of others are violated[14]. At the same time, conduct disorder (CD) involves behavior one would

consider cruel to animals[20]. Studies have shown that this kind of cruel behavior, albeit not so common in preschoolers, is possible[18].

Previous studies have shown that the disorders mentioned above are normative and common among preschool children[18,21]. These studies involving children with behavioral disorders have demonstrated a lesser degree of parental warmth and a higher degree of parental depression, anxiety, and stress. In addition, a considerable amount of research links parenting with behavioral disorders in preschoolers[14,22-24].

The present study focuses on the effects of parenting styles on the behavioral problems of preschoolers[23]. The study was conducted in seven kindergartens in Ma'an Shan city from October 2017 to May 2018. Data was collected with the "Children's Strength and Difficulties Questionnaire"[25], and 2253 valid responses were received from parents. The study concluded that parenting styles were closely related to children's behavioral and emotional problems. Findings showed that high levels of mother and father support and participation were inversely related to abnormal children conduct problems. This conclusion is in line with previous studies[14,22,24,26,27]. One study in literature revealed that some parental characteristics and styles, such as permissive, negligent, authoritarian, and inconsistent/harsh/punitive discipline, were considered to increase the risk for emotional and behavioral problems in children[22]. Conversely, in a previous study, Haslam *et al*[24] explained that parenting styles with cultural values impacted child development rather than parenting characteristics alone. The same parenting styles may have differential effects on child development depending on the socio-cultural context. The authors pointed out that authoritative parenting and permissive behaviors of parents may not be suitable in individualist cultures but it is suitable in collectivist cultures that promote interdependence and obedience. The differences in these studies may stem from the design and the related factors. In addition, the growing child is constantly affected not only by parenting but also several factors in the environment.

Another study showed suggestive evidence of the bidirectional effects that parenting has on child misbehaviors and that child misbehavior may affect parenting[27]. In addition, they found that more authoritarian, overprotective, and permissive parenting behaviors are related to greater child behavioral disorders, such as ADHD, ODD, and CD. At early ages, child misbehavior predicted greater paternal authoritarian parenting.

In detail, the authors emphasized that the effects of parenting also varied according to age levels. These results supported the findings of the main study that was conducted by Wang *et al*[23]. It showed evidence that maternal and paternal coercion/hostility and authoritativeness were related to conduct problems, hyperactivity, and peer communication problems. In contrast, there are supportive studies on reciprocal relations that focus on parenting and child misbehaviors, like the one by Allman *et al*[27].

In existing literature, there is growing evidence for the hereditary role in the development of prosocial behaviors and conduct problems in children[28-30]. It is of course possible that genetic influences are one of the reasons for the maturing basis for behavioral problems that endure throughout childhood.

Studies are clearly demonstrating that parenting that contributes to maladaptive child development constitutes both the absence of positive and supportive parenting behaviors. In a parent-child relationship, the child experiences the most immediate influences. In conclusion, parenting always impacts children's adjustment.

---

## CLINICAL IMPLICATIONS

Effective and supportive practices in child-parent relationships are positively associated with normal development for preschoolers. Parenting is shown as the first predictive factor in reducing prosocial behavior problems in children at early ages, and research suggests that behavioral and emotional disorders emerge in early childhood.

---

## CONCLUSION

Concerning the findings, studies suggest that positive parenting styles are related to emotional and behavioral disorders. Future research can seek to indicate the effective factors on children's misbehavior and development. Also, more intervention research is needed to explore the impacts of parenting on children's misbehaviors.

---

## ACKNOWLEDGEMENTS

Thanks to the authors of the main study who are focused on parenting style and preschoolers' behavioral problems and give an opportunity to me to comment on this issue.

---

## FOOTNOTES

**Author contributions:** Sarac E performed the design, literature search and writing of the study.

**Conflict-of-interest statement:** The author has no relevant financial or non-financial relationships to disclose.

**Open-Access:** This article is an open-access article that was selected by an in-house editor and fully peer-reviewed by external reviewers.

It is distributed in accordance with the Creative Commons Attribution NonCommercial (CC BY-NC 4.0) license, which permits others to distribute, remix, adapt, build upon this work non-commercially, and license their derivative works on different terms, provided the original work is properly cited and the use is non-commercial. See: <https://creativecommons.org/licenses/by-nc/4.0/>

**Country of origin:** Türkiye

**ORCID number:** Elif Sarac [0000-0002-4126-9327](https://orcid.org/0000-0002-4126-9327).

**S-Editor:** Liu JH

**L-Editor:** Filipodia

**P-Editor:** Ma XP

## REFERENCES

- 1 Santrock JW. Life span development [13th edition]. 2011. New York: McGraw-Hill
- 2 Pinquart M. Associations of parenting dimensions and styles with externalizing problems of children and adolescents: An updated meta-analysis. *Dev Psychol* 2017; **53**: 873-932 [PMID: [28459276](https://pubmed.ncbi.nlm.nih.gov/28459276/) DOI: [10.1037/dev0000295](https://doi.org/10.1037/dev0000295)]
- 3 King KA, Vidourek RA, Merianos AL. Authoritarian parenting and youth depression: Results from a national study. *J Prev Interv Community* 2016; **44**: 130-139 [PMID: [26939843](https://pubmed.ncbi.nlm.nih.gov/26939843/) DOI: [10.1080/10852352.2016.1132870](https://doi.org/10.1080/10852352.2016.1132870)]
- 4 Sumargi AM, Prasetyo E, Ardelia BW. Parenting Styles And Their Impacts On Child Problem Behaviors. *Jurnal Psikologi* 2020; **19**: 269-285 [DOI: [10.14710/jp.19.3.269-285](https://doi.org/10.14710/jp.19.3.269-285)]
- 5 Lansford JE, Sharma C, Malone PS, Woodlief D, Dodge KA, Oburu P, Pastorelli C, Skinner AT, Sorbring E, Tapanya S, Tirado LM, Zelli A, Al-Hassan SM, Alampay LP, Bacchini D, Bombi AS, Bornstein MH, Chang L, Deater-Deckard K, Di Giunta L. Corporal punishment, maternal warmth, and child adjustment: a longitudinal study in eight countries. *J Clin Child Adolesc Psychol* 2014; **43**: 670-685 [PMID: [24885184](https://pubmed.ncbi.nlm.nih.gov/24885184/) DOI: [10.1080/15374416.2014.893518](https://doi.org/10.1080/15374416.2014.893518)]
- 6 Sumargi A, Filus A, Morawska A, Sofronoff K. The Parenting and Family Adjustment Scales (PAFAS): an Indonesian Validation Study. *J Child Fam Stud* 2018; **27**: 756-770 [DOI: [10.1007/s10826-017-0926-y](https://doi.org/10.1007/s10826-017-0926-y)]
- 7 Guo M, Morawska A, Filus A. Validation of the Parenting and Family Adjustment Scales to Measure Parenting Skills and Family Adjustment in Chinese Parents. *Measurement and Evaluation in Counseling* 2016 [DOI: [10.1177/0748175615625754](https://doi.org/10.1177/0748175615625754)]
- 8 Breaux RP, Harvey EA, Lugo-Candelas CI. The role of parent psychopathology in the development of preschool children with behavior problems. *J Clin Child Adolesc Psychol* 2014; **43**: 777-790 [PMID: [24116918](https://pubmed.ncbi.nlm.nih.gov/24116918/) DOI: [10.1080/15374416.2013.836451](https://doi.org/10.1080/15374416.2013.836451)]
- 9 Nikoogoftar M, Seghatoleslam S. The Role of Parenting Styles In Predicting Adolescent Behavioral and Emotional Problems. *Pract Clin Psych* 2015; 23-30 Available from: <https://Sid.Ir/Paper/345831/En>
- 10 Murray J, Farrington DP. Risk factors for conduct disorder and delinquency: key findings from longitudinal studies. *Can J Psychiatry* 2010; **55**: 633-642 [PMID: [20964942](https://pubmed.ncbi.nlm.nih.gov/20964942/) DOI: [10.1177/070674371005501003](https://doi.org/10.1177/070674371005501003)]
- 11 Okorn A, Verhoeven M, Van Baar A. The Importance of Mothers' and Fathers' Positive Parenting for Toddlers' and Preschoolers' Social-Emotional Adjustment. *Parenting* 2022; **22**: 128-151 [DOI: [10.1080/15295192.2021.1908090](https://doi.org/10.1080/15295192.2021.1908090)]
- 12 Verhoeven M, van Baar AL, Deković M. Parenting Toddlers. *Handbook of Parenting* 2019 [DOI: [10.4324/9780429440847-2](https://doi.org/10.4324/9780429440847-2)]
- 13 Lee EH, Zhou Q, Ly J, Main A, Tao A, Chen SH. Neighborhood characteristics, parenting styles, and children's behavioral problems in Chinese American immigrant families. *Cultur Divers Ethnic Minor Psychol* 2014; **20**: 202-212 [PMID: [24041263](https://pubmed.ncbi.nlm.nih.gov/24041263/) DOI: [10.1037/a0034390](https://doi.org/10.1037/a0034390)]
- 14 Rolon-Arroyo B, Arnold DH, Breaux RP, Harvey EA. Reciprocal Relations Between Parenting Behaviors and Conduct Disorder Symptoms in Preschool Children. *Child Psychiatry Hum Dev* 2018; **49**: 786-799 [PMID: [29468356](https://pubmed.ncbi.nlm.nih.gov/29468356/) DOI: [10.1007/s10578-018-0794-8](https://doi.org/10.1007/s10578-018-0794-8)]
- 15 Besemer S, Loeber R, Hinshaw SP, Pardini DA. Bidirectional Associations Between Externalizing Behavior Problems and Maladaptive Parenting Within Parent-Son Dyads Across Childhood. *J Abnorm Child Psychol* 2016; **44**: 1387-1398 [PMID: [26780209](https://pubmed.ncbi.nlm.nih.gov/26780209/) DOI: [10.1007/s10802-015-0124-6](https://doi.org/10.1007/s10802-015-0124-6)]
- 16 Brown CA, Granero R, Ezpeleta L. The Reciprocal Influence of Callous-Unemotional Traits, Oppositional Defiant Disorder and Parenting Practices in Preschoolers. *Child Psychiatry Hum Dev* 2017; **48**: 298-307 [PMID: [27013514](https://pubmed.ncbi.nlm.nih.gov/27013514/) DOI: [10.1007/s10578-016-0641-8](https://doi.org/10.1007/s10578-016-0641-8)]
- 17 Al-biltagi M. Anxiety Disorder in Children: Review. *J Paedi Care Inol* 2016; **1**: 18-28 [DOI: [10.24218/jpci.2016.05](https://doi.org/10.24218/jpci.2016.05)]
- 18 American Psychiatric Association. Diagnostic and Statistical Manual of Mental Disorders. 5th ed. Arlington, VA: APA; 2013
- 19 Husby SM, Wichstrøm L. Interrelationships and Continuities in Symptoms of Oppositional Defiant and Conduct Disorders from Age 4 to 10 in the Community. *J Abnorm Child Psychol* 2017; **45**: 947-958 [PMID: [27783258](https://pubmed.ncbi.nlm.nih.gov/27783258/) DOI: [10.1007/s10802-016-0210-4](https://doi.org/10.1007/s10802-016-0210-4)]
- 20 Hong JS, Tillman R, Luby JL. Disruptive behavior in preschool children: distinguishing normal misbehavior from markers of current and later childhood conduct disorder. *J Pediatr* 2015; **166**: 723-30.e1 [PMID: [25598304](https://pubmed.ncbi.nlm.nih.gov/25598304/) DOI: [10.1016/j.jpeds.2014.11.041](https://doi.org/10.1016/j.jpeds.2014.11.041)]
- 21 Wakschlag LS, Briggs-Gowan MJ, Choi SW, Nichols SR, Kestler J, Burns JL, Carter AS, Henry D. Advancing a multidimensional, developmental spectrum approach to preschool disruptive behavior. *J Am Acad Child Adolesc Psychiatry* 2014; **53**: 82-96.e3 [PMID: [24342388](https://pubmed.ncbi.nlm.nih.gov/24342388/) DOI: [10.1016/j.jaac.2013.10.011](https://doi.org/10.1016/j.jaac.2013.10.011)]
- 22 Çöp E, Çengel Kültür SE, Şenses Dinç G. [Association Between Parenting Styles and Symptoms of Attention Deficit Hyperactivity Disorder]. *Türk Psikiyatri Derg* 2017; **28**: 25-32 [PMID: [28291295](https://pubmed.ncbi.nlm.nih.gov/28291295/)]
- 23 Wang SM, Yan SQ, Xie FF, Cai ZL, Gao GP, Weng TT, Tao FB. Association of preschool children behavior and emotional problems with the parenting behavior of both parents. *World J Clin Cases* 2024; **12**: 1084-1093 [PMID: [38464916](https://pubmed.ncbi.nlm.nih.gov/38464916/) DOI: [10.12998/wjcc.v12.i6.1084](https://doi.org/10.12998/wjcc.v12.i6.1084)]
- 24 Haslam D, Poniman C, Filus A, Sumargi A, Boediman L. Parenting Style, Child Emotion Regulation and Behavioral Problems: The Moderating Role of Cultural Values in Australia and Indonesia. *Marriage & Family Review* 2020; **56**: 320-342 [DOI: [10.1080/01494929.2020.1712573](https://doi.org/10.1080/01494929.2020.1712573)]
- 25 Famodu OO, Adebayo AM, Adebayo BE. Child labor and mental health status of in-school adolescents in a municipal local government area of Lagos state, Nigeria. *Int J Adolesc Med Health* 2018; **33** [PMID: [30367800](https://pubmed.ncbi.nlm.nih.gov/30367800/) DOI: [10.1515/ijamh-2018-0075](https://doi.org/10.1515/ijamh-2018-0075)]

- 26 **Larzelere RE**, Morris ASE, Harrist AW. Authoritative parenting: Synthesizing nurturance and discipline for optimal child development. 2013. Washington, DC: American Psychological Association. [DOI: [10.1037/13948-000](https://doi.org/10.1037/13948-000)]
- 27 **Allmann AES**, Klein DN, Kopala-Sibley DC. Bidirectional and transactional relationships between parenting styles and child symptoms of ADHD, ODD, depression, and anxiety over 6 years. *Dev Psychopathol* 2022; **34**: 1400-1411 [PMID: [34103100](https://pubmed.ncbi.nlm.nih.gov/34103100/) DOI: [10.1017/S0954579421000201](https://doi.org/10.1017/S0954579421000201)]
- 28 **Harvey EA**, Metcalfe LA. The interplay among preschool child and family factors and the development of ODD symptoms. *J Clin Child Adolesc Psychol* 2012; **41**: 458-470 [PMID: [22530755](https://pubmed.ncbi.nlm.nih.gov/22530755/) DOI: [10.1080/15374416.2012.673161](https://doi.org/10.1080/15374416.2012.673161)]
- 29 **McGrath LM**, Weill S, Robinson EB, Macrae R, Smoller JW. Bringing a developmental perspective to anxiety genetics. *Dev Psychopathol* 2012; **24**: 1179-1193 [PMID: [23062290](https://pubmed.ncbi.nlm.nih.gov/23062290/) DOI: [10.1017/S0954579412000636](https://doi.org/10.1017/S0954579412000636)]
- 30 **Lewis GJ**, Plomin R. Heritable influences on behavioural problems from early childhood to mid-adolescence: evidence for genetic stability and innovation. *Psychol Med* 2015; **45**: 2171-2179 [PMID: [25765219](https://pubmed.ncbi.nlm.nih.gov/25765219/) DOI: [10.1017/S0033291715000173](https://doi.org/10.1017/S0033291715000173)]



## Essential role of postoperative follow-up in the management of clear cell sarcoma

Zi-Han Zhang, Jin-Tao Guo, Ying Xie, Si-Yu Sun

**Specialty type:** Gastroenterology & hepatology

**Provenance and peer review:**

Invited article; Externally peer reviewed.

**Peer-review model:** Single blind

**Peer-review report's classification**

**Scientific Quality:** Grade B, Grade C

**Novelty:** Grade B, Grade C

**Creativity or Innovation:** Grade B, Grade C

**Scientific Significance:** Grade B, Grade C

**P-Reviewer:** Dey T, India; Sahin TT, Türkiye

**Received:** April 7, 2024

**Revised:** May 18, 2024

**Accepted:** June 4, 2024

**Published online:** August 16, 2024

**Processing time:** 89 Days and 2.6 Hours



**Zi-Han Zhang, Jin-Tao Guo, Ying Xie, Si-Yu Sun**, Department of Gastroenterology, Shengjing Hospital of China Medical University, Shenyang 110004, Liaoning Province, China

**Jin-Tao Guo, Si-Yu Sun**, Engineering Research Center of Ministry of Education for Minimally Invasive Gastrointestinal Endoscopic Techniques, Shenyang 110004, Liaoning Province, China

**Corresponding author:** Si-Yu Sun, MD, PhD, Chief Doctor, Director, Professor, Department of Gastroenterology, Shengjing Hospital of China Medical University, No. 36 Sanhao Street, Shenyang 110004, Liaoning Province, China. [sun-siyu@163.com](mailto:sun-siyu@163.com)

### Abstract

Clear cell sarcoma (CCS) is a rare melanocytic soft tissue sarcoma known for its propensity to metastasize to the lymph nodes and typically has an unfavorable prognosis. Currently, surgical resection is the primary treatment for localized CCS, while radiotherapy and chemotherapy are preferred for metastatic cases. The roles of adjuvant chemotherapy, radiotherapy, and lymph node dissection are controversial. Although immunotherapy has emerged as a promising avenue in CCS treatment research, there are no established clinical standards for postoperative follow-up. This editorial discusses a recent article by Liu *et al*, with a focus on current diagnostic modalities, treatment approaches, and the challenging prognosis associated with CCS. Our aim is to underscore the importance of long-term patient follow-up in CCS management.

**Key Words:** Clear cell carcinoma; Diagnosis; Treatment; Prognosis; Follow-up

©The Author(s) 2024. Published by Baishideng Publishing Group Inc. All rights reserved.

**Core Tip:** Clear cell sarcoma (CCS) is a rare subtype of melanocytic soft tissue sarcoma distinguished by its propensity for metastasis and recurrence. Survival rates markedly diminish in patients with advanced CCS compared with those with early-stage disease. The insidious nature of early occult onset and the limited responsiveness of CCS to chemoradiotherapy underscore the critical importance of routine postoperative follow-up for early detection of recurrent cases, which is crucial for enhancing patient prognosis.

**Citation:** Zhang ZH, Guo JT, Xie Y, Sun SY. Essential role of postoperative follow-up in the management of clear cell sarcoma. *World J Clin Cases* 2024; 12(23): 5299-5303

**URL:** <https://www.wjgnet.com/2307-8960/full/v12/i23/5299.htm>

**DOI:** <https://dx.doi.org/10.12998/wjcc.v12.i23.5299>

## INTRODUCTION

Clear cell sarcoma (CCS) is an uncommon and highly aggressive malignant soft tissue sarcoma (STS) it is characterized by melanocytic differentiation and is believed to originate in tendons and aponeuroses. Due to its insidious onset and slow growth in its early stages, CCS is frequently misdiagnosed as a benign lesion or is identified at an advanced stage. It poses a significant diagnostic challenge. Predominantly affecting the lower extremities, particularly the feet and ankles, CCS exhibits aggressive behavior, marked by local recurrence, lymph node metastasis, and distant metastasis[1,2]. At diagnosis, the majority of patients already present with lymph node or distant metastasis[3], contributing to the generally poor prognosis, with notably lower 5-year survival rates in advanced stages compared to those in early stages. Metastasis primarily occurs in the lungs, followed by the bones and brain[3]. While CCS of the gastrointestinal system is exceedingly rare[4], clear cell sarcoma-like gastrointestinal tumor (CCSLGT), initially reported by Zambrano *et al*[5] in 2003, is characterized by robust diffuse immunoreactivity of S-100 protein, negative melanocyte-specific markers, and the presence of osteoclast-like multinucleated giant cells. It primarily affects the walls of the small intestine, stomach, or large intestine. Although only two cases of primary pancreatic CCS have been reported to date[4,6], CCSLGT has a more aggressive phenotype compared with traditional CCS, often presenting with metastasis at diagnosis, particularly to the lymph nodes or liver[7].

Despite advancements in understanding the pathogenesis of STS, agreement on the management of CCS is lacking because it is a rare disease. This editorial sheds light on the latest developments in CCS diagnosis and treatment, underscoring the necessity of postoperative follow-up of patients with CCS.

## CURRENT DIAGNOSTIC METHODS FOR CCS

The diagnosis of CCS typically relies on a combination of medical history, clinical presentation, and imaging findings. Many patients are already at an advanced stage at symptom onset. CCSLGT predominantly affects the intestinal wall, manifesting as abdominal pain, intestinal obstruction, and occasionally nonspecific symptoms such as anorexia, night sweats, weight loss, or anemia[7]. Patients with pancreatic CCS commonly present with symptoms such as anorexia, jaundice, or other gastrointestinal symptoms[4,6].

Computed tomography (CT) is a primary diagnostic tool for identifying suspected cases, offering insights into sarcoma size and location[8]. Magnetic resonance imaging (MRI) aids in assessing tumor depth and its relationship with surrounding structures and is needed for preoperative planning. Liu *et al*[9] reported a rare case of CCS with pancreatic metastasis, elucidating the imaging features of pancreatic CCS. CT imaging revealed a round, mildly enhanced, heterogeneous lesion in the pancreatic tail and MRI depicted a vague boundary between the lesion and pancreatic body, with an equal to slightly lower signal on T1 and slightly higher signal on T2, along with progressive uneven enhancement. Given CCS's propensity for hematological or lymphatic metastasis, staging typically involves preoperative assessment with whole-body CT, positron emission tomography-CT, or bone scintigraphy[10]. Recent reports underscore the possibility of peripheral blood transmission of CCS, highlighting the utility of blood smears for rapid diagnosis[11].

A histological examination is imperative to confirm the diagnosis of CCS[12]. Additionally, preoperative confirmation through percutaneous biopsy is essential to ensure negative margins[13]. Multinucleated giant cells that have a wreath-like nuclear appearance are often present in CCS[14]. In contrast, CCSLGT typically lacks conspicuous nucleoli and multinucleated giant cells, replaced instead by CD68-positive multinucleated osteoclast-like giant cells[15]. Immunohistochemical analysis of CCS demonstrates striking similarities to malignant melanoma, commonly expressing S100 protein and melanocyte-specific markers such as HMB-45, melanin-A, and microphthalmia-associated transcription factor (MITF) [16-18]. While S100 protein is expressed in nearly all cases of CCSLGT, melanoma markers (melan A, HMB45) are typically negative[15].

Differential diagnosis is critical in distinguishing CCS from S100 protein-positive and/or melanocyte marker-positive tumors, including malignant melanoma, epithelioid malignant peripheral nerve sheath tumors, melanotic schwannomas, and perivascular epithelioid cell tumors[19]. Despite having morphological, ultrastructural, and histopathological similarities, CCS and melanoma differ in their molecular tumorigenesis[20]. Recent advancements have used fluorescence in situ hybridization and reverse transcription polymerase chain reaction to confirm CCS and distinguish it from malignant melanoma based on distinct genetic profiles[21]. Approximately 70%-90% of CCS cases are detected by the t(12;22)(q13;q12) translocation, which results in the Ewing sarcoma breakpoint region 1 (*EWSR1*)/activating transcription factor 1 (*ATF1*) chimeric gene. This translocation induces MITF expression, facilitating the acquisition of melanocytic characteristics and the expression of melanocyte markers[22]. Another specific mutation, the t(2;22)(q34;q12) translocation leading to *EWSR1* and cAMP response element-binding protein (*CREB1*) fusion, is found in a minority of CCS cases. More recently, *EWSR1*/cAMP responsive element modulator (*CREM*) fusion was identified in several CCS cases[21]. Ozenberger *et al*[23] used V5 labeled *EWSR1*/ATF1 to induce CCS in mice to observe genome distribution and found that

CREM may represent an important target gene and cofactor for EWSR1/ATF1 fusion. Notably, *BRAF* mutations, common in melanoma, are rare in CCS[24].

## CURRENT MANAGEMENT OF CCS

Currently, the preferred treatment for localized CCS is complete surgical resection with negative margins, and is often followed by local excision or partial amputation. While standards for metastasis detection remain elusive, radiation or chemotherapy is the preferred treatment modality[3]. The most frequent systemic sarcoma chemotherapy regimens include doxorubicin, sunitinib, gemcitabine, and pazopanib[25]. However, clinical trials evaluating MET inhibitors, such as tivantinib and crizotinib, have demonstrated limited antitumor activity, necessitating further research and improvement of treatment strategies[26,27]. Notably, trabectedin has recently been shown to induce cell cycle arrest in CCS cell lines, inhibit CCS tumor growth in mice, and elicit clinical and radiological tumor responses in patients[28,29].

CCS is generally regarded as unresponsive to radiotherapy and chemotherapy, with conflicting evidence of the survival advantage of adjuvant radiotherapy and chemotherapy[13,19,30,31]. A randomized prospective study by Beane *et al*[32] indicated that postoperative radiotherapy significantly reduced local recurrence rates in patients with STS, albeit without enhancing overall survival rates. The Japanese Orthopedic Association guidelines advocate for perioperative adjuvant radiotherapy in patients with STS, emphasizing the necessity for meticulous individual case assessment to optimize treatment outcome[33].

Recently, significant attention has been directed towards the development and application of immunotherapies for advanced sarcomas. The fundamental principle involves inhibiting the checkpoints that tumors use as a defense mechanism to evade detection by immune system. The use of immune checkpoints such as cytotoxic T-lymphocyte antigen-4 and programmed cell death-1 (PD-1) in melanoma treatment, and their parallels with CCS, have captured the interest of immunotherapists in the treatment of CCS. Marcrom *et al*[34] reported a case of recurrent, unresectable CCS with a complete clinical response to pembrolizumab and radiotherapy. This suggests that there is a synergistic effect between PD-1 therapy and radiotherapy. A phase I/II clinical trial conducted by Gordon *et al*[35] found the combined use of immune checkpoint inhibitors ipilimumab and nivolumab and the tumoricide trabectedin (the SAINT regimen) in early-stage disease significantly enhanced the survival outcomes of patients with advanced sarcoma, with CCS having a favorable responsive. However, large-scale studies are urgently needed to explore the therapeutic potential of immunotherapy in patients with CCS.

The prognosis of patients with CCS remains dismal, with 5- and 10-year survival rates ranging from 47% to 67% and 25% to 41%, respectively[19]. Notably, the 5-year overall survival rates of patients with stage III and IV CCS are substantially lower than those of patients with stage I and II CCS. Approximately one-third of patients with CCS have lymph node metastasis at diagnosis, a prevalence significantly higher than that observed in other soft tissue sarcomas[3]. In a retrospective analysis of 60 cases categorized as CCSLGT, Washimi *et al*[15] found that the frequency of lymph node metastasis at diagnosis was 62%, which was significantly higher than the metastasis rate observed in CCS. Previous research has highlighted tumor size, location, and metastasis as key prognostic factors[36]. A 2023 national database study by Fujiwara *et al*[33] identified primary tumor resection and metastatic lymph node dissection as independent factors associated with improved prognosis.

Moreover, CCS has a recurrence rate as high as 40%[37], with reports of late recurrences occurring after more than 10 years[13]. Fujiwara *et al*[33] reported cumulative local recurrence rates of 11% at 3 years and 19% at 5 years postoperatively. Tumor size was found to be significantly correlated with local recurrence, in contrast to other soft tissue sarcomas, in which surgical margins and the use of chemotherapy or radiotherapy typically has a more significant role. Nonetheless, the limited patient cohort in this study raises concerns about the reliability of this conclusion, necessitating further investigation.

The high recurrence rate and aggressive nature of CCS underscore the critical importance of comprehensive long-term follow-up for all patients. However, there is currently a lack of published data outlining the optimal routine follow-up strategy for surgically treated patients with localized disease. In the case reported by Liu *et al*[9], the patient declined regular disease monitoring and examination after the first operation, seeking follow-up only when symptoms manifested, resulting in delayed treatment. This highlights the crucial role of regular postoperative follow-ups in patients with CCS. The clinical practice guidelines established by ESMO-EURACAN-GENTURIS recommend risk assessment and a tailored follow-up strategy based on histological type and tumor grade, size, and location. Additionally, the use of appropriate imaging modalities, such as MRI to detect local recurrence in extremities and superficial recurrence in the trunk and CT to identify lung metastases, are useful for early detection of recurrence[38].

## CONCLUSION

Given the rarity of CCS, our understanding of the disease remains partial, necessitating further research to advance our understanding of its diagnosis and management. However, increased rates of metastasis and recurrence underscore the importance of prioritizing postoperative care and devising a structured follow-up regimen for patients. Early identification of at-risk individuals and prompt recognition of recurrent cases stand as crucial measures to improve patient prognosis and increase survival rates.

## FOOTNOTES

**Author contributions:** Zhang ZH, Guo JT, Xie Y, Sun SY contributed to this paper; Zhang ZH designed the outline of the manuscript and drafted the article; Guo JT was responsible for the revision of the manuscript; Xie Y contributed to the editing the manuscript; Sun SY was the study supervisor and was responsible for the revision of the manuscript.

**Supported by** Liaoning Province Applied Basic Research Program Joint Program Project, No. 2022JH2/101500076; Shenyang Young and Middle-aged Science and Technology Innovation Talent Support Program, No. RC200438; Tree Planting Program of Shengjing Hospital, No. M1595; and the Doctoral Start-up Foundation of Liaoning Province, No. 2022-BS-127.

**Conflict-of-interest statement:** All the authors report having no relevant conflicts of interest for this article.

**Open-Access:** This article is an open-access article that was selected by an in-house editor and fully peer-reviewed by external reviewers. It is distributed in accordance with the Creative Commons Attribution NonCommercial (CC BY-NC 4.0) license, which permits others to distribute, remix, adapt, build upon this work non-commercially, and license their derivative works on different terms, provided the original work is properly cited and the use is non-commercial. See: <https://creativecommons.org/Licenses/by-nc/4.0/>

**Country of origin:** China

**ORCID number:** Zi-Han Zhang 0000-0001-7636-9400; Jin-Tao Guo 0000-0001-5722-6359; Ying Xie 0000-0001-8226-4242; Si-Yu Sun 0000-0002-7308-0473.

**S-Editor:** Gong ZM

**L-Editor:** Filipodia

**P-Editor:** Chen YX

## REFERENCES

- Bianchi G, Charoenlap C, Cocchi S, Rani N, Campagnoni S, Righi A, Frisoni T, Donati DM. Clear cell sarcoma of soft tissue: a retrospective review and analysis of 31 cases treated at Istituto Ortopedico Rizzoli. *Eur J Surg Oncol* 2014; **40**: 505-510 [PMID: 24560887 DOI: 10.1016/j.ejso.2014.01.016]
- Enzinger FM. Clear-cell sarcoma of tendons and aponeuroses. An analysis of 21 cases. *Cancer* 1965; **18**: 1163-1174 [PMID: 14332545 DOI: 10.1002/1097-0142(196509)18:9<1163::aid-cnrc2820180916>3.0.co;2-0]
- Gonzaga MI, Grant L, Curtin C, Gootee J, Silberstein P, Voth E. The epidemiology and survivorship of clear cell sarcoma: a National Cancer Database (NCDB) review. *J Cancer Res Clin Oncol* 2018; **144**: 1711-1716 [PMID: 29961184 DOI: 10.1007/s00432-018-2693-6]
- Huang J, Luo RK, Du M, Zeng HY, Chen LL, Ji Y. Clear cell sarcoma of the pancreas: a case report and review of literature. *Int J Clin Exp Pathol* 2015; **8**: 2171-2175 [PMID: 25973121]
- Zambrano E, Reyes-Mugica M, Franchi A, Rosai J. An osteoclast-rich tumor of the gastrointestinal tract with features resembling clear cell sarcoma of soft parts: reports of 6 cases of a GIST simulator. *Int J Surg Pathol* 2003; **11**: 75-81 [PMID: 12754623 DOI: 10.1177/106689690301100202]
- Xiang H, Xiang W, Wang L. Primary clear cell-sarcoma of the pancreas: A case report. *Asian J Surg* 2023; **46**: 4842-4843 [PMID: 37308378 DOI: 10.1016/j.asjsur.2023.05.129]
- Wang J, Thway K. Clear cell sarcoma-like tumor of the gastrointestinal tract: an evolving entity. *Arch Pathol Lab Med* 2015; **139**: 407-412 [PMID: 25724038 DOI: 10.5858/arpa.2013-0547-RS]
- Sabaté JM, Fernández A, Torrubia S, Villanueva A, Monill JM. Clear cell sarcoma of the abdominal wall with peritoneal sarcomatosis: CT features. *Eur Radiol* 1999; **9**: 1550-1552 [PMID: 10525863 DOI: 10.1007/s003300050882]
- Liu YJ, Zou C, Wu YY. Metastatic clear cell sarcoma of the pancreas: A rare case report. *World J Clin Cases* 2024; **12**: 1448-1453 [PMID: 38576799 DOI: 10.12998/wjcc.v12.i8.1448]
- Ibrahim RM, Steenstrup Jensen S, Juel J. Clear cell sarcoma-A review. *J Orthop* 2018; **15**: 963-966 [PMID: 30210202 DOI: 10.1016/j.jor.2018.08.039]
- Zhang Y, Guo N, Shen N, Li K, Zheng J, Li T, Long F. Circulating tumor cells in clear cell sarcoma. *Br J Haematol* 2023; **201**: 1018 [PMID: 37096942 DOI: 10.1111/bjh.18803]
- Cortellini F, Carrara S, Fusaroli P. EUS-guided fine-needle biopsy for gastric submucosal tumors: Does one size fit all? *Endosc Ultrasound* 2022; **11**: 151-152 [PMID: 34755708 DOI: 10.4103/EUS-D-21-00095]
- Clark MA, Johnson MB, Thway K, Fisher C, Thomas JM, Hayes AJ. Clear cell sarcoma (melanoma of soft parts): The Royal Marsden Hospital experience. *Eur J Surg Oncol* 2008; **34**: 800-804 [PMID: 18042498 DOI: 10.1016/j.ejso.2007.10.006]
- Cornillie J, van Cann T, Wozniak A, Hompes D, Schöffski P. Biology and management of clear cell sarcoma: state of the art and future perspectives. *Expert Rev Anticancer Ther* 2016; **16**: 839-845 [PMID: 27253849 DOI: 10.1080/14737140.2016.1197122]
- Washimi K, Takagi M, Hisaoka M, Kawachi K, Takeyama M, Hiruma T, Narimatsu H, Yokose T. Clear cell sarcoma-like tumor of the gastrointestinal tract: A clinicopathological review. *Pathol Int* 2017; **67**: 534-536 [PMID: 28887884 DOI: 10.1111/pin.12573]
- De Beuckeleer LH, De Schepper AM, Vandevenne JE, Bloem JL, Davies AM, Oudkerk M, Hauben E, Van Marck E, Somville J, Vanel D, Steinbach LS, Guinebreteiere JM, Hogendoorn PC, Mooi WJ, Verstraete K, Zaloudek C, Jones H. MR imaging of clear cell sarcoma (malignant melanoma of the soft parts): a multicenter correlative MRI-pathology study of 21 cases and literature review. *Skeletal Radiol* 2000; **29**: 187-195 [PMID: 10855466 DOI: 10.1007/s002560050592]
- Hocar O, Le Cesne A, Berissi S, Terrier P, Bonvalot S, Vanel D, Auperin A, Le Pechoux C, Bui B, Coindre JM, Robert C. Clear cell sarcoma (malignant melanoma) of soft parts: a clinicopathologic study of 52 cases. *Dermatol Res Pract* 2012; **2012**: 984096 [PMID: 22693489 DOI: 10.1155/2012/984096]

- 18 **Coindre JM**, Hostein I, Terrier P, Bouvier-Labit C, Collin F, Michels JJ, Trassard M, Marques B, Ranchere D, Guillou L. Diagnosis of clear cell sarcoma by real-time reverse transcriptase-polymerase chain reaction analysis of paraffin embedded tissues: clinicopathologic and molecular analysis of 44 patients from the French sarcoma group. *Cancer* 2006; **107**: 1055-1064 [PMID: [16878328](#) DOI: [10.1002/encr.22099](#)]
- 19 **Ikuta K**, Nishida Y, Imagama S, Tanaka K, Ozaki T. The current management of clear cell sarcoma. *Jpn J Clin Oncol* 2023; **53**: 899-904 [PMID: [37451697](#) DOI: [10.1093/jjco/hyad083](#)]
- 20 **Potter AJ**, Dimitriou F, Karim RZ, Mahar A, Chan C, Long GV, Scolyer RA. Cutaneous clear cell sarcoma with an epidermal component mimicking melanoma. *Pathology* 2022; **54**: 369-371 [PMID: [34420793](#) DOI: [10.1016/j.pathol.2021.05.097](#)]
- 21 **Segawa K**, Sugita S, Aoyama T, Kubo T, Asanuma H, Sugawara T, Ito Y, Tsujiwaki M, Fujita H, Emori M, Hasegawa T. Detection of specific gene rearrangements by fluorescence in situ hybridization in 16 cases of clear cell sarcoma of soft tissue and 6 cases of clear cell sarcoma-like gastrointestinal tumor. *Diagn Pathol* 2018; **13**: 73 [PMID: [30219084](#) DOI: [10.1186/s13000-018-0752-6](#)]
- 22 **Li KK**, Goodall J, Goding CR, Liao SK, Wang CH, Lin YC, Hiraga H, Nojima T, Nagashima K, Schaefer KL, Lee KA. The melanocyte inducing factor MITF is stably expressed in cell lines from human clear cell sarcoma. *Br J Cancer* 2003; **89**: 1072-1078 [PMID: [12966428](#) DOI: [10.1038/sj.bjc.6601212](#)]
- 23 **Ozenberger BB**, Li L, Wilson ER, Lazar AJ, Barrott JJ, Jones KB. EWSR1::ATF1 Orchestrates the Clear Cell Sarcoma Transcriptome in Human Tumors and a Mouse Genetic Model. *Cancers (Basel)* 2023; **15** [PMID: [38136296](#) DOI: [10.3390/cancers15245750](#)]
- 24 **Park BM**, Jin SA, Choi YD, Shin SH, Jung ST, Lee JB, Lee SC, Yun SJ. Two cases of clear cell sarcoma with different clinical and genetic features: cutaneous type with BRAF mutation and subcutaneous type with KIT mutation. *Br J Dermatol* 2013; **169**: 1346-1352 [PMID: [23796270](#) DOI: [10.1111/bjd.12480](#)]
- 25 **Smrke A**, Frezza AM, Giani C, Somaiah N, Brahmi M, Czarnecka AM, Rutkowski P, Van der Graaf W, Baldi GG, Connolly E, Duffaud F, Huang PH, Gelderblom H, Bhadri V, Grimison P, Mahar A, Stacchiotti S, Jones RL. Systemic treatment of advanced clear cell sarcoma: results from a retrospective international series from the World Sarcoma Network. *ESMO Open* 2022; **7**: 100522 [PMID: [35717681](#) DOI: [10.1016/j.esmoop.2022.100522](#)]
- 26 **Schöffski P**, Wozniak A, Stacchiotti S, Rutkowski P, Blay JY, Lindner LH, Strauss SJ, Anthony A, Duffaud F, Richter S, Grünwald V, Leahy MG, Reichardt P, Sufliarsky J, van der Graaf WT, Sciort R, Debiec-Rychter M, van Cann T, Marréaud S, Lia M, Raveloarivahy T, Collette L, Bauer S. Activity and safety of crizotinib in patients with advanced clear-cell sarcoma with MET alterations: European Organization for Research and Treatment of Cancer phase II trial 90101 'CREATE'. *Ann Oncol* 2017; **28**: 3000-3008 [PMID: [28950372](#) DOI: [10.1093/annonc/mdx527](#)]
- 27 **Wagner AJ**, Goldberg JM, Dubois SG, Choy E, Rosen L, Pappo A, Geller J, Judson I, Hogg D, Senzer N, Davis IJ, Chai F, Waghorne C, Schwartz B, Demetri GD. Tivantinib (ARQ 197), a selective inhibitor of MET, in patients with microphthalmia transcription factor-associated tumors: results of a multicenter phase 2 trial. *Cancer* 2012; **118**: 5894-5902 [PMID: [22605650](#) DOI: [10.1002/encr.27582](#)]
- 28 **Galera M**, Álvarez R, Arregui M, Paniagua M, Álvarez A, González Crisostomo RA, Diazgranados A, Gutiérrez N, Calles A, Agra C. A Clear Cell Sarcoma Case: A Diagnostic and Treatment Challenge, with a Promising Response to Trabectedin. *Case Rep Oncol* 2023; **16**: 1542-1550 [PMID: [38074516](#) DOI: [10.1159/000534935](#)]
- 29 **Nakai T**, Imura Y, Tamiya H, Yamada S, Nakai S, Yasuda N, Kaneko K, Outani H, Takenaka S, Hamada K, Myoui A, Araki N, Ueda T, Itoh K, Yoshikawa H, Naka N. Trabectedin is a promising antitumor agent potentially inducing melanocytic differentiation for clear cell sarcoma. *Cancer Med* 2017; **6**: 2121-2130 [PMID: [28745431](#) DOI: [10.1002/cam4.1130](#)]
- 30 **Kawai A**, Hosono A, Nakayama R, Matsumine A, Matsumoto S, Ueda T, Tsuchiya H, Beppu Y, Morioka H, Yabe H; Japanese Musculoskeletal Oncology Group. Clear cell sarcoma of tendons and aponeuroses: a study of 75 patients. *Cancer* 2007; **109**: 109-116 [PMID: [17133413](#) DOI: [10.1002/encr.22380](#)]
- 31 **Mavrogenis A**, Bianchi G, Stavropoulos N, Papagelopoulos P, Ruggieri P. Clinicopathological features, diagnosis and treatment of clear cell sarcoma/melanoma of soft parts. *Hippokratia* 2013; **17**: 298-302 [PMID: [25031505](#)]
- 32 **Beane JD**, Yang JC, White D, Steinberg SM, Rosenberg SA, Rudloff U. Efficacy of adjuvant radiation therapy in the treatment of soft tissue sarcoma of the extremity: 20-year follow-up of a randomized prospective trial. *Ann Surg Oncol* 2014; **21**: 2484-2489 [PMID: [24756814](#) DOI: [10.1245/s10434-014-3732-4](#)]
- 33 **Fujiwara T**, Kunisada T, Nakata E, Mitsuhashi T, Ozaki T, Kawai A. Factors associated with survival in patients with clear cell sarcoma. *Bone Joint J* 2023; **105-B**: 1216-1225 [PMID: [37907082](#) DOI: [10.1302/0301-620X.105B11.BJJ-2022-0743.R3](#)]
- 34 **Marcrom S**, De Los Santos JF, Conry RM. Complete response of mediastinal clear cell sarcoma to pembrolizumab with radiotherapy. *Clin Sarcoma Res* 2017; **7**: 14 [PMID: [28725344](#) DOI: [10.1186/s13569-017-0079-1](#)]
- 35 **Gordon EM**, Chawla SP, Tellez WA, Younesi E, Thomas S, Chua-Alcala VS, Chomoyan H, Valencia C, Brigham DA, Moradkhani A, Quon D, Srikureja A, Wong SG, Tseng W, Federman N. SAINT: A Phase I/Expanded Phase II Study Using Safe Amounts of Ipilimumab, Nivolumab and Trabectedin as First-Line Treatment of Advanced Soft Tissue Sarcoma. *Cancers (Basel)* 2023; **15** [PMID: [36765863](#) DOI: [10.3390/cancers15030906](#)]
- 36 **Wetterwald L**, Riggi N, Kyriazoglou A, Dei Tos G, Dei Tos A, Digkila A. Clear cell sarcoma: state-of-the art and perspectives. *Expert Rev Anticancer Ther* 2023; **23**: 235-242 [PMID: [36811446](#) DOI: [10.1080/14737140.2023.2183846](#)]
- 37 **Kunisada T**, Nakata E, Fujiwara T, Hosono A, Takihira S, Kondo H, Ozaki T. Soft-tissue sarcoma in adolescents and young adults. *Int J Clin Oncol* 2023; **28**: 1-11 [PMID: [35084598](#) DOI: [10.1007/s10147-022-02119-7](#)]
- 38 **Gronchi A**, Miah AB, Dei Tos AP, Abecassis N, Bajpai J, Bauer S, Biagini R, Bielack S, Blay JY, Bolle S, Bonvalot S, Boukovinas I, Bovee JVMG, Boye K, Brennan B, Brodowicz T, Buonadonna A, De Álava E, Del Muro XG, Dufresne A, Eriksson M, Fagioli F, Fedenko A, Ferraresi V, Ferrari A, Frezza AM, Gasperoni S, Gelderblom H, Gouin F, Grignani G, Haas R, Hassan AB, Hecker-Nolting S, Hindi N, Hohenberger P, Joensuu H, Jones RL, Jungels C, Jutte P, Kager L, Kasper B, Kawai A, Kopeckova K, Krákorová DA, Le Cesne A, Le Grange F, Legius E, Leithner A, Lopez-Pousa A, Martin-Broto J, Merimsky O, Messiou C, Mir O, Montemurro M, Morland B, Morosi C, Palmerini E, Pantaleo MA, Piana R, Piperno-Neumann S, Reichardt P, Rutkowski P, Safwat AA, Sangalli C, Sbaraglia M, Scheipl S, Schöffski P, Sleijfer S, Strauss D, Strauss S, Sundby Hall K, Trama A, Unk M, van de Sande MAJ, van der Graaf WTA, van Houdt WJ, Frebourg T, Casali PG, Stacchiotti S; ESMO Guidelines Committee, EURACAN and GENTURIS. Soft tissue and visceral sarcomas: ESMO-EURACAN-GENTURIS Clinical Practice Guidelines for diagnosis, treatment and follow-up. *Ann Oncol* 2021; **32**: 1348-1365 [PMID: [34303806](#) DOI: [10.1016/j.annonc.2021.07.006](#)]



## Application of artificial intelligence in the diagnosis and treatment of Kawasaki disease

Yan Pan, Fu-Yong Jiao

**Specialty type:** Medicine, research and experimental

**Provenance and peer review:** Invited article; Externally peer reviewed.

**Peer-review model:** Single blind

**Peer-review report's classification**

**Scientific Quality:** Grade C

**Novelty:** Grade B

**Creativity or Innovation:** Grade C

**Scientific Significance:** Grade C

**P-Reviewer:** Singh A

**Received:** April 11, 2024

**Revised:** May 15, 2024

**Accepted:** June 4, 2024

**Published online:** August 16, 2024

**Processing time:** 84 Days and 23.1 Hours



**Yan Pan**, Department of Pediatrics, The First Affiliated Hospital of Yangtze University, Jingzhou 434000, Hubei Province, China

**Fu-Yong Jiao**, Shaanxi Kawasaki Disease Diagnosis and Treatment Center, Shaanxi Provincial People's Hospital, Xi'an 710000, Shaanxi Province, China

**Corresponding author:** Fu-Yong Jiao, MD, Research Scientist, Shaanxi Kawasaki Disease Diagnosis and Treatment Center, Shaanxi Provincial People's Hospital, No. 256 West Youyi Road, Xi'an 710000, Shaanxi Province, China. [3105089948@qq.com](mailto:3105089948@qq.com)

### Abstract

This editorial provides commentary on an article titled "Potential and limitations of ChatGPT and generative artificial intelligence (AI) in medical safety education" recently published in the *World Journal of Clinical Cases*. AI has enormous potential for various applications in the field of Kawasaki disease (KD). One is machine learning (ML) to assist in the diagnosis of KD, and clinical prediction models have been constructed worldwide using ML; the second is using a gene signal calculation toolbox to identify KD, which can be used to monitor key clinical features and laboratory parameters of disease severity; and the third is using deep learning (DL) to assist in cardiac ultrasound detection. The performance of the DL algorithm is similar to that of experienced cardiac experts in detecting coronary artery lesions to promoting the diagnosis of KD. To effectively utilize AI in the diagnosis and treatment process of KD, it is crucial to improve the accuracy of AI decision-making using more medical data, while addressing issues related to patient personal information protection and AI decision-making responsibility. AI progress is expected to provide patients with accurate and effective medical services that will positively impact the diagnosis and treatment of KD in the future.

**Key Words:** Artificial intelligence; Kawasaki disease; Diagnosis; Prediction; Image

©The Author(s) 2024. Published by Baishideng Publishing Group Inc. All rights reserved.

**Core Tip:** Artificial intelligence (AI) holds transformative potential in the diagnosis and treatment of Kawasaki Disease (KD). Utilizing machine learning algorithms, AI can analyze complex biomarkers to enhance diagnostic accuracy. Gene signal calculation tools can differentiate KD from similar inflammatory conditions, while deep learning algorithms can improve the precision of cardiac ultrasound detection. However, successful integration of AI into clinical practice requires addressing challenges such as data privacy, ethical considerations, and the need for robust, diverse datasets to ensure the reliability and accountability of AI systems.

**Citation:** Pan Y, Jiao FY. Application of artificial intelligence in the diagnosis and treatment of Kawasaki disease. *World J Clin Cases* 2024; 12(23): 5304-5307

**URL:** <https://www.wjgnet.com/2307-8960/full/v12/i23/5304.htm>

**DOI:** <https://dx.doi.org/10.12998/wjcc.v12.i23.5304>

## INTRODUCTION

Artificial intelligence (AI) is a sophisticated computational system that transcends the mere execution of pre-programmed instructions. AI systems possess the capacity to autonomously acquire knowledge from diverse datasets and make independent decisions. The pervasive utilization of the internet has facilitated the digitization of a vast array of resources. Moreover, the rise in smartphone usage and the growth of the “Internet of Things” have resulted in the quick gathering of information from people and electronic gadgets, which has contributed to the expansion of big data. Additionally, improvements in computer processing speeds have made it possible to analyze and handle large sets of data, which has enabled the creation of AI algorithms using vast amounts of data. This not only surpasses the limitations of conventional data analysis methods, but also has the ability to identify subtle data patterns that may elude human analysis, resulting in novel insights.

The rapid advancement of AI technology has ushered in a new era where its application is pervasive in various aspects of everyday life and business; it is widely used in various industries, such as commerce, weather prediction, and transportation, as well as in the medical field for tasks, such as automatic analysis of lung X-rays, bone age measurement, fracture diagnosis, and cancer diagnosis and treatment. While the healthcare sector is still in the early stages of incorporating AI technology compared to other industries, there is growing momentum for its development, and it is anticipated that AI will continue to expand across various fields in the future[1].

Kawasaki disease (KD), a systemic vasculitis with an unclear etiology, is the primary cause of acquired heart disease in developed countries[2]. The possibility of clinical similarities between KD and other conditions may lead to both KD being missed and misdiagnosed. Healthcare providers and scientists are currently focused on improving the accuracy and effectiveness of diagnosing KD. In this regard, AI is anticipated to serve as a valuable supplementary tool that has the potential to revolutionize KD management in practical clinical environments. This study presents several examples of how AI can be utilized in the realm of KD.

## POTENTIAL APPLICATIONS OF AI IN THE FIELD OF KD

### *Using machine learning to assist in KD diagnosis*

Machine learning (ML) is a branch of AI. The calculation method can acquire knowledge and predictions without relying on complex coding[3]. Portman *et al*[4] developed a blood biomarker group with high sensitivity and specificity for identifying children with KD. Blood samples were obtained from a single-center cohort of children with KD ( $n = 50$ ) and control children ( $n = 100$ ), and 11 candidates were selected to develop biomarkers according to the principle of clinical availability. ML was used to identify the 11 blood markers. The values for these markers were included in the model. The model provided a binary predictive risk score for KD as determined by the Youden index. The area under the final receiver operating characteristic curve (AUC) was 0.94 (95%CI: 0.90–0.98). Of the 97 non-KD patients 88 were diagnosed as negative, and of the 50 KD-positive patients 47 were diagnosed as positive. The sensitivity was 0.94 (95%CI: 0.87–1.0), and the specificity was 0.91 (95%CI: 0.85–0.96). When the biomarkers were reduced to three, C-reactive protein, NT pro-type natriuretic peptide, and thyroid hormone, the AUC of the prediction model was 0.92 (95%CI: 0.87–0.96), and the sensitivity and specificity were 86%. However, the generalizability of the research results is limited by its single-center design, small cohort size, and potential deviation from the control group[4]. Liu *et al*[5] conducted a retrospective study in China on 1398 KD patients hospitalized in seven hospitals affiliated with Chongqing Medical University from January 2015 to August 2020, and a prediction model was built based on the ML algorithm. A total of 1240 of the 1398 patients responded to intravenous immunoglobulin G (IVIG), while 158 were resistant to IVIG. According to the results of the logistic regression analysis of the training set, four independent risk factors were identified: total bilirubin [odds ratio (OR) = 1.115, 95%CI: 1.067–1.165], procalcitonin (OR = 1.511, 95%CI: 1.270–1.798), alanine aminotransferase (OR = 1.013, 95%CI: 1.008–1.018) and platelet count (OR = 0.998, 95%CI: 0.996–1). Using the ML algorithm to construct the KD prediction model, the model performed well in terms of sensitivity, specificity, and AUC. The results of this study can help clinicians predict IVIG-resistant KD early and adjust treatment plans over time[5]. Wang *et al*[6] retrospectively

collected the medical records of KD patients hospitalized at Fujian Maternal and Child Health Hospital from March 2013 to June 2019 using the electronic medical record system. The results showed that platelet count, blood calcium level, albumin-to-globulin ratio, days of fever before hospitalization, and body weight were predictive factors for IVIG-resistant KD. The AUC of this model was 0.74 (95%CI: 0.87–0.96), the sensitivity was 30%, and the specificity was 99%[6]. A retrospective cross-sectional study can assist ML study, but because the patient's condition is constantly changing, there may be some errors in judging from a single cross-sectional study.

### **Using the gene signal calculation toolbox to assist in identifying KD**

Ghosh *et al*[7] used the gene signal calculation toolbox (two types of gene signals developed in the context of a new coronal pneumonia infection, VIP/SVIP signal) to compare children with multiple system inflammatory syndrome (MIS-C) and KD. Using VIP/SVIP signals and 13 transcriptional signals to diagnose KD, they verified that KD and MIS-C were on the same host immune response continuum and that both were concentrated in the cytokine storm centered on IL15/IL15RA, indicating that there was a common immune pathogenesis between the two factors. However, they differed in other laboratory parameters (left ventricular ejection fraction, C-reactive protein, white blood cell count, and lymphocyte count) and cardiac phenotypes (cardiac function decline and coronary artery expansion). The VIP signal revealed the unique targeting cytokine pathway of MIS-c. SVIP signals indicated disease severity, and the signal in MIS-c was stronger than that in KD, indicating that the MIS-c condition was more serious than KD. Key clinical features (cardiac function decline) and laboratory parameters (thrombocytopenia and eosinophilia) can be used to monitor disease severity[7–9].

### **Using deep learning to assist cardiac ultrasound detection**

The workload of medical image labeling and manual interpretation is large and primarily depends on the expertise of professional doctors. In addition, there are limitations, such as misdiagnosis, missed diagnosis, and time consumption. The recent and continuous development of AI and big data has made computer-aided diagnosis possible. Compared to the traditional inspection mode, deep learning (DL) does not require significant preprocessing or manual feature extraction. It can automatically extract features that are difficult for humans to distinguish without losing information and realize end-to-end learning. This shows great potential for complex recognition of subtle patterns. Because the contour of echocardiography is not clear and the speckle noise is large, traditional manual segmentation is time consuming and error prone; an automatic segmentation algorithm based on DL can solve this problem. Incomplete KD is often misdiagnosed because of the lack of clinical manifestations of typical KD[10]. However, it was also associated with a significantly higher prevalence of coronary artery disease. It is important to identify coronary artery lesions using echocardiography for timely diagnosis and a good prognosis of KD. They obtained coronary artery images of children through echocardiography (KD,  $n = 138$ ; pneumonia,  $n = 65$ ) and used the collected data to train six DL networks (vgg19, xception, resnet50, resnext50, Se resnet50, and Se resnext50). Se-resnext50 shows the best performance in terms of classification, specificity, and accuracy. The accuracy, sensitivity, and specificity of Se resnext50 were 81.12%, 84.06%, and 58.46%, respectively. Research results have shown that the DL algorithm performs similarly to experienced cardiologists in detecting coronary artery lesions to promote the diagnosis of KD[11]. DL can guide untrained novices in diagnosing cardiac ultrasound to assess the size, function, and pericardial effusion of the left and right ventricles[12]. It has great application value in remote areas where resources are scarce; however, its safety and stability still need to be further verified.

## **RISKS OF AI UTILIZATION**

The primary obstacle hindering the clinical implementation of AI by clinicians is accountability. Controversies arise in assigning responsibility when the use of AI algorithms by pediatricians in clinical settings leads to misdiagnosis or unforeseen adverse reactions. The creation of AI algorithms involves multiple stakeholders, including clinical physicians, developers, data managers, and healthcare institutions. Therefore, it is crucial to determine the root causes of errors or defects and identify the specific timing and content of their occurrences to determine the responsibility when problems arise. Additionally, the need for a reproducibility assessment of the results generated from AI-driven studies is critical, especially in studies utilizing techniques such as DL on large datasets acquired across different institutions. This ensures that AI systems are not only effective, but also reliable and consistent across various clinical environments. Reproducibility assessments help validate the robustness of AI algorithms and their applicability to diverse patient populations and settings. Specifically, the development of AI systems requires access to large amounts of medical data. However, only essential data relevant to the intended purpose should be collected and utilized. Given the sensitivity of personal health information involved in AI development, obtaining appropriate legal authorization for data processing and ensuring that security measures are in place is essential.

## **CONCLUSION**

This study explored the use of AI in the diagnosis of KD. In addition to the applications discussed in this study, AI has several other potential applications. Before the actual implementation, it is necessary to improve the efficacy of AI algorithms through the accumulation of data from different healthcare institutions for AI training. Furthermore, to effectively integrate AI into KD management, comprehensive guidelines must be established to address patient privacy

concerns during the data collection process and the ethical and legal obligations associated with AI system decisions. It is expected that the real-world challenges associated with AI integration will gradually be addressed in the future. This will have a transformative impact on the treatment and delivery of medical services for patients with KD.

## FOOTNOTES

**Author contributions:** Jiao FY designed the study; Pan Y edited the manuscript significantly; Pan Y reviewed literature and provided input in writing the paper.

**Conflict-of-interest statement:** There is no conflict of interest associated with any of the senior authors or other coauthors who contributed their efforts to this manuscript.

**Open-Access:** This article is an open-access article that was selected by an in-house editor and fully peer-reviewed by external reviewers. It is distributed in accordance with the Creative Commons Attribution NonCommercial (CC BY-NC 4.0) license, which permits others to distribute, remix, adapt, build upon this work non-commercially, and license their derivative works on different terms, provided the original work is properly cited and the use is non-commercial. See: <https://creativecommons.org/licenses/by-nc/4.0/>

**Country of origin:** China

**ORCID number:** Yan Pan 0000-0003-0240-7085; Fu-Yong Jiao 0000-0002-8306-2543.

**S-Editor:** Liu H

**L-Editor:** Filipodia

**P-Editor:** Chen YX

## REFERENCES

- 1 Wang X, Liu XQ. Potential and limitations of ChatGPT and generative artificial intelligence in medical safety education. *World J Clin Cases* 2023; **11**: 7935-7939 [PMID: 38073698 DOI: 10.12998/wjcc.v11.i32.7935]
- 2 Jiao F, Jindal AK, Pandiarajan V, Khubchandani R, Kamath N, Sabui T, Mondal R, Pal P, Singh S. The emergence of Kawasaki disease in India and China. *Glob Cardiol Sci Pract* 2017; **2017**: e201721 [PMID: 29564342 DOI: 10.21542/gcsp.2017.21]
- 3 Kaul V, Enslin S, Gross SA. History of artificial intelligence in medicine. *Gastrointest Endosc* 2020; **92**: 807-812 [PMID: 32565184 DOI: 10.1016/j.gie.2020.06.040]
- 4 Portman MA, Magaret CA, Barnes G, Peters C, Rao A, Rhyne R. An Artificial Intelligence Derived Blood Test to Diagnose Kawasaki Disease. *Hosp Pediatr* 2023; **13**: 201-210 [PMID: 36775804 DOI: 10.1542/hpeds.2022-006868]
- 5 Liu J, Zhang J, Huang H, Wang Y, Zhang Z, Ma Y, He X. A Machine Learning Model to Predict Intravenous Immunoglobulin-Resistant Kawasaki Disease Patients: A Retrospective Study Based on the Chongqing Population. *Front Pediatr* 2021; **9**: 756095 [PMID: 34820343 DOI: 10.3389/fped.2021.756095]
- 6 Wang T, Liu G, Lin H. A machine learning approach to predict intravenous immunoglobulin resistance in Kawasaki disease patients: A study based on a Southeast China population. *PLoS One* 2020; **15**: e0237321 [PMID: 32853226 DOI: 10.1371/journal.pone.0237321]
- 7 Ghosh P, Katkar GD, Shimizu C, Kim J, Khandelwal S, Tremoulet AH, Kanegaye JT; Pediatric Emergency Medicine Kawasaki Disease Research Group; Bocchini J, Das S, Burns JC, Sahoo D. An Artificial Intelligence-guided signature reveals the shared host immune response in MIS-C and Kawasaki disease. *Nat Commun* 2022; **13**: 2687 [PMID: 35577777 DOI: 10.1038/s41467-022-30357-w]
- 8 Zhong H, Lv X, Sun X, Jiao W. Progress in the Diagnosis and Treatment of Kawasaki Disease and Other Multi-system Inflammatory Syndromes by Artificial Intelligence. *IJTDH* 2023; **44**: 52-57 [DOI: 10.9734/ijtdh/2023/v44i51408]
- 9 Zhong H, Sun X, Lv X, Jiao W. Advances in the Co-Host Immune Response to Multisystem Inflammatory Syndrome and Kawasaki Disease in Children with AI-Guided Features. *IJTDH* 2023; **44**: 51-58 [DOI: 10.9734/ijtdh/2023/v44i61415]
- 10 Zhong HP, Zhang YQ, Jiao W. A Short Review of Coronary Artery Lesions in Children. *IJTDH* 2023; **44**: 1-8 [DOI: 10.9734/ijtdh/2023/v44i131447]
- 11 Lee H, Eun Y, Hwang JY, Eun LY. Explainable Deep Learning Algorithm for Distinguishing Incomplete Kawasaki Disease by Coronary Artery Lesions on Echocardiographic Imaging. 2021 Preprint [DOI: 10.2196/preprints.27053]
- 12 Narang A, Bae R, Hong H, Thomas Y, Surette S, Cadieu C, Chaudhry A, Martin RP, McCarthy PM, Rubenson DS, Goldstein S, Little SH, Lang RM, Weissman NJ, Thomas JD. Utility of a Deep-Learning Algorithm to Guide Novices to Acquire Echocardiograms for Limited Diagnostic Use. *JAMA Cardiol* 2021; **6**: 624-632 [PMID: 33599681 DOI: 10.1001/jamacardio.2021.0185]



## Understanding the etiology of mental health problems in post-rehabilitation COVID-19 patients: Insights and strategies for effective intervention

Hai-Sheng Hu, Bao-Qing Sun

**Specialty type:** Medicine, research and experimental

**Provenance and peer review:** Invited article; Externally peer reviewed.

**Peer-review model:** Single blind

**Peer-review report's classification**

**Scientific Quality:** Grade C

**Novelty:** Grade B

**Creativity or Innovation:** Grade B

**Scientific Significance:** Grade B

**P-Reviewer:** Nambi G, Saudi Arabia

**Received:** April 19, 2024

**Revised:** May 22, 2024

**Accepted:** June 3, 2024

**Published online:** August 16, 2024

**Processing time:** 77 Days and 2.6 Hours



**Hai-Sheng Hu**, Guangzhou Respiratory Health Research Institute, The First Affiliated Hospital of Guangzhou Medical University, Guangzhou 510120, Guangdong Province, China

**Bao-Qing Sun**, Department of Clinical Laboratory, The First Affiliated Hospital of Guangzhou Medical University, Guangzhou 510120, Guangdong Province, China

**Corresponding author:** Bao-Qing Sun, PhD, Professor, Department of Clinical Laboratory, The First Affiliated Hospital of Guangzhou Medical University, No. 28 Qiaozhong Middle Road, Guangzhou 510120, Guangdong Province, China. [sunbaoqing@vip.163.com](mailto:sunbaoqing@vip.163.com)

### Abstract

In this editorial, we comment on an article by Alhammad *et al* that was published in a recent issue of the *World Journal of Clinical Cases* (Manuscript No.: 91134). We specifically focus on the mental health problems caused by coronavirus disease 2019 (COVID-19), their mechanisms, and targeted rehabilitation strategies. Severe acute respiratory syndrome coronavirus 2, *via* its spike protein, binds to angiotensin-converting enzyme 2 and other receptors prior to infiltrating diverse cells within the central nervous system, including endothelial cells, neurons, astrocytes, and oligodendrocytes, thereby contributing to the development of mental illnesses. Epidemiological data from 2020 underscored the global upsurge in major depressive and anxiety disorders by 27.6% and 25.6%, respectively, during the pandemic. The commented research show that 30% of post-intensive care unit discharge patients with COVID-19 in the Arabic region exhibited Hospital Anxiety and Depression Scale scores that were indicative of anxiety and depression. While acknowledging psychosocial factors, such as grief and loss, it is crucial to recognize the potential neurological impact of the virus through various mechanisms. Accordingly, interventions that encompass dietary measures, health supplements, and traditional Chinese medicine with neuroprotective properties are necessary. This editorial underscores the urgency to implement comprehensive rehabilitation approaches to address the intricate interplay between COVID-19 and mental well-being.

**Key Words:** COVID-19; Mental health; Rehabilitation therapy; Chronic COVID-19 syndrome; Social medicine

**Core Tip:** Epidemiological data from 2020 have revealed a worldwide escalation in major depressive disorders by 27.6% and in anxiety disorders by 25.6% amid the coronavirus disease 2019 (COVID-19) pandemic. The prevalence of mental health issues among patients with COVID-19 after rehabilitation is on the rise and is potentially linked to bereavement or the neurological impact of the virus. Implementing dietary interventions, health supplements, and traditional Chinese medicines with neuroprotective properties is imperative to safeguard the nervous systems of these individuals and improve their mental well-being.

**Citation:** Hu HS, Sun BQ. Understanding the etiology of mental health problems in post-rehabilitation COVID-19 patients: Insights and strategies for effective intervention. *World J Clin Cases* 2024; 12(23): 5308-5312

**URL:** <https://www.wjgnet.com/2307-8960/full/v12/i23/5308.htm>

**DOI:** <https://dx.doi.org/10.12998/wjcc.v12.i23.5308>

## INTRODUCTION

Severe acute respiratory syndrome coronavirus 2 (SARS-CoV-2), originating in December 2019, is an RNA virus classified within the coronavirus family. Its entry into the body is facilitated by the spike protein (S protein), which binds to the angiotensin-converting enzyme 2 and other receptors. This enables the virus to infiltrate a variety of cells within the central nervous system (CNS), including endothelial cells, neurons, astrocytes, and oligodendrocytes[1]. This broad cellular invasion has profound implications on the host. Evidence suggests that infection of these CNS-resident cells may lead to enduring consequences and potentially contribute to the development of neurodegenerative disorders over time [2]. Epidemiological data from 2020 revealed a global surge in patients with major depressive disorders by 27.6% and in anxiety disorders by 25.6% amidst the pandemic[3]. Furthermore, a survey that involved 402 coronavirus disease 2019 (COVID-19) survivors indicated varying rates of posttraumatic stress disorder, depression, anxiety, obsessive-compulsive symptoms, and insomnia, with percentages reaching as high as 42% for anxiety[4]. Neurological symptoms, including headache, altered consciousness, and paresthesia, have been documented in 36.4% of patients with COVID-19, particularly among the severely affected[5]. The neurological impact is notably high, reaching levels up to 88% in severely infected individuals[6]. Autopsy findings have revealed brain tissue edema and neuronal degeneration. The Beijing Ditan Hospital reported a case of viral encephalitis induced by SARS-CoV-2 attacking the CNS[7]. Additionally, genome sequencing has confirmed the presence of the virus in cerebrospinal fluid (CSF), which highlights the potential of COVID-19 to inflict nervous system damage[8]. The study of interest showed that 30% of patients with COVID-19 in the Arabic region exhibited Hospital Anxiety and Depression scales scores that reflect anxiety and depression following discharge from the intensive care unit[9]. This underscores the importance of analyzing the potential causes of poor mental health of and offering rehabilitation recommendations for patients with COVID-19.

## INFLUENCING FACTORS AND POSSIBLE MECHANISMS OF POOR MENTAL HEALTH IN PATIENTS WITH COVID-19

Years of trauma research indicate that, following negative life events, such as loss or exposure to disasters, most individuals experience either resilience, where there is minimal impact on symptoms of anxiety or depression, or recovery, marked by an initial increase in symptoms followed by improvement[10]. This trend aligns with the findings of extensive studies conducted during the COVID-19 pandemic. During this period, anxiety and depression symptoms peaked, likely as an acute response to an unforeseen crisis[11]. Therefore, we cannot rule out the possibility that the patients included in the study may have experienced mental health problems due to excessive longing or sadness caused by the passing of family or friends.

However, perturbations in the immune system triggered by an infection can also lead to psychopathological symptoms, as evidenced by past coronavirus outbreaks[12]. In a study conducted in India, postmortem examinations of the brains of rhesus and cynomolgus macaques following pulmonary disease induced by SARS-CoV-2 revealed T cell infiltration and microglial activation[13]. Damage to the immune system can diminish the ability of the nerve tissues to resist pathogen invasion and efficiently clear harmful substances, potentially resulting in mental health problems. Viral infections can also directly affect neurological function and potentially cause severe neurological damage. SARS-CoV-2 has been found to possess neurotropic properties and can induce neurological diseases. Evidence suggests that coronaviruses can be detected in the brain or colony-stimulating factor, thus potentially leading to psychopathological sequelae through direct infection of the CNS or indirectly *via* immune responses[14]. Various studies, including clinical observations, post-mortem analyses, animal experiments, and *in vitro* studies, have highlighted the neurotropic potential of coronaviruses and their ability to cause neuronal injury[15]. Additionally, research by Dantzer[16] suggests that the immune response to coronaviruses, characterized by a "cytokine storm," may contribute to psychiatric symptoms by

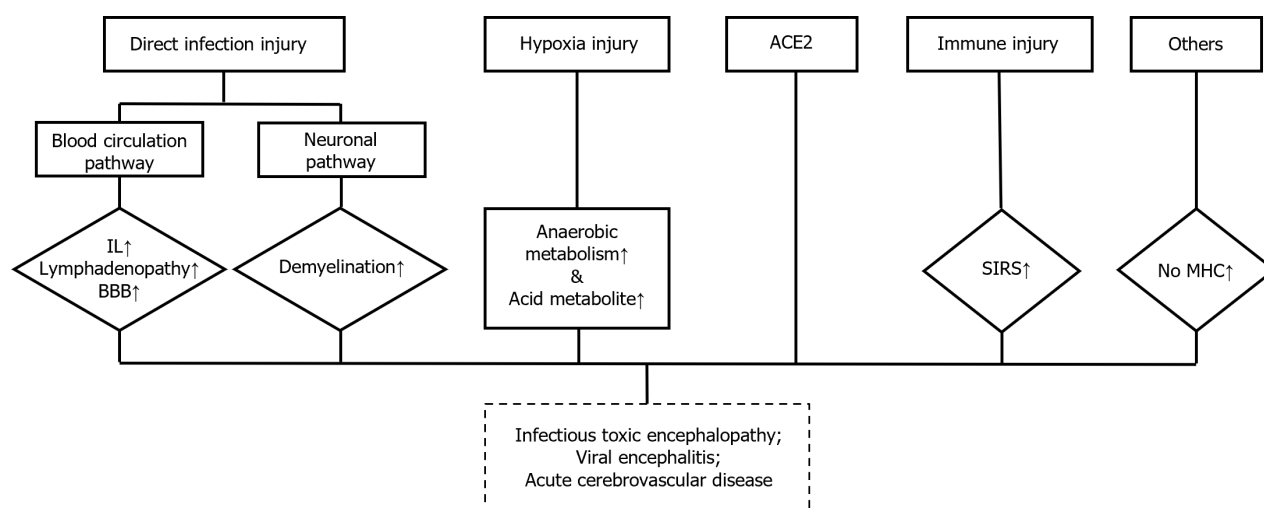


**Figure 1** Viral infections can directly cause imbalances in the circulatory system, such as increased interleukin release, lymphatic system disruption, and increased blood-brain barrier permeability. Additionally, infections can directly cause neuronal demyelination, potentially leading to mental health problems and inflammatory brain diseases. Moreover, the hypoxia induced by severe coronavirus disease 2019 can elevate anaerobic and acid metabolite levels, thus further affecting the nervous system. Additionally, viruses can infiltrate the brain through angiotensin converting enzyme-2 (ACE2) receptors, thereby disrupting the immune environment and causing damage. BBB: Blood-brain barrier; IL: Interleukin; MHC: Major histocompatibility complex; SIRS: Systemic inflammatory response syndrome.

triggering neuroinflammation. A possible mechanism for this is shown in [Figure 1](#). Furthermore, preliminary findings suggest that SARS-CoV-2 instigates molecular and cellular alterations akin to those observed in Alzheimer's disease[17]. Another study indicates that neurotoxic amyloidogenic peptides derived from SARS-CoV-2 could be responsible for triggering neurological symptoms in patients with COVID-19[18], such as  $\alpha$ -synuclein aggregates, which are involved in Parkinson's disease[19]. Moreover, a study from the United States suggested that SARS-CoV-2-infected mice displayed respiratory symptoms exhibiting increased expression of cytokines and chemokines, CCL11, in their CSF, resulting in hippocampal microglia activation. Subsequently, leading to impaired neurogenesis and loss of oligodendrocytes and myelinated axons[20]. Therefore, patients with severe clinical symptoms are more likely to experience mental-health problems.

## APPROPRIATE REHABILITATION TREATMENT IS FEASIBLE

Those with mental problems after a COVID-19 diagnosis should follow doctors' advice regarding the reasonable use of psychotherapeutic drugs during the recovery period[21]. Herein, we discuss the prevention of mental illness in convalescent patients with COVID-19 who are mentally healthy or in a sub-healthy state. Research has shown that *Hericium erinaceus* contains erinacines and hericenones, which stimulate the release of nerve growth factors, regulate inflammatory processes, reduce oxidative stress, protect nerve cells from apoptosis, and can be used as a functional food [22]. In addition, the products of some health care companies can also be used to prevent mental problems in patients with COVID-19 after rehabilitation, such as Sour jujube kernel  $\gamma$ -aminobutyric acid tablets (nutrilite®) and Broken wall Ganoderma spore powder (nutrilite®). Prior studies have shown that traditional Chinese medicine has significant efficacy in protecting the nervous system. The research of Liu *et al*[23] showed that Panax ginseng (Meyer) and Panax notoginseng (Burkill) contain important bioactive ingredients such as ginsenosides and exert multiple pharmacological effects on the nervous system and immune diseases. Therefore, these methods can be used to improve the prognosis of patients with COVID-19 and effectively reduce the occurrence of mental diseases.

## CONCLUSION

In general, mental illness or mental health issues are increasing in patients with COVID-19 after rehabilitation, which may be related to the loss of relatives or invasion of the nervous system of patients with COVID-19. Therefore, it is necessary to perform psychological rehabilitation for patients with COVID-19.

## ACKNOWLEDGEMENTS

We express our gratitude to Dr. Hong W, Marketing Manager Kuang Junjie, and Professor He YZ from Amway for their suggestions on relevant health products.

## FOOTNOTES

**Author contributions:** Hu HS and Sun BQ contributed to this study; Sun BQ designed the overall concept and outline of the manuscript; Hu HS contributed to the discussion and design of the manuscript; Hu HS and Sun BQ contributed to the writing and editing of the manuscript, illustrations, and literature review.

**Supported by** Guangzhou Laboratory Emergency Research Project, No. EKPG21-302.

**Conflict-of-interest statement:** The authors have no conflicts of interest related to this study or its publication.

**Open-Access:** This article is an open-access article that was selected by an in-house editor and fully peer-reviewed by external reviewers. It is distributed in accordance with the Creative Commons Attribution NonCommercial (CC BY-NC 4.0) license, which permits others to distribute, remix, adapt, build upon this work non-commercially, and license their derivative works on different terms, provided the original work is properly cited and the use is non-commercial. See: <https://creativecommons.org/licenses/by-nc/4.0/>

**Country of origin:** China

**ORCID number:** Hai-Sheng Hu 0000-0001-7873-6956; Bao-Qing Sun 0000-0002-1671-0723.

**S-Editor:** Gao CC

**L-Editor:** Filipodia

**P-Editor:** Chen YX

## REFERENCES

- Jackson CB, Farzan M, Chen B, Choe H. Mechanisms of SARS-CoV-2 entry into cells. *Nat Rev Mol Cell Biol* 2022; **23**: 3-20 [PMID: 34611326 DOI: 10.1038/s41580-021-00418-x]
- Weissert R. Nervous system-related tropism of SARS-CoV-2 and autoimmunity in COVID-19 infection. *Eur J Immunol* 2024; **54**: e2250230 [PMID: 37733584 DOI: 10.1002/eji.202250230]
- Daly M, Robinson E. Depression and anxiety during COVID-19. *Lancet* 2022; **399**: 518 [PMID: 35123689 DOI: 10.1016/S0140-6736(22)00187-8]
- Mazza MG, De Lorenzo R, Conte C, Poletti S, Vai B, Bollettini I, Melloni EMT, Furlan R, Ciceri F, Rovere-Querini P; COVID-19 BioB Outpatient Clinic Study group, Benedetti F. Anxiety and depression in COVID-19 survivors: Role of inflammatory and clinical predictors. *Brain Behav Immun* 2020; **89**: 594-600 [PMID: 32738287 DOI: 10.1016/j.bbi.2020.07.037]
- Mao L, Jin H, Wang M, Hu Y, Chen S, He Q, Chang J, Hong C, Zhou Y, Wang D, Miao X, Li Y, Hu B. Neurologic Manifestations of Hospitalized Patients With Coronavirus Disease 2019 in Wuhan, China. *JAMA Neurol* 2020; **77**: 683-690 [PMID: 32275288 DOI: 10.1001/jamaneurol.2020.1127]
- Iroegbu JD, Ifenatuoha CW, Ijomone OM. Potential neurological impact of coronaviruses: implications for the novel SARS-CoV-2. *Neurol Sci* 2020; **41**: 1329-1337 [PMID: 32424503 DOI: 10.1007/s10072-020-04469-4]
- Zhu N, Zhang D, Wang W, Li X, Yang B, Song J, Zhao X, Huang B, Shi W, Lu R, Niu P, Zhan F, Ma X, Wang D, Xu W, Wu G, Gao GF, Tan W; China Novel Coronavirus Investigating and Research Team. A Novel Coronavirus from Patients with Pneumonia in China, 2019. *N Engl J Med* 2020; **382**: 727-733 [PMID: 31978945 DOI: 10.1056/NEJMoa2001017]
- Scheuermeier M, Chaves KQ, Marin-Sanabria D, Acosta-Lazo H, Ulate-Campos A. First Pediatric Case of Autoimmune Encephalitis Associated With COVID-19 in Costa Rica. *Cureus* 2022; **14**: e30616 [PMID: 36426346 DOI: 10.7759/cureus.30616]
- Alhammad AM, Aldardeer NF, Alqahtani A, Aljawadi MH, Alnefaie B, Alonazi R, Almuqbil M, Alsaadon A, Alqahtani RM, Alballa R, Alshehri B, Alarifi MI, Alosaimi FD. Mental health status among COVID-19 patients survivors of critical illness in Saudi Arabia: A 6-month follow-up questionnaire study. *World J Clin Cases* 2024; **12**: 2560-2567 [DOI: 10.12998/wjcc.v12.i15.2560]
- Chen S, Bonanno GA. Psychological adjustment during the global outbreak of COVID-19: A resilience perspective. *Psychol Trauma* 2020; **12**: S51-S54 [PMID: 32538658 DOI: 10.1037/tra0000685]
- Robinson E, Sutin AR, Daly M, Jones A. A systematic review and meta-analysis of longitudinal cohort studies comparing mental health before vs during the COVID-19 pandemic in 2020. *J Affect Disord* 2022; **296**: 567-576 [PMID: 34600966 DOI: 10.1016/j.jad.2021.09.098]
- Hossain MM, Tasnim S, Sultana A, Faizah F, Mazumder H, Zou L, McKyer ELJ, Ahmed HU, Ma P. Epidemiology of mental health problems in COVID-19: a review. *F1000Res* 2020; **9**: 636 [PMID: 33093946 DOI: 10.12688/f1000research.24457.1]
- Philippens IHCHM, Böszörményi KP, Wubben JAM, Fagrouch ZC, van Driel N, Mayenburg AQ, Lozovaglia D, Roos E, Schurink B, Bugiani M, Bontrop RE, Middeldorp J, Bogers WM, de Geus-Oei LF, Langermans JAM, Verschoor EJ, Stammes MA, Verstrepen BE. Brain Inflammation and Intracellular  $\alpha$ -Synuclein Aggregates in Macaques after SARS-CoV-2 Infection. *Viruses* 2022; **14** [PMID: 35458506 DOI: 10.3390/v14040776]
- Wu Y, Xu X, Chen Z, Duan J, Hashimoto K, Yang L, Liu C, Yang C. Nervous system involvement after infection with COVID-19 and other coronaviruses. *Brain Behav Immun* 2020; **87**: 18-22 [PMID: 32240762 DOI: 10.1016/j.bbi.2020.03.031]
- Desforges M, Le Coupanec A, Dubeau P, Bourgouin A, Lajoie L, Dubé M, Talbot PJ. Human Coronaviruses and Other Respiratory Viruses: Underestimated Opportunistic Pathogens of the Central Nervous System? *Viruses* 2019; **12** [PMID: 31861926 DOI: 10.3390/v12010014]
- Dantzer R. Neuroimmune Interactions: From the Brain to the Immune System and Vice Versa. *Physiol Rev* 2018; **98**: 477-504 [PMID: 29351513 DOI: 10.1152/physrev.00039.2016]
- Shen WB, Elahi M, Logue J, Yang P, Baracco L, Reece EA, Wang B, Li L, Blanchard TG, Han Z, Rissman RA, Frieman MB, Yang P. SARS-CoV-2 invades cognitive centers of the brain and induces Alzheimer's-like neuropathology. *bioRxiv* 2022 [PMID: 35132414 DOI: 10.1101/2022.01.31.478476]
- Charnley M, Islam S, Bindra GK, Engwirda J, Ratcliffe J, Zhou J, Mezzenga R, Hulett MD, Han K, Berryman JT, Reynolds NP. Neurotoxic

- amyloidogenic peptides in the proteome of SARS-COV2: potential implications for neurological symptoms in COVID-19. *Nat Commun* 2022; **13**: 3387 [PMID: [35697699](#) DOI: [10.1038/s41467-022-30932-1](#)]
- 19 **Brundin P**, Nath A, Beckham JD. Is COVID-19 a Perfect Storm for Parkinson's Disease? *Trends Neurosci* 2020; **43**: 931-933 [PMID: [33158605](#) DOI: [10.1016/j.tins.2020.10.009](#)]
- 20 **Fernández-Castañeda A**, Lu P, Geraghty AC, Song E, Lee MH, Wood J, O'Dea MR, Dutton S, Shamardani K, Nwangwu K, Mancusi R, Yalçın B, Taylor KR, Acosta-Alvarez L, Malacon K, Keough MB, Ni L, Woo PJ, Contreras-Esquivel D, Toland AMS, Gehlhausen JR, Klein J, Takahashi T, Silva J, Israelow B, Lucas C, Mao T, Peña-Hernández MA, Tabachnikova A, Homer RJ, Tabacof L, Tosto-Mancuso J, Breyman E, Kontorovich A, McCarthy D, Quezado M, Vogel H, Hefti MM, Perl DP, Liddelow S, Folkerth R, Putrino D, Nath A, Iwasaki A, Monje M. Mild respiratory COVID can cause multi-lineage neural cell and myelin dysregulation. *Cell* 2022; **185**: 2452-2468.e16 [PMID: [35768006](#) DOI: [10.1016/j.cell.2022.06.008](#)]
- 21 **Mueller JK**, Riederer P, Müller WE. Neuropsychiatric Drugs Against COVID-19: What is the Clinical Evidence? *Pharmacopsychiatry* 2022; **55**: 7-15 [PMID: [35079985](#) DOI: [10.1055/a-1717-2381](#)]
- 22 **Li TJ**, Lee TY, Lo Y, Lee LY, Li IC, Chen CC, Chang FC. Hericium erinaceus mycelium ameliorate anxiety induced by continuous sleep disturbance in vivo. *BMC Complement Med Ther* 2021; **21**: 295 [PMID: [34865649](#) DOI: [10.1186/s12906-021-03463-3](#)]
- 23 **Liu H**, Lu X, Hu Y, Fan X. Chemical constituents of Panax ginseng and Panax notoginseng explain why they differ in therapeutic efficacy. *Pharmacol Res* 2020; **161**: 105263 [PMID: [33127555](#) DOI: [10.1016/j.phrs.2020.105263](#)]



## Discharging patients home from the intensive care unit: A new trend

Esraa M Hassan, Abbas B Jama, Ahmed Sharaf, Asim Shaikh, Mohamad El Labban, Salim Surani, Syed A Khan

**Specialty type:** Medicine, research and experimental

**Provenance and peer review:** Invited article; Externally peer reviewed.

**Peer-review model:** Single blind

**Peer-review report's classification**

**Scientific Quality:** Grade B, Grade B

**Novelty:** Grade B, Grade B

**Creativity or Innovation:** Grade B, Grade B

**Scientific Significance:** Grade B, Grade B

**P-Reviewer:** Nagase T; Su C

**Received:** February 27, 2024

**Revised:** June 7, 2024

**Accepted:** June 28, 2024

**Published online:** August 16, 2024

**Processing time:** 128 Days and 14.6 Hours



**Esraa M Hassan, Abbas B Jama, Syed A Khan,** Department of Critical Care Medicine, Mayo Clinic Health system, Mankato, MN 56001, United States

**Ahmed Sharaf,** Department of Internal Medicine, Baptist Hospital of Southeast Texas, Beaumont, TX 77701, United States

**Asim Shaikh,** Department of Medicine, Aga Khan University, Karachi 74200, Sindh, Pakistan

**Mohamad El Labban,** Department of Internal Medicine, Mayo Clinic Health System, Mankato, MN 56001, United States

**Salim Surani,** Department of Medicine and Pharmacology, Texas A&M University, College Station, TX 77843, United States

**Salim Surani,** Department of Anaesthesiology, Mayo Clinic Health System, Rochester, MN 55905, United States

**Corresponding author:** Salim Surani, FACP, FCCP, MD, MHSc, Adjunct Professor, Department of Medicine and Pharmacology, Texas A&M University, 40 Bizzell Street, College Station, TX 77843, United States. [srsurani@hotmail.com](mailto:srsurani@hotmail.com)

### Abstract

Discharging patients directly to home from the intensive care unit (ICU) is becoming a new trend. This review examines the feasibility, benefits, challenges, and considerations of directly discharging ICU patients. By analyzing available evidence and healthcare professionals' experiences, the review explores the potential impacts on patient outcomes and healthcare systems. The practice of direct discharge from the ICU presents both opportunities and complexities. While it can potentially reduce costs, enhance patient comfort, and mitigate complications linked to extended hospitalization, it necessitates meticulous patient selection and robust post-discharge support mechanisms. Implementing this strategy successfully mandates the availability of home-based care services and a careful assessment of the patient's readiness for the transition. Through critical evaluation of existing literature, this review underscores the significance of tailored patient selection criteria and comprehensive post-discharge support systems to ensure patient safety and optimal recovery. The insights provided contribute evidence-based recommendations for refining the direct discharge approach, fostering improved patient outcomes, heightened satisfaction, and streamlined healthcare processes. Ultimately, the review seeks to balance patient-centered care and effective resource utilization within ICU discharge strategies.

**Key Words:** Intensive care unit; Critical care; Early discharge; Cost effective critical care; Patient comfort; Early recovery

©The Author(s) 2024. Published by Baishideng Publishing Group Inc. All rights reserved.

**Core Tip:** Intensive care unit (ICU) discharge without transferring to a lower dependency unit is gaining attention as an alternative to traditional discharge methods. This approach offers potential cost savings, increased patient comfort, and reduced complications associated with prolonged hospital stays. However, successful implementation requires careful patient selection and robust post-discharge support services. Establishing specific criteria for patient selection and ensuring comprehensive post-discharge care is crucial, ultimately balancing patient-centered care with efficient resource utilization in ICU discharge practices. The potential for early patient recovery and cost saving is magnanimous, as seen in recent studies.

**Citation:** Hassan EM, Jama AB, Sharaf A, Shaikh A, El Labban M, Surani S, Khan SA. Discharging patients home from the intensive care unit: A new trend. *World J Clin Cases* 2024; 12(23): 5313-5319

**URL:** <https://www.wjgnet.com/2307-8960/full/v12/i23/5313.htm>

**DOI:** <https://dx.doi.org/10.12998/wjcc.v12.i23.5313>

## INTRODUCTION

Discharging patients from the intensive care unit (ICU) is critical in their recovery journey. It signifies a transition from acute care to a lower level of dependency, allowing patients to regain functional independence. Conventionally, patients are transferred from the ICU to a lower dependency unit (LDU) before being discharged home[1]. The bridges the presence of the continuous monitoring and support of the ICU to the lack of it in the outpatient setting. However, growing interest is in exploring the feasibility of discharging ICU patients directly without an LDU transfer[2].

This review aims to research the practice of discharging ICU patients directly and examine the potential outcomes and feasibility of this approach[3]. By exploring the available evidence and considering the experiences of healthcare professionals[3,4].

Direct disposition from the ICU can potentially reduce costs, preserve patient comfort, and prevent complications of prolonged hospitalization. A strict selection criterion, robust post-discharge support systems, and the availability of home-based care services are crucial factors to consider in ensuring the safety and success of this discharge strategy[5].

By critically analyzing the existing literature, this review aims to provide evidence-based recommendations for implementing an effective discharge process from the ICU that maintains optimized patient clinical and social outcomes.

### Why discharge directly from the ICU

Discharging ICU patients directly presents several potential advantages. First, it reduces healthcare costs. By bypassing the LDU stay, healthcare resources such as beds, personnel, and equipment can be utilized more efficiently. This approach may contribute to cost savings, particularly in healthcare systems with limited resources and high demand for ICU beds[2,6], as well as surgical patients, where it can reduce Medicare costs significantly[2,4] and reduce monthly costs by 10000 USD on average[2,5].

Second, direct discharge allows for preserving patient comfort and familiarity. Familiar surroundings and the support of family and loved ones can contribute to emotional well-being and aid in the patient's recovery process[6].

Furthermore, direct discharge can potentially prevent potential complications associated with LDU stays, such as hospital-acquired infections, physical and occupational deconditioning, malnutrition, and delirium[7].

There are some challenges that complicate the direct-to-discharge process. First, appropriate patient selection criteria are crucial to ensure patient safety. Not all ICU patients would be suitable for direct home discharge, and the studies we looked at did not provide or have access to the providers reasoning behind why certain patients were directly discharged to home. However, they noted among the cohort that were discharged directly home, patients tended to have minimal invasive intervention (*i.e.*, mechanical ventilation) requirements ( $P < 0.001$ ), lack significant comorbidities, and did not require vasopressors, which is an indirect marker of severity of illness[3,8].

Direct discharge requires robust follow-up care, including access to healthcare professionals, monitoring, and assistance with activities of daily living. Establishing effective post-discharge support systems, such as home care services and outpatient clinics, is essential to address ongoing medical needs and ensure the patient's well-being[3].

Collaboration between the healthcare team and community-based care providers is necessary to facilitate a smooth transition and ensure continuity of care[6,9-12].

## PATIENT SELECTION CRITERIA

The current guidelines from the society of critical care medicine published in 2016, and much of the literature on this topic do not provide guidelines or specific patient selection criteria for discharging ICU patients. However, the society of

critical care medicine recommends following a standardized process and stipulating a specific discharge criterion in every ICU admission, discharge, and transfer[13]. One study evaluating direct discharging (DD) in 174 ICUs found that the likelihood of discharge for an identical patient varied by a factor of two-fold depending on the ICU[7]. They concluded that practice variations between ICUs are one of the strongest predictors for discharging patients from the ICU. Furthermore, in our review of the literature, it became apparent that there were factors intrinsic and extrinsic to the patient that determined whether the patient would be discharged from the ICU. Extrinsic factors included the number of beds available in the acute care ward, better social home support, and the location (*i.e.*, hospital ward, operating room) from which they were admitted to the ICU[3,14-15]. The intrinsic included age, sex, and comorbidities.

### Adult

When examining the literature for patient characteristics, patients who had DD tended to be younger, with Stelfox *et al*[3] finding the median age of patients to be 47 years ( $P < 0.001$ ) in the cohort that was DD[7]. Martin *et al*[7] found 64% greater odds of having DD if patients were 18-39 years of age compared to patients who were 80-105 years of age. DD patients from the ICU had few comorbidities and were less critically ill at the time of ICU admission[3,6]. Studies generally reported a Charlson morbidity index score of 0-1 [odds ratio (OR): 1.74; 95% confidence interval (CI): 1.63-1.85] or a median acute physiology and chronic health evaluation II score of 15 ( $P < 0.001$ ) for patients among the DD cohort[3, 7]. Men tended to make up most of the DD cohort, with Lau *et al*[2] reporting that 66.4% of the DD patient cohort they examined were male.

Most studies did not include data based on race or ethnicity; however, Patel *et al*[8] showed that the DD patient cohort was 87.9% white and black patients. ICU length of stay ranged from 2-4 days with an average of 2.41 days ( $P < 0.001$ ). Patients were often admitted with a diagnosis of overdose/withdrawal, seizures, day procedure, or a diabetic complication[2,3,7,8,16].

### Pediatric

Patients who had DD patients in the pediatric population were similar to the adult studies we reviewed in regard to patients' age. The median age was two years in most of the studies[14,17]. However, age was not statistically significant, with Pizzuto *et al*[14] reporting the same distribution in age for patients who were transferred to an acute care ward ( $P = 0.21$ ). Kennedy and Numa[17] reported that 66.4% of the DD patient cohort were male. Admitting or discharge diagnoses included asthma, bronchiolitis, respiratory failure, and ones similar to what we have seen in the adult population of seizures, intoxication, diabetic ketoacidosis, and post-operative/procedure care[14,17-19]. A common theme among DD patients was the requirement of a home ventilator, with Pizzuto *et al*[14] finding that 24% of the DD *vs* 1% ( $P < 0.01$ ) of the acute care ward cohort required a home ventilator. In addition, if the patient required a vasoactive agent while in the ICU, they were less likely to have had DD, with Roumeliotis *et al*[19] finding decreased odds of 30% of being DD.

## IMPLEMENTING DIRECT HOME DISCHARGE

Empirical evidence suggests that patients with fewer diagnoses or comorbidities, with lower mortality index, who are younger, with stable housing, and with reduced requirement for ventilatory support are safe candidates for DD[2,6,18]. After an extensive analysis of 197089 patients in 174 ICUs, Martin *et al*[7] recommend implementing DD for: (1) Patients who were admitted for a day procedure or from a hospital clinic; (2) Patients with preexisting conditions such as chronic dialysis or diabetes, and (3) Patients with a discharge diagnosis of diabetic ketoacidosis or overdose after careful evaluation. A study by Shimogai *et al*[20] echoed the importance of the previously stated findings of patients' age, mortality index, and comorbidities for the patients' readiness for DD. They further added to the growing body of literature by suggesting implementing DD for patients with independence at home before admission and iterating early mobilization at the ICU as a strong predictive factor in patients being considered for DD[20]. Furthermore, Plotnikoff *et al* [21] examined the requirements for a successful discharge from the ICU, and they found involving patients and family members in the discharge process, and communication between healthcare providers was a common motif in a successful discharge. The details of the studies are shown in Table 1.

## OUTCOMES

A meta-analysis of > 40000 patients by Lau *et al*[15] found that observational data evaluating outcomes in patients who were directly discharged did not significantly differ in rates of events witnessed. No increase in 90-day mortality or readmissions was found. Another cohort study complemented the results of this meta-analysis by showing that in > 6000 patients, selective DD did not result in any increase in mortality or healthcare utilization[3].

One of the largest studies (> 140000 patients) evaluating the impact of DD on outcomes was conducted in 2015. This 2-year study found no significant difference in outcomes and identified a reduced length of hospital stay in DD patients. While numerous studies, though observational, continue to show a lack of difference in outcomes, interestingly, physician satisfaction is often lacking when practicing DD. Patients and their families are more satisfied with the DD practice[22].

Chawla *et al*[10] report a readmission rate of almost 25% in DD patients, much higher than that reported by Lau *et al* [15], which was only 8% of patients.

Table 1 Patient characteristics

Ref.	Sample size (n)	Age	Sex (%)	Race/ethnicity	Comorbidities (%)	Admitting/discharge diagnoses	Morbidity index	LOS (days)	Location before ICU (%)
Studies looking at adult population									
Martin <i>et al</i> [7]	197089	80-105 vs 18-39 (OR: 0.36; 95%CI: 0.34-0.39)	Male > female (OR > 1)	-	Chronic dialysis (OR > 1), diabetes (OR > 1)	Day procedure (OR: 2.82; 95%CI: 2.46-3.23), seizure, overdose or poisoning (OR: 1.35; 95%CI: 1.23-1.47), diabetic ketoacidosis or diabetic complications (OR: 1.35; 95%CI: 1.2-1.51), GI bleed (OR > 1)	Charlson comorbidity index of 0 and 1 (OR: 1.74; 95%CI: 1.63-1.85)	-	Day procedure (OR: 2.82; 95%CI: 2.46-3.23), clinic (OR > 1), prior ICU admission (OR > 1), prior hospitalization (OR > 1)
Lau <i>et al</i> [2]	137	44.5 ± 16.7 (P = 0.004)	Female 46 (33.6) (P = 0.13)	-	(P < 0.0001) hypertension (27), GERD (17.5), depression (16.1), diabetes (10.2), substance abuse/overdose (14.6)	Number of discharge diagnoses (P = 0.002) overdose, subglottic stenosis/angioedema/laryngospasm, trauma, pulmonary embolism, and seizure	Charlson comorbidity index score: 1.65 ± 2.1 (P = 0.01), NMES (at admission) 26.6 ± 7.2, NMES (at discharge/transfer) 16.85 ± 8.3 (P = 0.02)	2.7 ± 3.7 (P = 0.001)	Emergency department 188 (56.8), another hospital 78 (23.7), home (direct ICU admission) 17 (7.5), floor 25 (7.6), OR/PACU 9 (2.7), other/unknown 14 (4.2)
Patel <i>et al</i> [8]	331	54.1 ± 17.25	158 (47.7)	White (46.2), Black (41.7), Asian/pacific-islander (3.6), Hispanic/Latino (5.1), other/unknown (3.3)	-	Monitoring (n = 13), sepsis/septic shock (n = 25), diabetic ketoacidosis (n = 13), electrolyte abnormalities due to alcohol abuse (n = 7), hyperkalemia (n = 5), hemodynamic instability (n = 11), arrhythmia (n = 10), hypertensive urgency or emergency (n = 5), systolic and diastolic heart failure exacerbation (n = 5), angioedema (n = 29), medication desensitization (n = 19), pneumonia (n = 28), pulmonary embolism (n = 25), COPD exacerbation (n = 21), acute respiratory disease syndrome (n = 20), asthma exacerbation (n = 10), gastrointestinal hemorrhage (n = 34), hepatic failure (n = 9)	MPM0-III predicted mortality % 15.9 ± 11.1, NEMS on admission 19.45 ± 8.58	2.41 (P = 0.001)	-
Stelfox <i>et al</i> [3]	6732	47 (P < 0.001)	Female 393 (P = 0.67)	-	Diabetes 143 (P < 0.001), chronic lung disease 151 (P = 0.11), chronic kidney disease 23 (P < 0.001), liver disease 37 (P < 0.001), cancer 31 (P < 0.001), chronic heart or peripheral vascular disease 72 (P < 0.001), neurological disease 17 (P < 0.001), any comorbidity 360 (P < 0.001)	Admitting diagnosis (P < 0.001): Overdose, withdrawal, seizures, or metabolic coma 295, pneumonia 104, respiratory other 133, medical or neurological additional 107, trauma or orthopedic 79, cardiovascular 67, sepsis (non-pulmonary) 52, gastrointestinal 45, pregnancy or genitourinary 21, cancer 8	Charlson Score 0-1 (P < 0.001), APACHE II score, 15 (P < 0.001)	2.9 (P < 0.001)	Location before ICU (P < 0.001): Emergency department 607, ward 160, operating or recovery room 98, other Hospital 55
Basmaji <i>et al</i> [16]	-	-	-	-	-	-	-	-	-
Chawla <i>et al</i> [10]	95	61.1	Male (60)	-	-	Respiratory failure, sepsis, cardiac syndromes, gastrointestinal bleeding	MPM0II Score 31.4	4.5	-

Lau <i>et al</i> [6]	642	49	Male (54.9)	-	-	Overdose, pneumonia, seizures, diabetic ketoacidosis	Multiple organ dysfunction scores 7	3	-
Lam <i>et al</i> [22]	137	45.75	Male (66.4)	-	-	Overdose, upper airway compromise, trauma, pulmonary embolism, seizures	Multiple organ dysfunction scores 7	1.8	-
Martin <i>et al</i> [12]	46859	60.79 ± 17.42	Male (59)	-	COPD, diabetes, congestive heart failure, seizure, overdose	Overdose/poisoning, pneumonia (respiratory tract infection or empyema, sepsis-other, seizure/convulsions, diabetic ketoacidosis or complications of diabetes	-	0	-
Studies looking at pediatric population									
Pizzuto <i>et al</i> [14]	532	2	Female (44)	White or Caucasian (45), black or African American (27), American Indian or Alaska Native (3), Asian (2), other (19), unknown (4)	-	Respiratory failure; insufficiency; arrest (9), diabetic ketoacidosis (6), asthma (5), acute bronchiolitis (3), sleep apnea (3), pneumonia (3), acute tracheitis (3), septicemia (3), complication of device; implant or graft (3), anomalies of cerebrovascular system, congenital (2)	-	2.1	-
Gal <i>et al</i> [18]	308	4.6	Female (39)	-	Atrial or ventricular septal defects, valve replacement, or conduit replacement	Cardiac procedure [191 ( <i>i.e.</i> Catheterization)], cardiac surgery [70 ( <i>i.e.</i> implantable)], medical condition [53 ( <i>i.e.</i> Arrhythmia or infection)]	STAT Score 2	1	Emergency department (177), Operating room (45), post anesthesia (39), home (9), floor (8), clinic (5)
Kennedy <i>et al</i> [17]	702	2	Male (64.4)	-	-	Bronchiolitis, seizures, asthma, lower respiratory tract infection	-	Approximately 2	Emergency department directly admitted
Roumeliotis <i>et al</i> [19]	594	3	61.6	-	-	Acute intoxication, postoperative ear-nose-throat care, shock	95% of the cohort had PELOD 2 score of 0-8 ( <i>P</i> < 0.001)	83% of patients had LOS 1-6 days. 17% had LOS > 7 days	-

LOS: Length of stay; ICU: Intensive care unit; OR: Odds ratio; CI: Confidence interval; GI: Gastrointestinal; GERD: Gastroesophageal reflux disease; NMES: Neuromuscular electrical stimulation; PACU: Post-acute care unit; MPM0-III: Mortality probability admission model-III; COPD: Chronic obstructive pulmonary disease; STAT Score: The society of thoracic surgeons-European association of cardio-thoracic surgery; PELOD 2: Pediatric logistic organ dysfunction 2; APACHE II: Acute physiology and chronic health evaluation II.

## FUTURE DIRECTIONS

Studies have not shown a difference between complex outcomes such as length of hospital stay and mortality between DD and traditional ward discharge. While this represents a potential argument for using DD to curb resource waste and improve patient comfort, the observational nature of the studies needs to be considered. Before guidelines recommending DD are ushered into the norm, additional research must be conducted to prevent potential patient harm.

First, patient selection for DD needs to be refined and specified. Currently, physician discretion is the standard for patient selection criteria. A study found that younger patients suffering from overdose, withdrawal, seizures, and < 48 hours of mechanical ventilation were more likely to be discharged home than older patients, those with an acute high degree illness, or those who had received surgical care. While these parameters intuitively make sense, they need to be

studied in a blinded, randomized fashion to measure outcomes precisely[3].

Second, almost all studies focusing on DD have been observational, with various included participants. Additional, tightly controlled randomized trials are needed if confidence in outcome measures is required. A trial demonstrating non-inferiority would lend reliability to the practice of DD and help in tailoring patient-specific guidelines.

Finally, there is a need to explore the role of telemonitoring in DD patients. Combining modern, virtual healthcare delivery methods with DD can drastically reduce the burden on the intensive care system. When such methods were employed in COVID-19 patients, a weeklong reduction in hospital length of stay was noted[23]. This suggests the dearth of potential that is yet to be realized with such measures in everyday ICU care.

## CONCLUSION

Our review has highlighted the emerging concept of direct discharge from the ICU as an alternative to traditional transfer to LDU. The literature suggests that carefully selected patients with stable clinical conditions and robust support systems at home can benefit from this approach. While mortality rates and patient satisfaction appear comparable to those of the conventional LDU transfer, successful implementation hinges on stringent patient selection, robust risk assessment, and comprehensive post-discharge care strategies. Direct discharge offers potential benefits such as reduced strain on healthcare resources, minimized exposure to hospital-acquired infections, and improved patient experience within familiar surroundings. However, challenges include accurate patient identification, effective remote monitoring, and timely intervention in case of complications. Balancing these aspects is crucial to ensuring patient safety and successful outcomes. The findings of this review underscore the importance of further exploration and thoughtful implementation of direct discharge from the ICU. As we move forward, tailored patient selection based on rigorous criteria and risk assessment is paramount. Additionally, comprehensive post-discharge support mechanisms should be established to ensure patients' well-being beyond the hospital walls, including telehealth services and clear communication channels. Combining evidence-based approaches with multidisciplinary collaboration can pave the way for a more patient-centered and resource-efficient healthcare model. We hope that continued research and innovative strategies will lead to improved guidelines and practices, enhancing the viability of direct home discharge and benefiting patients and the healthcare system.

## FOOTNOTES

**Author contributions:** Hassan EM and Khan SA provided the conceptualization of the paper; Hassan EM, Shaikh A, Jama AB, El Labban M provided the literature review, drafting, and reviewing; Khan SA and Surani S provided supervision, idea generation, and critical final review of the manuscript; All authors agreed to the final accuracy of the work.

**Conflict-of-interest statement:** None of the authors have any conflict of interest to disclose.

**Open-Access:** This article is an open-access article that was selected by an in-house editor and fully peer-reviewed by external reviewers. It is distributed in accordance with the Creative Commons Attribution NonCommercial (CC BY-NC 4.0) license, which permits others to distribute, remix, adapt, build upon this work non-commercially, and license their derivative works on different terms, provided the original work is properly cited and the use is non-commercial. See: <https://creativecommons.org/licenses/by-nc/4.0/>

**Country of origin:** United States

**ORCID number:** Esraa M Hassan 0000-0002-1080-3224; Abbas B Jama 0000-0003-1181-7975; Asim Shaikh 0000-0001-6984-9465; Mohamad El Labban 0000-0003-4244-9204; Salim Surani 0000-0001-7105-4266; Syed A Khan 0000-0002-2452-2079.

**S-Editor:** Fan M

**L-Editor:** A

**P-Editor:** Cai YX

## REFERENCES

- 1 Bourne RS, Jennings JK, Panagioti M, Hodkinson A, Sutton A, Ashcroft DM. Medication-related interventions to improve medication safety and patient outcomes on transition from adult intensive care settings: a systematic review and meta-analysis. *BMJ Qual Saf* 2022; **31**: 609-622 [PMID: 35042765 DOI: 10.1136/bmjqs-2021-013760]
- 2 Lau VI, Lam JNH, Basmaji J, Priestap FA, Ball IM. Survival and Safety Outcomes of ICU Patients Discharged Directly Home-A Direct From ICU Sent Home Study. *Crit Care Med* 2018; **46**: 900-906 [PMID: 29494475 DOI: 10.1097/CCM.0000000000003074]
- 3 Stelfox HT, Soo A, Niven DJ, Fiest KM, Wunsch H, Rowan KM, Bagshaw SM. Assessment of the Safety of Discharging Select Patients Directly Home From the Intensive Care Unit: A Multicenter Population-Based Cohort Study. *JAMA Intern Med* 2018; **178**: 1390-1399 [PMID: 30128550 DOI: 10.1001/jamainternmed.2018.3675]
- 4 Safavi K, Wiener-Kronish J, Hanidziar D. The Complexity and Challenges of Intensive Care Unit Admissions and Discharges: Similarities With All Hospitalized Patients. *JAMA Intern Med* 2018; **178**: 1399-1400 [PMID: 30128564 DOI: 10.1001/jamainternmed.2018.3674]

- 5 Sy E, Gupta C, Shahab Z, Fortin N, Kassir S, Mailman JF, Lau VI. Long-term Safety of Directly Discharging Patients Home from the ICU Compared to Ward Transfer. *J Intensive Care Med* 2022; **37**: 1344-1352 [PMID: [35350921](#) DOI: [10.1177/08850666221090459](#)]
- 6 Lau VI, Priestap FA, Lam JNH, Ball IM. Factors Associated With the Increasing Rates of Discharges Directly Home From Intensive Care Units-A Direct From ICU Sent Home Study. *J Intensive Care Med* 2018; **33**: 121-127 [PMID: [27655852](#) DOI: [10.1177/0885066616668483](#)]
- 7 Martin CM, Lam M, Allen B, Richard L, Lau V, Ball IM, Wunsch H, Fowler RA, Scales DC. Determinants of Direct Discharge Home From Critical Care Units: A Population-Based Cohort Analysis. *Crit Care Med* 2020; **48**: 475-483 [PMID: [32205593](#) DOI: [10.1097/CCM.0000000000004178](#)]
- 8 Patel PM, Fiorella MA, Zheng A, McDonnell L, Yasuoka M, Yoo EJ. Characteristics and Outcomes of Patients Discharged Directly Home From a Medical Intensive Care Unit: A Retrospective Cohort Study. *J Intensive Care Med* 2021; **36**: 1431-1435 [PMID: [32954949](#) DOI: [10.1177/0885066620960637](#)]
- 9 Lusardi P, Jodka P, Stambovsky M, Stadnicki B, Babb B, Plouffe D, Doubleday N, Pizlak Z, Walles K, Montonye M. The going home initiative: getting critical care patients home with hospice. *Crit Care Nurse* 2011; **31**: 46-57 [PMID: [21965383](#) DOI: [10.4037/ccn2011415](#)]
- 10 Chawla S, D'Agostino RL, Pastores SM, Thirumala R, Kostecky N, Chou JF, Thaler HT, Halpern NA. Homeward bound: an analysis of patients discharged home from an oncologic intensive care unit. *J Crit Care* 2012; **27**: 681-687 [PMID: [22901403](#) DOI: [10.1016/j.jcrc.2012.05.009](#)]
- 11 Huang YC, Huang SJ, Ko WJ. Going home to die from surgical intensive care units. *Intensive Care Med* 2009; **35**: 810-815 [PMID: [19280177](#) DOI: [10.1007/s00134-009-1452-1](#)]
- 12 Martin CM, Lam M, Le B, Pinto R, Lau V, Ball IM, Wunsch H, Fowler RA, Scales DC. Outcomes After Direct Discharge Home From Critical Care Units: A Population-Based Cohort Analysis. *Crit Care Med* 2022; **50**: 1256-1264 [PMID: [35275594](#) DOI: [10.1097/CCM.0000000000005533](#)]
- 13 Nates JL, Nunnally M, Kleinpell R, Blosser S, Goldner J, Birriel B, Fowler CS, Byrum D, Miles WS, Bailey H, Sprung CL. ICU Admission, Discharge, and Triage Guidelines: A Framework to Enhance Clinical Operations, Development of Institutional Policies, and Further Research. *Crit Care Med* 2016; **44**: 1553-1602 [PMID: [27428118](#) DOI: [10.1097/CCM.0000000000001856](#)]
- 14 Pizzuto MF, Sutton AG, Schroeder KS, Bravo MA, Li L, Kihlstrom MJ. Characteristics and Outcomes of Patients Discharged Directly Home From the Pediatric Intensive Care Unit. *J Intensive Care Med* 2023; **38**: 737-742 [PMID: [36895117](#) DOI: [10.1177/08850666231162530](#)]
- 15 Lau VI, Donnelly R, Parvez S, Gill J, Bagshaw SM, Ball IM, Basmaji J, Cook DJ, Fiest KM, Fowler RA, Mailman JF, Martin CM, Rochwerg B, Scales DC, Stelfox HT, Iansavichene A, Sy EJ. Safety Outcomes of Direct Discharge Home From ICUs: An Updated Systematic Review and Meta-Analysis (Direct From ICU Sent Home Study). *Crit Care Med* 2023; **51**: 127-135 [PMID: [36519986](#) DOI: [10.1097/CCM.0000000000005720](#)]
- 16 Basmaji J, Lau V, Lam J, Priestap F, Ball IM. Lessons learned and new directions regarding Discharge Direct from Adult Intensive Care Units Sent Home (DISH): A narrative review. *J Intensive Care Soc* 2019; **20**: 165-170 [PMID: [31037110](#) DOI: [10.1177/1751143718794123](#)]
- 17 Kennedy TK, Numa A. Factors associated with discharge delay and direct discharge home from paediatric intensive care. *J Paediatr Child Health* 2020; **56**: 1101-1107 [PMID: [32100413](#) DOI: [10.1111/jpc.14829](#)]
- 18 Gal DB, Kwiatkowski DM, Cribb Fabersunne C, Kipps AK. Direct Discharge to Home From the Pediatric Cardiovascular ICU. *Pediatr Crit Care Med* 2022; **23**: e199-e207 [PMID: [35044343](#) DOI: [10.1097/PCC.0000000000002883](#)]
- 19 Roumeliotis N, Hassine CH, Ducruet T, Lacroix J. Discharge Directly Home From the PICU: A Retrospective Cohort Study. *Pediatr Crit Care Med* 2023; **24**: e9-e19 [PMID: [36053070](#) DOI: [10.1097/PCC.0000000000003061](#)]
- 20 Shimogai T, Izawa KP, Kawada M, Kuriyama A. Factors Affecting Discharge to Home of Medical Patients Treated in an Intensive Care Unit. *Int J Environ Res Public Health* 2019; **16** [PMID: [31698814](#) DOI: [10.3390/ijerph16224324](#)]
- 21 Plotnikoff KM, Krewulak KD, Hernández L, Spence K, Foster N, Longmore S, Straus SE, Niven DJ, Parsons Leigh J, Stelfox HT, Fiest KM. Patient discharge from intensive care: an updated scoping review to identify tools and practices to inform high-quality care. *Crit Care* 2021; **25**: 438 [PMID: [34920729](#) DOI: [10.1186/s13054-021-03857-2](#)]
- 22 Lam JNH, Lau VI, Priestap FA, Basmaji J, Ball IM. Patient, Family, and Physician Satisfaction With Planning for Direct Discharge to Home From Intensive Care Units: Direct From ICU Sent Home Study. *J Intensive Care Med* 2020; **35**: 82-90 [PMID: [28931361](#) DOI: [10.1177/0885066617731263](#)]
- 23 Grutters LA, Majoor KI, Mattern ESK, Hardeman JA, van Swol CFP, Vorselaars ADM. Home telemonitoring makes early hospital discharge of COVID-19 patients possible. *J Am Med Inform Assoc* 2020; **27**: 1825-1827 [PMID: [32667985](#) DOI: [10.1093/jamia/ocaa168](#)]



Case Control Study

# Correlation and predictive value of pathological complete response and ultrasound characteristic parameters in neoadjuvant chemotherapy for breast

Lei Zheng, Li-Xian Yang, Jing-Yi Liu, Zhe Jiang, Xiao-Wei Li, Peng-Peng Pu

**Specialty type:** Medicine, research and experimental

**Provenance and peer review:** Unsolicited article; Externally peer reviewed.

**Peer-review model:** Single blind

**Peer-review report's classification**

**Scientific Quality:** Grade B

**Novelty:** Grade B

**Creativity or Innovation:** Grade B

**Scientific Significance:** Grade B

**P-Reviewer:** Ankrah AO, Netherlands

**Received:** March 10, 2024

**Revised:** May 12, 2024

**Accepted:** June 11, 2024

**Published online:** August 16, 2024

**Processing time:** 116 Days and 19.2 Hours



**Lei Zheng, Li-Xian Yang, Jing-Yi Liu, Xiao-Wei Li, Peng-Peng Pu**, Department of Breast Surgery, Xingtai People's Hospital, Xingtai 054001, Hebei Province, China

**Zhe Jiang**, Department of Medical Imaging, Xingtai People's Hospital, Xingtai 054001, Hebei Province, China

**Corresponding author:** Lei Zheng, MM, Researcher, Department of Breast Surgery, Xingtai People's Hospital, No. 16 Hongxing Street, Qiaodong District, Xingtai 054001, Hebei Province, China. [zlys6699@163.com](mailto:zlys6699@163.com)

## Abstract

### BACKGROUND

Breast cancer ranks as one of the most prevalent malignant tumors among women, significantly endangering their health and lives. While radical surgery has been a pivotal method for halting disease progression, it alone is insufficient for enhancing the quality of life for patients.

### AIM

To investigate the correlation between ultrasound characteristic parameters of breast cancer lesions and clinical efficacy in patients undergoing neoadjuvant chemotherapy (NAC).

### METHODS

Employing a case-control study design, this research involved 178 breast cancer patients treated with NAC at our hospital from July 2019 to June 2022. According to the Miller-Payne grading system, the pathological response, *i.e.* efficacy, of the NAC in the initial breast lesion after NAC was evaluated. Of these, 59 patients achieved a pathological complete response (PCR), while 119 did not (non-PCR group). Ultrasound characteristics prior to NAC were compared between these groups, and the association of various factors with NAC efficacy was analyzed using univariate and multivariate approaches.

### RESULTS

In the PCR group, the incidence of posterior echo attenuation, lesion diameter  $\geq 2.0$  cm, and Alder blood flow grade  $\geq$  II were significantly lower compared to the non-PCR group ( $P < 0.05$ ). The area under the curve values for predicting NAC

efficacy using posterior echo attenuation, lesion diameter, and Alder grade were 0.604, 0.603, and 0.583, respectively. Also, rates of pathological stage II, lymph node metastasis, vascular invasion, and positive Ki-67 expression were significantly lower in the PCR group ( $P < 0.05$ ). Logistic regression analysis identified posterior echo attenuation, lesion diameter  $\geq 2.0$  cm, Alder blood flow grade  $\geq$  II, pathological stage III, vascular invasion, and positive Ki-67 expression as independent predictors of poor response to NAC in breast cancer patients ( $P < 0.05$ ).

## CONCLUSION

While ultrasound characteristics such as posterior echo attenuation, lesion diameter  $\geq 2.0$  cm, and Alder blood flow grade  $\geq$  II exhibit limited predictive value for NAC efficacy, they are significantly associated with poor response to NAC in breast cancer patients.

**Key Words:** Breast cancer; Ultrasound; Neoadjuvant chemotherapy; Efficacy; Pathological complete response

©The Author(s) 2024. Published by Baishideng Publishing Group Inc. All rights reserved.

**Core Tip:** This study explored the relationship between ultrasound characteristic parameters of breast cancer lesions and clinical efficacy in patients undergoing neoadjuvant chemotherapy (NAC). In all, 59 cases achieved pathological complete response and 119 cases did not. The ultrasound characteristics of the lesions before NAC were compared between both groups of patients, and the relationship between various factors and the efficacy of NAC in breast cancer was explored using univariate and multivariate analyses. In conclusion, the ultrasound characteristics of breast cancer lesions have limited value in predicting NAC efficacy but are closely related to poor outcomes in breast cancer patients undergoing NAC.

**Citation:** Zheng L, Yang LX, Liu JY, Jiang Z, Li XW, Pu PP. Correlation and predictive value of pathological complete response and ultrasound characteristic parameters in neoadjuvant chemotherapy for breast. *World J Clin Cases* 2024; 12(23): 5320-5328

**URL:** <https://www.wjgnet.com/2307-8960/full/v12/i23/5320.htm>

**DOI:** <https://dx.doi.org/10.12998/wjcc.v12.i23.5320>

## INTRODUCTION

Breast cancer ranks as one of the most prevalent malignant tumors among women, significantly endangering their health and lives. While radical surgery has been a pivotal method for halting disease progression, it alone is insufficient for enhancing the quality of life for patients[1,2]. In current clinical settings, a multifaceted treatment approach is predominantly utilized for managing breast cancer. The efficacy of neoadjuvant chemotherapy (NAC) in reducing tumor stages and facilitating surgical interventions has been well documented[3-5]. The assessment of pathological responses post-NAC is a standard measure of treatment efficacy[6]. However, studies indicate that the rates of pathological complete response (PCR) post-NAC are suboptimal[7], underscoring the importance of predicting pathological responsiveness for tailoring clinical management strategies[8]. Biomarkers such as Ki-67 are widely recognized for guiding therapy and monitoring response[9]. Furthermore, imaging technologies have been shown to reflect prognostic factors in breast cancer, sparking considerable interest among researchers globally[10-12]. Despite this, limited reports exist on the use of ultrasound to evaluate PCR in breast cancer post-NAC, and there is a paucity of literature confirming its validity.

Thus, this study analyzed clinical and ultrasound parameters to investigate the correlation between ultrasound characteristic parameters of breast cancer lesions and clinical outcomes in patients undergoing NAC, thereby providing a theoretical foundation for clinical application.

## MATERIALS AND METHODS

### General data

This study received approval from the Ethics Committee of Xingtai People's Hospital (Xingtai, China). Utilizing a case-control design, we enrolled 178 breast cancer patients who underwent NAC. The pathological response to NAC was evaluated using the Miller-Payne method, determining the efficacy on initial breast lesions. Of these participants, 59 achieved a PCR, while 119 did not (non-PCR group).

Inclusion criteria were as follows: (1) Patients were diagnosed according to the criteria outlined in the 'Breast Cancer Volume', employing ultrasound with a molybdenum target, magnetic resonance imaging, and lesion biopsy[13]; (2) Patients were at clinical stages II to III; (3) All patients were diagnosed for the first time; (4) Age ranged from 35 years to 59 years; (5) Breast cancer lesions were measurable by imaging; and (6) The study protocol received approval from the Medical Ethics Committee.

Exclusion criteria were as follows: (1) Patients presenting with distant metastases; (2) Patients with primary malignant tumors in tissues or organs other than the breast; (3) Patients diagnosed with immune system disorders; (4) Patients who did not complete the required chemotherapy cycles; (5) Patients with severe hepatic or renal dysfunction; (6) Patients suffering from significant immune system diseases, such as systemic lupus erythematosus; and (7) Patients lacking preoperative ultrasound data.

### **Preoperative ultrasound examination method**

Ultrasound examinations were conducted using the Sequoia 512 color Doppler ultrasound system (Siemens, Munich, Germany), which was equipped with a high-frequency probe operating between 8.0 MHz and 9.0 MHz. Patients were positioned supine with their arms elevated to ensure full exposure of both axillae and breasts. An acoustic coupling agent was applied to facilitate the scanning process. The ultrasound captured detailed images that included characteristic Breast Imaging Reporting and Data System descriptors such as the boundaries of breast cancer, microcalcification, mass morphology, peripheral high-echo halos, posterior echo attenuation, longest baseline diameter of the lesion, and blood flow classification. These images were subjected to a double-blind evaluation by two experienced breast pathologists.

### **NAC**

The NAC regimen was as follows: docetaxel + epirubicin + cyclophosphamide, epirubicin: 60 mg/m<sup>2</sup>, day 1; paclitaxel: 175 mg/m<sup>2</sup>, 3 h on day 1; cyclophosphamide: 500 mg/m<sup>2</sup> on day 1, 21 d as one cycle, with a total of four cycles. Surgical treatment began 2 wk after the last chemotherapy. Two days after the completion of NAC, all patients underwent ultrasound examination.

### **Chemotherapy efficacy evaluation**

The Miller-Payne method is employed to assess the efficacy of NAC in breast cancer patients[14]. The grading is as follows: Grade 1: no change observed in the lesions post-NAC; Grade 2: a reduction in tumor lesion density of less than 30% relative to pre-treatment, with no pathological changes; Grade 3: tumor lesion density decreases between 30% and 90% compared to before treatment; Grade 4: tumor lesion density reduces by more than 90% compared to pre-treatment levels; and Grade 5: complete disappearance of the tumor, indicative of complete remission on pathological examination.

### **Statistical analyses**

Statistical analyses were conducted using SPSS version 21.0 (IBM, Armonk, NY, United States). The quantitative variables, including age and body mass index, followed a normal distribution. Descriptive statistics for these parameters are presented as the mean ± standard deviation. The independent samples *t*-test was utilized for hypothesis testing between the two groups for these quantitative data. Categorical variables, such as the distribution of the affected side, menopausal status, and Ki-67 expression, were summarized as counts and percentages. Differences between groups were assessed using the  $\chi^2$  test. The predictive value of ultrasonic features for the efficacy of NAC in breast cancer was evaluated using the receiver operating characteristic (ROC) curve analysis. A logistic regression model was applied to perform multivariate analysis exploring the relationship between the efficacy of NAC and patient outcomes in breast cancer.

## **RESULTS**

### **Comparison of ultrasound characteristics between the PCR and non-PCR groups**

The proportion of patients exhibiting posterior echo attenuation, a lesion diameter of  $\geq 2.0$  cm, and an Alder blood flow classification of grade II or higher was significantly lower in the PCR group compared to the non-PCR group ( $P < 0.05$ ). Refer to Table 1 and Figure 1 for detailed data.

### **The value of ultrasound features before NAC in predicting the efficacy of NAC in breast cancer**

ROC curves were constructed for variables that showed statistical significance in univariate analysis, including posterior echo attenuation, lesion diameter, and Alder blood flow grade. The results indicated that the area under the curve (AUC) values for predicting the efficacy of NAC in breast cancer were 0.604 for posterior echo attenuation, 0.603 for lesion diameter  $\geq 2.0$  cm, and 0.583 for Alder grade  $\geq$  II. Refer to Figure 2 and Table 2 for detailed results.

### **Comparison of general data and pathological data between the PCR and non-PCR groups**

The proportion of patients in the PCR group presenting with pathological stage II, lymph node metastasis, vascular infiltration, and positive Ki-67 expression was significantly lower compared to the non-PCR group ( $P < 0.05$ ). Detailed data can be found in Table 3.

### **Multivariate analysis of the relationship between NAC efficacy and breast cancer patients**

In this study, logistic regression was utilized to assess the relationship between clinical outcomes post-NAC and various predictors, including posterior echo attenuation, lesion diameter, Alder blood flow classification, pathological staging, lymph node metastasis, vascular infiltration, and Ki-67 expression. These factors served as independent variables with the clinical efficacy of NAC as the dependent variable. The analysis identified posterior echo attenuation, lesion diameter  $\geq 2.0$  cm, Alder blood flow classification  $\geq$  grade II, pathological stage III, vascular infiltration, and positive Ki-67 expression as independent risk factors for poor NAC response in breast cancer patients ( $P < 0.05$ ). Results are detailed in

**Table 1 Comparison of ultrasound characteristics between pathological complete response group and non-pathological complete response group**

Ultrasonic feature	PCR group, <i>n</i> = 59	Non PCR group, <i>n</i> = 59	$\chi^2$	<i>P</i> value
Edge of lesion			1.374	0.241
Burr	41 (69.49)	72 (60.50)		
Smooth	18 (30.51)	47 (39.50)		
Calcification lesion			1.532	0.216
Yes	27 (45.76)	43 (36.13)		
No	32 (54.24)	76 (63.87)		
Peripheral echo halo			2.053	0.152
High and low echo dizziness	32 (54.24)	51 (42.86)		
No	27 (45.76)	68 (57.14)		
Posterior echo			6.767	0.009
Attenuation	38 (64.41)	52 (43.7)		
Unchanged	21 (35.59)	67 (56.3)		
Tumor morphology			1.464	0.226
Quasi-circular object	11 (18.64)	32 (26.89)		
Irregular	48 (81.36)	87 (73.11)		
Lesion diameter			6.769	0.006
≥ 2.0 cm	36 (61.02)	48 (40.34)		
< 2.0 cm	23 (38.98)	71 (59.66)		
Alder blood flow grading			4.448	0.035
≥ II stage	41 (69.49)	63 (52.94)		
< II stage	18 (30.51)	56 (47.06)		

Data are *n* (%). PCR: Pathological complete response.

**Table 2 The value of ultrasound features in predicting the efficacy of neoadjuvant chemotherapy in breast cancer**

Ultrasonic feature	Sensitivity	Specificity	Missed diagnosis	Misdiagnosis rate	AUC value
Posterior echo	64.41	56.30	35.59	43.70	0.604
Lesion diameter	61.02	59.66	38.98	40.34	0.603
Alder blood flow grading	69.49	47.06	30.51	52.94	0.583

Data are %. AUC: Area under the curve.

Table 4.

## DISCUSSION

The utilization of NAC for the treatment of breast cancer is increasingly prevalent. Early evaluation of NAC efficacy is crucial for optimizing treatment strategies and improving patient outcomes[15]. While pathological assessments, tumor markers, and genetic methods are traditionally employed to evaluate the effectiveness of NAC, these approaches are predominantly invasive[16-18]. In recent years, imaging techniques have gained traction in clinical practice as non-invasive alternatives for assessing NAC efficacy[19-21]. Despite this advancement, studies focusing on early evaluation using ultrasound are sparse. This study aimed to delineate the relationship between ultrasound characteristic parameters and PCR in NAC.

**Table 3 Comparison of general data and pathological data between pathological complete response group and non-pathological complete response group**

Index	PCR group, <i>n</i> = 59	Non PCR group, <i>n</i> = 119	<i>t</i> / $\chi^2$	<i>P</i> value
Age in year	44.8 ± 5.2	46.1 ± 6.4	-1.354	0.178
BMI in kg/m <sup>2</sup>	22.62 ± 1.33	22.85 ± 1.41	-1.044	0.298
Menstrual status			1.447	0.229
Menopause	16 (27.12)	43 (36.13)		
Premenopausal	43 (72.88)	76 (63.87)		
Affected side distribution			0.634	0.426
Left	27 (45.76)	62 (52.1)		
Right	32 (54.24)	57 (47.9)		
Pathological type			0.565	0.452
Infiltrating ductal carcinoma	48 (81.36)	102 (85.71)		
Other types	11 (18.64)	17 (14.29)		
Pathological staging			4.893	0.027
II stage	18 (30.51)	57 (47.9)		
III stage	41 (69.49)	62 (52.1)		
Lymph node metastasis			3.898	0.048
Yes	11 (18.64)	39 (32.77)		
No	48 (81.36)	80 (67.23)		
Vascular invasion			8.128	0.004
Yes	34 (57.63)	93 (78.15)		
No	25 (42.37)	26 (21.85)		
Ki-67			5.704	0.017
Positive	22 (37.29)	67 (56.3)		
Negative	37 (62.71)	52 (43.7)		
HER-2			2.706	0.100
Positive	33 (55.93)	51 (42.86)		
Negative	26 (44.07)	68 (57.14)		
ER			3.497	0.061
Positive	21 (35.59)	60 (50.42)		
Negative	38 (64.41)	59 (49.58)		

Data are *n* (%). BMI: Body mass index; PCR: Pathological complete response.

Ultrasound not only visualizes lesion characteristics but also detects changes in blood flow intensity at the lesion site [22]. The findings indicate that the rates of posterior echo attenuation, lesion diameter  $\geq 2.0$  cm, and Alder blood flow classification  $\geq$  grade II are significantly lower in the PCR group compared to the non-PCR group ( $P < 0.05$ ). Ultrasound effectively delineates the fine structure of tumors and precisely measures tumor diameters, while also depicting the boundary characteristics between lesions and surrounding tissues[23,24]. Prior studies utilizing ultrasound analysis to monitor lesion changes post-two cycles of NAC have demonstrated correlations with pathological assessments[25,26]. Moreover, ultrasound can evaluate changes in lesions before and after treatment by analyzing tumor blood flow classifications and hemodynamic parameters, offering the advantages of repeatability and ease of operation[27].

This study confirms that ultrasound can provide detailed internal images of lesions and inform prognostic evaluations of NAC outcomes. Notably, the AUC values for posterior echo attenuation, lesion diameter  $\geq 2.0$  cm, and Alder classification  $\geq$  grade II were 0.604, 0.603, and 0.583, respectively, indicating moderate predictive power. Future enhancements may include the integration of quantitative indicators such as lesion hardness and density to further refine the assessment of treatment efficacy.

Table 4 Multivariate analysis results

Index	$\beta$	SE	Walds	P value	OR	95%CI
Posterior echo	0.511	0.221	5.346	0.025	1.667	1.081 2.571
Lesion diameter	0.481	0.24	4.017	0.048	1.618	1.011 2.589
Alder blood flow grading	0.602	0.251	5.752	0.003	1.826	1.116 2.986
Pathological staging	0.648	0.238	7.413	0.000	1.912	1.199 3.048
Lymph node metastasis	0.392	0.203	3.729	0.073	1.480	0.994 2.203
Vascular invasion	0.711	0.251	8.024	0.000	2.036	1.245 3.330
Ki-67	0.641	0.227	7.974	0.000	1.898	1.217 2.962
Constant term	1.403	0.784	3.202	0.096	4.067	0.875 18.909

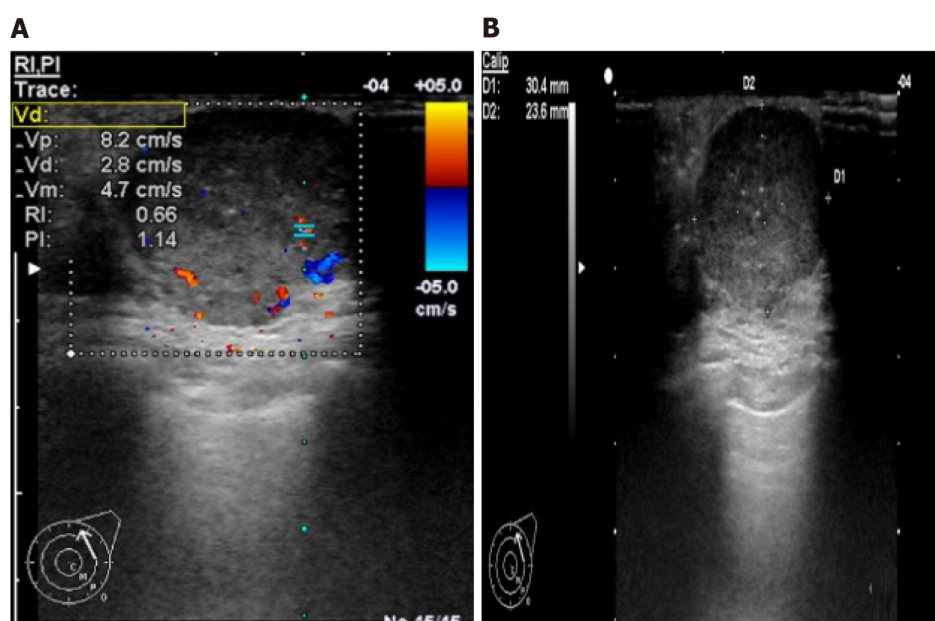


**Figure 1** A 43-yr-old female patient had a left breast mass with a diameter of 2.2 cm. The mass was irregular in shape and low echo in the rear. The Alder blood flow grade was grade II, and the pathological complete response effect was achieved after chemotherapy. A: Pre-chemotherapy; B: Post-chemotherapy.

This study demonstrated that the rates of pathological stage II, lymph node metastasis, and vascular invasion were significantly lower in the PCR group compared to the non-PCR group ( $P < 0.05$ ). Clinical data can often serve as a benchmark for determining whether patients have achieved PCR[28]. Numerous studies have analyzed clinical data from patients undergoing NAC, although results can vary due to differing inclusion criteria and patient heterogeneity. Previous research[29] has identified body weight and estrogen receptor levels as independent predictors of PCR post-NAC in breast cancer patients, with the number of chemotherapy cycles and lymph node metastasis also playing influential roles[30,31].

Pathological characteristics were found to be closely linked to the efficacy of NAC. Current clinical research in breast cancer increasingly emphasizes biological analysis, recognizing the significance of biological factor expression in evaluating and predicting NAC outcomes[32]. Ki-67, a protein related to cell proliferation, is noted for its utility in assessing tumor cell activity post-chemotherapy. High Ki-67 expression has been reported as a sensitive predictor of NAC response[33], corroborating findings from this study that high Ki-67 expression levels are significantly associated with NAC clinical efficacy.

Logistic regression analysis revealed that posterior echo attenuation, lesion diameter  $\geq 2.0$  cm, Alder blood flow classification  $\geq$  grade II, pathological stage III, vascular invasion, and positive Ki-67 expression are independent risk factors for ineffective NAC in breast cancer patients ( $P < 0.05$ ). Ultrasound imaging provides valuable insights into tumor size, shape, echo, and blood flow characteristics from various angles. Breast cancer lesions, which are typically vascular-rich with elastic-poor vessels, exhibit increased blood flow and reduced internal echo. Post-NAC, a significant reduction in cancer cells leads to diminished and narrowed blood vessels within the lesion, enhancing the internal echo. Furthermore, a decrease in lesion diameter and volume can reduce vascular pressure, improving internal echo characteristics. Higher Alder blood flow classifications, indicating elevated levels of blood perfusion, correlate with poorer clearance of lesions post-chemotherapy.

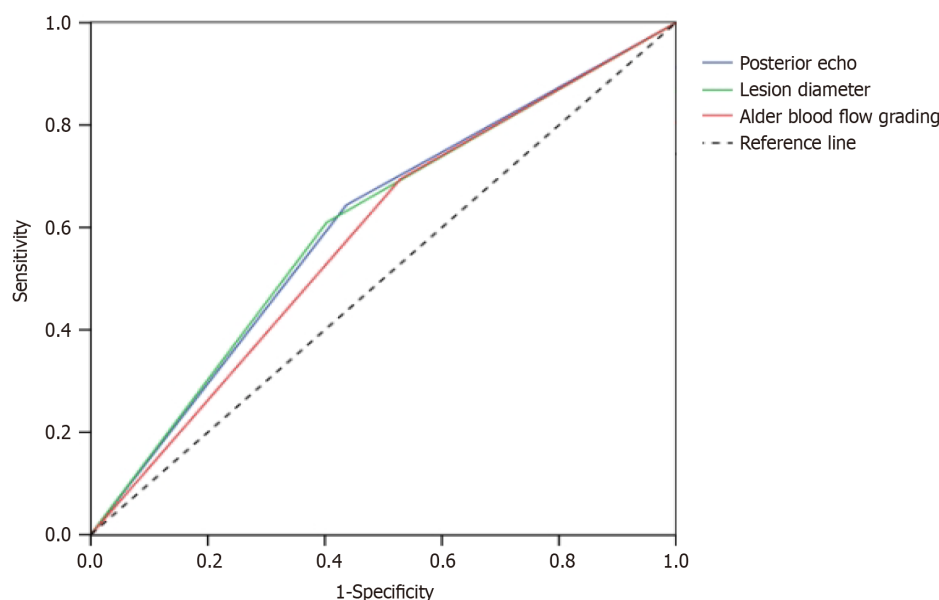


**Figure 2** Receiver operating characteristic curve of ultrasonographic features in predicting the efficacy of neoadjuvant chemotherapy in breast cancer.

In conclusion, posterior echo attenuation, lesion diameter  $\geq 2.0$  cm, and Alder blood flow classification are useful metrics for evaluating the efficacy of NAC. Ki-67 serves as a robust biological marker to gauge tumor proliferation activity after chemotherapy, with higher expression levels indicating less favorable postoperative outcomes. The study confirms that larger tumor diameters, vascular invasion, and advanced staging are predictive of poor response to NAC in breast cancer patients.

This study further substantiates the significance of vascular infiltration and positive Ki-67 expression in evaluating and predicting the efficacy of NAC. Previous research[34] has demonstrated that ultrasound is highly sensitive in reflecting the histological characteristics of residual tumors post-NAC. The technique provides comprehensive visualization of the tumor's size, shape, internal echo, and blood flow characteristics. Our analysis utilizes multiple parameters to evaluate PCR, with ROC analysis indicating that the integration of various ultrasound parameters with pathological data can enhance the prediction of NAC outcomes.

Advancements in ultrasound technology have notably improved resolution for detecting small lesions and facilitated more accurate quantitative tumor measurements. Analyzing ultrasound characteristics enables clinicians to tailor chemotherapy regimens effectively, potentially averting ineffective treatments and boosting PCR rates. Future research could benefit from incorporating additional advanced ultrasound technologies to refine the evaluation process further.

## CONCLUSION

The ultrasound characteristics of breast cancer lesions, specifically posterior echo attenuation, lesion diameter  $\geq 2.0$  cm, and Alder blood flow classification  $\geq \text{II}$ , demonstrate limited predictive value for the efficacy of NAC. Nonetheless, these parameters are closely associated with poorer outcomes in breast cancer patients undergoing NAC, underscoring their relevance in clinical assessment and treatment planning.

## FOOTNOTES

**Author contributions:** Zheng L, Yang LX, and Liu JY were the guarantors of the integrity of the entire study; Pu PP and Zheng L conceived the study and design; Yang LX and Jiang Z performed the literature search; Li XW and Pu PP conducted the study; Zheng L and Yang LX conducted the statistical analyses; Zheng L, Liu JY, and Pu PP wrote the manuscript; All authors have access to the data and played a role in writing the manuscript.

**Institutional review board statement:** This study was reviewed and approved by the Ethics Committee of Xingtai People's Hospital.

**Informed consent statement:** As this study was retrospective, no patient informed consent was required.

**Conflict-of-interest statement:** The authors have no conflicts of interest to declare.

**Data sharing statement:** Data for this study can be obtained from the corresponding authors.

**STROBE statement:** The authors have read the STROBE Statement-checklist of items, and the manuscript was prepared and revised according to the STROBE Statement-checklist of items.

**Open-Access:** This article is an open-access article that was selected by an in-house editor and fully peer-reviewed by external reviewers. It is distributed in accordance with the Creative Commons Attribution NonCommercial (CC BY-NC 4.0) license, which permits others to distribute, remix, adapt, build upon this work non-commercially, and license their derivative works on different terms, provided the original work is properly cited and the use is non-commercial. See: <https://creativecommons.org/licenses/by-nc/4.0/>

**Country of origin:** China

**ORCID number:** Lei Zheng 0009-0000-3725-9903.

**S-Editor:** Qu XL

**L-Editor:** Filipodia

**P-Editor:** Zhao YQ

## REFERENCES

- 1 **Zarotti C**, Papassotiropoulos B, Elfgen C, Dedes K, Vorburger D, Pestalozzi B, Trojan A, Varga Z. Biomarker dynamics and prognosis in breast cancer after neoadjuvant chemotherapy. *Sci Rep* 2022; **12**: 91 [PMID: 34997055 DOI: 10.1038/s41598-021-04032-x]
- 2 **Shafiee F**, Rabbani F, Yazdiniapour Z, Ghanadian M, Zolfaghari B, Maleki M. Cytotoxicity and apoptosis assay of novel cyclomyrsinol diterpenes against breast cancer cell lines. *World J Tradit Chin Med* 2022; **8**: 273 [DOI: 10.4103/wjtc.wjtc\_6\_21]
- 3 **Talamantes S**, Xie E, Costa RLB, Chen M, Rademaker A, Santa-Maria CA. Circulating immune cell dynamics in patients with triple negative breast cancer treated with neoadjuvant chemotherapy. *Cancer Med* 2020; **9**: 6954-6960 [PMID: 32757467 DOI: 10.1002/cam4.3358]
- 4 **Zhu Y**, Tzoras E, Matikas A, Bergh J, Valachis A, Zerdes I, Foukakis T. Expression patterns and prognostic implications of tumor-infiltrating lymphocytes dynamics in early breast cancer patients receiving neoadjuvant therapy: A systematic review and meta-analysis. *Front Oncol* 2022; **12**: 999843 [PMID: 36531050 DOI: 10.3389/fonc.2022.999843]
- 5 **Chen P**, Mao X, Ma N, Wang C, Yao G, Ye G, Zhou D. Dynamic changes in intrinsic subtype, immunity status, and risk score before and after neoadjuvant chemo- and HER2-targeted therapy without pCR in HER2-positive breast cancers: A cross-sectional analysis. *Medicine (Baltimore)* 2022; **101**: e29877 [PMID: 35945759 DOI: 10.1097/MD.00000000000029877]
- 6 **Ma G**, Wang J, Huang H, Han X, Xu J, Veeramootoo JS, Xia T, Wang S. Identification of the plasma total cfDNA level before and after chemotherapy as an indicator of the neoadjuvant chemotherapy response in locally advanced breast cancer. *Cancer Med* 2020; **9**: 2271-2282 [PMID: 32017472 DOI: 10.1002/cam4.2906]
- 7 **Geng SK**, Fu SM, Ma SH, Fu YP, Zhang HW. Tumor infiltrating neutrophil might play a major role in predicting the clinical outcome of breast cancer patients treated with neoadjuvant chemotherapy. *BMC Cancer* 2021; **21**: 68 [PMID: 33446143 DOI: 10.1186/s12885-021-07789-6]
- 8 **Graeser M**, Feuerhake F, Gluz O, Volk V, Hauptmann M, Jozwiak K, Christgen M, Kuemmel S, Grischke EM, Forstbauer H, Braun M, Warm M, Hackmann J, Uleer C, Aktas B, Schumacher C, Kolberg-Liedtke C, Kates R, Wuerstlein R, Nitz U, Kreipe HH, Harbeck N. Immune cell composition and functional marker dynamics from multiplexed immunohistochemistry to predict response to neoadjuvant chemotherapy in the WSG-ADAPT-TN trial. *J Immunother Cancer* 2021; **9** [PMID: 33963012 DOI: 10.1136/jitc-2020-002198]
- 9 **Drisis S**, El Adoui M, Flamen P, Benjelloun M, Dewind R, Paesmans M, Ignatiadis M, Bali M, Lemort M. Early prediction of neoadjuvant treatment outcome in locally advanced breast cancer using parametric response mapping and radial heterogeneity from breast MRI. *J Magn Reson Imaging* 2020; **51**: 1403-1411 [PMID: 31737963 DOI: 10.1002/jmri.26996]
- 10 **Spring LM**, Fell G, Arfe A, Sharma C, Greenup R, Reynolds KL, Smith BL, Alexander B, Moy B, Isakoff SJ, Parmigiani G, Trippa L, Bardia A. Pathologic Complete Response after Neoadjuvant Chemotherapy and Impact on Breast Cancer Recurrence and Survival: A Comprehensive Meta-analysis. *Clin Cancer Res* 2020; **26**: 2838-2848 [PMID: 32046998 DOI: 10.1158/1078-0432.CCR-19-3492]
- 11 **Nanda R**, Liu MC, Yau C, Shatsky R, Pusztai L, Wallace A, Chien AJ, Forero-Torres A, Ellis E, Han H, Clark A, Albain K, Boughey JC, Jaskowiak NT, Elias A, Isaacs C, Kemmer K, Helsten T, Majure M, Stringer-Reasor E, Parker C, Lee MC, Haddad T, Cohen RN, Asare S, Wilson A, Hirst GL, Singha R, Steeg K, Asare A, Matthews JB, Berry S, Sanil A, Schwab R, Symmans WF, van 't Veer L, Yee D, DeMichele A, Hyton NM, Melisko M, Perlmutter J, Rugo HS, Berry DA, Esserman LJ. Effect of Pembrolizumab Plus Neoadjuvant Chemotherapy on Pathologic Complete Response in Women With Early-Stage Breast Cancer: An Analysis of the Ongoing Phase 2 Adaptively Randomized I-SPY2 Trial. *JAMA Oncol* 2020; **6**: 676-684 [PMID: 32053137 DOI: 10.1001/jamaoncol.2019.6650]
- 12 **Graeser M**, Schrading S, Gluz O, Strobel K, Würstlein R, Kümmel S, Schumacher C, Grischke EM, Forstbauer H, Braun M, Christgen M, Adams J, Nitzsche H, Just M, Fischer HH, Aktas B, Potenberg J, von Schumann R, Kolberg-Liedtke C, Harbeck N, Kuhl CK, Nitz U. Early response by MR imaging and ultrasound as predictor of pathologic complete response to 12-week neoadjuvant therapy for different early breast cancer subtypes: Combined analysis from the WSG ADAPT subtrials. *Int J Cancer* 2021; **148**: 2614-2627 [PMID: 33533487 DOI: 10.1002/ijc.33495]
- 13 **Zhang BN**. Breast cancer booklet (standardization of malignant tumors. Standardized Diagnosis and Treatment Series). 2011. Available from: [https://xueshu.baidu.com/usercenter/paper/show?paperid=656b6e4d887ff8c5b87f5f824b775b34&site=xueshu\\_se](https://xueshu.baidu.com/usercenter/paper/show?paperid=656b6e4d887ff8c5b87f5f824b775b34&site=xueshu_se)
- 14 **Harbeck N**. Neoadjuvant and adjuvant treatment of patients with HER2-positive early breast cancer. *Breast* 2022; **62** Suppl 1: S12-S16 [PMID: 35148934 DOI: 10.1016/j.breast.2022.01.006]
- 15 **Candelaria RP**, Adrada BE, Lane DL, Rauch GM, Moulder SL, Thompson AM, Bassett RL, Arribas EM, Le-Petross HT, Leung JWT, Spak DA, Ravenberg EE, White JB, Valero V, Yang WT. Mid-treatment Ultrasound Descriptors as Qualitative Imaging Biomarkers of Pathologic Complete Response in Patients with Triple-Negative Breast Cancer. *Ultrasound Med Biol* 2022; **48**: 1010-1018 [PMID: 35300879 DOI: 10.1016/j.ultrasmedbio.2022.01.018]

- 16 **Jiang M**, Li CL, Luo XM, Chuan ZR, Lv WZ, Li X, Cui XW, Dietrich CF. Ultrasound-based deep learning radiomics in the assessment of pathological complete response to neoadjuvant chemotherapy in locally advanced breast cancer. *Eur J Cancer* 2021; **147**: 95-105 [PMID: 33639324 DOI: 10.1016/j.ejca.2021.01.028]
- 17 **Torrìsi R**, Marrazzo E, Agostinetti E, De Sanctis R, Losurdo A, Masci G, Tinteri C, Santoro A. Neoadjuvant chemotherapy in hormone receptor-positive/HER2-negative early breast cancer: When, why and what? *Crit Rev Oncol Hematol* 2021; **160**: 103280 [PMID: 33667658 DOI: 10.1016/j.critrevonc.2021.103280]
- 18 **Kim SY**, Cho N, Choi Y, Lee SH, Ha SM, Kim ES, Chang JM, Moon WK. Factors Affecting Pathologic Complete Response Following Neoadjuvant Chemotherapy in Breast Cancer: Development and Validation of a Predictive Nomogram. *Radiology* 2021; **299**: 290-300 [PMID: 33754824 DOI: 10.1148/radiol.2021203871]
- 19 **Gu J**, Tong T, Xu D, Cheng F, Fang C, He C, Wang J, Wang B, Yang X, Wang K, Tian J, Jiang T. Deep learning radiomics of ultrasonography for comprehensively predicting tumor and axillary lymph node status after neoadjuvant chemotherapy in breast cancer patients: A multicenter study. *Cancer* 2023; **129**: 356-366 [PMID: 36401611 DOI: 10.1002/cncr.34540]
- 20 **Thompson BM**, Chala LF, Shimizu C, Mano MS, Filassi JR, Geyer FC, Torres US, de Mello GGN, da Costa Leite C. Pre-treatment MRI tumor features and post-treatment mammographic findings: may they contribute to refining the prediction of pathologic complete response in post-neoadjuvant breast cancer patients with radiologic complete response on MRI? *Eur Radiol* 2022; **32**: 1663-1675 [PMID: 34716780 DOI: 10.1007/s00330-021-08290-1]
- 21 **Cui H**, Zhao D, Han P, Zhang X, Fan W, Zuo X, Wang P, Hu N, Kong H, Peng F, Wang Y, Tian J, Zhang L. Predicting Pathological Complete Response After Neoadjuvant Chemotherapy in Advanced Breast Cancer by Ultrasound and Clinicopathological Features Using a Nomogram. *Front Oncol* 2021; **11**: 718531 [PMID: 34888231 DOI: 10.3389/fonc.2021.718531]
- 22 **Sudhir R**, Koppula VC, Rao TS, Sannapareddy K, Rajappa SJ, Murthy SS. Accuracy of digital mammography, ultrasound and MRI in predicting the pathological complete response and residual tumor size of breast cancer after completion of neoadjuvant chemotherapy. *Indian J Cancer* 2022; **59**: 345-353 [PMID: 33753611 DOI: 10.4103/ijc.IJC\_795\_19]
- 23 **Cullinane C**, Brien AO, Shrestha A, Hanlon EO, Walshe J, Geraghty J, Evoy D, McCartan D, McDermott E, Prichard R. The association between breast density and breast cancer pathological response to neoadjuvant chemotherapy. *Breast Cancer Res Treat* 2022; **194**: 385-392 [PMID: 35606616 DOI: 10.1007/s10549-022-06616-1]
- 24 **Palshof FK**, Lanng C, Kroman N, Benian C, Vejborg I, Bak A, Talman ML, Balslev E, Tvedskov TF. Prediction of Pathologic Complete Response in Breast Cancer Patients Comparing Magnetic Resonance Imaging with Ultrasound in Neoadjuvant Setting. *Ann Surg Oncol* 2021; **28**: 7421-7429 [PMID: 34043094 DOI: 10.1245/s10434-021-10117-8]
- 25 **Rix A**, Piepenbrock M, Flege B, von Stillfried S, Koczera P, Opacic T, Simons N, Boor P, Thoröe-Boveleth S, Deckers R, May JN, Lammers T, Schmitz G, Stickeler E, Kiessling F. Effects of contrast-enhanced ultrasound treatment on neoadjuvant chemotherapy in breast cancer. *Theranostics* 2021; **11**: 9557-9570 [PMID: 34646386 DOI: 10.7150/thno.64767]
- 26 **Yam C**, Abuhadra N, Sun R, Adrada BE, Ding QQ, White JB, Ravenberg EE, Clayborn AR, Valero V, Tripathy D, Damodaran S, Arun BK, Litton JK, Ueno NT, Murthy RK, Lim B, Baez L, Li X, Buzdar AU, Hortobagyi GN, Thompson AM, Mittendorf EA, Rauch GM, Candelaria RP, Huo L, Moulder SL, Chang JT. Molecular Characterization and Prospective Evaluation of Pathologic Response and Outcomes with Neoadjuvant Therapy in Metaplastic Triple-Negative Breast Cancer. *Clin Cancer Res* 2022; **28**: 2878-2889 [PMID: 35507014 DOI: 10.1158/1078-0432.CCR-21-3100]
- 27 **Yin W**, Wang Y, Wu Z, Ye Y, Zhou L, Xu S, Lin Y, Du Y, Yan T, Yang F, Zhang J, Liu Q, Lu J. Neoadjuvant Trastuzumab and Pyrotinib for Locally Advanced HER2-Positive Breast Cancer (NeoATP): Primary Analysis of a Phase II Study. *Clin Cancer Res* 2022; **28**: 3677-3685 [PMID: 35713517 DOI: 10.1158/1078-0432.CCR-22-0446]
- 28 **Heil J**, Kuerer HM, Pfof A, Rauch G, Sinn HP, Golatta M, Liefers GJ, Vrancken Peeters MJ. Eliminating the breast cancer surgery paradigm after neoadjuvant systemic therapy: current evidence and future challenges. *Ann Oncol* 2020; **31**: 61-71 [PMID: 31912797 DOI: 10.1016/j.annonc.2019.10.012]
- 29 **Gluz O**, Nitz U, Kolberg-Liedtke C, Prat A, Christgen M, Kuemmel S, Mohammadian MP, Gebauer D, Kates R, Paré L, Grischke EM, Forstbauer H, Braun M, Warm M, Hackmann J, Uleer C, Aktas B, Schumacher C, Wuerstlein R, Graeser M, Pelz E, Jóźwiak K, Zu Eulenburg C, Kreipe HH, Harbeck N; ADAPT TN investigators. De-escalated Neoadjuvant Chemotherapy in Early Triple-Negative Breast Cancer (TNBC): Impact of Molecular Markers and Final Survival Analysis of the WSG-ADAPT-TN Trial. *Clin Cancer Res* 2022; **28**: 4995-5003 [PMID: 35797219 DOI: 10.1158/1078-0432.CCR-22-0482]
- 30 **Joo S**, Ko ES, Kwon S, Jeon E, Jung H, Kim JY, Chung MJ, Im YH. Multimodal deep learning models for the prediction of pathologic response to neoadjuvant chemotherapy in breast cancer. *Sci Rep* 2021; **11**: 18800 [PMID: 34552163 DOI: 10.1038/s41598-021-98408-8]
- 31 **Gong C**, Cheng Z, Yang Y, Shen J, Zhu Y, Ling L, Lin W, Yu Z, Li Z, Tan W, Zheng C, Zheng W, Zhong J, Zhang X, Zeng Y, Liu Q, Huang RS, Komorowski AL, Yang ES, Bertucci F, Ricci F, Orlandi A, Franceschini G, Takabe K, Klimberg S, Ishii N, Toss A, Tan MP, Cherian MA, Song E. A 10-miRNA risk score-based prediction model for pathological complete response to neoadjuvant chemotherapy in hormone receptor-positive breast cancer. *Sci China Life Sci* 2022; **65**: 2205-2217 [PMID: 35579777 DOI: 10.1007/s11427-022-2104-3]
- 32 **Ueno T**, Kitano S, Masuda N, Ikarashi D, Yamashita M, Chiba T, Kadoya T, Bando H, Yamanaka T, Ohtani S, Nagai S, Nakayama T, Takahashi M, Saji S, Aogi K, Velaga R, Kawaguchi K, Morita S, Haga H, Ohno S, Toi M. Immune microenvironment, homologous recombination deficiency, and therapeutic response to neoadjuvant chemotherapy in triple-negative breast cancer: Japan Breast Cancer Research Group (JBCRG)22 TR. *BMC Med* 2022; **20**: 136 [PMID: 35462552 DOI: 10.1186/s12916-022-02332-1]
- 33 **van den Ende NS**, Nguyen AH, Jager A, Kok M, Debets R, van Deurzen CHM. Triple-Negative Breast Cancer and Predictive Markers of Response to Neoadjuvant Chemotherapy: A Systematic Review. *Int J Mol Sci* 2023; **24** [PMID: 36769287 DOI: 10.3390/ijms24032969]
- 34 **Haque W**, Verma V, Schwartz MR, Lim B, Mangalampalli N, Butler EB, Teh BS. Neoadjuvant Chemotherapy for Metaplastic Breast Cancer: Response Rates, Management, and Outcomes. *Clin Breast Cancer* 2022; **22**: e691-e699 [PMID: 35193807 DOI: 10.1016/j.clbc.2022.01.006]



Retrospective Study

# Hounsfield units in assessing bone mineral density in ankylosing spondylitis patients with cervical fracture-dislocation

Zhong-Ya Gao, Wei-Lin Peng, Yang Li, Xu-Hua Lu

**Specialty type:** Orthopedics

**Provenance and peer review:**

Unsolicited article; Externally peer reviewed.

**Peer-review model:** Single blind

**Peer-review report's classification**

**Scientific Quality:** Grade C

**Novelty:** Grade B

**Creativity or Innovation:** Grade B

**Scientific Significance:** Grade B

**P-Reviewer:** Oommen AT

**Received:** March 2, 2024

**Revised:** May 29, 2024

**Accepted:** June 19, 2024

**Published online:** August 16, 2024

**Processing time:** 125 Days and 9.9 Hours



**Zhong-Ya Gao, Wei-Lin Peng, Yang Li, Xu-Hua Lu**, Department of Orthopaedics, Shanghai Changzheng Hospital, Naval Medical University, Shanghai 200003, China

**Co-first authors:** Zhong-Ya Gao and Wei-Lin Peng.

**Corresponding author:** Xu-Hua Lu, PhD, Doctor, Department of Orthopaedics, Shanghai Changzheng Hospital, Naval Medical University, No. 415 Fengyang Road, Shanghai 200003, China. [xuhualu415@163.com](mailto:xuhualu415@163.com)

## Abstract

### BACKGROUND

Cervical spine fracture-dislocations in patients with ankylosing spondylitis (AS) are mostly unstable and require surgery. However, osteoporosis, one of the comorbidities for AS, could lead to detrimental prognoses. There are few accurate assessments of bone mineral density in AS patients.

### AIM

To analyze Hounsfield units (HUs) for assessing bone mineral density in AS patients with cervical fracture-dislocation.

### METHODS

The HUs from C2 to C7 of 51 patients obtained from computed tomography (CT) scans and three-dimensional reconstruction of the cervical spine were independently assessed by two trained spinal surgeons and statistically analyzed. Inter-reader reliability and agreement were assessed by interclass correlation coefficient.

### RESULTS

The HUs decreased gradually from C2 to C7. The mean values of the left and right levels were significantly higher than those in the middle. Among the 51 patients, 25 patients (49.02%) may be diagnosed with osteoporosis, and 16 patients (31.37%) may be diagnosed with osteopenia.

### CONCLUSION

The HUs obtained by cervical spine CT are feasible for assessing bone mineral density with excellent agreement in AS patients with cervical fracture-dislocation.

**Key Words:** Hounsfield unit; Ankylosing spondylitis; Fracture-dislocation; Cervical spine;

Osteoporosis

©The Author(s) 2024. Published by Baishideng Publishing Group Inc. All rights reserved.

**Core Tip:** In this study, we analyzed Hounsfield units (HU) for assessing bone mineral density in patients with ankylosing spondylitis who developed cervical spine fracture-dislocation. The HU obtained by cervical spine computed tomography are feasible for assessing bone mineral density with excellent agreement. Subsequently, by analyzing the HU, we described the distribution of vertebral HU in ankylosing spondylitis patients with cervical fracture-dislocation. Among the 51 cervical fracture-dislocation patients with AS, 25 patients (49.02%) were diagnosed with osteoporosis, whereas 16 patients (31.37%) were diagnosed with osteopenia.

**Citation:** Gao ZY, Peng WL, Li Y, Lu XH. Hounsfield units in assessing bone mineral density in ankylosing spondylitis patients with cervical fracture-dislocation. *World J Clin Cases* 2024; 12(23): 5329-5337

**URL:** <https://www.wjgnet.com/2307-8960/full/v12/i23/5329.htm>

**DOI:** <https://dx.doi.org/10.12998/wjcc.v12.i23.5329>

## INTRODUCTION

Ankylosing spondylitis (AS), characterized by syndesmophytes and ankylosis, is an inflammatory spondyloarthropathy that causes spinal stiffness and reduced mobility[1]. Minor trauma can lead to vertebral fractures due to the increased fragility of the spine, as observed in long bones, with cervical fracture-dislocations as the most severe type[2].

Most cervical fracture-dislocations in patients with AS involve the three columns, resulting in extreme instability and inevitable neurological deterioration[3]. Early surgical intervention can significantly enhance neurological recovery, reduce the incidence of complications, and increase the survival rate[4-6]. However, spinal surgeons face challenges when treating cervical fractures in these patients, including high surgical risks, limited control during surgery, a high risk of internal fixation failure, and postoperative refracture[7,8]. One of the underlying complications contributing to these challenges is osteoporosis, which is frequently mentioned but not adequately addressed[9-12].

Therefore, obtaining reliable bone density measurements is essential for guiding treatment in cervical spine fracture patients with AS. Dual-energy X-ray absorptiometry (DXA) is the international gold standard for the diagnosis of osteoporosis. However, DXA has limitations in measuring bone density in patients with AS[12]. Ligamentous calcification, tissue hyperplasia, and bone redundancy at the measurement site can result in normal or even abnormally high bone density values[13]. Quantitative computed tomography (CT) can accurately measure bone density at specific sites, but its high cost and complex operation limits its availability in most hospitals[14].

CT produces Hounsfield units (HU), offering unique advantages in assessing spinal osteoporosis. In addition, they provide a means of evaluating bone density without the requirement of additional tests and patient costs[15]. Hinze[12] highlighted the feasibility of using HU to assess osteoporosis in AS patients requiring surgical treatment, indicating the value of HU assessment in these patients.

Only a few studies have explored the evaluation of osteoporosis in AS patients with cervical fractures. Consequently, we conducted a retrospective study to investigate the HU patterns in cervical vertebrae of these patients and explored the application of HU in assessing their vertebral bone density.

## MATERIALS AND METHODS

### Study design and patient population

This retrospective case study was based on data from AS patients who exhibited cervical spine fracture-dislocation and were admitted to The Second Affiliated Hospital of Naval Medical University between June 2018 and June 2023. The inclusion criteria comprised patients with cervical fractures occurring between C1-C7 and those with completely fused cervical segments due to AS. The exclusion criteria included patients with spinal infection, lack of patient consent, and subjects who had undergone spinal surgery previously.

The study cohort comprised 51 patients (44 males, 7 females). Each patient underwent a CT scan and three-dimensional reconstruction of the cervical spine after injury. Subsequently, patients were immobilized using Halo vests and underwent closed reduction immediately after CT or magnetic resonance imaging examinations. After achieving satisfactory reduction outcomes, patients underwent posterior or combined anterior-posterior surgeries under general anesthesia following successful awake nasotracheal intubation.

The ethics review board of our institution granted approval to conduct this study.

### HU imaging assessments

The HUs of C2-C7 vertebrae were measured with Neusoft PACS system by two trained spinal surgeons using the images from the CT scan and three-dimensional reconstruction of the cervical spine. Three sagittal plane reconstruction images, right, middle, and left, were selected for each vertebra. Each vertebrae were divided into approximately 16 regions, and the HUs were measured within each region, excluding areas of bone abnormality such as cortical bone, bone islands, and blood vessels. A detailed description of the measurement process is provided in [Figure 1](#).

### Statistical and conformity analysis

The HUs were measured and averaged for every region of each vertebrae. Inter-reader reliability and consistency were evaluated using the interclass correlation coefficient (ICC). An ICC greater than 0.7 indicated consistency between the two datasets. SPSS 22.0 software (IBM Corp., Armonk, NY, United States) was used for statistical analysis.

## RESULTS

### Demographics and clinical data

Among the 51 patients enrolled in this study, 25 were diagnosed with low-energy spinal injuries, whereas 26 patients suffered high-energy injuries. Each patient sustained a single spinal segment injury involving the three columns. The fracture-dislocation levels were distributed as follows: C1/2 in 5 patients, C2/3 in 2 patients, C3/4 in 2 patients, C4/5 in 6 patients, C5/6 in 16 patients, and C6/7 in 20 patients. All patients presented with neurological deficits. Detailed demographics and clinical data for the patients are presented in [Table 1](#).

### HU imaging assessments

Of the 306 vertebrae examined, 298 (97.39%) were fully assessable for the HUs. Eight vertebrae were excluded from complete assessment due to severe fractures and dislocations affecting all regions. However, the measurable regions of the eight vertebrae were evaluated, and the outcomes were averaged. Statistical analysis of HUs at the right, middle, and left levels of each vertebrae was conducted by the two spinal surgeons. Detailed information on the data is provided in [Table 2](#).

### Distribution of vertebral HUs

Both readers observed a cascading decrease in HUs from C2 to C7 ([Table 3](#)). At both levels, the highest mean HU values were recorded at C2 (322.83 and 322.10), whereas the lowest values were recorded at C7 (190.20 and 190.41).

In addition, the mean HU values at different levels of the sagittal plane were analyzed. The results showed that the mean HU values of the left (251 and 252) and right (247 and 247) levels were significantly higher than those at the middle level (215 and 216) level for the two readers ( $P < 0.5$ ; [Table 2](#)).

### Reliability and agreement of HUs

The inter-reader reliability was excellent, with ICCs ranging from 0.91 to 0.99 across the cervical spine. The C6 vertebrae exhibited the highest concordance with ICC of 0.99, whereas the C5 vertebrae showed the lowest with an ICC of 0.91 ([Table 3](#)).

## DISCUSSION

In this study, we evaluated bone mineral density using HUs obtained through CT scan and three-dimensional reconstruction of the cervical spine. The findings demonstrated that HUs are a feasible method for accessing bone mineral density assessment in patients with AS who develop cervical spine fracture-dislocation.

CT examination is associated with additional costs and exposure to increased radiation compared to X-ray examination and DXA. However, using HUs to assess bone mineral density offers several advantages. Firstly, CT scan and three-dimensional reconstructions of the cervical spine are routine procedures for all patients with cervical fracture-dislocations and AS, making them accessible with no additional financial burden on patients. Moreover, the reduced risk of secondary nerve damage resulting from displacements eliminate the need for strict positioning and spatial requirements associated with other examinations such as magnetic resonance imaging and DXA[16]. Secondly, with advancements in CT equipment and supporting software, surgeons can quickly obtain high-definition images and measure the vertebral HUs digitally from images without requiring additional training from radiography specialists. In addition, CT scan is an important diagnostic tool for AS with cervical spine fracture-dislocations, helping prevent missed diagnoses and misdiagnoses often encountered with other examination methods[17]. Moreover, HUs, as a tool for assessing bone mineral density, offer users the ability to set regions of interest. This capability helps to avoid inaccuracies caused by osteochondritis, bone islands, and vascular plexus, significantly enhancing the accuracy of bone mineral density in patients with AS [18]. Furthermore, HUs can be used to predict internal fixation loosening and detect changes in bone mineral density[19].

Marques *et al*[20] conducted a cross-sectional study and reported that low-dose CT measurement of the HUs is a feasible method to assess vertebral bone density in r-axSpa (AS), demonstrating excellent inter-reader reliability across C3-L5 by two trained readers. This study, comprising 50 patients with r-axSpa, revealed that the HU values decreased from C3 to C7, with ICCs ranging from 0.90 to 1.00 in cervical vertebrae, consistent with the results of our study. The

Table 1 Demographics and clinical data of 51 ankylosing spondylitis patients with cervical spine fracture-dislocation			
Feature	Male, n = 44	Female, n = 7	Total, n = 51
Age (years)	55.14	59.57	55.4
Injury level			
C1/2	5 (11.36)	0 (0)	5 (9.80)
C2/3	2 (4.55)	0 (0)	2 (3.92)
C3/4	2 (4.55)	0 (0)	2 (3.92)
C4/5	5 (11.36)	1 (14.28)	6 (11.76)
C5/6	13 (29.54)	3 (42.86)	16 (31.37)
C6/7	17 (38.64)	3 (42.86)	20 (39.23)
ASIA grade			
A	2 (4.55)	1 (14.28)	3 (5.88)
B	5 (11.36)	2 (28.58)	7 (13.73)
C	14 (31.82)	3 (42.86)	17 (33.33)
D	23 (52.27)	1 (14.28)	24 (47.06)

Data are n (%). ASIA: American Spinal Injury Association.

Table 2 Hounsfield units from three levels of sagittal plane reconstruction images of two readers						
Segment	Reader 1-Housfield units			Reader 2-Housfield units		
	Right	Middle	Left	Right	Middle	Left
C2	337	296	334	336	297	334
C3	266	228	261	266	229	260
C4	250	215	249	253	215	250
C5	233	198	226	235	198	225
C6	218	181	214	217	182	215
C7	201	173	196	202	174	196
Average	251	215	247	252	216	247

Table 3 Reliability and agreement of Hounsfield units			
Segment	Readers 1-Housfield units	Readers 2-Housfield units	ICC
C2	322.83	322.10	0.96
C3	252.23	251.55	0.94
C4	238.95	239.57	0.96
C5	219.60	218.47	0.91
C6	204.49	205.02	0.99
C7	190.20	190.41	0.98
Average	238.05	237.85	0.93

ICC: Interclass correlation coefficient.

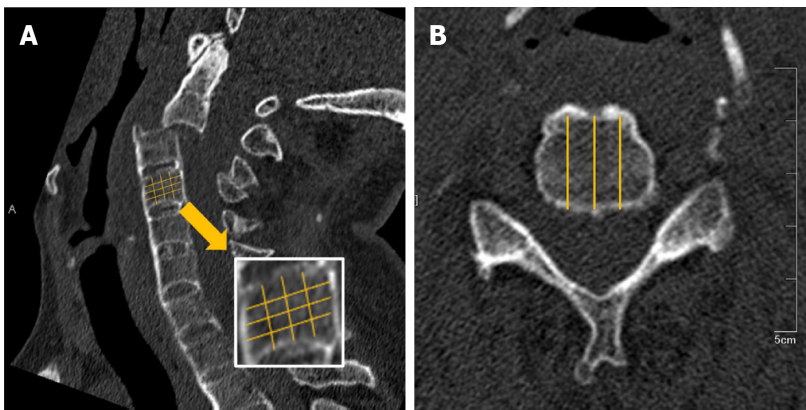


**Figure 1 Hounsfield unit imaging assessments.** A: A 60-year-old male cervical fracture-dislocation patient with ankylosing spondylitis. Using a three-dimensional reconstruction, the middle sagittal plane was selected. Using nine reference lines, every vertebra was equally divided into 16 regions; B: The right, middle, and left sagittal planes were selected according to three reference lines.

distribution pattern of HU values in cervical vertebrae is presented in Table 2. Notably, the HU values gradually decreased from C2 (322) to C7(190), with the lowest ICC observed at C5 (ICC = 0.91), consistent with the results from Marques *et al*[20].

In addition, a comparative analysis of the HUs of three levels showed that the HU values of the left and the right sagittal levels were significantly higher than those at the middle sagittal level. This observation may be attributed to the mechanical support provided by extraspinal bone, which can divert gravitational, emotional, and compressive stresses away from the vertebral trabeculae. This phenomenon results in diminished trabecular density, as predicted by Wolf's law[21].

Swart *et al*[22] provided insights into the mechanism of osteoporosis in AS/diffuse idiopathic skeletal hyperostosis patients, highlighting that HUs were significantly reduced in the middle of long-segment autofusion, consistent with stress shielding. Alexander also emphasized the variation in bone mineral density between fused and unfused segments, a point that was not addressed by Marques *et al*[20]. In our study, all patients were diagnosed with AS with completely fused cervical segments. However, it is essential to recognize that the mechanism of cervical spine injuries may differ in patients with incomplete fusion.

Marques *et al*[20] reported that lower HU values indicated a lower CT attenuation and less dense bones. Despite DXA being the international gold standard for bone mineral density assessment, it has limitations in measuring bone density in patients with AS[12]. Clinical studies have indicated a correlation between the DXA results and the HUs from the same vertebra[23,24]. However, there is no universally accepted standard for diagnosing osteoporosis based on HUs from the cervical spine. Moreover, due to differences in anatomical areas and lack of adequate techniques for cervical bone mineral density, the relationship between DXA results and the HUs from cervical vertebrae remains controversial[25].

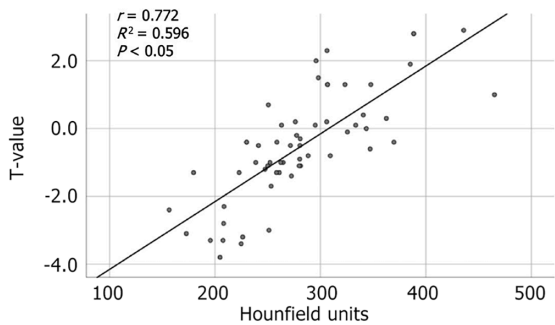
Colantonio *et al*[26] evaluated the relationship between HUs from the C4 vertebra and femur neck bone mineral density, given that the C4 vertebra is considered the least degenerative segment. Han *et al*[27] conducted a retrospective analysis of cervical vertebral HUs and lumbar T-values obtained by DXA in 439 patients. This analysis demonstrated that the C2 and C3 vertebrae exhibited relatively higher correlation values than other subaxial spinal segments. A strong correlation ( $r = 0.64-0.70$ ) was observed between cervical spine HUs and spine DXA results, indicating that cervical spine HUs could be a reliable measure for bone mineral density across different measurement planes, age groups, sex, or degrees of degeneration. In addition, Han *et al*[27] proposed a formula ( $T\text{-score} = 0.01 \times \text{HUs} - 4.55$ ) and suggested cutoff HU values for osteoporosis and osteopenia as 231.5 and 284.0, respectively.

We conducted a retrospective analysis involving 57 patients, excluding patients with AS, diffuse idiopathic skeletal hyperostosis, pathological fractures, and previous spinal surgeries. All the patients underwent a CT scan and three-dimensional reconstruction of the cervical spine within 1 mo of DXA. The method for measuring HUs in C2-C7 vertebrae was consistent with the approach described in the previous studies on AS. Our analysis revealed a strong correlation between HUs in cervical vertebrae and T-scores from DXA ( $r = 0.772$ ) (Figure 2). We determined HU thresholds for osteopenia and osteoporosis to be 274.33 and 228.08, respectively (Table 4), which were consistent with the data reported by Han *et al*[27]. Receiver operation characteristic curves (Figure 3) demonstrated that the HU measurement had a sensitivity of 92.2% and specificity of 87.5% with an area under the curve of 0.931 ( $P < 0.05$ ) in diagnosing osteoporosis and a sensitivity of 80.0% and specificity of 91.7% with an area under the curve of 0.919 ( $P < 0.05$ ) in diagnosing osteopenia.

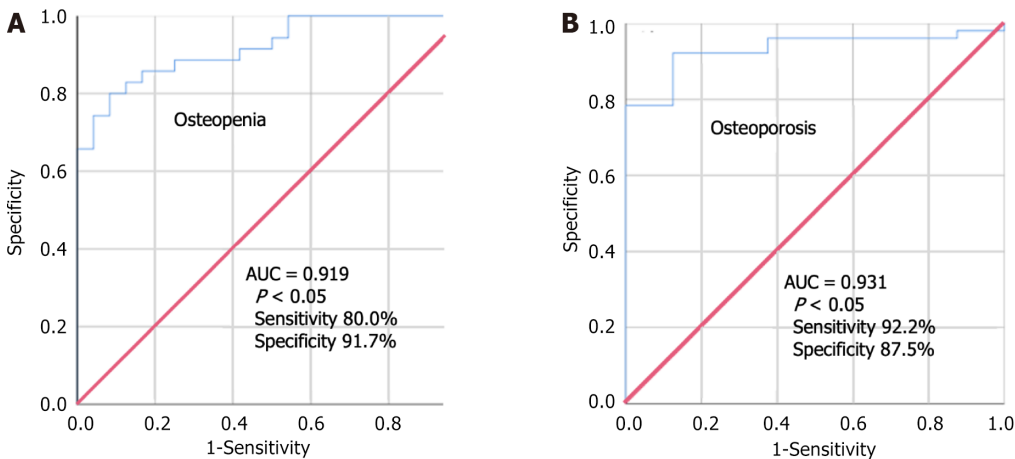
The findings showed that among the 51 cervical fracture-dislocation patients with AS, 25 patients (49.02%) were diagnosed with osteoporosis, whereas 16 patients (31.37%) were diagnosed with osteopenia. These results indicated that the prevalence of osteoporosis is approximately 49.02% among patients with AS who experience cervical spine fracture-dislocation. This prevalence exceeds the reported osteoporosis rate in normal patients with AS, which is 25% as reported by the World Health Organization[28]. This increased prevalence could be attributed to the higher risk of vertebral fracture among AS patients who develop osteoporosis.

Table 4 Hounsfield unit thresholds for osteopenia and osteoporosis		
Bone mineral Density	T-value	HU
Normal	-1 or greater	≤ 274.33
Osteopenia	-1 to -2.5	228.08-274.33
Osteoporosis	-2.5 or less	≤ 228.08

HU: Hounsfield unit.



**Figure 2** Scatter plot showing the correlation between the Hounsfield units obtained from cervical vertebrae and T-values obtained from dual-energy X-ray absorptiometry of the lumbar vertebrae of 59 normal patients. A significant correlation was found ( $r = 0.772$ ,  $r^2 = 0.596$ ,  $P < 0.05$ ).



**Figure 3** Receiver operation characteristic curve to diagnose osteopenia and osteoporosis. A: Hounsfield unit measurement had a sensitivity of 92.2% and specificity of 87.5% with an area under the curve (AUC) of 0.931 ( $P < 0.05$ ) in diagnosing osteopenia; B: Hounsfield unit measurement had a sensitivity of 80.0% and specificity of 91.7% with an AUC of 0.919 ( $P < 0.05$ ) in diagnosing osteoporosis.

It seems contradictory that AS, characterized by aberrant ossification of extraosseous tissues, often coexists with osteoporosis. However, various studies have shown that AS patients have a significantly higher rate of bone loss compared to healthy people, with osteoporosis occurring even in the early stages of the disease[29]. The cause of osteoporosis in association with AS remains controversial, with the most likely scenario involving a combination of several mechanisms leading to bone loss. These mechanisms include genetic factors, chronic inflammation, medication side effects, asymptomatic bowel disease, and a gradual decrease in spinal mobility due to worsening of ankylosing joints. Notably, persistent inflammation that cannot be effectively alleviated by medications is the main predictor of bone loss in these patients[30].

Most elderly AS patients have reduced bone mass, making them susceptible to vertebral fractures from minor trauma [31]. These fractures are often extremely unstable and frequently associated with neurological dysfunction, complex complications, and high mortality rates[32]. Surgical treatment is typically required for most AS patients who develop cervical spine fracture-dislocations[33]. Stronger internal fixations are required for reduction and stabilization due to the spinal fusion and deformity characteristic of AS. However, osteoporosis in the vertebrae of these patients reduces the grip strength for internal fixation, increasing the surgical difficulty for spinal surgeons[34]. Furthermore, patients with cervical fracture-dislocations often suffer from severe cervical cord injuries resulting in quadriplegia. These patients require prolonged postoperative immobilization, which may exacerbate the progression of osteoporosis.

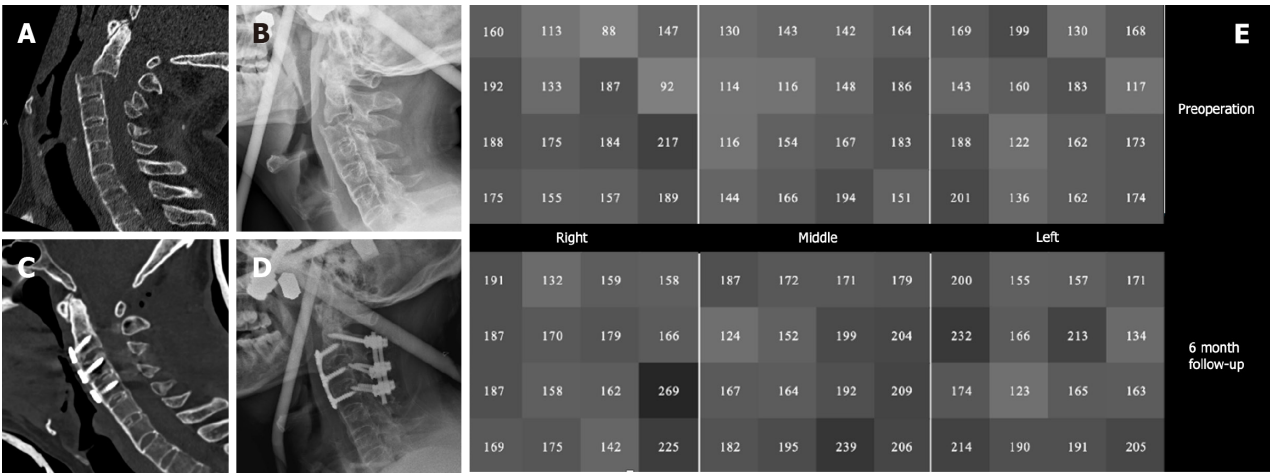


**Figure 4** A 68-year-old man developed paralysis after a traffic accident. A: Preoperative computed tomography suggested ankylosing spondylitis combined with C2/3 fracture-dislocation; B and C: We performed a reduction with a Halo vest and an anterior combined posterior surgery; D: Postoperative bisphosphonates were used for anti-osteoporosis treatment, and cervical computed tomography was repeated at 6 mo postoperatively; E: We calculated the Hounsfield unit values of the C5 vertebra and found that the postoperative Hounsfield unit values (179.67) were significantly higher than preoperative (157.44).

Therefore, initiating anti-osteoporotic therapy for patients with AS is essential. However, current studies indicate that only a few patients, especially those with compromised self-care abilities, received anti-osteoporotic therapy[35]. Clinical guidelines for treating osteoporosis in AS are not available. Bisphosphonates are currently the first-line drugs for osteoporosis treatment. Previous studies demonstrated that bisphosphonates inhibit osteoclast activity, thereby reducing bone destruction. In addition, they have anti-inflammatory properties, which may alleviate inflammation and bone marrow edema in AS patients[30]. Furthermore, tumor necrosis factor inhibitors are effective in treating osteoporosis by increasing bone mineral density and mitigating the progression of AS[36,37]. A bioinformatic analysis study identified 241 overlapping genes associated with AS and osteoporosis. The study proposed carlumab, bermekimab, rilonacept, rilatumumab, and ficalatuzumab as potential drugs for treating osteoporosis[38]. Although progress has been made in studying drugs for osteoporosis treatment in AS, further research should be conducted to explore the optimal anti-osteoporosis treatment regimen.

Furthermore, regular follow-up to evaluate bone mineral destiny is crucial alongside anti-osteoporosis treatment, whereby HU measurements are valuable. We measured and analyzed the HU values of cervical vertebrae in non-operated segments to evaluate the effectiveness of postoperative anti-osteoporotic treatment. Figure 4 illustrates a case of a 68-year-old man who developed paralysis after a traffic accident. Preoperative CT scans indicated AS combined with C2/3 fracture-dislocation. We performed an anterior combined posterior surgery after fixation and repositioning with a Halo vest. Bisphosphonates were administered postoperatively for anti-osteoporosis treatment, and cervical CT scans were conducted for 6 mo after the surgery. The HU values of C5 vertebra showed a significant increase in the postoperative HU value (179.67) compared to the preparative value (157.44), as shown in the gray scale diagram.

This study had some shortcomings. Firstly, most studies on the measurement of cervical HU refer to the methodology established by Schreiber *et al*[24]. In addition, previous research has shown that the average HU of several slices from the same vertebra does not significantly differ from the HU obtained from a single slice[39]. However, in our study, we divided each vertebra into 48 regions to explore the distribution of HUs, which significantly increased the workload. We anticipate leveraging artificial intelligence and upgrading software to streamline this process in future. Secondly, the preliminary diagnostic criteria proposed in this study, based on the relationship between cervical HUs and lumbar T-values obtained from DXA, may not be sufficiently rigorous. Multicenter and large sample clinical studies are required to confirm these findings.

## CONCLUSION

In summary, use of the HUs obtained from cervical spine CT is a feasible approach for assessing bone mineral density in patients with AS who experience cervical spine fracture-dislocation. Although further clinical studies are necessary to refine this approach, it provides a promising and effective method for evaluating bone mineral density of cervical spine.

## ACKNOWLEDGEMENTS

We thank the Second Affiliated Hospital of Naval Medical University for assistance with planning statistical analyses. Gratitude is also extended to the patients who participated in our study, providing invaluable data. In addition, we appreciate the editorial team of this journal for their insightful review and guidance.

## FOOTNOTES

**Author contributions:** Gao ZY and Lu XH contributed to conceptualization; Gao ZY, Li Y, and Peng WL contributed to methodology; Gao ZY and Peng WL contributed to case collection and collation; Gao ZY and Li Y contributed to data statistics and analysis; Gao ZY contributed to writing-original draft preparation; Lu Xa contributed to supervision; Li Y, Peng WL, and Lu XH contributed to review of the manuscript.

**Institutional review board statement:** This study was performed in line with the principles of the Declaration of Helsinki. This study was approved by the Ethics Committee of The Second Affiliated Hospital of Naval Medical University (IRB: 2022-12-0628).

**Informed consent statement:** Both verbal and written informed consent were obtained from all individual participants included in the study.

**Conflict-of-interest statement:** All authors declare no conflicts of interest.

**Data sharing statement:** All data can be obtained from the corresponding author (Xu-Hua Lu, No. 415 Fengyang Road, Shanghai, 200003, China. E-mail address: [xuhualu415@163.com](mailto:xuhualu415@163.com)).

**Open-Access:** This article is an open-access article that was selected by an in-house editor and fully peer-reviewed by external reviewers. It is distributed in accordance with the Creative Commons Attribution NonCommercial (CC BY-NC 4.0) license, which permits others to distribute, remix, adapt, build upon this work non-commercially, and license their derivative works on different terms, provided the original work is properly cited and the use is non-commercial. See: <https://creativecommons.org/licenses/by-nc/4.0/>

**Country of origin:** China

**ORCID number:** Xu-Hua Lu [0009-0004-2537-8293](https://orcid.org/0009-0004-2537-8293).

**S-Editor:** Liu JH

**L-Editor:** Filipodia

**P-Editor:** Zhang XD

## REFERENCES

- Braun J, Sieper J. Ankylosing spondylitis. *Lancet* 2007; **369**: 1379-1390 [PMID: [17448825](#) DOI: [10.1016/S0140-6736\(07\)60635-7](#)]
- Mei J, Hu H, Ding H, Huang Y, Zhang W, Chen X, Fang X. Investigating the causal relationship between ankylosing spondylitis and osteoporosis in the European population: a bidirectional Mendelian randomization study. *Front Immunol* 2023; **14**: 1163258 [PMID: [37359532](#) DOI: [10.3389/fimmu.2023.1163258](#)]
- Graham B, Van Peteghem PK. Fractures of the spine in ankylosing spondylitis. Diagnosis, treatment, and complications. *Spine (Phila Pa 1976)* 1989; **14**: 803-807 [PMID: [2781394](#) DOI: [10.1097/00007632-198908000-00005](#)]
- Huang J, Bai H, Tan Q, Hao D, Wu A, Wang Q, Wang B, Wang L, Liu H, Chen X, Jiang Z, Ma X, Liu X, Liu P, Cai W, Lu M, Mao N, Wang Y, Fu S, Zhao S, Zang X, Xie Y, Yu H, Song R, Sun J, Xiang L, Liu X, Li S, Liao B, Wu Z. Instantaneous death risk, conditional survival and optimal surgery timing in cervical fracture patients with ankylosing spondylitis: A national multicentre retrospective study. *Front Immunol* 2022; **13**: 971947 [PMID: [36189242](#) DOI: [10.3389/fimmu.2022.971947](#)]
- Weinstein PR, Karpman RR, Gall EP, Pitt M. Spinal cord injury, spinal fracture, and spinal stenosis in ankylosing spondylitis. *J Neurosurg* 1982; **57**: 609-616 [PMID: [7131059](#) DOI: [10.3171/jns.1982.57.5.0609](#)]
- Lukasiewicz AM, Bohl DD, Varthi AG, Basques BA, Webb ML, Samuel AM, Grauer JN. Spinal Fracture in Patients With Ankylosing Spondylitis: Cohort Definition, Distribution of Injuries, and Hospital Outcomes. *Spine (Phila Pa 1976)* 2016; **41**: 191-196 [PMID: [26579959](#) DOI: [10.1097/BRS.0000000000001190](#)]
- Lazennec JY, d'Astorg H, Rousseau MA. Cervical spine surgery in ankylosing spondylitis: Review and current concept. *Orthop Traumatol Surg Res* 2015; **101**: 507-513 [PMID: [25863707](#) DOI: [10.1016/j.otsr.2015.02.005](#)]
- An SB, Kim KN, Chin DK, Kim KS, Cho YE, Kuh SU. Surgical outcomes after traumatic vertebral fractures in patients with ankylosing spondylitis. *J Korean Neurosurg Soc* 2014; **56**: 108-113 [PMID: [25328647](#) DOI: [10.3340/jkns.2014.56.2.108](#)]
- Liu J, Zhao L, Yang X, Liu C, Kong N, Yu Y, Xuan D, Wan W, Xue Y. Bone mineral density, bone metabolism-related factors, and microRNA-218 are correlated with disease activities in Chinese ankylosing spondylitis patients. *J Clin Lab Anal* 2022; **36**: e24223 [PMID: [34984723](#) DOI: [10.1002/jcla.24223](#)]
- Meyer B. Editorial. Is a meta-analysis of a few low-level publications helpful in guiding surgical strategies? *Neurosurg Focus* 2021; **51**: E10 [PMID: [34598130](#) DOI: [10.3171/2021.7.FOCUS21432](#)]
- Davey-Ranasinghe N, Deodhar A. Osteoporosis and vertebral fractures in ankylosing spondylitis. *Curr Opin Rheumatol* 2013; **25**: 509-516 [PMID: [23719363](#) DOI: [10.1097/BOR.0b013e3283620777](#)]
- Hinze AM, Louie GH. Osteoporosis Management in Ankylosing Spondylitis. *Curr Treatm Opt Rheumatol* 2016; **2**: 271-282 [PMID: [28620575](#) DOI: [10.1007/s40674-016-0055-6](#)]
- Klingberg E, Lorentzon M, Mellström D, Geijer M, Göthlin J, Hilme E, Hedberg M, Carlsten H, Forsblad-d'Elia H. Osteoporosis in ankylosing spondylitis - prevalence, risk factors and methods of assessment. *Arthritis Res Ther* 2012; **14**: R108 [PMID: [22569245](#) DOI: [10.1186/ar3833](#)]
- Korkosz M, Gąsowski J, Grzanka P, Gorczowski J, Pluskiewicz W, Jeka S, Grodzicki T. Baseline new bone formation does not predict bone loss in ankylosing spondylitis as assessed by quantitative computed tomography (QCT): 10-year follow-up. *BMC Musculoskelet Disord* 2011;

- 12: 121 [PMID: [21627836](#) DOI: [10.1186/1471-2474-12-121](#)]
- 15 **Pickhardt PJ**, Pooler BD, Lauder T, del Rio AM, Bruce RJ, Binkley N. Opportunistic screening for osteoporosis using abdominal computed tomography scans obtained for other indications. *Ann Intern Med* 2013; **158**: 588-595 [PMID: [23588747](#) DOI: [10.7326/0003-4819-158-8-201304160-00003](#)]
- 16 **Schiefer TK**, Milligan BD, Bracken CD, Jacob JT, Krauss WE, Pichelmann MA, Clarke MJ. In-hospital neurologic deterioration following fractures of the ankylosed spine: a single-institution experience. *World Neurosurg* 2015; **83**: 775-783 [PMID: [25545552](#) DOI: [10.1016/j.wneu.2014.12.041](#)]
- 17 **Zhang Z**, Liu C, Hu F, You Y, Hu W, Zhang X. Are Both Preoperative Full-Spine 3Dimensional Computed Tomography Scans and X-Ray Films Necessary for Patients with Ankylosing Spondylitis Kyphosis? *Orthop Surg* 2022; **14**: 2618-2624 [PMID: [36102171](#) DOI: [10.1111/os.13461](#)]
- 18 **Pu M**, Zhang B, Zhu Y, Zhong W, Shen Y, Zhang P. Hounsfield Unit for Evaluating Bone Mineral Density and Strength: Variations in Measurement Methods. *World Neurosurg* 2023; **180**: e56-e68 [PMID: [37544597](#) DOI: [10.1016/j.wneu.2023.07.146](#)]
- 19 **Pickhardt PJ**, Lauder T, Pooler BD, Muñoz Del Rio A, Rosas H, Bruce RJ, Binkley N. Effect of IV contrast on lumbar trabecular attenuation at routine abdominal CT: correlation with DXA and implications for opportunistic osteoporosis screening. *Osteoporos Int* 2016; **27**: 147-152 [PMID: [26153046](#) DOI: [10.1007/s00198-015-3224-9](#)]
- 20 **Marques ML**, Pereira da Silva N, van der Heijde D, Reijnierse M, Baraliakos X, Braun J, van Gaalen FA, Ramiro S. Low-dose CT hounsfield units: a reliable methodology for assessing vertebral bone density in radiographic axial spondyloarthritis. *RMD Open* 2022; **8** [PMID: [35732346](#) DOI: [10.1136/rmdopen-2021-002149](#)]
- 21 **Frost HM**. Wolff's Law and bone's structural adaptations to mechanical usage: an overview for clinicians. *Angle Orthod* 1994; **64**: 175-188 [PMID: [8060014](#) DOI: [10.1043/0003-3219\(1994\)064<0175:WLABSA>2.0.CO;2](#)]
- 22 **Swart A**, Hamouda A, Pennington Z, Lakomkin N, Mikula AL, Martini ML, Shafi M, Subramaniam T, Sebastian AS, Freedman BA, Nassr AN, Fogelson JL, Elder BD. Significant Reduction in Bone Density as Measured by Hounsfield Units in Patients with Ankylosing Spondylitis or Diffuse Idiopathic Skeletal Hyperostosis. *J Clin Med* 2024; **13** [PMID: [38592686](#) DOI: [10.3390/jcm13051430](#)]
- 23 **Choi MK**, Kim SM, Lim JK. Diagnostic efficacy of Hounsfield units in spine CT for the assessment of real bone mineral density of degenerative spine: correlation study between T-scores determined by DEXA scan and Hounsfield units from CT. *Acta Neurochir (Wien)* 2016; **158**: 1421-1427 [PMID: [27177734](#) DOI: [10.1007/s00701-016-2821-5](#)]
- 24 **Schreiber JJ**, Anderson PA, Rosas HG, Buchholz AL, Au AG. Hounsfield units for assessing bone mineral density and strength: a tool for osteoporosis management. *J Bone Joint Surg Am* 2011; **93**: 1057-1063 [PMID: [21655899](#) DOI: [10.2106/JBJS.J.00160](#)]
- 25 **Amin MFM**, Zakaria WMW, Yahya N. Correlation between Hounsfield unit derived from head, thorax, abdomen, spine and pelvis CT and t-scores from DXA. *Skeletal Radiol* 2021; **50**: 2525-2535 [PMID: [34021364](#) DOI: [10.1007/s00256-021-03801-z](#)]
- 26 **Colantonio DF**, Saxena SK, Vanier A, Rodkey D, Tittle S, Wagner SC. Cervical Spine Computed Tomography Hounsfield Units Accurately Predict Low Bone Mineral Density of the Femoral Neck. *Clin Spine Surg* 2020; **33**: E58-E62 [PMID: [31498274](#) DOI: [10.1097/BSD.0000000000000879](#)]
- 27 **Han K**, You ST, Lee HJ, Kim IS, Hong JT, Sung JH. Hounsfield unit measurement method and related factors that most appropriately reflect bone mineral density on cervical spine computed tomography. *Skeletal Radiol* 2022; **51**: 1987-1993 [PMID: [35419706](#) DOI: [10.1007/s00256-022-04050-4](#)]
- 28 **Dubrovsky AM**, Lim MJ, Lane NE. Osteoporosis in Rheumatic Diseases: Anti-rheumatic Drugs and the Skeleton. *Calcif Tissue Int* 2018; **102**: 607-618 [PMID: [29470611](#) DOI: [10.1007/s00223-018-0401-9](#)]
- 29 **El Maghraoui A**. Extra-articular manifestations of ankylosing spondylitis: prevalence, characteristics and therapeutic implications. *Eur J Intern Med* 2011; **22**: 554-560 [PMID: [22075279](#) DOI: [10.1016/j.ejim.2011.06.006](#)]
- 30 **El Maghraoui A**. Osteoporosis and ankylosing spondylitis. *Joint Bone Spine* 2004; **71**: 291-295 [PMID: [15288853](#) DOI: [10.1016/j.jbspin.2003.06.002](#)]
- 31 **Montala N**, Juanola X, Collantes E, Muñoz-Gomariz E, Gonzalez C, Gratacos J, Zarco P, Fernandez Sueiro JL, Mulero J, Torre-Alonso JC, Batlle E, Carmona L. Prevalence of vertebral fractures by semiautomated morphometry in patients with ankylosing spondylitis. *J Rheumatol* 2011; **38**: 893-897 [PMID: [21362760](#) DOI: [10.3899/jrheum.100851](#)]
- 32 **Thumbikat P**, Hariharan RP, Ravichandran G, McClelland MR, Mathew KM. Spinal cord injury in patients with ankylosing spondylitis: a 10-year review. *Spine (Phila Pa 1976)* 2007; **32**: 2989-2995 [PMID: [18091492](#) DOI: [10.1097/BRS.0b013e31815cddfc](#)]
- 33 **Charles YP**, Buy X, Gangi A, Steib JP. Fracture in ankylosing spondylitis after minor trauma: radiological pitfalls and treatment by percutaneous instrumentation. A case report. *Orthop Traumatol Surg Res* 2013; **99**: 115-119 [PMID: [23270725](#) DOI: [10.1016/j.otsr.2012.09.018](#)]
- 34 **Sari I**, Haroon N. Radiographic Progression in Ankylosing Spondylitis: From Prognostication to Disease Modification. *Curr Rheumatol Rep* 2018; **20**: 82 [PMID: [30406859](#) DOI: [10.1007/s11926-018-0795-4](#)]
- 35 **Khosla S**, Hofbauer LC. Osteoporosis treatment: recent developments and ongoing challenges. *Lancet Diabetes Endocrinol* 2017; **5**: 898-907 [PMID: [28689769](#) DOI: [10.1016/S2213-8587\(17\)30188-2](#)]
- 36 **Haroon NN**, Sriganthan J, Al Ghanim N, Inman RD, Cheung AM. Effect of TNF-alpha inhibitor treatment on bone mineral density in patients with ankylosing spondylitis: a systematic review and meta-analysis. *Semin Arthritis Rheum* 2014; **44**: 155-161 [PMID: [24909809](#) DOI: [10.1016/j.semarthrit.2014.05.008](#)]
- 37 **Molnar C**, Scherer A, Baraliakos X, de Hooge M, Micheroli R, Exer P, Kissling RO, Tamborrini G, Wildi LM, Nissen MJ, Zufferey P, Bernhard J, Weber U, Landewé RBM, van der Heijde D, Ciurea A; Rheumatologists of the Swiss Clinical Quality Management Program. TNF blockers inhibit spinal radiographic progression in ankylosing spondylitis by reducing disease activity: results from the Swiss Clinical Quality Management cohort. *Ann Rheum Dis* 2018; **77**: 63-69 [PMID: [28939631](#) DOI: [10.1136/annrheumdis-2017-211544](#)]
- 38 **Wang C**, Wang L, Li Q, Wu W, Yuan J, Wang H, Lu X. Computational Drug Discovery in Ankylosing Spondylitis-Induced Osteoporosis Based on Data Mining and Bioinformatics Analysis. *World Neurosurg* 2023; **174**: e8-e16 [PMID: [36716856](#) DOI: [10.1016/j.wneu.2023.01.092](#)]
- 39 **Schreiber JJ**, Anderson PA, Hsu WK. Use of computed tomography for assessing bone mineral density. *Neurosurg Focus* 2014; **37**: E4 [PMID: [24981903](#) DOI: [10.3171/2014.5.FOCUS1483](#)]



Retrospective Study

## Establishment and performance analysis of a new multiplex detection method for influenza an and B virus antigen

Cheng-Jing Xia, Bao-Hua Li, Yan-Ni Guo, Xiao-He Zhou, Run-Ling Zhang, Ying-No Niu

**Specialty type:** Medical laboratory technology

**Provenance and peer review:**

Unsolicited article; Externally peer reviewed.

**Peer-review model:** Single blind

**Peer-review report's classification**

**Scientific Quality:** Grade C

**Novelty:** Grade B

**Creativity or Innovation:** Grade C

**Scientific Significance:** Grade B

**P-Reviewer:** Daskalakis M

**Received:** April 13, 2024

**Revised:** June 4, 2024

**Accepted:** June 20, 2024

**Published online:** August 16, 2024

**Processing time:** 82 Days and 22.4 Hours



**Cheng-Jing Xia, Bao-Hua Li, Yan-Ni Guo, Xiao-He Zhou, Run-Ling Zhang,** Department of Clinical Laboratory, West Wing, Shenzhen Hospital (Guangming) of University of Chinese Academy of Sciences, Shenzhen 518106, Guangdong Province, China

**Ying-No Niu,** Laboratory, Nanjing Vazyme Biotech Co. Ltd, Nanjing 210033, Jiangsu Province, China

**Corresponding author:** Cheng-Jing Xia, Doctor, Associate Chief Technician, Department of Clinical Laboratory, West Wing, Shenzhen Hospital (Guangming) of University of Chinese Academy of Sciences, No. 4253 Songbai Road, Matian Street, Guangming District, Shenzhen 518106, Guangdong Province, China. [cjxia1976@163.com](mailto:cjxia1976@163.com)

### Abstract

#### BACKGROUND

Influenza A and B virus detection is pivotal in epidemiological surveillance and disease management. Rapid and accurate diagnostic techniques are crucial for timely clinical intervention and outbreak prevention. Quantum dot-encoded microspheres have been widely used in immunodetection. The integration of quantum dot-encoded microspheres with flow cytometry is a well-established technique that enables rapid analysis. Thus, establishing a multiplex detection method for influenza A and B virus antigens based on flow cytometry quantum dot microspheres will help in disease diagnosis.

#### AIM

To establish a codetection method of influenza A and B virus antigens based on flow cytometry quantum dot-encoded microsphere technology, which forms the foundation for the assays of multiple respiratory virus biomarkers.

#### METHODS

Different quantum dot-encoded microspheres were used to couple the monoclonal antibodies against influenza A and B. The known influenza A and B antigens were detected both separately and simultaneously on a flow cytometer, and the detection conditions were optimized to establish the influenza A and B antigen codetection method, which was utilized for their detection in clinical samples. The results were compared with the fluorescence quantitative polymerase chain reaction (PCR) method to validate the clinical performance of this method.

## RESULTS

The limits of detection of this method were 26.1 and 10.7 pg/mL for influenza A and B antigens, respectively, which both ranged from 15.6 to 250000 pg/mL. In the clinical sample evaluation, the proposed method well correlated with the fluorescent quantitative PCR method, with positive, negative, and overall compliance rates of 57.4%, 100%, and 71.6%, respectively.

## CONCLUSION

A multiplex assay for quantitative detection of influenza A and B virus antigens has been established, which is characterized by high sensitivity, good specificity, and a wide detection range and is promising for clinical applications.

**Key Words:** Influenza A; Influenza B; Quantum dot microspheres; Antigen detection; Multiplex detection

©The Author(s) 2024. Published by Baishideng Publishing Group Inc. All rights reserved.

**Core Tip:** Respiratory viruses primarily target and affect the respiratory system, such as the influenza A and B viruses, highly contagious and can spread through various means. The detection of influenza A and B virus antigens is significant for the diagnosis, treatment, and prevention of influenza. In this study, a multiplex detective method for influenza A and B virus antigens was developed using flow cytometry quantum dot microspheres. The multiplex assay is characterized by high sensitivity, good specificity, and a broad detection range, making it a promising tool for clinical applications.

**Citation:** Xia CJ, Li BH, Guo YN, Zhou XH, Zhang RL, Niu YN. Establishment and performance analysis of a new multiplex detection method for influenza an and B virus antigen. *World J Clin Cases* 2024; 12(23): 5338-5345

**URL:** <https://www.wjgnet.com/2307-8960/full/v12/i23/5338.htm>

**DOI:** <https://dx.doi.org/10.12998/wjcc.v12.i23.5338>

## INTRODUCTION

Infections caused by respiratory viruses and their prevention and control are common public health challenges worldwide. The coronavirus disease 2019 pandemic that occurred in recent years has increased the attention of the public, public health agencies, and policy makers worldwide to infections caused by respiratory viruses[1,2]. Because different respiratory viruses and different subtypes of the same virus may have different treatment modalities and preventive and control measures, rapid and accurate identification of these viruses and their subtypes provide not only a sufficient basis for disease diagnosis and treatment but also a solid foundation for epidemiological investigations and prevention and control of outbreaks[3,4]. Therefore, developing a rapid, sensitive, and multiplexed method for the detection of respiratory viruses is necessary. The bead array technology has a unique advantage in multiplexed detection because it can detect multiple viral proteins (antigens or antibodies) in a rapid, high-throughput, parallelized manner[5-7]. The core principle of bead array technology is to use specific molecules linked to differently labeled microspheres to recognize the corresponding detectors; thus, how to prepare encoded microspheres is the key to achieving high-throughput, high sensitivity, and multiplexed detection. Currently, the bead array technology in the market is mainly dominated by Luminex, which is expensive and requires expensive multichannel detection instruments. Compared with traditional dyes, quantum dots (QDs), which have the advantages of broad absorption spectrum, narrow excitation fluorescence spectrum, high luminescence efficiency, adjustable luminescence spectrum with particle size, and good photostability, have gradually become the focus of fluorescence coding particles in bead array[8-12].

In this study, we proposed to develop a multiplex flow cytometry (FCM) detection method for influenza A and Influenza B virus antigens, using QD-encoded microspheres as reaction carriers to establish a multiplex detection of influenza A and Influenza B virus antigens based on the FCM QD-encoded microsphere technology and lay the foundation for the multiplex detection of common respiratory viruses.

## MATERIALS AND METHODS

### Study subjects

In this retrospective study, throat swab samples were collected from 81 patients with suspected respiratory viral infections attending the outpatient clinic of the University of Chinese Academy of Sciences, Shenzhen Hospital (Guangming) West Campus between May and August 2022. Of these patients, 43 were male and 38 were female, aged 1-63 years. Patient samples were clinically diagnosed with influenza A and B virus infections using the colloidal gold antigen detection kit (Guangzhou Wondfo), and the remaining pharyngeal swab samples were frozen at -80°C. Patients with clinical symptomatic manifestations of respiratory viral infections were included, whereas those who had taken anti-

influenza medications within 1 month before sampling were excluded.

### Instruments and reagents

DxFlex flow cytometer (Beckman Coulter, CA, United States); ABI 7,500 real-time fluorescence quantitative polymerase chain reaction (PCR) instrument (Life Technologies, CA, United States); influenza A and B virus NP proteins, influenza A virus NP protein monoclonal antibodies (clone nos. FluA6 and FluA8), influenza B virus NP protein monoclonal antibodies (clone nos. FluB15, FluB66, and FluB79) were obtained from Nanjing Novozymes Medical Technology Co., Ltd. (China). Influenza A virus NP protein monoclonal antibodies (clone nos. FluB15, FluB66, and FluB79) are from Nanjing Novozymes Medical Technology Co., Ltd. Microspheres and QD reagents included fluorescence-encoded microspheres (Bangs Laboratories, Inc., IN, United States), polystyrene microspheres (Suzhou Institute of Nano-Tech and Nano-Bionics, China), CdSe/ZnS QD nanocrystals (Wuhan Jiayuan, China). N-hydroxysuccinimide N-hydroxysuccinimide (sulfo-NHS), 1-ethyl-3-(3-dimethylaminopropyl) carbodiimide hydrochloride (EDC), and 2-morpholine ethanesulfonic acid (MES) (Sigma Aldrich, MA, United States); biotin labeling kit (Thermo Fisher Scientific, MA, United States); flow cytometer quality control microspheres and flow cytometer sheath solution (Beckman Coulter); and fluorescence quantitative PCR reagents and consumables (Daan Gene Co., Ltd., China).

### Methods

**QD-encoded microsphere detection system construction:** (1) For QD-encoded microsphere preparation, polystyrene microspheres were firstly dissolved, and then fluorescent staining was performed by adding different concentrations of CdSe/ZnS QDs in the dissolution system. The microspheres were transferred from the organic-phase dissolution system to the aqueous-phase preservation system after staining. By adjusting the concentration ratio of QDs and polystyrene microspheres, multi-peak QD-encoded microspheres with different brightness could be obtained. Because polystyrene microspheres have a carboxyl group modification on the surface, they can be used for subsequent antibody coupling; (2) For antibody coupling to microspheres, the microsphere concentration was first determined using a blood counting plate, then approximately one million microspheres were removed for activation, and the microspheres were washed to MES buffer as the activation system. After rapid addition of EDC (0.2 mg) and sulfo-NHS (0.2 mg) to the microspheres, they were vortexed rapidly for 10 s and placed on a turnover mixer to react for 20 min. The activated microspheres were washed twice using MES buffer, and the antibody was added, rapidly vortexed for 10 s, and placed on a turnover mixer for 2 hours. The coupled microspheres were washed, the concentration was determined, the yield was calculated, and coupling was confirmed. To compare the performance of different antibodies, different mouse anti-influenza A/B virus NP protein monoclonal antibodies (clone no. Flu A6, Flu A8, Flu B15, Flu B66, and Flu B79) were coupled to select the optimal combination of antibody pairs in subsequent tests; and (3) In the preparation of biotinylated antibodies, the ultrafiltration column was initially used to replace the influenza A and B antibodies into the phosphate-buffered saline solution, and then the concentrations of influenza A and B antibodies were measured. The biotinylated reagent was added to the solution-exchanged antibody, mixed upside down for 10 s, and then turned over and mixed for 1 h at room temperature to complete the biotin labeling of the antibody. After the reaction, the reaction product was purified using an ultrafiltration column to remove the unreacted biotinylated reagent, and the concentration of the biotinylated antibody was then determined using an enzyme marker. The concentration of biotin (B) bound to IgG was determined by the HABA reaction, and the molar ratio (B/P) of biotin to IgG antibody (P) was then calculated.

**Performance testing of the single test for influenza A and B virus antigens:** The development of the encoded microsphere-based multiple detection method for influenza A and B virus antigens requires the establishment and validation of a single test for influenza A and B antigens, and the single test must be subjected to cotesting of this single test method.

The influenza A antigen single test mainly consists of the following steps: (1) Preparation of standards: Dilute the influenza A antigen masterbatch to a series of concentrations such as  $1 \times 10^6$ ,  $2 \times 10^5$ , 40000, 8000, 1600, 320, 64, 12.8, and 2.56 pg/mL by serial dilution; (2) Immunoassay: Add the diluent, standards/samples, and biotinylated antibody for detection of influenza A antigen, and capture the microspheres coupled to the antibody for the influenza A antigen to a 96-well filtration plate. After incubation for 2.5 hours away from light, add streptavidin-phycoerythrin and incubate for 0.5 hours away from light, then use a vacuum filtration device for filtration, and use a cleaning solution two times, and resuspend the microspheres into the cleaning solution for testing; (3) Testing and data processing: The flow cytometer was used to collect data from each microsphere, and the obtained median fluorescence intensity (MFI) data were imported into GraphPad Prism software for analysis; and (4) A calibration curve was drawn between a series of MFI values of the standards and the concentration of the standards, and the concentration of samples was deduced using the calibration curve. The steps for the single test for influenza B virus antigens were the same as those for influenza A virus, with different antibodies only. The initial performance evaluation of the single test method mainly included the measurement range and cross-reactivity. By observing the distribution of different concentrations of standards on the calibration curve, the measurement range of the method for influenza A and B antigens concentration was determined.

**Performance test of influenza A and B virus antigens codetection:** The codetection test of influenza A and B antigens is based on a single detection test in which two types of capture microspheres of influenza A and B viruses and two types of biotinylated detection antibodies of influenza A and B viruses are directly added to the same reaction system to establish the formation of the detection sandwich of influenza A and B virus antigens, respectively, at the same time, and ultimately output the fluorescence signal of the antigens on the flow cytometer using the encoded microspheres as the medium. The fluorescence signals of the influenza A and B detection microspheres were then used to obtain the results of the calibration curves and sample concentrations (Figure 1). Referring to the description of the relevant literature[12,13], a

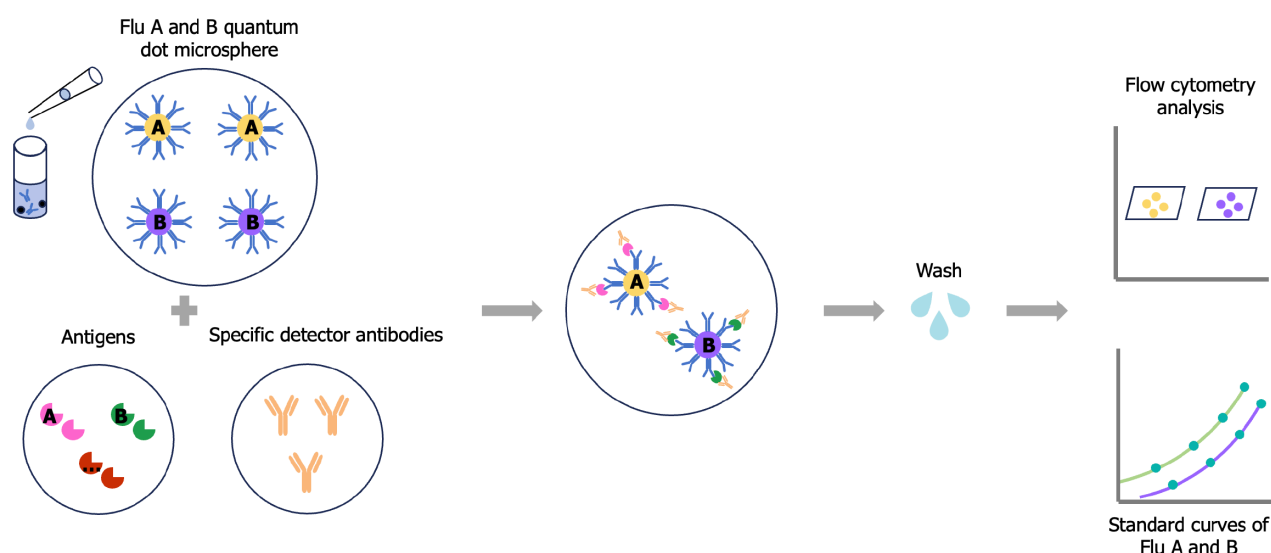


**Figure 1** Schematic diagram of the principle of quantum dot encoded microsphere-based multiplexed detection of Influenza A and B virus antigens.

performance evaluation was performed on QD microsphere-based codetection methods, including detection limit, measurement range, and cross-reactivity.

**Validation and method comparison of clinical samples on an FCM QD microsphere technology-based influenza A and B codetection platform:** The clinical pharyngeal swab samples stored at  $-80^{\circ}\text{C}$  were thawed at room temperature for 30 minutes, then added with 500  $\mu\text{L}$  of extraction solution, and rotated along the wall of the tube for approximately 10 times to dissolve the specimens into the extraction solution as much as possible. The extracted sample solution was divided into two: one was used for this method and the other for nucleic acid detection by real-time fluorescence quantitative PCR (the specific procedure was performed in accordance with the instructions for the use of the reagents). The detection limit of the influenza A and B virus antigen detection was used as the critical value for negative and positive judgments, and the negative and positive results were compared with those of PCR to analyze the clinical sensitivity and specificity.

### Statistical analysis

The results were statistically analyzed using Microsoft Excel. Measurement information was expressed as mean  $\pm$  SD and  $\text{CV} = 100\% \times s/x$ . The standard curves were plotted using GraphPad Prism 9 software.

## RESULTS

### Preparation of reagent raw materials

By the solvent-embedding method, a set of fluorescent microspheres based on QD encoding was obtained. FCM analyses showed that the fluorescent microspheres had good clustering performance; theoretically, the simultaneous detection of six analytes could be achieved (Figure 2). To demonstrate the feasibility of antibody coupling, conventional fluorescent dye-based encoded microspheres, BAL1 and BAL2, were first used to couple with influenza A and B antibodies, whereas a species-specific fluorescent-labeled antibody (FITC-Donkey-anti-mouse IgG at a concentration of 10  $\mu\text{g}/\text{mL}$ ) was used for labeling the coupled microspheres, and the relevant characterization parameters were determined (Table 1), which were consistent with previously reported coupling results[14,15]. On the basis of the results, QD-encoded microspheres were used for the labeling of antibodies against influenza A and B, and the relevant characterization parameters were also determined. As a result, the microsphere recovery and antibody coverage and coupling uniformity (CV%) after antibody coupling were good and could be used for subsequent detection. The overall recoveries of biotinylated antibodies before and after labeling were 55%–70%. The B/P of the biotinylated antibodies to influenza A and B viruses was between 4 and 6, which are consistent with the ideal labeling results reported previously[16], proving that these reagents can meet the needs of subsequent tests.

### Preliminary assessment of influenza A and B virus antigen detection performance

In the early stage of the study, to explore the feasibility of the single detection technique for influenza A and B virus antigens, BAL1- and BAL2-encoded microspheres were initially used for the preliminary establishment of the performance, and parameters such as the antibody concentration, 1-Stearoyl-2-arachidonoyl-sn-glycero-3-phosphorylethanolamine dye quantity, incubation time, and incubation steps, were optimized, and analytical performances, such as the

Table 1 Characterization parameters of microsphere coupling			
	Microsphere recovery, %	MEFL value	CV, %
BAL1, BAL2	> 80	$2 \times 10^5$ - $6 \times 10^5$	< 25
Quantum dot microspheres	> 80	$1 \times 10^6$ - $1.5 \times 10^6$	< 25

BAL1: B-aggressive lymphoma 1; BAL2: B-aggressive lymphoma 2; MEFL: Molecules of equivalent fluorescein; CV: Coefficient of variation.

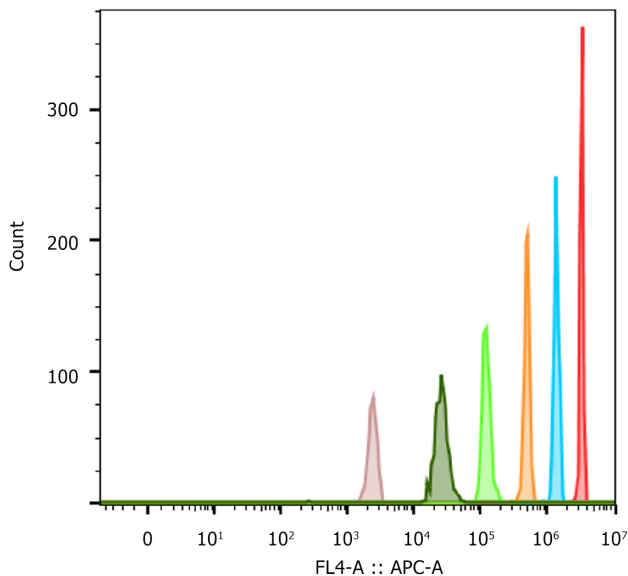


Figure 2 Histogram of fluorescence intensity of six quantum dot encoded microspheres with different brightness.

measurement range, and cross-reactivity, were also initially investigated. These research results laid the technical foundation of the microsphere multiplex immunoassay. In the preliminary study, the measurement range of influenza A and B combined assay was  $7.81\text{--}1 \times 10^6$  pg/mL, and the signal generated by influenza A antigens on influenza B capture microspheres at a concentration of  $2 \times 10^5$  pg/mL was 0.21%. Influenza B antigen at a concentration of  $2 \times 10^5$  pg/mL produced a signal of 0.01% on influenza A capture microspheres (Table 2). These results demonstrate that the method can be used for the simultaneous detection of influenza A and B virus antigens. Thereafter, BAL1- and BAL2-encoded microspheres were replaced with QD-encoded microspheres, and a preliminary sensitivity assessment was performed for the single detection of influenza A and B virus antigens. The blank limits of the single test system using QD-encoded microspheres were 10.5 and 2.9 pg/mL for the detection of influenza A and B virus antigens, respectively.

**Analytical performance of influenza A and B virus antigen codetection**

On the basis of the above preliminary study, a QD-encoded microsphere-based codetection method for influenza A and B virus antigens was established, and a systematic study of sensitivity and measurement range was then performed. The calibration curve of influenza A and B antigen codetection is shown in Figure 3. The detection limit of the multiplexed detection system using QD-encoded microspheres was 26.1 (range,  $15.6\text{--}2.5 \times 10^5$  pg/mL) for the detection of influenza A antigens. The detection limit of the detection of influenza B antigens was 10.7 (range,  $15.6\text{--}2.5 \times 10^5$ ) pg/mL.

**Comparison of multiple detection methods with fluorescent quantitative PCR results**

Based on the analytical performance study, the results of the multiple detection of influenza A and B virus antigens were compared with those of fluorescent quantitative PCR influenza A and B nucleic acid detection. Among the 81 samples, 54 were positive in the influenza A PCR (Table 3), with CT values ranging from 25.59 to 39.12, and 27 samples were negative in the influenza A PCR, with CT values > 40. The results of the QD-encoded microsphere-based detection of influenza A virus antigens showed that 31 samples were positive for influenza A antigens, with concentrations ranging from 26.1 to 83,019.1 pg/mL, and 50 samples were negative for influenza A antigens, with detected concentrations < 26.1 pg/mL. Accordingly, a positive compliance rate (sensitivity) of 57.4%, negative compliance rate (specificity) of 100%, and overall compliance rate of 71.6% were calculated, which is superior to the currently commonly used clinical reagents for colloidal gold antigen detection, such as Wondfo’s positive compliance rate of 56.49% and a negative compliance rate of 99.75% (taken from the instructions for the reagent). Among the 81 samples, one was positive in the PCR for influenza B, with a CT value of 36.5, which was also positive in the multiplex method, with a concentration of 261.2 pg/mL of influenza B antigens, and the remaining 80 samples negative in the PCR for influenza B were also fully compatible with this multiplex method, with a sensitivity and specificity of 100%.

**Table 2** Cross-reactivity results of influenza A and B antigens detection

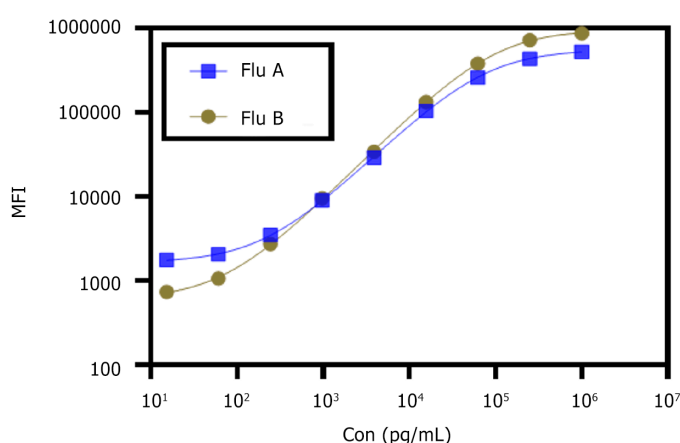
Microspheres	Proteins concentration (pg/mL)		Cross-reaction rate, %
	Influenza B NP proteins	Influenza A NP proteins	
Influenza A	$2 \times 10^5$		0.01
	$1 \times 10^6$		0.01
Influenza B		$2 \times 10^5$	0.21
		$1 \times 10^6$	0.16

NP: Nucleoprotein.

**Table 3** Comparison of the results of the multiple detection of influenza A and B antigens and polymerase chain reaction influenza A and B nucleic acid detection results

Antigen multiplexing detection	q-PCR assay		Sensitivity, %	Idiosyncrasy, %
	Positive	Negative		
Influenza A virus				
Positive	31	0	57.4	100
Negative	23	27		
Influenza B virus				
Positive	1	0	100	100
Negative	0	80		

q-PCR: Quantitative polymerase chain reaction.

**Figure 3** Calibration curve for fluorescence detection of influenza A and B virus antigens. MFI: Median fluorescence intensity.

## DISCUSSION

In this study, a QD-encoded microsphere FCM immunoassay method for influenza A and B virus antigens was developed. Multiple QD-encoded microspheres, antibody coupled encoded microspheres, and biotinylated antibodies were successfully prepared, and their analytical performances, such as sensitivity, measurement range, and cross-reactivity, for the influenza A and B antigen detection were investigated. The results confirmed that the codetection method can be used for the subsequent testing of clinical samples. In response to the problems of QD leakage and fluorescence intensity fluctuations encountered during development and testing, QD-encoded microspheres with long-term stability were obtained by optimizing the solvent system, preservation conditions, and surface modification.

In a test of 81 clinical samples, 31 positive samples and 50 negative samples for influenza were measured using this method. When compared with the results of the fluorescent quantitative PCR, the negative and positive compliance rates were 100% and 57.4%, respectively. This indicates that this method is effective in avoiding false-positive results; however,

for false-negative results, it suggests an inherent difference in the detection sensitivity between immunoassays and nucleic acid detection methods[3,17,18], which is due to the ability of PCR amplification to detect very low amounts of nucleic acid sequences and maybe because this method requires further optimization to improve the sensitivity. Subsequent optimization of the conditions can be referred to the protocol of multiple microspheres[19], where the sensitivity can be improved by decreasing the initial incubation volume of microspheres and samples, increasing the initial incubation time, decreasing the amount of capture antibody coupled to microspheres, and screening for antibodies with a higher affinity to be used as capture or detection antibodies to achieve increased sensitivity. On the contrary, PCR is used to determine viral nucleic acid sequences, which may also produce positive results for inactive viruses, with a certain false-positive rate. Quantitative immunological assays are more effective in assessing changes in viral activity status and viral load and have fewer false-positive results, making them valuable not only for diagnosis but also for determining disease severity and prognosis. In addition, the clinical samples used were secondary eluates performed on pharyngeal swab samples that had already undergone primary extract elution; thus, their results may have a greater likelihood of false-negative results relative to PCR, which also exceeds the sensitivity and specificity of the colloidal gold immunoassay when compared with detection by colloidal gold immunoassay after the first elution. This demonstrates the superiority of the method. Follow-up research work is needed to evaluate the antigen concentrations in real pharyngeal swab samples to obtain more complete data for performance studies. Meanwhile, very few influenza B virus-positive samples resulted in the evaluation of the sensitivity of this method for influenza B virus to be verified by more positive specimens; however, the specificity also reached 100% in comparison with PCR, which was consistent with the results for influenza A, proving the feasibility of this method in multiplex detection. As its main advantage, this method can be used for multiplex detection of respiratory viruses using the FCM detection platform, which is also the direction of our next research.

As study limitations, FCM QD microspheres are not sensitive enough compared with PCR; thus, more clinical samples are needed to validate the method.

## CONCLUSION

This study demonstrated the feasibility of using QD-encoded microsphere for codetection of influenza A and B viruses. Therefore, we will continue to work on the development of immunoassays for various respiratory viruses and develop them into a rapid diagnostic technology platform that can be used for the immediate detection of multiple viruses by taking advantage of the unique advantages of QD-encoded microspheres to make rapid respiratory viruses testing more affordable, easy to use, and universally accessible.

## FOOTNOTES

**Author contributions:** Xia CJ contributed to the manuscript writing, data collection and analysis; Xia CJ, Li BH, Guo YN, Zhou XH, Zhang RL and Niu YN collected data; Xia CJ and Niu YN were involved in the conceptualization and supervision of this manuscript; and all authors approved the final manuscript.

**Supported by** Shenzhen Guangming District Soft Science Research Project, No. 2021R01097.

**Institutional review board statement:** This study was approved by the Ethic Committee of West Wing, Shenzhen Hospital (Guangming) of University of Chinese Academy of Sciences.

**Informed consent statement:** Patients were not required to give informed consent to the study because the analysis used anonymous clinical data that were obtained after each patient agreed to treatment by written consent.

**Conflict-of-interest statement:** We have no financial relationships to disclose.

**Data sharing statement:** No additional data are available.

**Open-Access:** This article is an open-access article that was selected by an in-house editor and fully peer-reviewed by external reviewers. It is distributed in accordance with the Creative Commons Attribution NonCommercial (CC BY-NC 4.0) license, which permits others to distribute, remix, adapt, build upon this work non-commercially, and license their derivative works on different terms, provided the original work is properly cited and the use is non-commercial. See: <https://creativecommons.org/licenses/by-nc/4.0/>

**Country of origin:** China

**ORCID number:** Cheng-Jing Xia 0009-0009-7228-5053.

**S-Editor:** Liu JH

**L-Editor:** A

**P-Editor:** Zhang XD

## REFERENCES

- 1 **Qiu J.** Covert coronavirus infections could be seeding new outbreaks. *Nature* 2020 [PMID: 32203376 DOI: 10.1038/d41586-020-00822-x]
- 2 **Xu XL, Ge SW, Chen CN, Wei M, Fu JY.** Analysis of etiology and epidemic characteristics of children respiratory tract virus infection in Shijiazhuang area. *Xiandai Jianyan Yixue Zazhi* 2021; **36**: 140-143 [DOI: 10.3969/j.issn.1671-7414.2021.02.033]
- 3 **Zhang N, Wang L, Deng X, Liang R, Su M, He C, Hu L, Su Y, Ren J, Yu F, Du L, Jiang S.** Recent advances in the detection of respiratory virus infection in humans. *J Med Virol* 2020; **92**: 408-417 [PMID: 31944312 DOI: 10.1002/jmv.25674]
- 4 **Lu X, Wang Q, Zhang Y.** Detection of respiratory viruses by multiplex RT-PCR with a GeXP analyzer. *Int J Infect Dis* 2014; **21**: 444 [DOI: 10.1016/j.ijid.2014.03.1336]
- 5 **Graham H, Chandler DJ, Dunbar SA.** The genesis and evolution of bead-based multiplexing. *Methods* 2019; **158**: 2-11 [PMID: 30659874 DOI: 10.1016/j.ymeth.2019.01.007]
- 6 **Dincer C, Bruch R, Kling A, Ditttrich PS, Urban GA.** Multiplexed Point-of-Care Testing - xPOCT. *Trends Biotechnol* 2017; **35**: 728-742 [PMID: 28456344 DOI: 10.1016/j.tibtech.2017.03.013]
- 7 **Rho J, Jang W, Hwang I, Lee D, Lee CH, Chung TD.** Multiplex immunoassays using virus-tethered gold microspheres by DC impedance-based flow cytometry. *Biosens Bioelectron* 2018; **102**: 121-128 [PMID: 29128714 DOI: 10.1016/j.bios.2017.11.027]
- 8 **Bian F, Sun L, Cai L, Wang Y, Zhao Y.** Quantum dots from microfluidics for nanomedical application. *Wiley Interdiscip Rev Nanomed Nanobiotechnol* 2019; **11**: e1567 [PMID: 31257723 DOI: 10.1002/wnan.1567]
- 9 **Cheng Y, Ling SD, Geng Y, Wang Y, Xu J.** Microfluidic synthesis of quantum dots and their applications in bio-sensing and bio-imaging. *Nanoscale Adv* 2021; **3**: 2180-2195 [PMID: 36133767 DOI: 10.1039/d0na00933d]
- 10 **Şahin S, Ünlü C, Trabzon L.** Affinity biosensors developed with quantum dots in microfluidic systems. *Emergent Mater* 2021; **4**: 187-209 [PMID: 33718778 DOI: 10.1007/s42247-021-00195-5]
- 11 **Singh S, Dhawan A, Karhana S, Bhat M, Dinda AK.** Quantum Dots: An Emerging Tool for Point-of-Care Testing. *Micromachines (Basel)* 2020; **11** [PMID: 33260478 DOI: 10.3390/mi11121058]
- 12 **Li J, Liu H, Han JX, Hou WJ, Sun ZZ, Fu Y, Yang BC, Shi ZH.** Preparation and performance evaluation on novel corona virus (SARS-CoV-2) S1 antigen quantum dots fluorescence immunoassay reagent. *Xiandai Jianyan Yixue Zazhi* 2022; **37**: 148-152 [DOI: 10.3969/j.issn.1671-7414.2022.02.030]
- 13 **Tan YH, Cao CL, Zhang RF, Pan XF, Li GC, She HJ, Liang TC, Feng JM.** Establishment and performance evaluation of a time-resolved fluorescence immunoassay for the detection of placental growth Factor. *Xiandai Jianyan Yixue Zazhi* 2023; **38**: 112-116+146 [DOI: 10.3969/j.issn.1671-7414.2023.01.021]
- 14 **Clotilde LM, Bernard C 4th, Salvador A, Lin A, Lauzon CR, Muldoon M, Xu Y, Lindpaintner K, Carter JM.** A 7-plex microbead-based immunoassay for serotyping Shiga toxin-producing Escherichia coli. *J Microbiol Methods* 2013; **92**: 226-230 [PMID: 23228591 DOI: 10.1016/j.mimet.2012.11.023]
- 15 **de Jager W, te Velthuis H, Prakken BJ, Kuis W, Rijkers GT.** Simultaneous detection of 15 human cytokines in a single sample of stimulated peripheral blood mononuclear cells. *Clin Diagn Lab Immunol* 2003; **10**: 133-139 [PMID: 12522051 DOI: 10.1128/cdli.10.1.133-139.2003]
- 16 **Hermanson GT.** Bioconjugate Techniques. 2013 [DOI: 10.1016/C2009-0-64240-9]
- 17 **Vemula SV, Zhao J, Liu J, Wang X, Biswas S, Hewlett I.** Current Approaches for Diagnosis of Influenza Virus Infections in Humans. *Viruses* 2016; **8**: 96 [PMID: 27077877 DOI: 10.3390/v8040096]
- 18 **Zhang Y, Zhou ZQ, Wang ZX, Li Y, Xiao M, Xu YC, Wang H.** Discussion on the clinical value of combined detection of SARS-CoV-2 nucleic acid, antigen and antibody. *Xiandai Jianyan Yixue Zazhi* 2020; **35**: 99-102, 109 [DOI: 10.3969/j.issn.1671-7414.2020.05.025]
- 19 **Das S, Dunbar S.** Multiplex Immunoassay Approaches Using Luminex® xMAP® Technology for the Study of COVID-19 Disease. *Adv Exp Med Biol* 2023; **1412**: 479-489 [PMID: 37378784 DOI: 10.1007/978-3-031-28012-2\_26]

## Retrospective Study

# Evaluating the role of interleukin-2 and interleukin-12 in pediatric patients with concurrent *Mycoplasma pneumoniae* and Epstein-Barr virus infections

Yan-Ping Hao

**Specialty type:** Pediatrics**Provenance and peer review:**

Unsolicited article; Externally peer reviewed.

**Peer-review model:** Single blind**Peer-review report's classification****Scientific Quality:** Grade B**Novelty:** Grade B**Creativity or Innovation:** Grade B**Scientific Significance:** Grade B**P-Reviewer:** Ordoñez-González I, Mexico**Received:** April 29, 2024**Revised:** May 24, 2024**Accepted:** June 11, 2024**Published online:** August 16, 2024**Processing time:** 67 Days and 6.5 Hours**Yan-Ping Hao**, Department of Pediatrics, Maternal and Child Health Hospital, Shaoxing 312400, Zhejiang Province, China**Corresponding author:** Yan-Ping Hao, MBBS, Doctor, Department of Pediatrics, Maternal and Child Health Hospital, No. 261 Shanhu Road, Shengzhou, Shaoxing 312400, Zhejiang Province, China. [yanpingh0021@163.com](mailto:yanpingh0021@163.com)

## Abstract

### BACKGROUND

*Mycoplasma pneumoniae* (MP) frequently causes respiratory infections in children, whereas Epstein-Barr virus (EBV) typically presents subclinical manifestations in immunocompetent pediatric populations. The incidence of MP and EBV co-infections is often overlooked clinically, with the contributory role of EBV in pulmonary infections alongside MP remaining unclear.

### AIM

To evaluate the serum concentrations of interleukin-2 (IL-2) and interleukin-12 (IL-12) in pediatric patients with MP pneumonia co-infected with EBV and assess their prognostic implications.

### METHODS

We retrospectively analyzed clinical data from patients diagnosed with MP and EBV co-infection, isolated MP infection, and a control group of healthy children, spanning from January 1, 2018 to December 31, 2021. Serum IL-2 and IL-12 levels were quantified using enzyme-linked immunosorbent assay. Logistic regression was employed to identify factors influencing poor prognosis, while receiver operating characteristic (ROC) curves evaluated the prognostic utility of serum IL-2 and IL-12 levels in co-infected patients.

### RESULTS

The co-infection group exhibited elevated serum IL-2 and C-reactive protein (CRP) levels compared to both the MP-only and control groups, with a reverse trend observed for IL-12 ( $P < 0.05$ ). In the poor prognosis cohort, elevated CRP and IL-2 levels, alongside prolonged fever duration, contrasted with reduced IL-12 levels ( $P < 0.05$ ). Logistic regression identified elevated IL-2 as an independent risk factor and high IL-12 as a protective factor for adverse outcomes ( $P < 0.05$ ).

ROC analysis indicated that the area under the curves for IL-2, IL-12, and their combination in predicting poor prognosis were 0.815, 0.895, and 0.915, respectively.

## CONCLUSION

Elevated serum IL-2 and diminished IL-12 levels in pediatric patients with MP and EBV co-infection correlate with poorer prognosis, with combined IL-2 and IL-12 levels offering enhanced predictive accuracy.

**Key Words:** Interleukin-2; Interleukin-12; *Mycoplasma pneumoniae*; Epstein-Barr virus; Coinfection

©The Author(s) 2024. Published by Baishideng Publishing Group Inc. All rights reserved.

**Core Tip:** This study presents a novel exploration of the interaction between immune response markers and co-infection outcomes in pediatric respiratory infections, focusing on *Mycoplasma pneumoniae* and Epstein-Barr virus. Our research addresses a critical gap in understanding the immunological dynamics in co-infected pediatric patients, offering insights into the prognostic values of interleukins interleukin-2 and interleukin-12. Through a comprehensive analysis of clinical data and a robust methodological approach, we provide evidence that serum levels of these cytokines are significantly associated with disease prognosis in co-infected individuals. The findings suggest a nuanced role of the immune system in managing co-infections, with potential implications for therapeutic strategies.

**Citation:** Hao YP. Evaluating the role of interleukin-2 and interleukin-12 in pediatric patients with concurrent *Mycoplasma pneumoniae* and Epstein-Barr virus infections. *World J Clin Cases* 2024; 12(23): 5346-5353

**URL:** <https://www.wjgnet.com/2307-8960/full/v12/i23/5346.htm>

**DOI:** <https://dx.doi.org/10.12998/wjcc.v12.i23.5346>

## INTRODUCTION

*Mycoplasma pneumoniae* (MP), a common respiratory infection, is the cause of over 40% of community-acquired pneumonia cases in children. It often presents as mycoplasma pneumonia, which is characterized by fever and a persistent, dry cough[1,2]. Simultaneously, Epstein-Barr virus (EBV), a DNA virus, is recognized for its high infectivity, specifically targeting the respiratory system and other organs, and has the potential to remain in a dormant state within the host indefinitely[3,4]. Recent studies have shown an increasing tendency in co-infections involving MP and EBV. This clinical scenario is sometimes difficult to diagnose because it lacks unique symptoms, which worsens lung damage, prolongs episodes of fever, and complicates treatment interventions[5,6]. It is worth mentioning that there have been reports of children with MP and EBV co-infection experiencing more severe clinical symptoms, often affecting several organ systems[7,8].

MP, a primary causative agent of respiratory infections, triggers inflammation and increased sensitivity in the airways when transmitted through respiratory droplets[1,9]. Due to their developing immune systems, children are especially vulnerable to experiencing severe symptoms when they have both MP and EBV infections. This may be because these pathogens trigger a combined immunological response that worsens the symptoms. Interleukin-2 (IL-2) and interleukin-12 (IL-12) are important cytokines primarily produced by activated Th1 cells that have significant functions in the immune system[10]. IL-2 stimulates the growth and development of T and B lymphocytes by binding to their receptors on target cells, coordinating a cellular immune response[11]. On the other hand, IL-12, which plays a crucial role in the body's natural defense system, is essential for cellular immunological functions[12]. The participation of IL-2 in the development of MP and the significance of IL-12 as a crucial Th1 cytokine in regulating innate immunity highlight the intricate nature of the immune response to MP and EBV infections. While the exact pathogenic mechanisms behind co-infections of MP and EBV are not yet fully understood, existing literature highlights their connection with immune-mediated processes. The impaired immune response in pediatric MP pneumonia is commonly recognized, however there are differing views on the prevalence of Th subtypes (Th1/Th2)[10,13].

This study seeks to clarify the functions of IL-2 and IL-12 in the cellular immune response to co-infection of MP and EBV. It will achieve this by analyzing the levels of IL-2 and IL-12 in the blood serum of children who have MP pneumonia and EBV co-infection. The study aims to provide insights into the prognostic significance of these cytokines.

## MATERIALS AND METHODS

### Study population

This study conducted a retrospective analysis of clinical data from patients who were diagnosed with MP co-infected with EBV, patients with isolated MP infection, and a control group consisting of healthy youngsters. The participants were enlisted from Maternal and Child Health Hospital between January 1, 2018 and December 31, 2021.

Inclusion criteria encompassed: (1) Clinical presentation of pneumonia at admission characterized by symptoms such as fever, cough, abnormal pulmonary sounds upon auscultation, and novel infiltrative patterns observable on chest radiographs; and (2) Confirmation of MP infection through positive MP polymerase chain reaction (PCR) assays<sup>[14]</sup>, and EBV infection validated by EBV PCR positive results.

The exclusion criteria were established to exclude instances with inadequate data, poor immune function, concurrent bacterial or viral infections, and other respiratory diseases such as pulmonary tuberculosis and bronchial asthma.

Before the patients' guardians participated, they were given informed consent. The study's approach strictly followed the ethical principles specified in the Declaration of Helsinki and obtained clearance from the Hospital's Medical Ethics Committee.

### Data collection

Data encompassing demographic details, clinical manifestations, laboratory findings, and radiological assessments were collated retrospectively. Specimens for laboratory analysis, including blood, nasopharyngeal aspirate (NPA), and bronchoalveolar lavage fluid were collected. Initial blood samples were analyzed to determine white blood cell counts, neutrophil percentages, platelet counts, levels of C-reactive protein (CRP), and cytokines such as IL-2 and IL-12. To rigorously exclude the presence of other common viral (*e.g.*, respiratory syncytial virus, influenza, metapneumovirus, adenovirus, and parainfluenza virus) and bacterial co-infections, NPA samples were collected within 24 hours of admission for comprehensive viral antigen detection and bacterial culture. Additionally, to mitigate the low sensitivity of blood cultures and limited viral detection, we employed a multi-panel PCR assay capable of identifying a broader range of bacterial and viral pathogens. This assay complements our standard procedures by enhancing the specificity of our infectious agent detection, thereby reducing the potential for undetected co-infections that could influence cytokine levels.

The prognosis of pediatric patients, including cases involving negative outcomes such as death or long-term damage to lung function caused by co-infection of MP and EBV, were thoroughly recorded. The exclusion criterion for unfavorable outcomes involved mortality or functional impairments resulting from dysfunctions in other organs, as established through autopsy.

### Measurement of CRP and serum cytokines

After collecting 3 mL of fasting venous blood samples, the samples were subjected to centrifugation at a speed of 2500 rpm for a duration of 10 minutes. This process was done to separate the serum, which was thereafter stored at a temperature of -80°C. CRP levels were measured using an automated biochemistry analyzer (AU5800; Beckman Coulter, Brea, CA, United States). IL-2 and IL-12 serum levels were measured using enzyme-linked immunosorbent assays (ELISA) following the manufacturer's protocol (Shanghai Jianglai Biotechnology Co., Ltd., Shanghai, China). The duration of the fever was also documented.

### Statistical analyses

The statistical analysis was performed using SPSS version 20.0 (IBM Corp., Armonk, NY, United States). The categorical variables were represented as frequencies and percentages. Chi-square tests were used to compare the different groups. The continuous variables were reported as the mean  $\pm$  standard deviation. Pairwise comparisons were conducted using *t*-tests, while multigroup comparisons were performed using one-way ANOVA. Post-hoc analysis was conducted using SNK-*q* tests. Utilizing multivariate logistic regression, we analyzed the characteristics that contribute to a negative outcome in pediatric patients with MP and EBV co-infection. The diagnostic efficacy of serum IL-2 and IL-12 levels in predicting negative outcomes was assessed using receiver operating characteristic (ROC) curves. A *P* value less than 0.05 was considered statistically significant.

## RESULTS

### Clinical characteristics

Upon comparing the general characteristics across the MP group, the co-infection group (MP and EBV), and the control group, no significant disparities were observed in age or sex distribution among these groups (*P* > 0.05). Notably, serum CRP levels were markedly elevated in the co-infection group compared to both the MP group and the control group, with the MP group also displaying higher CRP levels than the control group (*P* < 0.05). Furthermore, the duration of fever in the co-infection group significantly exceeded that in the MP group (*P* < 0.05, [Table 1](#)).

In the comparison between the poor prognosis and the non-poor prognosis groups, age and sex did not significantly differ. However, the CRP levels and fever durations were significantly higher in the poor prognosis group compared to the non-poor prognosis group (*P* < 0.05, [Table 2](#)).

### Serum interleukin levels

Analysis of serum IL-2 and IL-12 levels among the MP group, the co-infection group, and the control group revealed that IL-2 levels in the co-infection group were significantly elevated compared to both the MP group and the control group, with the MP group also having higher IL-2 levels than the control group. Conversely, IL-12 levels in the co-infection group were significantly lower than those in both the MP group and the control group, with the MP group exhibiting lower IL-12 levels than the control group (*P* < 0.05, [Table 3](#)).

**Table 1 Comparison of general data among *Mycoplasma pneumoniae* group, coinfection group and control group**

Group	n	Age	Male/female	CRP in mg/L	Fever in days
Coinfection	165	5.31 ± 2.09	79/86	35.36 ± 10.09 <sup>e,f</sup>	8.16 ± 2.15 <sup>f</sup>
MP	165	5.26 ± 2.06	89/76	25.26 ± 8.06 <sup>e</sup>	5.16 ± 1.06
Control	165	5.19 ± 2.45	83/82	15.30 ± 4.09	-
<i>F/t/χ<sup>2</sup></i>	-	0.031	0.632	219.653	9.863
<i>P</i> value	-	0.965	0.075	< 0.001	< 0.001

<sup>e</sup>*P* < 0.001 vs control group.<sup>f</sup>*P* < 0.001 vs *Mycoplasma pneumoniae* (MP) group. Coinfection: Epstein-Barr virus coinfection in MP pneumonia; Control: Healthy children; CRP: C-reactive protein.**Table 2 Comparison of general data between poor prognosis group and non-poor prognosis group**

Group	n	Age	Male/female	CRP in mg/L	Fever in days
Poor prognosis	56	5.31 ± 2.19	32/24	36.36 ± 9.09 <sup>f</sup>	9.73 ± 2.84 <sup>f</sup>
Non-poor prognosis	109	5.16 ± 2.56	61/48	29.16 ± 7.31	5.83 ± 1.84
<i>t/χ<sup>2</sup></i>	-	0.231	0.684	2.546	3.858
<i>P</i> value	-	0.865	0.076	< 0.001	< 0.001

<sup>f</sup>*P* < 0.001 vs non-poor prognosis group. CRP: C-reactive protein.**Table 3 Comparison of the serum interleukin-2 and interleukin-12 levels among *Mycoplasma pneumoniae* group, coinfection group and control group**

Group	n	IL-2	IL-12
Coinfection	165	3.75 ± 0.95 <sup>e,f</sup>	14.09 ± 3.95 <sup>e,f</sup>
MP	165	2.76 ± 0.66 <sup>e</sup>	23.75 ± 7.19 <sup>e</sup>
Control	165	1.89 ± 0.53	38.21 ± 10.74
<i>F</i>	-	98.62	267.83
<i>P</i> value	-	< 0.001	< 0.001

<sup>e</sup>*P* < 0.001 vs control group.<sup>f</sup>*P* < 0.001 vs *Mycoplasma pneumoniae* (MP) group. Coinfection: Epstein-Barr virus coinfection in MP pneumonia; Control: Healthy children; IL-2: Interleukin-2; IL-12: Interleukin-12.

When comparing the poor prognosis group with the non-poor prognosis group, the poor prognosis group showed significantly higher serum IL-2 levels and significantly lower IL-12 levels (*P* < 0.05, Table 4).

### Logistic regression analysis

A logistic regression analysis incorporating serum IL-2, IL-12, CRP levels, and fever duration as independent variables, and the poor prognosis of children with EBV co-infection in MP pneumonia as the dependent variable, identified high serum IL-2 as an independent risk factor for poor prognosis. Conversely, high serum IL-12 emerged as a protective factor against poor prognosis in these patients (*P* < 0.05, Table 5).

### Predictive values of independent correlation factors

ROC curve analysis illustrated that the area under the curve (AUC) for serum IL-2 in predicting poor prognosis in children with MP and EBV co-infection was 0.815 (95%CI 0.653-0.903, *P* < 0.001), with a cutoff value of 3.265 ng/L, a sensitivity of 73.3%, and a specificity of 90.2%. The AUC for serum IL-12 in this context was 0.895 (95%CI 0.836-0.953, *P* < 0.001), with a cutoff value of 13.895 ng/L, a sensitivity of 94.2%, and a specificity of 82.5%. The combined AUC for serum IL-2 and IL-12 was 0.915 (95%CI 0.858-0.971, *P* < 0.001), yielding a sensitivity of 85.1% and a specificity of 84.3% (Figure 1).

Table 4 Comparison of the serum interleukin-2 and interleukin-12 levels between poor prognosis group and non-poor prognosis group			
Group	n	IL-2	IL-12
Poor prognosis	56	4.63 ± 1.27 <sup>f</sup>	11.26 ± 3.63 <sup>f</sup>
Non-poor prognosis group	109	2.41 ± 0.53	18.47 ± 4.63
t	-	7.974	8.764
P value	-	< 0.001	< 0.001

<sup>f</sup>P < 0.001 vs non-poor prognosis group.

Table 5 Logistic regression analysis of factors affecting poor prognosis in children with Epstein-Barr virus coinfection in <i>Mycoplasma pneumoniae</i> pneumonia						
Variate	β	SE	Wald χ <sup>2</sup>	P value	OR	95%CI
IL-2	1.186	0.496	5.847	0.013	3.865	1.235-7.475
IL-12	1.074	0.426	6.194	0.012	0.384	0.156-0.836
CRP	0.516	0.319	2.496	0.136	1.858	0.843-3.285
Fever	0.173	0.264	0.395	0.586	1.124	0.656-2.184

CRP: C-reactive protein; IL-2: Interleukin-2; IL-12: Interleukin-12.

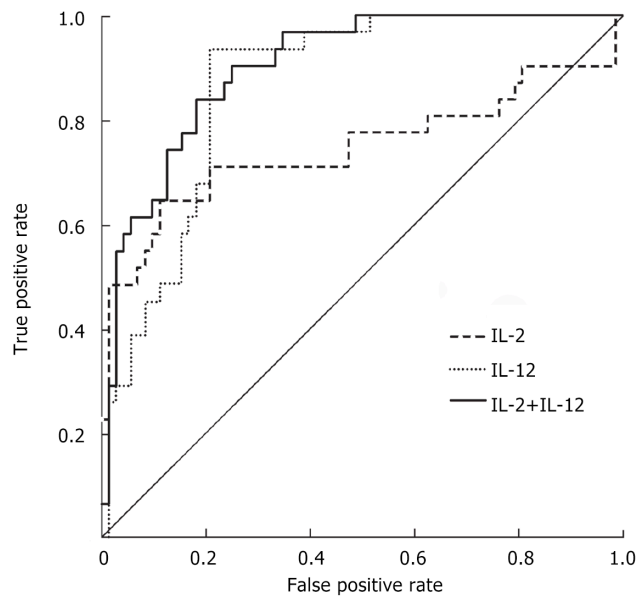


Figure 1 Receiver operator characteristic curves for serum interleukin-2, interleukin-12, and the combination of serum interleukin-2 and interleukin-12 in evaluating the poor prognosis of children with Epstein-Barr virus coinfection in *Mycoplasma pneumoniae* pneumonia.

DISCUSSION

The medical community has rarely reported or acknowledged cases of co-infections involving both MP and EBV in juvenile respiratory infections among patients with normal immune function[1,9,15]. Our analysis found that the clinical and radiological characteristics of children with simultaneous MP and EBV infections closely resemble those of MP infection alone. Nevertheless, the group of patients with co-infections displayed extended periods of fever and increased CRP levels, indicating more severe clinical symptoms in these individuals. This finding is consistent with similar case studies in scientific literature, such as the report by Li *et al*[7] on a patient with co-infection who experienced splenic infarction, and the description by Yenson *et al*[16] of a 7-year-old with MP and EBV co-infection who had agglutination of white and red blood cells. These reports further support the idea that co-infection can result in more severe manifestations of the disease.

IL-2 is essential for the immune response and is mostly produced by activated Th1 cells. It helps regulate immunological responses by activating regulatory T lymphocytes[17]. The findings of our study revealed a notable increase in serum IL-2 levels in the co-infection group compared to both the MP group and the control group. This suggests that co-infection might stimulate a heightened release of IL-2, which in turn could result in an intensified inflammatory response. The atypical manifestation of IL-2, linked to immunological dysfunction, could be a crucial element in the development of MP and EBV co-infection. Significantly, the study found that higher IL-2 levels were strongly linked to a negative prognosis in the group being studied. This suggests that IL-2 levels may have the capacity to predict unfavorable outcomes. Logistic regression study revealed that elevated blood IL-2 is an autonomous risk factor for worse prognosis in children with MP and EBV co-infection. Additionally, ROC curve analysis confirmed the predictive significance of serum IL-2 levels for undesirable outcomes.

IL-12, mostly released by mononuclear macrophages, plays a crucial role in stimulating Th1 cellular immune responses and controlling the equilibrium between Th1 and Th2 cells[18,19]. Extensive studies on IL-12 have revealed its ability to boost T cell function, promote Th1 responses, and regulate the balance between Th1 and Th2 cellular immune responses. This plays a vital role in cellular immunity during viral infections[10,20]. The results of this work suggest that individuals with co-infection have a dominant Th1 response, which is associated with an enhanced cellular immunological reactivity resulting in systemic immune damage and more severe clinical symptoms. The co-infection group exhibited a significant decrease in blood IL-12 levels compared to both the MP-only and control groups. Similarly, within the MP group, serum IL-12 levels were lower compared to the control group. These findings imply that serum IL-12 concentrations could potentially be used as indications of the severity of infection[21]. Moreover, the reduced levels of IL-12 in the group with bad prognosis, compared to the group with non-poor prognosis, suggest an imbalance in the Th1/Th2 cellular immune response in co-infected children. This highlights the importance of IL-12 as a crucial regulatory component in determining their prognosis.

The investigation demonstrated that elevated blood IL-12 levels serve as a safeguard against unfavorable prognosis in children with MP and EBV co-infection, confirming the strong correlation between IL-12 levels and patient outcomes. There was a correlation between the decrease in serum IL-12 levels and a higher probability of experiencing a negative prognosis. The ROC curve study revealed that serum IL-12 is a strong predictor of bad prognosis in co-infected children, with an AUC value of 0.895. The sensitivity of the test was 94.2%, meaning it correctly identified 94.2% of the children with poor prognosis. The specificity of the test was 82.5%, indicating that it correctly identified 82.5% of the children without poor prognosis. An association was found between a serum IL-12 threshold of  $\leq 13.895$  ng/L and an increased likelihood of experiencing negative outcomes. In addition, when serum IL-2 and IL-12 levels were analyzed together, the AUC was found to be 0.915. This analysis showed a sensitivity of 85.1% and a specificity of 84.3%. These results suggest that the combined assessment of these cytokines provides a more accurate prediction of outcomes for children with co-infections and could be an important prognostic marker.

Due to the notable increase in CRP levels observed in our study, it is essential to understand the complex interplay between EBV and MP co-infection. While EBV infections are typically subclinical in immunocompetent children, the scenario may differ substantially when co-infection with another pathogen such as MP is present. Studies have shown that EBV can enhance the host's inflammatory response, especially when co-infected with other pathogens[22]. Furthermore, MP is known to provoke a significant inflammatory response, potentially leading to elevated CRP levels [23]. In the context of co-infection, as in our study, the synergistic effects of EBV and MP may intensify the inflammatory response, thereby causing an increase in CRP levels beyond what is typically observed with viral infections alone. Moreover, CRP, as an acute-phase protein, is a sensitive marker of inflammation and is elevated in various infectious contexts. Our findings of elevated CRP levels are corroborated by the existing literature suggesting that the presence of additional pro-inflammatory stimuli, such as a bacterial infection with MP, can significantly enhance the CRP response even in the setting of a primary viral infection[24]. Therefore, the apparent anomaly in CRP elevation in our study is consistent with the expected biological response to EBV and MP co-infection, rather than an indication of data error. This response underscores the importance of considering co-infections and their cumulative impact on inflammatory markers in clinical assessments and research.

This study had significant limitations, particularly its retrospective approach, which prevented the determination of an ideal sample size and may have led to selection bias and reduced testing effectiveness due to the very small number of participants. Additionally, due to the study being conducted at a single center, there is a possibility of biases that may restrict the applicability of the results to a broader population. Future research should focus on establishing cooperation between other centers to validate these findings and expand our understanding of the role of IL-12 in predicting the outcome of young patients with MP and EBV co-infections.

## CONCLUSION

Our study reveals that elevated serum IL-2 and reduced IL-12 levels in pediatric MP pneumonia with EBV co-infection are indicative of poor prognosis, with their combined assessment offering superior predictive accuracy. This underscores the necessity for further investigation into the underlying mechanisms and interactions of MP/EBV co-infection to enhance clinical management and outcomes.

## ACKNOWLEDGEMENTS

Thank you to the patients who participated in this study.

## FOOTNOTES

**Author contributions:** Hao YP independently completed the following tasks: conceptualization, data curation, formal analysis, methodology development, resource acquisition, software implementation, and original draft writing; The final writing and editing were conducted by Hao YP.

**Institutional review board statement:** This study was approved by the Ethics committee of Maternal and Child Health Hospital.

**Informed consent statement:** Written informed consent for publication was obtained from all patients and their families included in this retrospective analysis.

**Conflict-of-interest statement:** The authors report no relevant conflicts of interest for this article.

**Data sharing statement:** The datasets used and/or analyzed during the present study are available from the corresponding author on reasonable request.

**Open-Access:** This article is an open-access article that was selected by an in-house editor and fully peer-reviewed by external reviewers. It is distributed in accordance with the Creative Commons Attribution NonCommercial (CC BY-NC 4.0) license, which permits others to distribute, remix, adapt, build upon this work non-commercially, and license their derivative works on different terms, provided the original work is properly cited and the use is non-commercial. See: <https://creativecommons.org/licenses/by-nc/4.0/>

**Country of origin:** China

**ORCID number:** Yan-Ping Hao 0009-0008-3577-8089.

**S-Editor:** Gong ZM

**L-Editor:** Filipodia

**P-Editor:** Zhang XD

## REFERENCES

- 1 **Kashyap S**, Sarkar M. Mycoplasma pneumonia: Clinical features and management. *Lung India* 2010; **27**: 75-85 [PMID: 20616940 DOI: 10.4103/0970-2113.63611]
- 2 **Jiang W**, Wu M, Zhou J, Wang Y, Hao C, Ji W, Zhang X, Gu W, Shao X. Etiologic spectrum and occurrence of coinfections in children hospitalized with community-acquired pneumonia. *BMC Infect Dis* 2017; **17**: 787 [PMID: 29262797 DOI: 10.1186/s12879-017-2891-x]
- 3 **Cohen JI**. Epstein-Barr virus infection. *N Engl J Med* 2000; **343**: 481-492 [PMID: 10944566 DOI: 10.1056/NEJM200008173430707]
- 4 **Nowalk A**, Green M. Epstein-Barr Virus. *Microbiol Spectr* 2016; **4** [PMID: 27337443 DOI: 10.1128/microbiolspec.DMIH2-0011-2015]
- 5 **Zhang X**, Chen Z, Gu W, Ji W, Wang Y, Hao C, He Y, Huang L, Wang M, Shao X, Yan Y. Viral and bacterial co-infection in hospitalised children with refractory Mycoplasma pneumoniae pneumonia. *Epidemiol Infect* 2018; **146**: 1384-1388 [PMID: 29970200 DOI: 10.1017/S0950268818000778]
- 6 **Xu Y**, Li S, Liu J, Zhou J, Jin F, Chen X, Wang Y, Jiang Y, Chen Z. Impact of Epstein-Barr virus coinfection in Mycoplasma pneumoniae pneumonia. *Medicine (Baltimore)* 2020; **99**: e19792 [PMID: 32311992 DOI: 10.1097/MD.00000000000019792]
- 7 **Li Y**, Pattan V, Syed B, Islam M, Yousif A. Splenic infarction caused by a rare coinfection of Epstein-Barr virus, cytomegalovirus, and Mycoplasma pneumoniae. *Pediatr Emerg Care* 2014; **30**: 636-637 [PMID: 25186505 DOI: 10.1097/PEC.0000000000000211]
- 8 **Martínez Roig A**, Busquets Monge RM, López Segura N, Herrero Pérez S, Esteban Torné E. [Epstein-Barr virus and Mycoplasma pneumoniae coinfection in two girls with community-acquired pneumonia]. *An Esp Pediatr* 2002; **56**: 69-70 [PMID: 11792250 DOI: 10.1016/S1695-4033(02)77771-0]
- 9 **Ferwerda A**, Moll HA, de Groot R. Respiratory tract infections by Mycoplasma pneumoniae in children: a review of diagnostic and therapeutic measures. *Eur J Pediatr* 2001; **160**: 483-491 [PMID: 11548186 DOI: 10.1007/s004310100775]
- 10 **Vignali DA**, Kuchroo VK. IL-12 family cytokines: immunological playmakers. *Nat Immunol* 2012; **13**: 722-728 [PMID: 22814351 DOI: 10.1038/ni.2366]
- 11 **Tanaka H**, Honma S, Abe S, Tamura H. Effects of interleukin-2 and cyclosporin A on pathologic features in Mycoplasma pneumonia. *Am J Respir Crit Care Med* 1996; **154**: 1908-1912 [PMID: 8970385 DOI: 10.1164/ajrccm.154.6.8970385]
- 12 **Salvatore CM**, Fonseca-Aten M, Katz-Gaynor K, Gomez AM, Mejias A, Somers C, Chavez-Bueno S, McCracken GH, Hardy RD. Respiratory tract infection with Mycoplasma pneumoniae in interleukin-12 knockout mice results in improved bacterial clearance and reduced pulmonary inflammation. *Infect Immun* 2007; **75**: 236-242 [PMID: 17074851 DOI: 10.1128/IAI.01249-06]
- 13 **Li W**, Liu YJ, Zhao XL, Shang SQ, Wu L, Ye Q, Xu H. Th1/Th2 Cytokine Profile and Its Diagnostic Value in Mycoplasma pneumoniae Pneumonia. *Iran J Pediatr* 2016; **26**: e3807 [PMID: 26848377 DOI: 10.5812/ijp.3807]
- 14 **Xu D**, Li S, Chen Z, Du L. Detection of Mycoplasma pneumoniae in different respiratory specimens. *Eur J Pediatr* 2011; **170**: 851-858 [PMID: 21107602 DOI: 10.1007/s00431-010-1360-y]
- 15 **Oumei H**, Xuefeng W, Jianping L, Kunling S, Rong M, Zhenze C, Li D, Huimin Y, Lining W, Zhaolan L, Xinmin L, Hua X, Zhiyan J,

- Yanning L, Yan H, Baoqing Z, Xiaochun F, Chunhui H, Yonghong J, Xue Z, Wei W, Zi W. Etiology of community-acquired pneumonia in 1500 hospitalized children. *J Med Virol* 2018; **90**: 421-428 [PMID: 28975629 DOI: 10.1002/jmv.24963]
- 16 Yenson PR, Fleming A, Kaikov Y, Wadsworth LD. Combined neutrophil and erythrocyte agglutination in a 7-year-old boy. *J Pediatr Hematol Oncol* 2007; **29**: 664-665 [PMID: 17805049 DOI: 10.1097/MPH.0b013e3181461662]
- 17 Mitra S, Leonard WJ. Biology of IL-2 and its therapeutic modulation: Mechanisms and strategies. *J Leukoc Biol* 2018; **103**: 643-655 [PMID: 29522246 DOI: 10.1002/JLB.2RI0717-278R]
- 18 Dittrich A, Hessenkemper W, Schaper F. Systems biology of IL-6, IL-12 family cytokines. *Cytokine Growth Factor Rev* 2015; **26**: 595-602 [PMID: 26187858 DOI: 10.1016/j.cytogfr.2015.07.002]
- 19 Sutterwala FS, Mosser DM. The taming of IL-12: suppressing the production of proinflammatory cytokines. *J Leukoc Biol* 1999; **65**: 543-551 [PMID: 10331481 DOI: 10.1002/jlb.65.5.543]
- 20 Komastu T, Ireland DD, Reiss CS. IL-12 and viral infections. *Cytokine Growth Factor Rev* 1998; **9**: 277-285 [PMID: 9918125 DOI: 10.1016/S1359-6101(98)00017-3]
- 21 Li H, Li S, Zheng J, Cai C, Ye B, Yang J, Chen Z. Cerebrospinal fluid Th1/Th2 cytokine profiles in children with enterovirus 71-associated meningoencephalitis. *Microbiol Immunol* 2015; **59**: 152-159 [PMID: 25611005 DOI: 10.1111/1348-0421.12227]
- 22 Jangra S, Yuen KS, Botelho MG, Jin DY. Epstein-Barr Virus and Innate Immunity: Friends or Foes? *Microorganisms* 2019; **7** [PMID: 31238570 DOI: 10.3390/microorganisms7060183]
- 23 Shi S, Zhang X, Zhou Y, Tang H, Zhao D, Liu F. Immunosuppression Reduces Lung Injury Caused by Mycoplasma pneumoniae Infection. *Sci Rep* 2019; **9**: 7147 [PMID: 31073201 DOI: 10.1038/s41598-019-43451-9]
- 24 Sproston NR, Ashworth JJ. Role of C-Reactive Protein at Sites of Inflammation and Infection. *Front Immunol* 2018; **9**: 754 [PMID: 29706967 DOI: 10.3389/fimmu.2018.00754]



## Observational Study

# Perception of dental appearance and aesthetic analysis among patients, laypersons and dentists

Alhanoof Aldegheishem, Hadeel Mohammed Alfayadh, Munirah AlDossary, Shahad Asaad, Elzahraa Eldwakhly, Nour AL Huda AL Refaei, Dana Alsenan, Mai Soliman

**Specialty type:** Medicine, research and experimental

**Provenance and peer review:**

Invited article; Externally peer reviewed.

**Peer-review model:** Single blind

**Peer-review report's classification**

**Scientific Quality:** Grade D

**Novelty:** Grade B

**Creativity or Innovation:** Grade B

**Scientific Significance:** Grade B

**P-Reviewer:** O'Brien T

**Received:** February 25, 2024

**Revised:** May 5, 2024

**Accepted:** June 14, 2024

**Published online:** August 16, 2024

**Processing time:** 131 Days and 9.2 Hours



**Alhanoof Aldegheishem, Elzahraa Eldwakhly, Nour AL Huda AL Refaei, Dana Alsenan, Mai Soliman,** Department of Clinical Dental Sciences, College of Dentistry, Princess Nourah Bint Abdulrahman University, Riyadh 11671, Saudi Arabia

**Hadeel Mohammed Alfayadh,** Department of Oral Medicine and Pathology, Ministry of Health, Riyadh 11176, Saudi Arabia

**Munirah AlDossary,** Department of Prosthodontics, Ministry of Health, Riyadh 11176, Saudi Arabia

**Shahad Asaad,** Department of Pediatric, Ministry of Health, Riyadh 11176, Saudi Arabia

**Corresponding author:** Mai Soliman, PhD, Associate Professor, Department of Clinical Dental Sciences, College of Dentistry, Princess Nourah Bint Abdulrahman University, King Khaled Airport Road, Riyadh 11671, Saudi Arabia. [msmustafa@pnu.edu.sa](mailto:msmustafa@pnu.edu.sa)

## Abstract

### BACKGROUND

Current concepts of beauty are increasingly subjective, influenced by the viewpoints of others. The aim of the study was to evaluate divergences in the perception of dental appearance and smile esthetics among patients, laypersons and dental practitioners. The study goals were to evaluate the influence of age, sex, education and dental specialty on the participants' judgment and to identify the values of different esthetic criteria. Patients sample included 50 patients who responded to a dental appearance questionnaire (DAQ). Two frontal photographs were taken, one during a smile and one with retracted lips. Laypersons and dentists were asked to evaluate both photographs using a Linear Scale from (0-10), where 0 represent (absolutely unaesthetic) and 10 represent (absolutely aesthetic). One-way analysis of variance (ANOVA) and *t*-test analysis were measured for each group. Most patients in the sample expressed satisfaction with most aspects of their smiles and dental appearance. Among laypersons (including 488 participants), 47 pictures "with lips" out of 50 had higher mean aesthetic scores compared to pictures "without lips". Among the dentist sample, 90 dentists' perception towards the esthetic smile and dental appearance for photos "with lips" and "without lips" were the same for 23 out of 50 patients. Perception of smile aesthetics differed between patients, laypersons and dentists. Several

factors can contribute to shape the perception of smile aesthetic.

### AIM

To compare the perception of dental aesthetic among patients, laypersons, and professional dentists, to evaluate the impact of age, sex, educational background, and income on the judgments made by laypersons, to assess the variations in experience, specialty, age, and sex on professional dentists' judgment, and to evaluate the role of lips, skin shade and tooth shade in different participants' judgments.

### METHODS

Patients sample included 50 patients who responded to DAQ. Two frontal photographs were taken: one during a smile and one with retracted lips. Laypersons and dentists were asked to evaluate both photographs using a Linear Scale from (0-10), where 0 represent (absolutely unaesthetic) and 10 represent (absolutely aesthetic). One-way ANOVA and *t*-test analysis were measured for each group.

### RESULTS

Most patients in the sample expressed satisfaction with most aspects of their smiles and dental appearance. Among laypersons (including 488 participants), 47 pictures "with lips" out of 50 had higher mean aesthetic scores compared to pictures "without lips". Whereas among the dentist sample, 90 dentists' perception towards the esthetic smile and dental appearance for photos "with lips" and "without lips" were the same for 23 out of 50 patients. Perception of smile aesthetics differed between patients, laypersons and dentists.

### CONCLUSION

Several factors can contribute to shape the perception of smile aesthetic.

**Key Words:** Aesthetic perception; Laypersons; Dental appearance; Dentists; Smile analysis; Dental aesthetic

©The Author(s) 2024. Published by Baishideng Publishing Group Inc. All rights reserved.

**Core Tip:** An aesthetically pleasing smile is not only dependent on elements such as tooth position, size, shape, and color, but also on the amount of gingiva exposed and lip positioning. All of these facial features are essential to achieve a harmonious form, emphasizing the importance of physical appearance and facial attractiveness. However, the concept of attractiveness varies between individuals influenced by uncontrollable factors such as cultural differences, as well as their personal and social background. Several studies have shown significant differences in aesthetic perception concerning various factors, including the presence of a black triangle, inflamed gingiva, diastema, malocclusion, midline shift, facial asymmetry, buccal corridor and gingival display. Many studies have reported significant differences on the aesthetic perception among laypersons and dentists. Although there is an existing body of research, a deeper comprehension of how dental appearances are perceived is required. Additionally, there are limited scientific data regarding the relationship between variations in skin color and tooth shade values in terms of perceived attractiveness. There was no widely recognized scientific relationship between skin color and smile perception. Therefore, the aim of this study was to compare perception of dental aesthetic among patients, laypersons, and professional dentists.

**Citation:** Aldegheishem A, Alfayadh HM, AlDossary M, Asaad S, Eldwakhly E, AL Refaei NAH, Alsenan D, Soliman M. Perception of dental appearance and aesthetic analysis among patients, laypersons and dentists. *World J Clin Cases* 2024; 12(23): 5354-5365

**URL:** <https://www.wjgnet.com/2307-8960/full/v12/i23/5354.htm>

**DOI:** <https://dx.doi.org/10.12998/wjcc.v12.i23.5354>

## INTRODUCTION

Over the past few years, there has been notable public awareness regarding dental treatment, emphasizing the importance of teeth in both function and facial aesthetics. During interpersonal communication, it is common for people to direct their attention toward the center of the face, which is the mouth, where the smile plays a crucial role in facial expression and enhancing one's appearance[1].

An aesthetically pleasing smile is not only dependent on elements such as tooth position, size, shape, and color, but also on the amount of gingiva exposed and lip positioning[2]. All of these facial features are essential to achieve a harmonious form, emphasizing the importance of physical appearance and facial attractiveness.

However, the concept of attractiveness varies between individuals influenced by uncontrollable factors such as cultural differences, as well as their personal and social background[3]. Several studies have shown significant differences in aesthetic perception concerning various factors, including the presence of a black triangle, inflamed gingiva[1], diastema [5,6], malocclusion[6], midline shift[7], facial asymmetry, buccal corridor and gingival display[8,9]. Many studies have reported significant differences on the aesthetic perception among laypersons and dentists[7,10,11].

It is widely accepted that a trained and observant eye can easily distinguish the imbalances and disharmony within its environment[10]. Moreover, several studies have shown that the aesthetic perception of dental features is influenced not only by an individual's level of education but also by other factors including sex, age and cultural background[1,12-15].

Although there is an existing body of research, a deeper comprehension of how dental appearances are perceived is required. Additionally, there are limited scientific data regarding the relationship between variations in skin color and tooth shade values in terms of perceived attractiveness[16]. There was no widely recognized scientific relationship between skin color and smile perception. Therefore, the aim of this study was to compare perceptions of dental aesthetic among patients, laypersons, and professional dentists, as follows:

To evaluate the impact of age, sex, educational background, and income on the judgments made by laypersons.

To assess the variations in experience, specialty, age, and sex on professional dentists' judgment.

To evaluate the role of lips, skin shade and tooth shade in different participants' judgments.

## MATERIALS AND METHODS

The data collection phase was divided into three stages: (1) Dental photography and dental appearance questionnaire (DAQ) for participants; (2) Questionnaire for dentist; and (3) Questionnaire targeting laypersons.

### **Ethical approval**

This cross-sectional study received approval from the Deanship of Scientific Research, Princess Norah University under the study number 17-0183.

### **Patient selection criteria**

Fifty female patients aged between 18 years and 40 years were randomly selected from active patients treated in the dental clinic. Patients having orthodontic appliance or any aesthetic dental treatment such as veneers, full coverage crown or any aesthetic fillings were excluded from the study.

### **Dental appearance questionnaire**

The participants were asked to answer DAQ (Table 1), which had been translated into Arabic. The reliability and validity of this questionnaire were tested[17]. The questionnaire consists of 11 elements, and it was developed to assess the satisfaction of the participants. Furthermore, patients were asked about their history of orthodontic treatment or the use of lip fillers.

### **Criteria measured for each patient**

(1) Measurement of length-width of central incisor, laterals and canines using digital caliper.

(2) Recording of skin shade based on Fitzpatrick scale (Figure 1)[18,19].

(3) Recording of teeth shade using digital shade detector (Ray Plicker, Borea, France), and the shade was validated by Vita classic shade guide (Figure 2).

and (4) Age of patient and level of education were also recorded.

The shade of each patient's teeth was measured using the digital shade detector (Ray Plicker) scale (A1-D4), where (A1-A4) represents Reddish-Brownish tooth shade, (B1-B4) represents Reddish-Yellowish tooth shade, (C1-C4) represents Greyish tooth shade, and (D1-D4) represents Reddish Grey tooth shade. In addition to the shade categorization, tooth brightness was rated on a scale from 1 to 4, with 1 representing the lightest and 4 representing the darkest tooth brightness.

### **Patients Photographing**

Two frontal photographs were taken in compliance with standard dental photography (AACD) using a Nikon digital camera. The camera was positioned at a fixed angle of 90 degrees with adjustable height on camera holder. Participants were positioned at a distance of 22 inches from the camera, and their head position was stabilized using Facebow ear pieces in a vertical position connected to a stand perpendicular to the head (Figure 3). The first photograph was taken with the patient smiling to document the maximum number of teeth and gingiva displayed during laughing or broadly smiling. The second photograph was taken with retracted lips, and the same retractor was used to ensure standardization (Figure 4).

### **Tested esthetic criteria**







The tested criteria affecting aesthetic perception included golden proportion, recurrent esthetic dental proportion, width to height ratio, apparent contact dimension, upper lip position, upper lip curvature, parallelism of the maxillary anterior incisal curve with the lower lip (smile arc), relationship between the maxillary anterior teeth and the lower lip, number of maxillary teeth displayed in the smile, presence of diastema between the maxillary central incisors, smile arc/lower lip distance, upper lip height, lower lip height, midline discrepancy, lateral incisor edge position and skin and teeth shade on aesthetic perception.

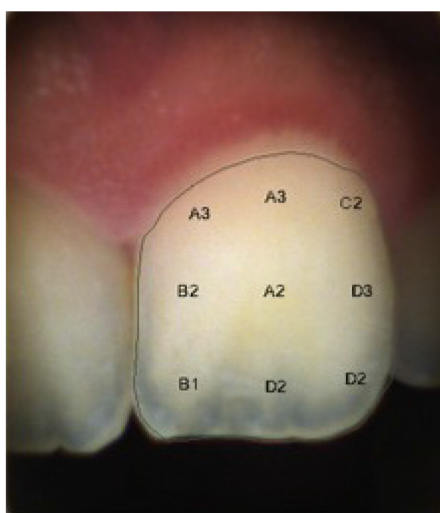
### **Assessment of dental appearance performed by laypersons and dentists**

The assessment of dental appearance was performed by laypersons, dentists representing various specialties, experiences,

**Table 1 Dental appearance questionnaire**

Number	Question
Q1	I am content with the appearance of my teeth
Q2	I am content with the size of my teeth
Q3	I am content with the shape of my teeth
Q4	I am content with the color of my teeth
Q5	I am content with the position of my teeth
Q6	I am content with the appearance of my gum
Q7	I tend to hide my teeth
Q8	I wish I had other teeth
Q9	I feel rather old because of my teeth
Q10	I am dissatisfied with the black hole disease between my teeth.
Q11	I am dissatisfied that my teeth are recognized as artificial

Fitzpatrick scale					
					
<b>Type I</b>	<b>Type II</b>	<b>Type III</b>	<b>Type IV</b>	<b>Type V</b>	<b>Type VI</b>
Light, pale white	White, fair	Medium, white to olive	Olive, moderate brown	Brown, dark brown	Black, very dark brown to black
Always burns, never tans	Usually burns, tans with difficulty	Sometimes mild burns, gradually tans to olive	Rarely burns, tans with ease to a moderate brown	Very rarely burns, tans very easily	Never burns, tans very easy deeply pigmented

**Figure 1** Fitzpatrick scale.**Figure 2** Representative image for digital shade mapping using digital shade detector "Ray Picker".

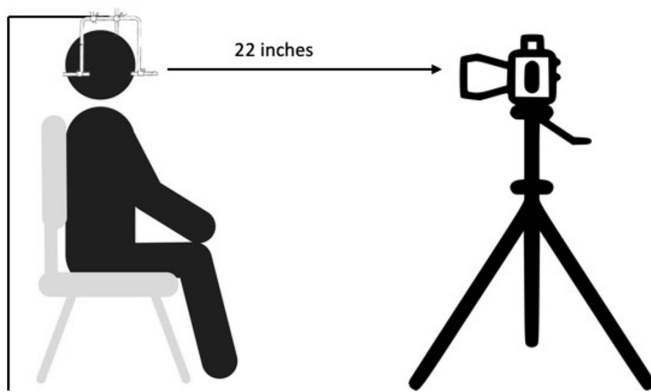


**Figure 3** Patient position in reference to camera.



**Figure 4** Frontal views. A: Smiling with lips; B: Smiling with retracted lips.

and sexes. They were requested to evaluate the dental appearance using standardized digital photographs. Additionally, laypersons, and dentists were requested to judge the photographs based on aesthetic appearance using a Visual Analogue Scale (VAS).

Laypersons received training how to use (VAS) by being shown two photos of patients not included in the study. Once they felt comfortable with the process, they were asked to use the VAS to analyze the photos. The VAS was graded on a scale from 0 to 10, with 0 representing absolutely unaesthetic and 10 representing absolutely aesthetic. Demographic information collected from dentists included sex, age, nationality, place of work, specialty, and years of experience. Laypersons were asked about their sex, age, educational level, and income.

### Statistical analysis

The collected data were analyzed using Statistical Software SPSS version 23. Descriptive statistics were calculated using parametric tests (*t*-test and one-way analysis of variance) as well as non-parametric tests (Mann-Whitney and Kruskal-Wallis). To assess the normality testing, Shapiro-Wilk test was used.

## RESULTS

The results of this study are presented according to the following: patient sample characteristics, layperson sample characteristics, dentist sample characteristics, comparison among patients, laypersons and dentists' perception, and the aesthetic analysis of patients' photographs.

### Patient sample characteristics

The patient sample included 50 female participants. Most of the patients were in the age group of 20 years to 29 years, with only 2 patients falling into the age group of 50 to 69. In terms of treatment, 62.0% of the patients underwent orthodontic treatment while 38.0% did not. Additionally, only 8.0% of the patients underwent filler treatment, while the 92.0% did not choose this option.

Regarding patient satisfaction, 66.0% of patients expressed satisfaction (satisfied/highly satisfied) regarding the size of their teeth, 42.0% of patients reported satisfaction (satisfied/highly satisfied) concerning the color of their teeth. 54.0% of patients were satisfied (satisfied/highly satisfied) with the appearance of their gum, whereas 30.0% of patients could not decide whether they are satisfied or not with the appearance of their gum (Table 2).

**Table 2** Distribution of patients' satisfaction level on their smile and dental appearance

Variable	Highly dissatisfied	Dissatisfied	Cannot decide/do not know	Satisfied	Highly satisfied	Total
Appearance of teeth		9 (18.0)	9 (18.0)	19 (38.0)	13 (26.0)	50 (100.0)
Size of teeth		8 (16.0)	9 (18.0)	23 (46.0)	10 (20.0)	50 (100.0)
Shape of teeth		8 (16.0)	10 (20.0)	22 (44.0)	10 (20.0)	50 (100.0)
Color of teeth	2 (4.0)	16 (32.0)	11 (22.0)	14 (28.0)	7 (14.0)	50 (100.0)
Position of teeth		9 (18.0)	8 (16.0)	21 (42.0)	12 (24.0)	50 (100.0)
Appearance of gum	2 (4.0)	6 (12.0)	15 (30.0)	16 (32.0)	11 (22.0)	50 (100.0)

Data are *n* (%).

Assessments of patient's behavioral attitudes related to their dental appearance was performed on a five-point Likert scale where a score of 1 indicated "strongly disagree" and a score of 5 represented "strongly agree". It was found that 74% of patients responded either "strongly disagree" or "disagree" regarding hiding their teeth. Similarly, 68% of patients' responses were "strongly disagree" or "disagree" considering their desire for replacing their teeth, and 76% of patients reported "strongly disagree" or "disagree" concerning evaluating if their teeth made them look older. A total of 16.0% of patients could not decide whether they are satisfied or not with in their response to these behavioral attitudes.

Patients' satisfaction level towards six measures describing their teeth, which included appearance, size, shape, color, position, and the appearance of the gum, was assessed. The patients' sample indicated satisfaction with mean scores of 3.56 for gum appearance, and 3.72 for teeth appearance and the positioning of teeth. However, patients provided a lower satisfaction level regarding their teeth color (Figure 5).

Patients' agreement level regarding the five negative self-behavioral attitudes related to their reaction to smile and teeth appearance was assessed. In general, the patients' sample disagreed with most items, giving mean scores of 1.84 for "strange teeth" and 2.32 for "black space". Patients strongly disagreed that their teeth could make them look older, with mean score of 1.68. Moreover, patients who did not undergo orthodontic treatment showed lower satisfaction with gum appearance scoring 3.32 and tended to hide their teeth with mean score 2.58 compared to those who received orthodontic treatment. Furthermore, patients who did not have filler treatment expressed lower satisfaction with tooth size (mean score: 3.67) when compared with those who had filler treatment (mean score: 4.00).

### Laypersons' sample characteristics

The layperson sample consisted of 488 randomly selected participants, with 86.1% female and 13.9% male. In terms of age distribution, the majority (60.2%) were aged 27 or younger, while 28.0% were aged between 28-years-old and 43-years-old, and the lowest percentage was aged 44 or older. Moreover, most of the participants had a bachelor's degree and their monthly income extended from 10000 to 30000 Saudi Riyal.

In the laypersons' sample, there was a significant difference in their perception of aesthetic smiles and dental appearances in photos "with lips" and "without lips". Among the patients' photos, 46 had higher aesthetic perception when lips were present. The highest-rated aesthetic photo, according to laypersons' perception achieved a maximum mean value of  $(8.18 \pm 1.99)$  "with lips" and  $(6.53 \pm 2.74)$  "without lips". In contrast, the photos that were considered (absolutely unaesthetic) by laypersons received scores of  $1.73 \pm 1.95$  "with lips" and  $1.08 \pm 1.74$  "without lips". These findings show a significant difference in mean perception scores among laypersons for photos "with lips" compared to those "without lips" in most of the pictures.

Furthermore, female laypersons had higher perception mean scores compared to males. There were significant differences in perception mean scores among laypersons based on their educational background. The least significant difference post-hoc test was used to determine the significant differences within the educational background categories for laypersons. The mean scores for laypersons with an intermediate level of education were higher than those for laypersons in the Secondary, Bachelor, and PhD groups, with *P* values < 0.05 (0.001, 0.002, and 0.048) and mean differences of 1.89, 1.62 and 1.80, respectively. These findings suggest that laypersons with an intermediate level of education tend to have a higher aesthetical mean score when compared to laypersons in the Secondary, Bachelor, and PhD education groups.

Regarding laypersons' income, significant differences were observed in perception mean scores. Laypersons with an income of more than 30000 obtained a higher aesthetical mean score for the group "without lips" compared to laypersons in both the less than 10000 and the 10000-30000 income groups.

### Dentist sample characteristics

Out of the 90 randomly selected dentists, the majority were females representing 82.2% of the sample, and the remaining 17.8% consisted of males. More than 57.8% were under the age of 30. The majority (85.6%) of the dentists' sample were Saudi, while the remaining were non-Saudi, regardless of the nationality. The highest percentage (97.7%) of the dentists' sample worked in academic institutes and governmental hospitals, while only 2.2% held jobs in the private sector. Most dentists in the sample had between 1 year to 4 years of professional experience, which is compatible with the sample's age.

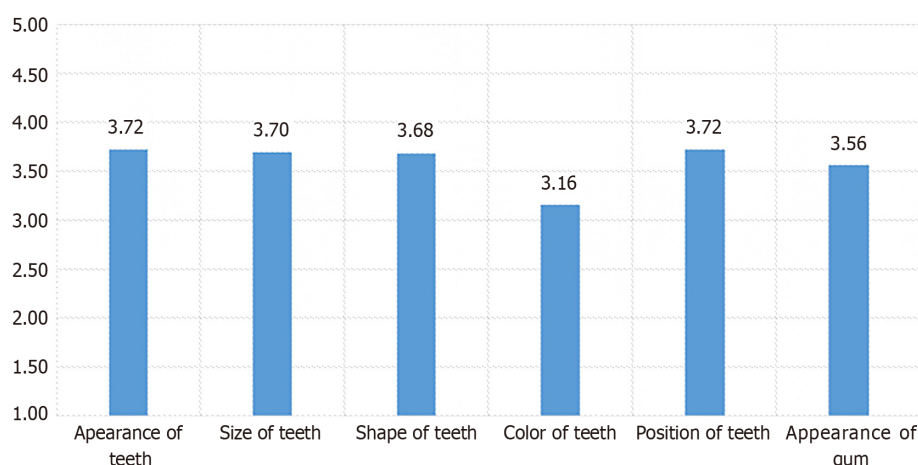


**Figure 5** Patients' mean response scores for satisfaction about dental appearance.

For the dentist sample, the perception of aesthetic smile and dental appearance in photos, “with lips” and “without lips”, was similar among 23 of the patients. The highest mean value for dentists' perceptions was recorded with photos that included lips, with a mean score of  $7.83 \pm 1.962$ , and for the same photo without lips, the mean score was  $7.67 \pm 2.208$ . These findings suggest that the smile and dental appearance were both considered as aesthetic parameters from dentists' points of view. Furthermore, the lowest mean value for dentists' perceptions were recorded in photos “with lips”, with a mean score of  $2.20 \pm 1.819$  and for the same photo “without lips”, the mean score was  $1.97 \pm 1.839$ . This suggests that both the smile and dental appearance were considered unaesthetic parameter according to dentists' opinion. In general, female dentists tended to give higher perception scores in comparison to males in the same profession.

### Comparison among patients, laypersons and dentist's perception

A positive moderate correlation existed between patients' satisfaction with their dental appearance and the assessments made by both laypersons and dentists for patients' pictures, whether with or without lips. Furthermore, there was a strong and positive significant relationship between laypersons' perception and dentists' perception mean scores for pictures, with and without lips. There was no significant difference in perception mean scores between dentists and laypersons when evaluating pictures “with lips”, whereas the main difference was found in the evaluation of pictures “without lips”. Laypersons gave a mean score of  $5.26 \pm 2.54$  for pictures “with lips” and  $2.65 \pm 2.53$  for pictures “without lips”. In contrast, dentists' mean scores were  $5.33 \pm 2.32$  for pictures “with lips” and  $4.77 \pm 2.52$  for pictures “without lips” (Figure 6).

### Aesthetic analysis

Based on this study, patient satisfaction was significantly affected by certain aesthetic criteria, such as midline discrepancy, tooth shade, smile arc, width of smile line, presence of diastema, upper lip position, and upper lip curvature. However, there was no statistical evidence that patients' satisfaction was affected by other criteria, including occlusal plane *vs* commissural line, upper inter-incisal line *vs* midline, labial corridor, as well as incisal curve *vs* lower lip.

Furthermore, there were statistically significant differences in laypersons' perception mean scores between smile line, and incisal curve *vs* lower lip, with *P* values less than 0.05. There were no statistically significant differences in layperson's perception mean scores for tooth exposure at rest, incisal curve *vs* lower lip (contacting), smile width, labial corridor, and occlusal plane *vs* commissural line, with *P* values greater than 0.05.

Additionally, there were statistically significant differences in dentists' perception mean scores for labial corridor, smile line, and incisal curve *vs* lower lip, with *P* values less than 0.05. In contrast, there was no statistical evidence that dentists' perception was affected by upper inter-incisal line *vs* midline, incisal curve *vs* lower lip (contacting), and tooth exposure at rest aesthetic criteria.

### Facial analysis

**Skin shade:** Within the sample of patients, the majority, 60.0%, exhibited a light brown skin shade, while 24.0% had a medium brown skin tone. Beige and black skin shades each comprised 8% of the sample based on Fitzpatrick scale.

**Upper lip position:** Within the patient group, the distribution of upper lip position was as follows (Figure 7): 50% had an average upper lip position (Figure 7A), 46.0% had a low position upper lip (Figure 7B), and 14% had a high position or gummy smile (Figure 7C).

**Upper lip curvature:** Within the patient group, 62.0% exhibited a straight upper lip curvature (Figure 7A), 24.0% had a downward curvature (Figure 7E) and only 14.0% of the patients' sample had an upward upper lip curvature during smiling (Figure 7D).

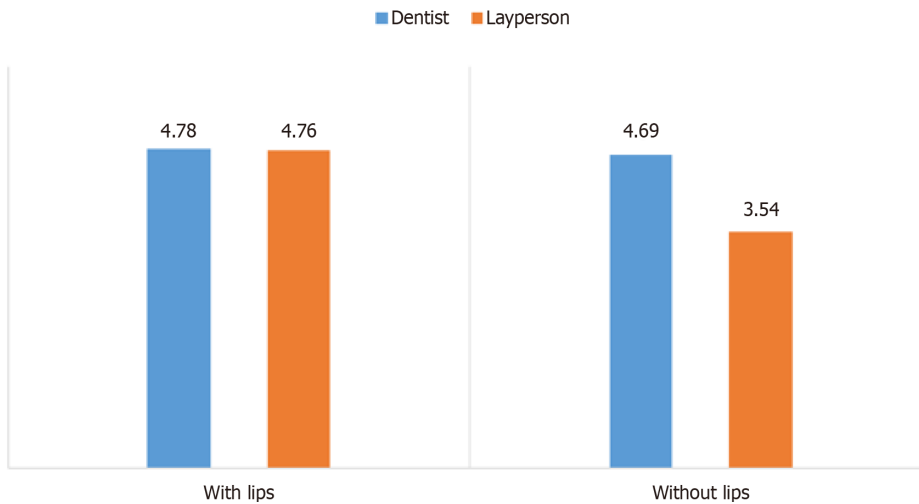


**Figure 6** Comparison between dentist and laypersons mean score for pictures with lips and without lips.



**Figure 7 Extra-oral photograph.** A: Average upper lip position, straight upper lip curvature, coincident between upper inter-incisal line and midline, normal buccal corridor, occlusal plane parallel to the commissural line; B: Low upper lip position, straight smile arc, narrow smile line width; C: High upper lip position, the bottom line of the upper teeth formed a consistent curve with the lower lip; D: Upward upper lip curvature; E: Downward upper lip curvature, midline discrepancy to the right, intermediate smile line width; F: Midline discrepancy to the left; G: Proper dental midline coincidence, the bottom line of the upper teeth does not form a consistent curve with the lower lip, wide smile line width; H: Diastema between their central incisors.

**Upper inter-incisal line *vs* midline:** Most patients (60.0%) exhibited alignment in upper inter-incisal line *vs* midline (Figure 7A).

**Buccal corridor:** In the present study, 42.0% of the sample had a normal buccal corridor (Figure 7A).

**Occlusal plane *vs* commissural line:** The dental measurements revealed that (74.0%) of patients had an occlusal plane parallel to the commissural line (Figure 7A).

### Dental aesthetics

**Midline discrepancy:** In this study, 48% of patients presented proper dental midline coincidence (Figure 7G). In addition, 40.0% showed a midline discrepancy to the right, while 12.0% had a mild discrepancy to the left (Figure 7E and F).

**Tooth shade:** Among the patients' sample, the highest percent (48.0%) had Reddish-Brownish tooth shade, at brightness level 1 and 2, with A2 being the highest. Next, 34.0% of the sample displayed Reddish-Yellowish tooth shades, at brightness level 1, 2 and 3, with shade B1 being the highest. Furthermore, 16.0% of the sample revealed greyish tooth shade at brightness level 1,2 and 3, with shade C1 being the highest. Lastly, only 2.0% of the patients' sample had Reddish-Grey tooth shade at brightness level 2, with shade D1.

**Smile arc:** In 36% of the patients' sample, the bottom line of the upper teeth formed a consistent curve with the lower lip (Figure 7C). On the other hand, in 34% of patients, this alignment was not constant with the lower lip (Figure 7G), and only 30% had a straight smile arc (Figure 7B).

**Width of smile line:** The study found that most patients (76.0%) showed their first premolars during smiling. In contrast, 20.0% of patients tended to show their second premolars, and only 4.0% of patients showed their first molar when smiling. This smile line width can be categorized as narrow (Figure 7B), intermediate (Figure 7E), or wide (Figure 7G).

**Presence of diastema between the central incisors:** Diastema between the central incisors was absent for 94.0% of patients. Only 6.0% displayed a diastema between their central incisors (Figure 7H).

## DISCUSSION

This study evaluated the aesthetic perception towards dental appearance as perceived by three entities: patients, laypersons and dentists. The patients were selected from diverse backgrounds as well as socioeconomic levels in order to explore their satisfaction with different aesthetic elements.

Patients' teeth shade was measured using the digital shade detector (Ray Plicker). As, traditional chairside shade selection is known to be subjective due to various factors, including differences in viewer interpretation, external influences such as eye fatigue, aging, emotional state, lighting conditions, level of experience, and physiological variable such as color blindness. Therefore, electronic shade matching devices are used to address the limitations of traditional shade selection[20].

In the present study, most of the patients have a light brown skin shade. Vadavadagi *et al*[21] found a correlation between skin tone and tooth shade, suggesting that individuals with medium to dark skin tend to have teeth categorized with a high value resulting in darker shaded teeth compared to individuals with fair skin tones whose teeth have a low value[21]. The study by Esan *et al*[22] did not reveal any significant relationship between tooth shade and skin color[22].

In this study, patients were categorized according to the lip position to average upper lip position, low lip position, and high lip position (gummy smile). According to literature, the exposure of gingival tissue at smiling is not considered a negative aesthetic feature[23,24]. Kokich *et al*[24] evaluated female smiles and found that laypersons generally considered a 3 mm display of gingival tissue as aesthetically pleasing[24].

Notably in this study, most patients exhibited a straight upper lip curvature during smiling. In agreement with this finding, Hulsye's mean score data indicated that the group with an upward lip curvature contained the largest number of subjects, while the group with a straight lip curvature included the fewest subjects. Additionally, this study reported that most patients displayed normal buccal corridors[25]. However, Krishnan *et al*[26] reported that intermediate buccal corridors are generally considered the most aesthetically pleasing when compared to wider or narrower buccal corridors [26].

In the current study, most patients exhibited parallel alignment of the occlusal plane with the commissural line. AlShamsi and AbuZayda[27] reported that the occlusal plane parallel to the commissural line is most preferred by both dental professionals and laypersons[27]. This aligns with the suggestions of Goldstein *et al*[28] and Dawson[29], suggesting that maintaining a parallel occlusal plane to a commissural line is essential for preserving natural facial harmony.

Most of the patients in this study displayed proper dental midline alignment. This observation is consistent with the findings of a study conducted by Priyadharshni *et al*[30], which reported that the dental midline coincided with facial midline for most of the female population[30].

In the present study, the parallel smile arc was the predominant smile amongst patients. This finding aligns with Tjan *et al*[31] study which suggested that the parallel smile arc was found to be the normal type of smile arc in untreated individuals, and generally is considered optimal and aesthetically pleasing[31]. Regarding smile width, our results indicate a higher prevalence of exposure to the first premolar (76.0%). This finding is consistent with Tjan *et al*[31], who found a high prevalence of first premolar exposure (48.6%). However, other studies have reported a greater prevalence of exposure to the second premolar[32,33]. This variance may be attributed to differences in the age composition of the sample studied.

In this study, it was observed that the presence of a diastema had an adverse effect on the perceived attractiveness of the smile, receiving the lowest score amongst all pictures (Figure 7H). The lower rating could be attributed to violation of the aesthetic principle of unity, harmony and balance. Kokich *et al*[24] and Geevarghese *et al*[7] observed that the midline diastema was not perceived as unattractive to neither dentists nor the public except when the gap between the central incisors exceeded 2.0 mm to 3.0 mm. Sabri *et al*[5], on the other hand, reported that a diastema exceeding 4 mm was

linked with an unfavorable perception of an individual's smile. Studies have shown that smiles that create a sense of unity are generally considered to be more attractive[2,34,35].

The majority of female patients expressed satisfaction according to their responses. This high satisfaction level could be attributed to several reasons; specifically, 62.0% of the sample had undergone orthodontic treatment while 8.0% had received lip fillers, indicating a greater motivational attitude to achieve an aesthetically pleasing smile. In line with our findings Negruțiu *et al*[9] and An *et al*[36] concluded that patients who had previously undergone orthodontic treatment exhibited a superior aesthetic perception compared to the control group without such treatment. Additionally, Alhaj *et al* [15] reported that individuals who have undergone orthodontic treatment or plastic surgery exhibited a positive impact on aesthetic perception.

However, when it comes to category of teeth color, most of the patients reported lower satisfaction levels[15]. The finding aligns with the findings of Alhaj *et al*[15], who also reported that teeth color received the lowest ratings when compared to facial and frontal profile assessments[15]. This emphasizes that teeth color is a sensitive and significant component of smile attractiveness[37]. This finding may be attributed to factors such as sex and age distribution within the sample. Research conducted by Vallittu *et al*[38], revealed that younger patients tend to prefer lighter tooth shade compared to the older individuals[38]. Similarly, Labban *et al*[19] found that female participants preferred lighter teeth shade than male participants[19].

The results of this study revealed that female laypersons tend to have higher mean scores perception than males. This aligns with Geron and Atalia[39], who reported statistically significant higher scores among female participants when evaluating smiles with upper gingival exposure[39]. This suggest that females may be more tolerant of upper gingival exposure. In contrast, our results differ from those of Zaugg *et al*[14], Alhaj *et al*[15] and Dudea *et al*[40] who reported that women tended to be more critical than men when assessing the presence of minor or major defects, while men were more accepting of different smiles. These differences could be attributed to a combination of sociocultural factors, individual preferences, and the specific characteristic of the study populations.

Furthermore, this study found that laypersons in the intermediate education group recorded higher level of aesthetical perception compared to laypersons in the Secondary, Bachelor, and PhD education groups. This observation agrees with Türkahraman *et al*[41] findings, who noted that individuals with a primary school education had a lower ability to notice skeletal dysplasia compared to those with university level of education[41]. Furthermore, Alhaj *et al*[15] reported that individuals with a higher level of education tended to rate their orofacial appearance more favorably than those with low or no education[15]. Hence, it can be concluded that there is a positive correlation between education level and the refinement of aesthetic preferences.

In our study, age was found to play a significant factor in the perception of laypersons. This agrees with the results reported by Zaugg *et al*[14] and Rodrigues *et al*[42], who found differences in perception among various age groups, with younger individuals exhibiting a more critical assessment. Regarding the presence of a black triangle, a statistically significant difference was observed, indicating a decline in aesthetic perception for black triangle among patient aged over 40 years. These data are consistent with the research conducted by Pithon *et al*[43], who observed a decline in the aesthetic perception with advancing age. However, Sriphadungporn and Chamnannidiadha[44] found that older individuals exhibited a greater tolerance for a large black triangle size compared to younger individuals[44]. Additionally, Alomari *et al*[4] reported that certain gingival characteristics were found to have more significant aesthetic impact among laypersons than the presence of a black triangle[4]. These differences may be attributed to differences in cultural and regional factors, which may have an influence on smile aesthetics and perceptions.

The findings of this study indicated that professional judgment of aesthetics, particularly in cases involving images "without lips", varies significantly. Dentist may apply precise scientific criteria to evaluate such images, setting them apart from non-experts. Our research aligns with Kusnoto *et al*[45] who found that education within the dental field and knowledge acquisition can influence and alter individuals' perceptions[45]. This finding is consistent with the results of Geevarghese *et al*[7], Khalaf *et al*[11] and Kokich *et al*[24] who reported that dentists possess a high ability to detect the most subtle changes in smile aesthetics compared to the general population.

It is important to acknowledge several limitations of this study. Firstly, the study focused on a sample of 50 female patients aged 18 to 40, which may not accurately reflect the broader population. Additionally, the study findings may be influenced by the specific demographics and cultural factors of the patients, as it was conducted exclusively within PNU dental clinics, potentially limiting the generalization of the results to different population. Moreover, it is worth noting that patients who volunteered for the study may have different aesthetic concerns or treatment histories which could have affected the study's outcomes. Lastly, the use of two-dimensional, static images in the assessment, both for laypersons and dentists, may not fully capture the dynamic nature of aesthetic outcomes, which could impact the accuracy of assessments.

## CONCLUSION

According to our analyses, the following conclusions could be drawn: (1) Orthodontic treatment positively affected patient satisfaction; (2) The presence of diastema negatively impacted the patient's smile attractiveness; (3) Female laypersons had a better perception of aesthetic when compared to male laypersons; (4) Higher education level with higher socioeconomic status enhanced aesthetic perception; (5) Younger aged laypersons displayed a more critical eye for aesthetics when compared to the older population; and (6) Dentists' aesthetic evaluation was more precise when compared to laypersons' aesthetic judgement.

## FOOTNOTES

**Author contributions:** Aldegheishem A, Alfayadh HM, AlDossary M, Asaad S, Eldwakhly E, AL Refaei NAH, AlSenan D, Soliman M conceptualized the study; Alfayadh HM, AL Refaei NAH, AlSenan D performed data collation; Aldegheishem A contributed funding acquisition and project management; Alfayadh HM, Asaad S, Eldwakhly E conducted the survey; Aldegheishem A, AlDossary M, AlSenan D, Soliman M designed the research methodology; Aldegheishem A, Alfayadh HM, AlDossary M, Asaad S, Eldwakhly E, AlSenan D wrote the original manuscript; AL Refaei NAH, Soliman M wrote and edited the manuscript the review and editing; All authors have read and agreed to the published version of the manuscript.

**Supported by** Princess Nourah Bint Abdulrahman University Researchers, No. PNURSP2024R115.

**Institutional review board statement:** The ethical approvals were obtained from the Deanship of Scientific Research, Princess Nourah Bint Abdulrahman University under IRB study number 17-0183.

**Informed consent statement:** Informed consent was obtained from all subjects involved in the study.

**Conflict-of-interest statement:** The authors declare no conflict of interest.

**Data sharing statement:** The data presented in this study are available upon request from the corresponding author.

**STROBE statement:** The authors have read the STROBE Statement-checklist of items, and the manuscript was prepared and revised according to the STROBE Statement-checklist of items.

**Open-Access:** This article is an open-access article that was selected by an in-house editor and fully peer-reviewed by external reviewers. It is distributed in accordance with the Creative Commons Attribution NonCommercial (CC BY-NC 4.0) license, which permits others to distribute, remix, adapt, build upon this work non-commercially, and license their derivative works on different terms, provided the original work is properly cited and the use is non-commercial. See: <https://creativecommons.org/licenses/by-nc/4.0/>

**Country of origin:** Saudi Arabia

**ORCID number:** Hadeel Mohammed Alfayadh 0000-0003-1690-8470; Mai Soliman 0000-0003-2417-8754.

**S-Editor:** Liu H

**L-Editor:** Filipodia

**P-Editor:** Zhang L

## REFERENCES

1. Werner LL, der Graaff JV, Meeus WH, Branje SJ. Depressive Symptoms in Adolescence: Longitudinal Links with Maternal Empathy and Psychological Control. *J Abnorm Child Psychol* 2016; **44**: 1121-1132 [PMID: 26627889 DOI: 10.1207/s15326950dp3801\_6]
2. Van der Geld P, Oosterveld P, Van Heck G, Kuijpers-Jagtman AM. Smile attractiveness. Self-perception and influence on personality. *Angle Orthod* 2007; **77**: 759-765 [PMID: 17685777 DOI: 10.2319/082606-349]
3. Almanea R, Modimigh A, Almogren F, Alhazzani E. Perception of smile attractiveness among orthodontists, restorative dentists, and laypersons in Saudi Arabia. *J Conserv Dent* 2019; **22**: 69-75 [PMID: 30820086 DOI: 10.4103/JCD.JCD\_429\_18]
4. Alomari SA, Alhaija ESA, AlWahadni AM, Al-Tawachi AK. Smile microaesthetics as perceived by dental professionals and laypersons. *Angle Orthod* 2022; **92**: 101-109 [PMID: 34520516 DOI: 10.2319/020521-108.1]
5. Sabri NABM, Ridzwan SBB, Soo SY, Wong L, Tew IM. Smile Attractiveness and Treatment Needs of Maxillary Midline Diastema with Various Widths: Perception among Laypersons, Dental Students, and Dentists in Malaysia. *Int J Dent* 2023; **2023**: 9977868 [PMID: 37095900 DOI: 10.1155/2023/9977868]
6. Zorlu M, Camcı H. The relationship between different levels of facial attractiveness and malocclusion perception: an eye tracking and survey study. *Prog Orthod* 2023; **24**: 29 [PMID: 37599306 DOI: 10.1186/s40510-023-00483-2]
7. Geevarghese A, Baskaradoss JK, Alsalem M, Aldahash A, Alfayez W, Alduhaimi T, Alehaideb A, Alsammahi O. Perception of general dentists and laypersons towards altered smile aesthetics. *J Orthod Sci* 2019; **8**: 14 [PMID: 31497573 DOI: 10.4103/jos.JOS\_103\_18]
8. Aldhorae K, Alqadasi B, Altawili ZM, Assiry A, Shamalah A, Al-Haidari SA. Perception of Dental Students and Laypersons to Altered Dentofacial Aesthetics. *J Int Soc Prev Community Dent* 2020; **10**: 85-95 [PMID: 32181225 DOI: 10.4103/jispcd.JISPCD\_340\_19]
9. Negruțiu BM, Moldovan AF, Staniș CE, Pusta CTJ, Moca AE, Vaida LL, Romanec C, Luchian I, Zetu IN, Todor BI. The Influence of Gingival Exposure on Smile Attractiveness as Perceived by Dentists and Laypersons. *Medicina (Kaunas)* 2022; **58** [PMID: 36143942 DOI: 10.3390/medicina58091265]
10. Miller CJ. The smile line as a guide to anterior esthetics. *Dent Clin North Am* 1989; **33**: 157-164 [PMID: 2656315]
11. Khalaf K, Seraj Z, Hussein H. Perception of Smile Aesthetics of Patients with Anterior Malocclusions and Lips Influence: A Comparison of Dental Professionals', Dental Students,' and Laypersons' Opinions. *Int J Dent* 2020; **2020**: 8870270 [PMID: 33133189 DOI: 10.1155/2020/8870270]
12. Ward DH. Proportional Smile Design: Using the Recurring Esthetic Dental Proportion to Correlate the Widths and Lengths of the Maxillary Anterior Teeth with the Size of the Face. *Dent Clin North Am* 2015; **59**: 623-638 [PMID: 26140969 DOI: 10.1016/j.cden.2015.03.006]
13. Raj V, Heymann HO, Hershey HG, Ritter AV, Casko JS. The apparent contact dimension and covariates among orthodontically treated and nontreated subjects. *J Esthet Restor Dent* 2009; **21**: 96-111 [PMID: 19368599 DOI: 10.1111/j.1708-8240.2009.00240.x]
14. Zaugg FL, Molinero-Mourelle P, Abou-Ayash S, Schimmel M, Brägger U, Wittneben JG. The influence of age and gender on perception of

- orofacial esthetics among laypersons in Switzerland. *J Esthet Restor Dent* 2022; **34**: 959-968 [PMID: 35324054 DOI: 10.1111/jerd.12906]
- 15 **Alhajj MN**, Ariffin Z, Celebić A, Alkheraif AA, Amran AG, Ismail IA. Perception of orofacial appearance among laypersons with diverse social and demographic status. *PLoS One* 2020; **15**: e0239232 [PMID: 32941532 DOI: 10.1371/journal.pone.0239232]
  - 16 **Sabherwal RS**, Gonzalez J, Naini FB. Assessing the influence of skin color and tooth shade value on perceived smile attractiveness. *J Am Dent Assoc* 2009; **140**: 696-705 [PMID: 19491166 DOI: 10.14219/jada.archive.2009.0256]
  - 17 **Mehl CJ**, Harder S, Kern M, Wolfart S. Patients' and dentists' perception of dental appearance. *Clin Oral Investig* 2011; **15**: 193-199 [PMID: 20232095 DOI: 10.1007/s00784-010-0393-y]
  - 18 **Sachdeva S**. Fitzpatrick skin typing: applications in dermatology. *Indian J Dermatol Venereol Leprol* 2009; **75**: 93-96 [PMID: 19172048 DOI: 10.4103/0378-6323.45238]
  - 19 **Labban N**, Al-Otaibi H, Alayed A, Alshankiti K, Al-Enizy MA. Assessment of the influence of gender and skin color on the preference of tooth shade in Saudi population. *Saudi Dent J* 2017; **29**: 102-110 [PMID: 28725127 DOI: 10.1016/j.sdentj.2017.05.001]
  - 20 **Kim M**, Kim B, Park B, Lee M, Won Y, Kim CY, Lee S. A Digital Shade-Matching Device for Dental Color Determination Using the Support Vector Machine Algorithm. *Sensors (Basel)* 2018; **18** [PMID: 30213046 DOI: 10.3390/s18093051]
  - 21 **Vadavadagi SV**, Kumari KV, Choudhury GK, Vilekar AM, Das SS, Jena D, Kataraki B, B L B. Prevalence of Tooth Shade and its Correlation with Skin Colour - A Cross-sectional Study. *J Clin Diagn Res* 2016; **10**: ZC72-ZC74 [PMID: 27042590 DOI: 10.7860/JCDR/2016/16918.7324]
  - 22 **Esan TA**, Olusile AO, Akeredolu PA. Factors influencing tooth shade selection for completely edentulous patients. *J Contemp Dent Pract* 2006; **7**: 80-87 [PMID: 17091143]
  - 23 **Suzuki L**, Machado AW, Bittencourt MAV. An Evaluation of the Influence of Gingival Display Level in Smile Aesthetics. *Dent Press J Orthod* 2011; **16**: 37-39 [DOI: 10.1590/S2176-94512011000500005]
  - 24 **Kokich VO Jr**, Kiyak HA, Shapiro PA. Comparing the perception of dentists and lay people to altered dental esthetics. *J Esthet Dent* 1999; **11**: 311-324 [PMID: 10825866 DOI: 10.1111/j.1708-8240.1999.tb00414.x]
  - 25 **Hulsey CM**. An esthetic evaluation of lip-teeth relationships present in the smile. *Am J Orthod* 1970; **57**: 132-144 [PMID: 5263359 DOI: 10.1016/0002-9416(70)90260-5]
  - 26 **Krishnan V**, Daniel ST, Lazar D, Asok A. Characterization of posed smile by using visual analog scale, smile arc, buccal corridor measures, and modified smile index. *Am J Orthod Dentofacial Orthop* 2008; **133**: 515-523 [PMID: 18405815 DOI: 10.1016/j.ajodo.2006.04.046]
  - 27 **AlShamsi A**, AbuZayda M. The Evaluation of Smile Design by Lay People and Dentists in the UAE. *Int J Dent Oral Health* 2020; **6** [DOI: 10.16966/2378-7090.318]
  - 28 **Goldstein RE**, Belinfante L, Nahai F. Change Your Smile. 3rd ed. United States: Quintessence, 1997
  - 29 **Dawson PE**. Evaluation, Diagnosis and Treatment of Occlusal Problems. 2nd ed. United States: Mosby, 1989
  - 30 **Priyadharshni S**, Felicita A Sumathi. Prevalence of Maxillary Midline Shift in Female Patients Reported to Saveetha Dental College. *Drug Inven Today* 2019; **11**: 77-80
  - 31 **Tjan AH**, Miller GD, The JG. Some esthetic factors in a smile. *J Prosthet Dent* 1984; **51**: 24-28 [PMID: 6583388 DOI: 10.1016/s0022-3913(84)80097-9]
  - 32 **Al-Johany SS**, Alqahtani AS, Alqahtani FY, Alzahrani AH. Evaluation of different esthetic smile criteria. *Int J Prosthodont* 2011; **24**: 64-70 [PMID: 21210007]
  - 33 **Maulik C**, Nanda R. Dynamic smile analysis in young adults. *Am J Orthod Dentofacial Orthop* 2007; **132**: 307-315 [PMID: 17826598 DOI: 10.1016/j.ajodo.2005.11.037]
  - 34 **Valo TS**. Anterior esthetics and the visual arts: beauty, elements of composition, and their clinical application to dentistry. *Curr Opin Cosmet Dent* 1995; **24**-32 [PMID: 7550877]
  - 35 **Lombardi RE**. The principles of visual perception and their clinical application to denture esthetics. *J Prosthet Dent* 1973; **29**: 358-382 [PMID: 4570911 DOI: 10.1016/s0022-3913(73)80013-7]
  - 36 **An SM**, Choi SY, Chung YW, Jang TH, Kang KH. Comparing esthetic smile perceptions among laypersons with and without orthodontic treatment experience and dentists. *Korean J Orthod* 2014; **44**: 294-303 [PMID: 25473645 DOI: 10.4041/kjod.2014.44.6.294]
  - 37 **Pavicic DK**, Spalj S, Uhac I, Lajnert V. A Cross-Sectional Study of the Influence of Tooth Color Elements on Satisfaction with Smile Esthetics. *Int J Prosthodont* 2017; **30**: 156-159 [PMID: 28267826 DOI: 10.11607/ijp.5070]
  - 38 **Vallittu PK**, Vallittu AS, Lassila VP. Dental aesthetics--a survey of attitudes in different groups of patients. *J Dent* 1996; **24**: 335-338 [PMID: 8916647 DOI: 10.1016/0300-5712(95)00079-8]
  - 39 **Geron S**, Atalia W. Influence of sex on the perception of oral and smile esthetics with different gingival display and incisal plane inclination. *Angle Orthod* 2005; **75**: 778-784 [PMID: 16283815 DOI: 10.1043/0003-3219(2005)75
  - 40 **Dudea D**, Lasserre JF, Alb C, Culic B, Pop Ciutrla IS, Colosi H. Patients' perspective on dental aesthetics in a South-Eastern European community. *J Dent* 2012; **40** Suppl 1: e72-e81 [PMID: 22330323 DOI: 10.1016/j.jdent.2012.01.016]
  - 41 **Türkkahraman H**, Gökalp H. Facial profile preferences among various layers of Turkish population. *Angle Orthod* 2004; **74**: 640-647 [PMID: 15529499 DOI: 10.1043/0003-3219(2004)074<0640:FPPAVL>2.0.CO;2]
  - 42 **Rodrigues Cde D**, Magnani R, Machado MS, Oliveira OB. The perception of smile attractiveness. *Angle Orthod* 2009; **79**: 634-639 [PMID: 19537851 DOI: 10.2319/030508-131.1]
  - 43 **Pithon MM**, Bastos GW, Miranda NS, Sampaio T, Ribeiro TP, Nascimento LE, Coqueiro Rda S. Esthetic perception of black spaces between maxillary central incisors by different age groups. *Am J Orthod Dentofacial Orthop* 2013; **143**: 371-375 [PMID: 23452971 DOI: 10.1016/j.ajodo.2012.10.020]
  - 44 **Sriphadungporn C**, Chamnannidiadha N. Perception of smile esthetics by laypeople of different ages. *Prog Orthod* 2017; **18**: 8 [PMID: 28317085 DOI: 10.1186/s40510-017-0162-4]
  - 45 **Kusnoto J**, Haryanto ST. Perceptions Differences in Smile Attractiveness Between Dental Students and Laypersons. *J Indonesian Dent Assoc* 2021; **4**: 29-34 [DOI: 10.32793/JIDA.V4I1.670]



Observational Study

# Effects of pulmonary surfactant combined with noninvasive positive pressure ventilation in neonates with respiratory distress syndrome

Ze-Ning Shi, Xin Zhang, Chun-Yuan Du, Bing Zhao, Shu-Gang Liu

**Specialty type:** Health care sciences and services

**Provenance and peer review:** Unsolicited article; Externally peer reviewed.

**Peer-review model:** Single blind

**Peer-review report's classification**

**Scientific Quality:** Grade B

**Novelty:** Grade B

**Creativity or Innovation:** Grade B

**Scientific Significance:** Grade B

**P-Reviewer:** Han G, United States

**Received:** March 22, 2024

**Revised:** May 25, 2024

**Accepted:** June 12, 2024

**Published online:** August 16, 2024

**Processing time:** 104 Days and 22.8 Hours



**Ze-Ning Shi, Shu-Gang Liu,** Department of Pediatrics, Army Military Medical University Officer School Affiliated Hospital, Shijiazhuang 050000, Hebei Province, China

**Xin Zhang, Bing Zhao,** Department of Anesthesiology, Army Military Medical University Officer School Affiliated Hospital, Shijiazhuang 050000, Hebei Province, China

**Chun-Yuan Du,** Department of Gynecology and Obstetrics, Army Military Medical University Officer School Affiliated Hospital, Shijiazhuang 050000, Hebei Province, China

**Corresponding author:** Xin Zhang, PhD, Research Fellow, Department of Anesthesiology, Army Military Medical University Officer School Affiliated Hospital, No. 346 Shenglibei Street, Shijiazhuang 050000, Hebei Province, China. [zhangxing202309@163.com](mailto:zhangxing202309@163.com)

## Abstract

### BACKGROUND

Neonatal respiratory distress syndrome (NRDS) is one of the most common diseases in neonatal intensive care units, with an incidence rate of about 7% among infants. Additionally, it is a leading cause of neonatal death in hospitals in China. The main mechanism of the disease is hypoxemia and hypercapnia caused by lack of surfactant

### AIM

To explore the effect of pulmonary surfactant (PS) combined with noninvasive positive pressure ventilation on keratin-14 (KRT-14) and endothelin-1 (ET-1) levels in peripheral blood and the effectiveness in treating NRDS.

### METHODS

Altogether 137 neonates with respiratory distress syndrome treated in our hospital from April 2019 to July 2021 were included. Of these, 64 control cases were treated with noninvasive positive pressure ventilation and 73 observation cases were treated with PS combined with noninvasive positive pressure ventilation. The expression of KRT-14 and ET-1 in the two groups was compared. The deaths, complications, and  $\text{PaO}_2$ ,  $\text{PaCO}_2$ , and  $\text{PaO}_2/\text{FiO}_2$  blood gas indexes in the two groups were compared. Receiver operating characteristic curve (ROC) analysis was used to determine the diagnostic value of KRT-14 and ET-1 in the treatment of NRDS.

### RESULTS

The observation group had a significantly higher effectiveness rate than the control group. There was no significant difference between the two groups in terms of neonatal mortality and adverse reactions, such as bronchial dysplasia, cyanosis, and shortness of breath. After treatment, the levels of PaO<sub>2</sub> and PaO<sub>2</sub>/FiO<sub>2</sub> in both groups were significantly higher than before treatment, while the level of PaCO<sub>2</sub> was significantly lower. After treatment, the observation group had significantly higher levels of PaO<sub>2</sub> and PaO<sub>2</sub>/FiO<sub>2</sub> than the control group, while PaCO<sub>2</sub> was notably lower in the observation group. After treatment, the KRT-14 and ET-1 levels in both groups were significantly decreased compared with the pre-treatment levels. The observation group had a reduction of KRT-14 and ET-1 levels than the control group. ROC curve analysis showed that the area under the curve (AUC) of KRT-14 was 0.791, and the AUC of ET-1 was 0.816.

## CONCLUSION

Combining PS with noninvasive positive pressure ventilation significantly improved the effectiveness of NRDS therapy. KRT-14 and ET-1 levels may have potential as therapeutic and diagnostic indicators.

**Key Words:** Pulmonary surfactant; Non-invasive positive pressure ventilation; Neonatal respiratory distress syndrome; Keratin-14; Endothelin-1

©The Author(s) 2024. Published by Baishideng Publishing Group Inc. All rights reserved.

**Core Tip:** The purpose of this study was to explore the effect of pulmonary surfactant (PS) combined with noninvasive positive pressure ventilation on the levels of keratin-14 (KRT-14) and endothelin-1 (ET-1) in peripheral blood and the effectiveness for treating neonatal respiratory distress syndrome (NRDS). KRT-14 and ET-1 expression in the two groups was compared. The therapeutic effectiveness, occurrence of death and complications, and the blood gas indexes PaO<sub>2</sub>, PaCO<sub>2</sub> and PaO<sub>2</sub>/FiO<sub>2</sub> in the two groups were compared. Receiver operating characteristic curve analysis was used to determine the diagnostic value of KRT-14 and ET-1 for the effectiveness of NRDS therapy. PS combined with noninvasive positive pressure ventilation significantly improved the effectiveness of NRDS therapy. KRT-14 and ET-1 levels may have potential as diagnostic indicators of therapy.

**Citation:** Shi ZN, Zhang X, Du CY, Zhao B, Liu SG. Effects of pulmonary surfactant combined with noninvasive positive pressure ventilation in neonates with respiratory distress syndrome. *World J Clin Cases* 2024; 12(23): 5366-5373

**URL:** <https://www.wjgnet.com/2307-8960/full/v12/i23/5366.htm>

**DOI:** <https://dx.doi.org/10.12998/wjcc.v12.i23.5366>

## INTRODUCTION

Neonatal respiratory distress syndrome (NRDS) is one of the most common conditions in neonatal intensive care units. The incidence is about 7% and it is one of the main causes of neonatal death in hospitals in China[1,2]. The main mechanism of the disease is hypoxemia and hypercapnia caused by lack of surfactant. The diffusion efficiency of oxygen through the alveolar-capillary exchange barrier is disturbed owing to various factors, and lung injury in neonates leads to asthma, septicemia, pneumonia, and other complex symptoms[3]. Premature delivery of pregnant women and pregnancy disease may lead to morbidity. Only early diagnosis and treatment can improve the quality of life of neonates[4,5].

As the pathogenesis of NRDS is the lack of pulmonary surfactant, exogenous pulmonary surfactant (PS) replacement therapy has been found to be an effective treatment[6]. When neonates suffer from respiratory failure, respiratory support can also improve their condition. However, invasive ventilation tends to cause a series of complications such as lung infection, ventilator-associated lung injury, *etc* that draws attention to its widespread use[7]. It has been found in many studies that noninvasive positive pressure ventilation significantly improves NRDS neonates and has good safety[8,9]. At the same time, some studies have found that PS combined with non-invasive positive pressure ventilation can further improve clinical efficacy[10].

Keratin-14 (KRT-14) is a cytoskeleton protein that has good diagnostic value for lung tissue injury[11]. A study by Confalonieri[12] reported that KRT-14 was a viable biomarker for activation and repair/regeneration of lung cells. It is involved in the repair and regeneration of alveoli when the alveoli collapse, and lung cells are severely damaged in neonates with NRDS. Therefore, KRT14 may be used as an indicator of the improvement of the condition of neonates with RDS. Endothelin-1 (ET-1) is a vasoactive substance, which is mainly produced in lung tissue. It promotes the gradual change of pulmonary vascular reactivity through angiogenesis. It participates in vascular regulation, bronchoconstriction, and inflammatory reactions in the respiratory system. Endothelial and epithelial dysfunction in RDS patients can be induced of pro-inflammatory mechanisms. The use of endothelin receptor antagonists can regulate lung injury[13,14]. El Shemi *et al* team[15] examined the plasma ET-1 concentration of 69 premature neonates from 28 to 34 wk of age and diagnosed with NRDS. They found that the ET-1 concentration increased significantly 3 d after birth, and was predictive of the development of bronchopulmonary dysplasia. At present, there are few study results on the correlation of KRT-14

and ET-1 with the curative effect of NRDS neonates. Therefore, this study aimed to provide a basis and direction for clinical research on PS combined with noninvasive positive pressure ventilation to treat NRDS in neonates and observe the KRT-14 and ET-1 levels in peripheral blood.

## MATERIALS AND METHODS

### Study population

A total of 137 neonates with NRDS were treated in our hospital between April 2019 and July 2021 and were included in the study. The neonates had been admitted to the hospital and received basic treatment to ensure smooth breathing, protect against infection, and maintain water and electrolyte balance. Sixty-four infants, 37 males and 27 females, were included in a control group that received noninvasive positive pressure ventilation and basic treatment. The other 73 infants, 38 males and 35 females, were included in an observation group treated with PS combined with noninvasive positive pressure ventilation in addition to basic treatment. The study was approved by the Medical Ethics Committee, and the parents of all infants signed an informed consent form.

### Inclusion and exclusion criteria

Inclusion criteria: All neonates included in the study had complete clinical data, were diagnosed NRDS by imaging using the diagnostic criteria established by the 2016 update of the European Consensus Guidelines on the management of respiratory distress syndrome[16]. All families agreed with the treatment and follow-up. Exclusion criteria: Neonates with congenital immune defects, status complicated by other respiratory diseases, acute infectious disease, liver and kidney insufficiency, or allergic to therapeutic drugs or methods were excluded.

### Therapies

After admission, the two groups of neonates were treated with 21%-80% oxygen at a 6-8 L/min gas flow rate, and 4-7 cmH<sub>2</sub>O pressure. If the continuous positive airway pressure decreased to 2-3 cmH<sub>2</sub>O and the oxygen concentration decreased to 25%, and dyspnea was significantly relieved or had disappeared, the treatment was terminated. If the oxygen concentration was > 80%, the pressure was > 6-7 cmH<sub>2</sub>O, and the oxygen saturation was < 85% after 6-8 h of treatment, or if type II respiratory failure occurred, the treatment was changed to mechanical ventilation. Based on the above, neonates in the observation group were given exogenous PS[17] by tracheal administration as soon as possible.

### Sample collection and ELISA detection

After hospital admission and at 7:00 am the morning after treatment began, 5 mL of sterile venous blood was collected into a coagulation tube, serum was separated by centrifugation at 3000 g at 4 °C for 10 min and stored -80 °C. KRT-14 and ET-1 levels were determined by ELISA. The assay wells included a blank with 0 µL standard; a standard with 50 µL of standard substance at different concentrations, and a sample-to-be tested with 10 µL of sample and 40 µL diluent. Nothing was added to the blank well. In addition to the blank wells, 100 µL of horseradish peroxidase-labeled detection antibody was added to each of the standard wells and the sample wells. The reaction wells were sealed and incubated in a water bath at 37 °C for 65 min. The liquid was discarded, and the absorbent paper was patted dry. Each well was filled with washing liquid and allowed to stand for 2 min. The washing liquid was discarded, and the absorbent paper was patted dry. This procedure was repeated six times before 50 µL of substrate A and B solution was added to each well and incubated at 37 °C in the dark for 10 min. The optical density (OD) of each well was measured at 450 nm within 15 min after adding 50 µL of stop solution to each well, and the concentration was calculated.

### Efficacy evaluation

After effective treatment, clinical symptoms resolved or improved, abnormal shadows in the lungs disappeared or improved on X-ray films, and blood gas indexes normalized or improved. After Ineffective treatment, the clinical symptoms worsened or did not improve, or the neonate died, X-ray films showed enlarged shadow areas or lack of improvement. Blood gas indexes worsened or did not improve.

### Outcome measures

Main the outcome measures were KRT-14 and ET-1 expression in the observation and control groups. The therapeutic effect, death, and complications in the two groups were compared. The secondary outcomes were the clinical data of the two groups of neonates. The blood gas indexes PaO<sub>2</sub>, PaO<sub>2</sub>, and PaO<sub>2</sub>/FiO<sub>2</sub> of the two groups of neonates were compared and the value of KRT-14 and ET-1 for predicting the therapeutic effect in NRDS neonates was evaluated by ROC curve analysis.

### Statistical analysis

SPSS 20.0 (IBM Corp., Armonk, NY, United States) was used to perform the statistical analysis. GraphPad Prism 7 (GraphPad, La Jolla, CA, United States) was used to graph the collected data. Enumeration data were reported as numbers and percentages (%), and compared by chi-square tests. Measurement data were reported as means ± SD and independent sample *t*-tests were used to compare measurement data that were normally distributed. ROC was used to evaluate the diagnostic value of KRT-14 and ET-1 in the therapeutic effect of NRDS neonates. *P* < 0.05 was regarded as statistically significant.

**Table 1 Clinical data**

Parameter	Observation group, <i>n</i> = 73	Control group, <i>n</i> = 64	$\chi^2/t$	<i>P</i> value
Sex			0.456	0.499
Male	38 (52.05)	37 (57.81)		
Female	35 (47.95)	27 (42.19)		
Gestational age in wk	33.37 ± 2.12	32.87 ± 2.05	1.399	0.164
Body mass in kg	2.82 ± 0.69	2.71 ± 0.58	1.002	0.318
Apgar score	8.47 ± 1.31	8.28 ± 1.26	0.862	0.390
Age of pregnant woman in yr	27.3 ± 4.8	26.5 ± 4.1	1.041	0.230
Hypertension of Pregnant Women	9 (12.33)	5 (7.81)	0.758	0.384
Diabetes of pregnant women	11 (15.07)	7 (10.94)	0.510	0.475
Premature rupture of membranes	9 (12.33)	10 (15.63)	0.310	0.578
Delivery mode				
Eutocia	41 (56.16)	40 (62.50)	0.566	0.452
Cesarean section	32 (43.84)	24 (37.50)		
Premature delivery				
Yes	52 (71.23)	41 (64.06)	0.804	0.370
No	21 (28.77)	23 (35.94)		
Delivery history			0.027	0.870
Primiparity	50 (68.49)	43 (67.19)		
Multiparity	23 (31.51)	21 (32.81)		

## RESULTS

### Clinical data

Comparison of the clinical data (Table 1) found no significant differences between the two groups in sex, gestational age, body mass, Apgar score, age at pregnancy, hypertension during pregnancy, maternal diabetes, premature rupture of membranes, delivery mode, premature delivery, and delivery history.

### Comparison of therapeutic effect and adverse reactions between the two groups

We observed and compared the therapeutic effects of the two groups of neonates after treatment. The effectiveness of treatment was significantly better in the observation group than in the control group. As shown in Table 2 between-group differences in death, bronchial dysplasia, cyanosis, and shortness of breath were not significant.

### Blood gas indexes in the study groups

Comparing the blood gas indexes PaO<sub>2</sub>, PaCO<sub>2</sub>, and PaO<sub>2</sub>/FiO<sub>2</sub> before and after treatment, found no significant difference between the control and observation groups before treatment. After treatment, PaO<sub>2</sub> and PaO<sub>2</sub>/FiO<sub>2</sub> in both groups were significantly higher than before treatment, and PaCO<sub>2</sub> was notably lower than before treatment. The levels of PaO<sub>2</sub>, PaO<sub>2</sub>/FiO<sub>2</sub> in the observation group were considerably higher than the control group, while PaCO<sub>2</sub> was considerably lower than the control group, as shown in Figure 1.

### Levels of KRT-14 and ET-1 before and after treatment in the two groups

A comparison of the levels of KRT-14 and ET-1 before and after treatment in the two groups revealed that there is no difference between the two groups before the treatment. After treatment, the levels of KRT-14 and ET-1 were significantly reduced in both groups when compared to their pre-treatment levels. Moreover, the levels in the observation group were significantly lower than those in the control group, as shown in Figure 2.

### Diagnostic value of therapeutic effects of KRT-14 and ET-1

After comparing the levels of KRT-14 and ET-1 in neonates with effective and ineffective curative effects, we found that neonates with ineffective curative effects had significantly higher levels of KRT-14 and ET-1 than neonates with effective curative effects (*P* < 0.05). ROC curve analysis of the diagnostic value of KRT-14 and ET-1 in the curative effectiveness of NRDS neonates found that the area under the curve (AUC) of KRT-14 was 0.791, and the AUC of ET-1 was 0.816, as shown in Table 3 and Figure 3.

**Table 2 Effective therapy and adverse reactions**

Outcome	Observation group, <i>n</i> = 73	Control group, <i>n</i> = 64	<i>t</i>	<i>P</i> value
Effective curative effect	67 (91.78)	51 (79.69)	4.175	0.041
Ineffective curative effect	6 (8.22)	13 (20.31)		
Death	3 (4.11)	6 (9.38)	1.540	0.215
Bronchial dysplasia	6 (8.22)	11 (17.19)	2.514	0.112
Cyanopathy	8 (10.96)	10 (15.63)	0.651	0.420
Shortness of breath	9 (12.33)	14 (21.88)	2.225	0.136

**Table 3 Receiver operating characteristic curve analysis**

Index	AUC	95%CI	Specificity, %	Sensitivity, %	Youden index, %	Cut-off
KRT-14	0.791	0.665-0.917	85.47	60.00	45.47	> 3.645
ET-1	0.816	0.726-0.907	76.07	70.00	46.07	> 40.060

AUC: Area under the curve; ET-1: Endothelin-1; KRT-14: Keratin-14.

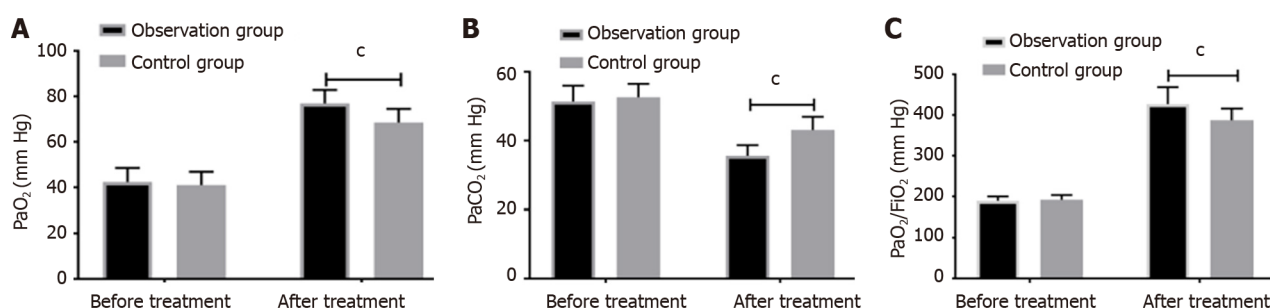


**Figure 1 Changes in blood gas indexes before and after treatment.** A: There was no significant difference in the  $\text{PaO}_2$  in the observation group ( $42.39 \pm 6.14$ ) and in the control group ( $41.01 \pm 5.89$ ) ( $t = 1.338$ ,  $P = 0.183$ ). The  $\text{PaO}_2$  in both groups was significantly increased after treatment ( $P < 0.05$ ), and it was significantly higher than the control group ( $68.54 \pm 5.96$ ) than in the observation group ( $76.92 \pm 5.94$ ) ( $t = 8.226$ ,  $P < 0.001$ ); B: There was no significant difference in the  $\text{PaCO}_2$  in the observation group ( $51.38 \pm 4.57$ ) and the control group ( $52.64 \pm 3.89$ ) ( $t = 1.725$ ,  $P = 0.087$ ). The  $\text{PaCO}_2$  in both groups was significantly decreased after treatment ( $P < 0.05$ ), and in the observation group ( $35.58 \pm 3.10$ ) it was significantly lower than the control group ( $43.08 \pm 3.83$ ) ( $t = 12.659$ ,  $P < 0.001$ ); C: There was no significant difference in the  $\text{PaO}_2/\text{FiO}_2$  of the observation group ( $189.19 \pm 10.95$ ) and in the control group ( $192.05 \pm 11.55$ ) ( $t = 1.487$ ,  $P = 0.139$ ). The  $\text{PaO}_2/\text{FiO}_2$  was significantly increased in both groups after treatment ( $P < 0.05$ ), and in the observation group ( $426.97 \pm 41.39$ ), it was significantly higher than the control group ( $387.18 \pm 28.86$ ) ( $t = 6.115$ ,  $P < 0.001$ ).  $^cP < 0.001$ .

## DISCUSSION

The pathogenesis of NRDS involves acute diffuse alveolar-capillary injury, which leads to increased pulmonary capillary permeability, and alveolar and interstitial edema, and ultimately gives rise to type II alveolar cell damage. This kind of damage reduces PS, leading to an increase in alveolar surface tension, contraction of alveolar groups, and abnormal pulmonary ventilation/blood flow ratio, eventually triggering severe hypoxemia[18,19]. Noninvasive positive pressure ventilation can relax the alveoli of neonates, improve the compliance of neonate lungs, maintain the pressure in alveoli, and maintain smooth breathing. Exogenous PS can supplement the lack of PS in neonates, thus reducing the tension of alveoli in neonates, preventing alveoli atrophy, improving lung respiratory function and lung compliance, and increasing blood oxygen saturation in NRDS, thus reducing the mechanical ventilation time of neonates[20,21].

We compared the therapeutic effect and adverse reactions of the two groups after treatment and found that the combination of PS and noninvasive positive pressure ventilation had a significantly better therapeutic effect than noninvasive positive pressure ventilation alone. However, the difference of the mortality rates in the two groups was not significant. We also compared the blood gas indexes  $\text{PaO}_2$ ,  $\text{PaCO}_2$ , and  $\text{PaO}_2/\text{FiO}_2$  of the two groups before and after treatment. After treatment,  $\text{PaO}_2$ ,  $\text{PaO}_2/\text{FiO}_2$  increased in both groups, and  $\text{PaCO}_2$  decreased significantly. After treatment, the  $\text{PaO}_2$  and  $\text{PaO}_2/\text{FiO}_2$  levels were significantly higher and  $\text{PaCO}_2$  was significantly lower in the observation group than in the control group. The blood gas levels of neonates with NRDS are significantly worse than those of healthy newborns as a result of differences in lung oxygenation and respiratory function. After the symptoms are controlled and pulmonary function improves, the blood gas index of the neonates returns to normal[22]. The study

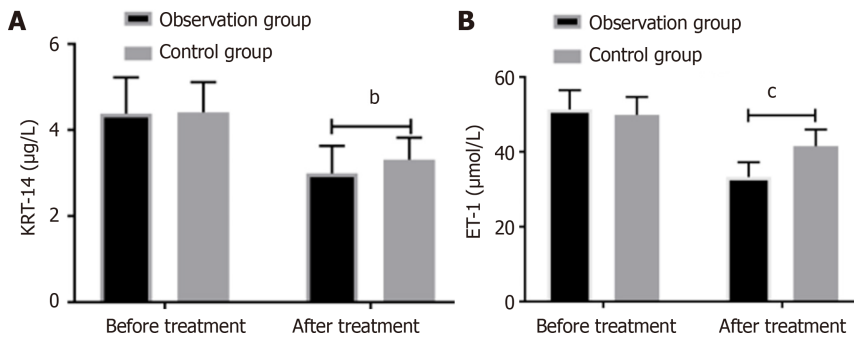


**Figure 2 Levels of keratin-14 and endothelin-1 before and after treatment.** A: There was no significant difference in keratin-14 (KRT-14) in the observation group ( $4.38 \pm 0.84$ ) and in the control group ( $4.41 \pm 0.70$ ) ( $t = 0.822$ ,  $P = 0.225$ ). KRT-14 was significantly decreased in both groups after treatment ( $P < 0.05$ ), and in the observation group ( $2.99 \pm 0.64$ ), the decrease was significantly lower than the control group ( $3.31 \pm 0.51$ ) ( $t = 3.206$ ,  $P < 0.002$ ); B: There was no significant difference in endothelin-1 (ET-1) between the observation group ( $51.34 \pm 5.13$ ) and the control group ( $49.90 \pm 4.75$ ) ( $t = 1.697$ ,  $P = 0.092$ ). ET-1 was significantly decreased in both groups after treatment ( $P < 0.05$ ), and it was significantly lower in the observation group ( $33.29 \pm 3.93$ ), than in the control group ( $41.51 \pm 4.48$ ) ( $t = 11.441$ ,  $P < 0.001$ ). <sup>b</sup> $P < 0.01$ , <sup>c</sup> $P < 0.001$ .

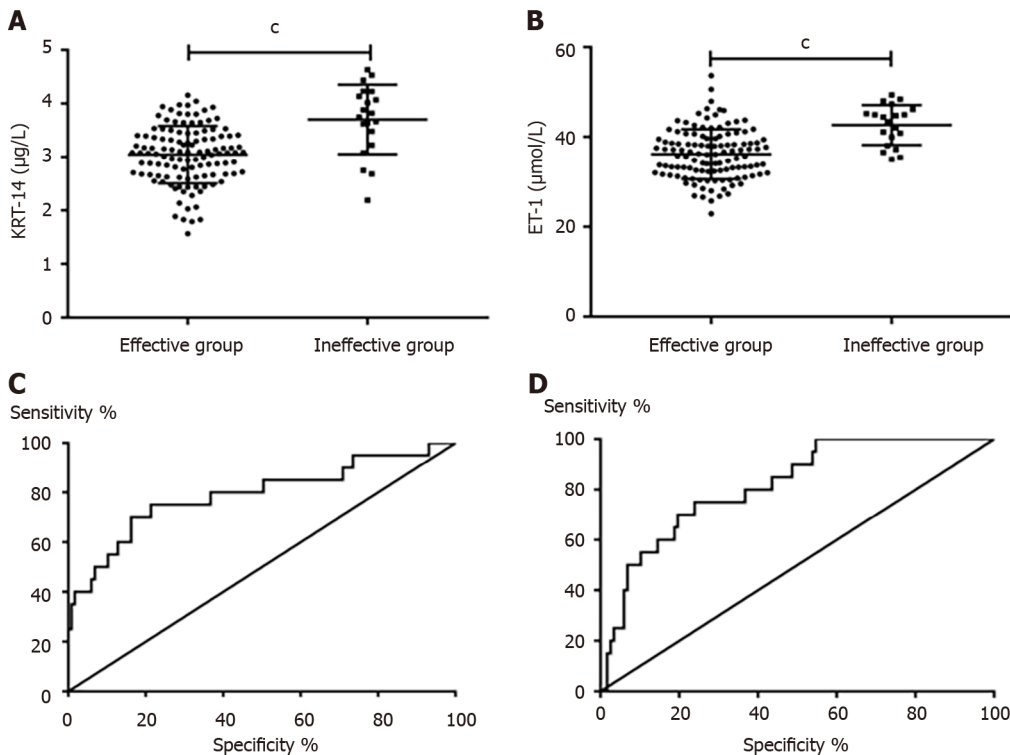


**Figure 3 Diagnostic value of the curative effectiveness of keratin-14 and endothelin-1.** A: Keratin-14 was significantly lower in neonates with effective therapy ( $2.94 \pm 0.56$ ) than in neonates with ineffective therapy ( $3.70 \pm 0.65$ ) ( $t = 5.472$ ,  $P < 0.001$ ); B: Endothelin-1 (ET-1) was significantly lower in neonates with effective therapy ( $33.80 \pm 5.36$ ) than that in neonates with ineffective therapy ( $42.68 \pm 4.48$ ) ( $t = 6.997$ ,  $P < 0.001$ ); C: Receiver operating characteristic (ROC) curves of keratin-14 in the diagnosis of effective therapy; D: ROC of ET-1 in diagnosis of therapeutic effect after treatment.

results shows that the combined treatment was more effective.

We measured the levels of KRT-14 and ET-1 in both groups of neonates. KRT-14 and ET-1 are lung tissue factors[23,24] and KRT14 increases rapidly in response to lung injury. Previous studies reported a negative correlation between KRT14 and PaO<sub>2</sub>/FiO<sub>2</sub>, and KRT14 is elevated in RDS. We found that KRT-14 and ET-1 levels in both were significantly lower after treatment than they were before treatment, and they were significantly lower in the observation group than in the control group after treatment. Additionally, our findings indicate that KRT-14 and ET-1 levels were significantly elevated in neonates who did not respond effectively to therapy compared with those who did. This suggests that KRT-14 and ET-1 could potentially be valuable diagnostic indicators for neonates with NRDS who are undergoing treatment. Therefore, we the value of KRT-14 and ET-1 for diagnosing therapeutic effectiveness by ROC curve analysis, and the AUC of each factor indicated that both were specific and sensitive. Both factors have diagnostic value in assessing the effectiveness of NRDS treatment in neonates and could potentially serve as diagnostic indices of effective treatment. Thus, KRT-14 can serve as an indicator of improvement in RDS patients, decreasing as their condition improves.

The study has some weaknesses. The subjects included in our study were all sick neonates and healthy newborns were not included for comparison. We did not explore differences between the measures tested in this study and the indexes measured in healthy newborns. Secondly, various types of PS are available for treatment[25], and therefore it is expected that further research can be conducted to assess the differences of the therapeutic effectiveness of different PS preparations. Finally, we found that some complications occurred during the treatment of the neonates, but we did not explore the risk factors of these complications. We hope to add to this discussion after completing our follow-up study.

## CONCLUSION

In conclusion, PS combined with noninvasive positive pressure ventilation significantly improved the effectiveness of NRDS therapy. KRT-14 and ET-1 levels are potential therapeutic diagnostic indicators.

## FOOTNOTES

**Author contributions:** Shi ZN, Zhang X, and Du CY were the guarantors of the integrity of the entire study; Zhang X and Zhao B performed the study concept and design; Shi ZN and Liu SG performed the literature study; Shi ZN and Zhang Xin pro conducted the study; Shi ZN and Zhang X conducted the statistical analysis; Shi ZN and Zhang X wrote the manuscript; All authors have access to the data and played a role in writing this manuscript.

**Institutional review board statement:** This study was approved by the Ethics Committee of the Hospital affiliated to the Military Medical University (Approval No. 2024007).

**Informed consent statement:** As this study was retrospective, informed consent of patients was not required.

**Conflict-of-interest statement:** All authors have no conflicts of interest to disclose.

**Data sharing statement:** Data for this study were obtained from the corresponding authors.

**STROBE statement:** The authors have read the STROBE Statement – checklist of items, and the manuscript was prepared and revised according to the STROBE Statement – checklist of items.

**Open-Access:** This article is an open-access article that was selected by an in-house editor and fully peer-reviewed by external reviewers. It is distributed in accordance with the Creative Commons Attribution NonCommercial (CC BY-NC 4.0) license, which permits others to distribute, remix, adapt, build upon this work non-commercially, and license their derivative works on different terms, provided the original work is properly cited and the use is non-commercial. See: <https://creativecommons.org/licenses/by-nc/4.0/>

**Country of origin:** China

**ORCID number:** Xin Zhang 0009-0005-7236-7631.

**S-Editor:** Liu JH

**L-Editor:** Filipodia

**P-Editor:** Yu HG

## REFERENCES

- 1 Zhang B, Dai Y, Chen H, Yang C. Neonatal Mortality in Hospitalized Chinese Population: A Meta-Analysis. *Biomed Res Int* 2019; **2019**: 7919501 [PMID: 30756086 DOI: 10.1155/2019/7919501]
- 2 Luo J, Chen J, Li Q, Feng Z. Differences in Clinical Characteristics and Therapy of Neonatal Acute Respiratory Distress Syndrome (ARDS) and Respiratory Distress Syndrome (RDS): A Retrospective Analysis of 925 Cases. *Med Sci Monit* 2019; **25**: 4992-4998 [PMID: 31278248 DOI: 10.12659/MSM.915213]
- 3 Mei H, Zhang Y, Liu C, Zhang Y, Liu C, Song D, Xin C, Wang J, Josephs-Spaulding J, Zhu Y, Tang F. Messenger RNA sequencing reveals similar mechanisms between neonatal and acute respiratory distress syndrome. *Mol Med Rep* 2018; **17**: 59-70 [PMID: 29115600 DOI: 10.3892/mmr.2017.7891]
- 4 Ye W, Zhang T, Shu Y, Fang C, Xie L, Peng K, Liu C. The influence factors of neonatal respiratory distress syndrome in Southern China: a case-control study. *J Matern Fetal Neonatal Med* 2020; **33**: 1678-1682 [PMID: 30369276 DOI: 10.1080/14767058.2018.1526918]
- 5 Lu CQ, Lin J, Yuan L, Zhou JG, Liang K, Zhong QH, Huang JH, Xu LP, Wu H, Zheng Z, Ping LL, Sun Y, Li ZK, Liu L, Lyu Q, Chen C. Pregnancy induced hypertension and outcomes in early and moderate preterm infants. *Pregnancy Hypertens* 2018; **14**: 68-71 [PMID: 30527121 DOI: 10.1016/j.preghy.2018.06.008]
- 6 Bae CW, Kim CY, Chung SH, Choi YS. History of Pulmonary Surfactant Replacement Therapy for Neonatal Respiratory Distress Syndrome in Korea. *J Korean Med Sci* 2019; **34**: e175 [PMID: 31243934 DOI: 10.3346/jkms.2019.34.e175]
- 7 Zhu XW, Shi Y, Shi LP, Liu L, Xue J, Ramanathan R; NHFOV Study Group. Non-invasive high-frequency oscillatory ventilation vs nasal continuous positive airway pressure in preterm infants with respiratory distress syndrome: Study protocol for a multi-center prospective

- randomized controlled trial. *Trials* 2018; **19**: 319 [PMID: 29898763 DOI: 10.1186/s13063-018-2673-9]
- 8 **Clément G**, Reschke MF. Relationship between motion sickness susceptibility and vestibulo-ocular reflex gain and phase. *J Vestib Res* 2018; **28**: 295-304 [PMID: 29689763 DOI: 10.3233/VES-180632]
- 9 **Anwaar O**, Hussain M, Shakeel M, Ahsan Baig MM. Outcome Of Use Of Nasal Continuous Positive Airway Pressure Through Infant Flow Drivers In Neonates With Respiratory Distress In A Tertiary Care Hospital In Pakistan. *J Ayub Med Coll Abbottabad* 2018; **30**: 511-555 [PMID: 30632326]
- 10 **Soll RF**, Barkhuff W. Noninvasive Ventilation in the Age of Surfactant Administration. *Clin Perinatol* 2019; **46**: 493-516 [PMID: 31345543 DOI: 10.1016/j.clp.2019.05.002]
- 11 **Da Silva Melo AR**, Barroso H, Uchôa De Araújo D, Ruidomar Pereira F, De Oliveira NF. The influence of sun exposure on the DNA methylation status of MMP9, miR-137, KRT14 and KRT19 genes in human skin. *Eur J Dermatol* 2015; **25**: 436-443 [PMID: 26424515 DOI: 10.1684/ejd.2015.2598]
- 12 **Confalonieri M**, Buratti E, Grassi G, Bussani R, Chilosi M, Farra R, Abrami M, Stuardi C, Salton F, Ficial M, Confalonieri P, Zandonà L, Romano M. Keratin14 mRNA expression in human pneumocytes during quiescence, repair and disease. *PLoS One* 2017; **12**: e0172130 [PMID: 28199407 DOI: 10.1371/journal.pone.0172130]
- 13 **Mei M**, Cheng G, Sun B, Yang L, Wang H, Sun J, Zhou W. EDN1 Gene Variant is Associated with Neonatal Persistent Pulmonary Hypertension. *Sci Rep* 2016; **6**: 29877 [PMID: 27425626 DOI: 10.1038/srep29877]
- 14 **Jiang Y**, Zeng Y, Huang X, Qin Y, Luo W, Xiang S, Sooranna SR, Pinhu L. Nur77 attenuates endothelin-1 expression via downregulation of NF- $\kappa$ B and p38 MAPK in A549 cells and in an ARDS rat model. *Am J Physiol Lung Cell Mol Physiol* 2016; **311**: L1023-L1035 [PMID: 27765761 DOI: 10.1152/ajplung.00043.2016]
- 15 **El Shemi MS**, Tawfik S, Khafagy SM, Hamza MT, Youssef AM. Endothelin 1 as a predictor marker for bronchopulmonary dysplasia in preterm neonates with respiratory distress syndrome. *J Neonatal Perinatal Med* 2017; **10**: 79-83 [PMID: 28304322 DOI: 10.3233/NPM-1653]
- 16 **Sweet DG**, Carnielli V, Greisen G, Hallman M, Ozek E, Plavka R, Saugstad OD, Simeoni U, Speer CP, Vento M, Visser GH, Halliday HL. European Consensus Guidelines on the Management of Respiratory Distress Syndrome - 2016 Update. *Neonatology* 2017; **111**: 107-125 [PMID: 27649091 DOI: 10.1159/000448985]
- 17 **Zhang C**, Zhu X. Clinical effects of pulmonary surfactant in combination with nasal continuous positive airway pressure therapy on neonatal respiratory distress syndrome. *Pak J Med Sci* 2017; **33**: 621-625 [PMID: 28811782 DOI: 10.12669/pjms.333.12227]
- 18 **Dimache G**, Stoean C, Durbacă S, Croitoru M, Ionescu M, Nedelcu IN, Corbu I. Study of specific immune response to unadsorbed concentrated tetanus vaccine administered by intradermal route to non-immunized persons in the last ten years. *Arch Roum Pathol Exp Microbiol* 1990; **49**: 51-62 [PMID: 2101203]
- 19 **Speer CP**. Neonatal respiratory distress syndrome: an inflammatory disease? *Neonatology* 2011; **99**: 316-319 [PMID: 21701203 DOI: 10.1159/000326619]
- 20 **Fan YZ**, Wen ZL. [Efficacy of different dosages of ambroxol hydrochloride in the prevention of neonatal respiratory distress syndrome]. *Zhongguo Dang Dai Er Ke Za Zhi* 2009; **11**: 771-772 [PMID: 19755033]
- 21 **Wu X**, Li S, Zhang J, Zhang Y, Han L, Deng Q, Wan X. Meta-analysis of high doses of ambroxol treatment for acute lung injury/acute respiratory distress syndrome based on randomized controlled trials. *J Clin Pharmacol* 2014; **54**: 1199-1206 [PMID: 25174313 DOI: 10.1002/jcph.389]
- 22 **Xiang J**, Wang P. Efficacy of pulmonary surfactant combined with high-dose ambroxol hydrochloride in the treatment of neonatal respiratory distress syndrome. *Exp Ther Med* 2019; **18**: 654-658 [PMID: 31258703 DOI: 10.3892/etm.2019.7615]
- 23 **Goraça A**, Kleniewska P, Skibska B. ET-1 mediates the release of reactive oxygen species and TNF- $\alpha$  in lung tissue by protein kinase C  $\alpha$  and  $\beta$ 1. *Pharmacol Rep* 2016; **68**: 121-126 [PMID: 26721363 DOI: 10.1016/j.pharep.2015.07.007]
- 24 **Ghosh M**, Brechbuhl HM, Smith RW, Li B, Hicks DA, Titchner T, Runkle CM, Reynolds SD. Context-dependent differentiation of multipotential keratin 14-expressing tracheal basal cells. *Am J Respir Cell Mol Biol* 2011; **45**: 403-410 [PMID: 21131447 DOI: 10.1165/ajrcmb.2010-0283OC]
- 25 **Chen C**, Tian T, Liu L, Zhang J, Fu H. Gender-related efficacy of pulmonary surfactant in infants with respiratory distress syndrome: A STROBE compliant study. *Medicine (Baltimore)* 2018; **97**: e0425 [PMID: 29702992 DOI: 10.1097/MD.00000000000010425]



## Observational Study

# Impact of interleukin 6 levels on acute lung injury risk and disease severity in critically ill sepsis patients

Ya Liu, Li Chen

**Specialty type:** Medicine, research and experimental

**Provenance and peer review:** Unsolicited article; Externally peer reviewed.

**Peer-review model:** Single blind

**Peer-review report's classification**

**Scientific Quality:** Grade C

**Novelty:** Grade B

**Creativity or Innovation:** Grade B

**Scientific Significance:** Grade B

**P-Reviewer:** Basu A, United States

**Received:** April 24, 2024

**Revised:** May 16, 2024

**Accepted:** June 4, 2024

**Published online:** August 16, 2024

**Processing time:** 71 Days and 21 Hours



**Ya Liu, Li Chen**, Department of Intensive Care Unit, Ninth People's Hospital Affiliated to Shanghai Jiao Tong University School of Medicine, Shanghai 201900, China

**Corresponding author:** Li Chen, MS, Doctor, Department of Intensive Care Unit, Ninth People's Hospital Affiliated to Shanghai Jiao Tong University School of Medicine, Room 504, Building 14, Baosteel Ba Village Community, Baoshan District, Shanghai 201900, China.  
[wwqh480@163.com](mailto:wwqh480@163.com)

## Abstract

### BACKGROUND

Sepsis is a life-threatening condition characterized by a dysregulation of the host response to infection that can lead to acute lung injury (ALI) and multiple organ dysfunction syndrome (MODS). Interleukin 6 (IL-6) is a pro-inflammatory cytokine that plays a crucial role in the pathogenesis of sepsis and its complications.

### AIM

To investigate the relationship among plasma IL-6 levels, risk of ALI, and disease severity in critically ill patients with sepsis.

### METHODS

This prospective and observational study was conducted in the intensive care unit of a tertiary care hospital between January 2021 and December 2022. A total of 83 septic patients were enrolled. Plasma IL-6 levels were measured upon admission using an enzyme-linked immunosorbent assay. The development of ALI and MODS was monitored during hospitalization. Disease severity was evaluated by Acute Physiology and Chronic Health Evaluation II (APACHE II) and Sequential Organ Failure Assessment (SOFA) scores.

### RESULTS

Among the 83 patients with sepsis, 38 (45.8%) developed ALI and 29 (34.9%) developed MODS. Plasma IL-6 levels were significantly higher in patients who developed ALI than in those without ALI (median: 125.6 pg/mL vs 48.3 pg/mL;  $P < 0.001$ ). Similarly, patients with MODS had higher IL-6 levels than those without MODS (median: 142.9 pg/mL vs 58.7 pg/mL;  $P < 0.001$ ). Plasma IL-6 levels were strongly and positively correlated with APACHE II ( $r = 0.72$ ;  $P < 0.001$ ) and SOFA scores ( $r = 0.68$ ;  $P < 0.001$ ).

## CONCLUSION

Elevated plasma IL-6 levels in critically ill patients with sepsis were associated with an increased risk of ALI and MODS. Higher IL-6 levels were correlated with greater disease severity, as reflected by higher APACHE II and SOFA scores. These findings suggest that IL-6 may serve as a biomarker for predicting the development of ALI and disease severity in patients with sepsis.

**Key Words:** Sepsis; Acute lung injury; Multiple organ dysfunction syndrome; Interleukin-6; Biomarker; Disease severity

©The Author(s) 2024. Published by Baishideng Publishing Group Inc. All rights reserved.

**Core Tip:** Elevated plasma interleukin-6 (IL-6) levels in septic patients indicate a higher risk of acute lung injury and multiple organ dysfunction syndrome. Monitoring IL-6 levels can help predict disease severity and the development of complications in critically ill patients with sepsis, making it a potential valuable biomarker for early intervention and management strategies.

**Citation:** Liu Y, Chen L. Impact of interleukin 6 levels on acute lung injury risk and disease severity in critically ill sepsis patients. *World J Clin Cases* 2024; 12(23): 5374-5381

**URL:** <https://www.wjgnet.com/2307-8960/full/v12/i23/5374.htm>

**DOI:** <https://dx.doi.org/10.12998/wjcc.v12.i23.5374>

## INTRODUCTION

Sepsis is a life-threatening condition that arises from a dysregulated host response to infection and is associated with organ dysfunction and a high mortality rate[1]. Despite significant advances in medical care and treatment strategies, sepsis remains a major public health concern, with an estimated global incidence of 48.9 million cases and 11 million sepsis-related deaths annually[2]. One of the most severe and challenging complications associated with sepsis is acute lung injury (ALI), which can progress to acute respiratory distress syndrome (ARDS) and contribute to the development of multiple organ dysfunction syndrome (MODS)[3].

The pathogenesis of sepsis is complex and involves a dysregulated inflammatory response characterized by the excessive production of pro-inflammatory cytokines, chemokines, and other mediators[4]. Among these mediators, interleukin 6 (IL-6) has been identified as a key player in the inflammatory cascade and has been implicated in the development of various complications associated with sepsis, including ALI, ARDS, and MODS[5-7]. IL-6 is a pleiotropic cytokine produced by various cell types, including immune cells, endothelial cells, and fibroblasts[8] and plays a crucial role in the acute-phase response and regulation of inflammatory processes. During sepsis, IL-6 levels are markedly elevated and contribute to the systemic inflammatory response and development of organ dysfunction[9].

Several studies have suggested a potential link between elevated IL-6 levels and the risk of ALI and MODS in patients with sepsis. However, the specific relationship between plasma IL-6 levels and the development of these complications, as well as the association between IL-6 levels and disease severity, have yet to be fully elucidated.

In this prospective and observational study, we investigated the correlation between plasma IL-6 levels and the risk of ALI and MODS in critically ill patients with sepsis. In addition, we evaluated the association between IL-6 levels and disease severity, as assessed by two widely used scoring systems: The Acute Physiology and Chronic Health Evaluation II (APACHE II) score and the Sequential Organ Failure Assessment (SOFA) score.

## MATERIALS AND METHODS

### Study design and participants

This prospective and observational study was conducted in the intensive care unit (ICU) of a tertiary care hospital between January 2021 and December 2022. Adult patients ( $\geq 18$ -years-old) admitted to the ICU with a diagnosis of sepsis according to the Sepsis-3 criteria[8] were eligible for inclusion. The Sepsis-3 criteria define sepsis as a life-threatening organ dysfunction caused by a dysregulated host response to infection, with an increase in the SOFA score of 2 or more points[10]. Patients with preexisting lung diseases, such as chronic obstructive pulmonary disease, asthma, or interstitial lung disease, were excluded from the study to avoid potential confounding factors that could influence the development of ALI or ARDS. In addition, we excluded patients with known autoimmune or inflammatory disorders and those receiving immunosuppressive therapies to minimize the impact of these conditions on the inflammatory response and cytokine levels.

The research protocol was reviewed and approved by the Ethics Committee of Ninth People's Hospital Affiliated to Shanghai Jiao Tong University School of Medicine, and written informed consent from all participants or their legal representatives is obtained before enrollment.

## Data collection and measurements

Upon admission to the ICU, we collated a range of demographic and clinical data for each patient, including age, sex, body mass index (BMI), comorbidities (*e.g.*, diabetes, hypertension, and cardiovascular disease), source of infection, and vital signs (temperature, blood pressure, heart rate, and respiratory rate).

For each patient, we calculated the APACHE II and SOFA scores to evaluate disease severity and the degree of organ dysfunction, respectively[11,12]. The APACHE II score is a widely used scoring system that considers the patient's age, acute physiological measurements, and comorbidities, to provide an estimate of the risk of hospital mortality[11]. The SOFA score, on the other hand, evaluates the degree of organ dysfunction across six organ systems (respiratory, cardiovascular, renal, hepatic, neurological, and coagulation) and is commonly used to evaluate the severity of sepsis and predict clinical outcomes[12].

Blood samples were collected from each patient within 24 h of ICU admission to measure plasma IL-6 levels. Blood samples were centrifuged and plasma was separated and stored at -80 °C to await analysis. Plasma IL-6 levels were quantified using a commercially available enzyme-linked immunosorbent assay (ELISA) kit (R&D Systems, Minneapolis, MN, United States) in accordance with the manufacturer's instructions. ELISA is a widely accepted and reliable method for measuring the levels of cytokines in biological samples with high levels of sensitivity and specificity.

## Outcome measures

The primary outcome measures of the study were the development of ALI and MODS during hospitalization. ALI was defined according to the Berlin Definition criteria[13], which include the following: (1) Acute onset of hypoxemia (arterial oxygen pressure [ $\text{PaO}_2$ ]/fraction of inspired oxygen [ $\text{FiO}_2$ ]  $\leq 300$  mmHg) with or without positive end-expiratory pressure; (2) Bilateral opacities on chest imaging (*e.g.*, chest radiography and computed tomography) that were not fully explained by effusions, lobar/lung collapse, or nodules; and (3) Respiratory failure that could not be fully explained by cardiac failure or fluid overload.

The severity of ALI was further classified into mild ( $200 \text{ mmHg} < \text{PaO}_2/\text{FiO}_2 \leq 300 \text{ mmHg}$ ), moderate ( $100 \text{ mmHg} < \text{PaO}_2/\text{FiO}_2 \leq 200 \text{ mmHg}$ ), and severe ( $\text{PaO}_2/\text{FiO}_2 \leq 100 \text{ mmHg}$ ), in accordance with the Berlin Definition criteria.

MODS was defined as alteration of organ function in two or more organ systems requiring medical intervention to maintain homeostasis[14]. The presence and severity of MODS were evaluated by the SOFA score; a score of 2 or higher in any organ system indicated organ dysfunction.

Throughout hospitalization, patients were closely monitored for the development of ALI and MODS by the attending physicians and the study team. We systematically collected and analyzed a range of clinical data to determine the presence and severity of these complications, including respiratory parameters, laboratory findings, imaging studies, and organ function assessments.

## Statistical analysis

Continuous variables were presented as the mean  $\pm$  standard deviation or median (interquartile range) depending on whether the data were normally distributed. Normality was assessed using the Shapiro-Wilk test and by the visual inspection of histograms. Categorical variables are reported as frequencies and percentages.

Differences in continuous variables between groups (*e.g.*, ALI *vs* no ALI and MODS *vs* no MODS) were analyzed by the Student's *t*-test or by the non-parametric Mann-Whitney *U* test, as appropriate, based on the distribution of data. For categorical variables, the differences between groups were analyzed by the  $\chi^2$  test or Fisher's exact test, as appropriate.

Correlations between plasma IL-6 levels and disease severity scores (APACHE II and SOFA) were assessed by Spearman's rank correlation analysis. Spearman's correlation coefficient (*r*) was calculated and the strength of each correlation was interpreted as follows: 0.00–0.19 (very weak), 0.20–0.39 (weak), 0.40–0.59 (moderate), 0.60–0.79 (strong), and 0.80–1.00 (very strong)[15].

Receiver operating characteristic (ROC) curve analysis was performed to evaluate the ability of plasma IL-6 levels to predict the development of ALI and MODS. The area under the curve (AUC) was calculated, and the optimal cut-off values for IL-6 levels were determined based on the maximum Youden index (sensitivity + specificity - 1). Additionally, the sensitivity, specificity, positive predictive value (PPV), and negative predictive value (NPV) were reported for the identified cut-off values.

Multivariate logistic regression analysis was conducted to evaluate the association between plasma IL-6 levels and the risk of developing ALI and MODS while adjusting for potential confounders such as age, sex, BMI, and comorbidities (*e.g.*, diabetes, hypertension, and cardiovascular disease). Odds ratios (ORs) and corresponding 95% confidence intervals (Cis) were calculated to estimate the risk of developing ALI and MODS associated with elevated IL-6 levels.

Statistical significance was set at  $P < 0.05$  for all analyze. All statistical analyses were performed using SPSS (version 25.0; IBM Corp., Armonk, NY, United States) and GraphPad Prism version 8.0 (GraphPad Software, San Diego, CA, United States).

# RESULTS

## Patient characteristics

A total of 83 patients with sepsis (49 males and 34 females) were included in this study. Mean patient age was  $62.4 \pm 16.8$  years (range: 22–88 years). The most common sources of infection were pneumonia (38.6%), intra-abdominal infections (24.1%), urinary tract infections (18.1%), and skin and soft tissue infections (9.6%). The median APACHE II score was 22

(interquartile range [IQR]: 17–27) and the median SOFA score was 8 (IQR: 5–11), thus indicating a high degree of disease severity and organ dysfunction within the study population (Table 1).

### The development of ALI and MODS

During hospitalization, 38 patients (45.8%) developed ALI and 29 patients (34.9%) developed MODS. The distribution of ALI severity was as follows: mild (18 patients, 21.7%), moderate (14 patients, 16.9%), and severe (six patients, 7.2%).

Patients who developed ALI had significantly higher plasma IL-6 levels than those without ALI (median: 125.6 pg/mL, IQR: 88.4–172.9 pg/mL *vs* median: 48.3 pg/mL, IQR: 32.1–72.6 pg/mL;  $P < 0.001$ ). Similarly, patients with MODS had higher IL-6 levels than those without MODS (median: 142.9 pg/mL, IQR: 102.4–196.7 pg/mL *vs* median: 58.7 pg/mL, IQR: 37.8–85.2 pg/mL;  $P < 0.001$ ), as shown in Table 2.

### The correlation between IL-6 levels and disease severity

Plasma IL-6 levels were strongly and positively correlated with APACHE II ( $r = 0.72$ ;  $P < 0.001$ ) and SOFA scores ( $r = 0.68$ ;  $P < 0.001$ ), thus indicating a significant association between elevated IL-6 levels and increased disease severity and organ dysfunction (Tables 3 and 4).

### Predictive value of IL-6 levels

ROC curve analysis revealed that plasma IL-6 levels exhibited a good predictive value for the development of ALI (AUC = 0.84; 95%CI: 0.75–0.93) and MODS (AUC = 0.82; 95%CI: 0.72–0.91). The optimal cut-off value for predicting ALI was 92.5 pg/mL, with a sensitivity of 76.3% (95%CI: 60.4%–87.6%), a specificity of 80.0% (95%CI: 66.2%–89.1%), a PPV of 72.7% (95%CI: 57.2%–84.4%), and a NPV of 82.9% (95%CI: 69.0%–91.6%). For the prediction of MODS, the optimal cut-off value for IL-6 was 118.7 pg/mL, with a sensitivity of 72.4% (95%CI: 54.3%–85.5%), a specificity of 85.2% (95%CI: 72.9%–92.5%), a PPV of 75.0% (95%CI: 57.8%–87.1%), and a NPV of 83.8% (95%CI: 71.5%–91.6%), as shown in Table 5.

### Multivariate logistic regression analysis

After adjusting for age, sex, BMI, and comorbidities (diabetes, hypertension, cardiovascular disease), multivariate logistic regression analysis revealed that higher plasma IL-6 levels were independently associated with an increased risk of developing ALI (OR: 1.22; 95%CI: 1.09–1.37;  $P = 0.001$ ) and MODS (OR: 1.18, 95%CI: 1.06–1.32;  $P = 0.003$ ).

## DISCUSSION

This prospective and observational study investigated the relationship between plasma IL-6 levels and the risk of developing ALI and MODS, as well as the association between IL-6 levels and disease severity in critically ill patients with sepsis.

Our analysis revealed that patients with sepsis who developed ALI or MODS had significantly higher plasma IL-6 levels than those without such complications. Furthermore, plasma IL-6 levels were strongly and positively correlated with disease severity scores (APACHE II and SOFA), indicating that higher IL-6 levels were associated with more severe illness and organ dysfunction. Elevated IL-6 levels demonstrated good predictive value for the development of ALI and MODS, and identified optimal cut-off values for each outcome. We also found that higher plasma IL-6 levels were independently associated with an increased risk of developing ALI and MODS, even after adjusting for potential confounders. These findings are consistent with those of previous studies that reported an association between elevated IL-6 levels and the development of ALI, ARDS, and MODS in patients with sepsis[5-7,16-18]. IL-6 is a key mediator of the inflammatory response and plays a crucial role in the pathogenesis of sepsis and its complications. Increased levels of IL-6 can lead to endothelial dysfunction, increased vascular permeability, and the recruitment of inflammatory cells, thus contributing to the development of ALI and MODS[13,14,19].

The strong positive correlation between plasma IL-6 levels and disease severity scores (APACHE II and SOFA) observed in this study further supports the potential role of IL-6 as a biomarker of disease severity in patients with sepsis. Higher IL-6 levels may reflect a more dysregulated inflammatory response and a greater degree of organ dysfunction, ultimately leading to worse clinical outcomes[20,21]. This finding is consistent with previous studies that reported a correlation between elevated IL-6 levels and increased disease severity and mortality in patients with sepsis[22,23].

The ability of plasma IL-6 levels to predict the development of ALI and MODS, as demonstrated by our ROC curve analysis, highlights the potential clinical utility of IL-6 as a prognostic biomarker for patients with sepsis. We also identified optimal cut-off values for IL-6 levels which could facilitate risk stratification and guide early interventions to prevent or mitigate the development of these complications[24,25]. The early identification of patients at high risk of developing ALI and MODS could encourage more intensive monitoring, the early implementation of protective ventilation strategies, and the initiation of targeted therapies to modulate the inflammatory response. This evidence was strengthened further by multivariate logistic regression analysis which demonstrated that higher plasma IL-6 levels were independently associated with an increased risk of developing ALI and MODS, even after adjusting for potential confounders such as age, sex, BMI, and comorbidities. This finding suggests that IL-6 may play a direct role in the pathogenesis of these complications rather than simply representing an independent marker of inflammation.

**Table 1** Baseline characteristics of the study participants

Characteristic	All Patients	ALI	No ALI	MODS	No MODS
Age in yr	62.4 ± 16.8	65.2 ± 15.1	60.1 ± 17.9	67.3 ± 14.2	59.8 ± 17.5
Male sex	49 (59.0)	23 (60.5)	26 (57.8)	18 (62.1)	31 (57.4)
BMI (kg/m <sup>2</sup> )	26.8 ± 4.9	27.2 ± 5.3	26.5 ± 4.6	27.6 ± 5.1	26.4 ± 4.8
Comorbidities					
Diabetes mellitus	22 (26.5)	12 (31.6)	10 (22.2)	10 (34.5)	12 (22.2)
Hypertension	35 (42.2)	19 (50.0)	16 (35.6)	16 (55.2)	19 (35.2)
Cardiovascular disease	16 (19.3)	9 (23.7)	7 (15.6%)	7 (24.1%)	9 (16.7%)
Source of infection					
Pneumonia	32 (38.6)	21 (55.3)	11 (24.4)	14 (48.3)	18 (33.3)
Intra-abdominal	20 (24.1)	7 (18.4)	13 (28.9)	6 (20.7)	14 (25.9)
Urinary tract	15 (18.1)	5 (13.2)	10 (22.2)	4 (13.8)	11 (20.4)
Skin/soft tissue	8 (9.6)	2 (5.3)	6 (13.3)	2 (6.9%)	6 (11.1)
APACHE II score, median (IQR)	22 (17-27)	26 (21-31)	18 (14-23)	28 (24-33)	19 (15-24)
SOFA score, median (IQR)	8 (5-11)	11 (8-14)	6 (4-8)	13 (10-16)	6 (4-8)

Data are *n* (%) or mean ± standard deviation. ALI: Acute lung injury; APACHE II: Acute Physiology and Chronic Health Evaluation II; BMI: Body mass index; IQR: Interquartile range; MODS: Multiple organ dysfunction syndrome; SOFA: Sequential Organ Failure Assessment.

**Table 2** Distribution of plasma interleukin 6 levels in patients with and without acute lung injury and multiple organ dysfunction syndrome

Groups	Median IL-6 in pg/mL	Interquartile range
ALI	125.6	88.4-172.9
No ALI	48.3	32.1-72.6
MODS	142.9	102.4-196.7
No MODS	58.7	37.8-85.2

Data are mean ± standard deviation. ALI: Acute lung injury; IL: Interleukin; MODS: Multiple organ dysfunction syndrome.

**Table 3** Correlation between plasma interleukin 6 levels and Acute Physiology and Chronic Health Evaluation II scores

APACHE II score	Median IL-6 in pg/mL	Interquartile range
10-14	32.8	25.6-41.2
15-19	62.1	48.7-79.3
20-24	98.5	75.4-122.7
25-29	146.2	115.8-176.4
≥ 30	198.6	162.7-235.8

Data are mean ± standard deviation. Spearman's *r* = 0.72 (*P* < 0.001). APACHE II: Acute Physiology and Chronic Health Evaluation II; IL: Interleukin.

## CONCLUSION

This prospective and observational study demonstrated a significant correlation between elevated plasma IL-6 levels and an increased risk of developing ALI and MODS in critically ill patients with sepsis. Furthermore, we found that higher IL-6 levels were associated with a greater disease severity, as reflected by higher APACHEII and SOFA scores. These findings suggest that IL-6 may serve as a potential biomarker for predicting the development of ALI and MODS as well

**Table 4 Correlation between plasma interleukin 6 levels and Sequential Organ Failure Assessment scores**

SOFA score	Median IL-6 in pg/mL	Interquartile range
2-4	39.7	28.9-51.6
5-7	72.5	53.2-94.7
8-10	121.8	95.6-149.5
11-13	167.3	137.8-203.2
≥ 14	221.6	185.9-264.7

Data are mean ± standard deviation. Spearman's  $r = 0.68$  ( $P < 0.001$ ). IL-6: Interleukin 6; SOFA: Sequential Organ Failure Assessment.

**Table 5 Receiver operating characteristic curve analysis for the prediction of acute lung injury and multiple organ dysfunction syndrome using plasma interleukin 6 levels**

Outcome	Cut-off in pg/mL	Sensitivity	Specificity	PPV	NPV	AUC (95%CI)
ALI	92.5	76.3	80.0	72.7	82.9	0.84 (0.75-0.93)
MODS	118.7	72.4	85.2	75.0	83.8	0.82 (0.72-0.91)

ALI: Acute lung injury; AUC: Area under the curve; CI: Confidence interval; MODS: Multiple organ dysfunction syndrome; NPV: Negative predictive value; PPV: Positive predictive value.

as for assessing disease severity in patients with sepsis.

It is important to note that this study has certain limitations that should be considered when interpreting the results. First, the sample size was relatively small, and the study was conducted at a single center; these factors may limit the generalizability of our findings. Second, we did not evaluate the prognostic value of serial IL-6 measurements or the effect of interventions targeting IL-6 on clinical outcomes. Future studies, with larger sample sizes, multicenter designs, and longitudinal IL-6 measurements, are now required to validate these findings and investigate the potential therapeutic implications of targeting IL-6 in patients with sepsis. Furthermore, it is important to recognize that IL-6 is not the only mediator involved in the inflammatory response during sepsis, and that other cytokines, chemokines, and inflammatory markers may also contribute to the development of ALI and MODS. Future research should investigate the potential synergistic or additive effects of combining IL-6 with other biomarkers to improve risk stratification and the prognosis of patients with sepsis.

Despite these limitations, the present study provides valuable insights into the role of IL-6 as a biomarker for predicting the development of ALI and MODS, as well as its association with disease severity in critically ill patients with sepsis. Collectively, our findings contribute to a better understanding of the pathophysiology of sepsis and its complications and may pave the way for the development of novel therapeutic strategies targeting the IL-6 pathway.

## FOOTNOTES

**Author contributions:** The concept of this study was jointly proposed by Liu Y and Chen L, who participated in the data collection; Liu Y contributed to the formal analysis of this study, and drafted the initial draft; Chen L conducted the research, methodology, and visualization of the manuscript; Liu Y and Chen L participated in this study, validated it, and jointly reviewed and edited the manuscript.

**Institutional review board statement:** This study has been reviewed and approved by the Ethics Committee of the Ninth Affiliated People's Hospital of Shanghai Jiao Tong University School of Medicine.

**Informed consent statement:** This study has obtained informed consent forms signed by patients and guardians.

**Conflict-of-interest statement:** The authors have no conflicts of interest to declare.

**Data sharing statement:** No data available.

**STROBE statement:** The authors have read the STROBE Statement-checklist of items, and the manuscript was prepared and revised according to the STROBE Statement-checklist of items.

**Open-Access:** This article is an open-access article that was selected by an in-house editor and fully peer-reviewed by external reviewers. It is distributed in accordance with the Creative Commons Attribution NonCommercial (CC BY-NC 4.0) license, which permits others to

distribute, remix, adapt, build upon this work non-commercially, and license their derivative works on different terms, provided the original work is properly cited and the use is non-commercial. See: <https://creativecommons.org/licenses/by-nc/4.0/>

**Country of origin:** China

**ORCID number:** Ya Liu 0009-0008-0157-3798; Li Chen 0009-0005-1314-6038.

**S-Editor:** Liu H

**L-Editor:** Filipodia

**P-Editor:** Yu HG

## REFERENCES

- 1 Singer M, Deutschman CS, Seymour CW, Shankar-Hari M, Annane D, Bauer M, Bellomo R, Bernard GR, Chiche JD, Coopersmith CM, Hotchkiss RS, Levy MM, Marshall JC, Martin GS, Opal SM, Rubenfeld GD, van der Poll T, Vincent JL, Angus DC. The Third International Consensus Definitions for Sepsis and Septic Shock (Sepsis-3). *JAMA* 2016; **315**: 801-810 [PMID: 26903338 DOI: 10.1001/jama.2016.0287]
- 2 Rubenfeld GD, Caldwell E, Peabody E, Weaver J, Martin DP, Neff M, Stern EJ, Hudson LD. Incidence and outcomes of acute lung injury. *N Engl J Med* 2005; **353**: 1685-1693 [PMID: 16236739 DOI: 10.1056/NEJMoa050333]
- 3 Sakr Y, Lobo SM, Moreno RP, Gerlach H, Ranieri VM, Michalopoulos A, Vincent JL; SOAP Investigators. Patterns and early evolution of organ failure in the intensive care unit and their relation to outcome. *Crit Care* 2012; **16**: R222 [PMID: 23158219 DOI: 10.1186/cc11868]
- 4 Angus DC, van der Poll T. Severe sepsis and septic shock. *N Engl J Med* 2013; **369**: 840-851 [PMID: 23984731 DOI: 10.1056/NEJMra1208623]
- 5 Meduri GU, Headley S, Kohler G, Stentz F, Tolley E, Umberger R, Leeper K. Persistent elevation of inflammatory cytokines predicts a poor outcome in ARDS. Plasma IL-1 beta and IL-6 Levels are consistent and efficient predictors of outcome over time. *Chest* 1995; **107**: 1062-1073 [PMID: 7705118 DOI: 10.1378/chest.107.4.1062]
- 6 Park WY, Goodman RB, Steinberg KP, Ruzinski JT, Radella F 2nd, Park DR, Pugin J, Skerrett SJ, Hudson LD, Martin TR. Cytokine balance in the lungs of patients with acute respiratory distress syndrome. *Am J Respir Crit Care Med* 2001; **164**: 1896-1903 [PMID: 11734443 DOI: 10.1164/ajrcm.164.10.2104013]
- 7 Oberholzer A, Oberholzer C, Moldawer LL. Interleukin-10: A complex role in the pathogenesis of sepsis syndromes and its potential as an anti-inflammatory drug. *Crit Care Med* 2002; **30**: S58-S63 [DOI: 10.1097/00003246-200201001-00008]
- 8 Remick DG. Interleukin-8. *Crit Care Med* 2005; **33**: S466-S467 [PMID: 16340423 DOI: 10.1097/01.CCM.0000186783.34908.18]
- 9 ARDS Definition Task Force, Ranieri VM, Rubenfeld GD, Thompson BT, Ferguson ND, Caldwell E, Fan E, Camporota L, Slutsky AS. Acute respiratory distress syndrome: the Berlin Definition. *JAMA* 2012; **307**: 2526-2533 [PMID: 22797452 DOI: 10.1001/jama.2012.5669]
- 10 Knaus WA, Draper EA, Wagner DP, Zimmerman JE. APACHE II: a severity of disease classification system. *Crit Care Med* 1985; **13**: 818-829 [PMID: 3928249 DOI: 10.1097/00003246-198510000-00009]
- 11 Vincent JL, Moreno R, Takala J, Willatts S, De Mendonça A, Bruining H, Reinhart CK, Suter PM, Thijs LG. The SOFA (Sepsis-related Organ Failure Assessment) score to describe organ dysfunction/failure. On behalf of the Working Group on Sepsis-Related Problems of the European Society of Intensive Care Medicine. *Intensive Care Med* 1996; **22**: 707-710 [PMID: 8844239 DOI: 10.1007/BF01709751]
- 12 Apel K, Hirt H. Reactive oxygen species: metabolism, oxidative stress, and signal transduction. *Annu Rev Plant Biol* 2004; **55**: 373-399 [PMID: 15377225 DOI: 10.1146/annurev.arplant.55.031903.141701]
- 13 Savill J. Apoptosis and the kidney. *J Am Soc Nephrol* 1994; **5**: 12-21 [PMID: 7948779 DOI: 10.1681/ASN.V5112]
- 14 Marshall JC, Cook DJ, Christou NV, Bernard GR, Sprung CL, Sibbald WJ. Multiple organ dysfunction score: a reliable descriptor of a complex clinical outcome. *Crit Care Med* 1995; **23**: 1638-1652 [PMID: 7587228 DOI: 10.1097/00003246-199510000-00007]
- 15 Mukaka MM. Statistics corner: A guide to appropriate use of correlation coefficient in medical research. *Malawi Med J* 2012; **24**: 69-71 [PMID: 23638278]
- 16 Meduri GU, Kohler G, Headley S, Tolley E, Stentz F, Postlethwaite A. Inflammatory cytokines in the BAL of patients with ARDS. Persistent elevation over time predicts poor outcome. *Chest* 1995; **108**: 1303-1314 [PMID: 7587434 DOI: 10.1378/chest.108.5.1303]
- 17 Ware LB, Koyama T, Zhao Z, Janz DR, Wickersham N, Bernard GR, May AK, Calfee CS, Matthay MA. Biomarkers of lung epithelial injury and inflammation distinguish severe sepsis patients with acute respiratory distress syndrome. *Crit Care* 2013; **17**: R253 [PMID: 24156650 DOI: 10.1186/cc13080]
- 18 Damas P, Ledoux D, Nys M, Vrindts Y, De Groote D, Franchimont P, Lamy M. Cytokine serum level during severe sepsis in human IL-6 as a marker of severity. *Ann Surg* 1992; **215**: 356-362 [PMID: 1558416 DOI: 10.1097/00000658-199204000-00009]
- 19 Oppenheim JJ. Cytokines: past, present, and future. *Int J Hematol* 2001; **74**: 3-8 [PMID: 11530802 DOI: 10.1007/BF02982543]
- 20 Abe R, Hirasawa H, Oda S, Sadahiro T, Nakamura M, Watanabe E, Nakada TA, Hatano M, Tokuhisa T. Up-regulation of interleukin-10 mRNA expression in peripheral leukocytes predicts poor outcome and diminished human leukocyte antigen-DR expression on monocytes in septic patients. *J Surg Res* 2008; **147**: 1-8 [PMID: 17720196 DOI: 10.1016/j.jss.2007.07.009]
- 21 Pinsky MR, Vincent JL, Deviere J, Alegre M, Kahn RJ, Dupont E. Serum cytokine levels in human septic shock. Relation to multiple-system organ failure and mortality. *Chest* 1993; **103**: 565-575 [PMID: 8432155 DOI: 10.1378/chest.103.2.565]
- 22 de Pablo R, Monserrat J, Reyes E, Diaz-Martin D, Rodriguez Zapata M, Carballo F, de la Hera A, Prieto A, Alvarez-Mon M. Mortality in patients with septic shock correlates with anti-inflammatory but not proinflammatory immunomodulatory molecules. *J Intensive Care Med* 2011; **26**: 125-132 [PMID: 21464065 DOI: 10.1177/0885066610384465]
- 23 Gelderman KA, Hultqvist M, Olsson LM, Bauer K, Pizzolla A, Olofsson P, Holmdahl R. Rheumatoid arthritis: the role of reactive oxygen species in disease development and therapeutic strategies. *Antioxid Redox Signal* 2007; **9**: 1541-1567 [PMID: 17678439 DOI: 10.1089/ars.2007.1569]
- 24 Agrawal A, Zhuo H, Brady S, Levitt J, Steingrub J, Siegel MD, Soto G, Peterson MW, Chesnutt MS, Matthay MA, Liu KD. Pathogenetic and

predictive value of biomarkers in patients with ALI and lower severity of illness: results from two clinical trials. *Am J Physiol Lung Cell Mol Physiol* 2012; **303**: L634-L639 [PMID: 22865551 DOI: 10.1152/ajplung.00195.2012]

- 25 **Bajwa EK**, Yu CL, Gong MN, Thompson BT, Christiani DC. Pre-B-cell colony-enhancing factor gene polymorphisms and risk of acute respiratory distress syndrome. *Crit Care Med* 2007; **35**: 1290-1295 [PMID: 17414088 DOI: 10.1097/01.CCM.0000260243.22758.4F]



## Knowledge domain and emerging trends in the rupture risk of intracranial aneurysms research from 2004 to 2023

Jun-Chen Chen, Cheng Luo, Yong Li, Dian-Hui Tan

**Specialty type:** Medicine, research and experimental

**Provenance and peer review:** Unsolicited article; Externally peer reviewed.

**Peer-review model:** Single blind

**Peer-review report's classification**

**Scientific Quality:** Grade A

**Novelty:** Grade A

**Creativity or Innovation:** Grade A

**Scientific Significance:** Grade A

**P-Reviewer:** Soreq L

**Received:** May 12, 2024

**Revised:** June 20, 2024

**Accepted:** June 26, 2024

**Published online:** August 16, 2024

**Processing time:** 53 Days and 20.2 Hours



**Jun-Chen Chen, Cheng Luo, Yong Li, Dian-Hui Tan**, Department of Neurosurgery, The First Affiliated Hospital of Shantou University Medical College, Shantou 515041, Guangdong Province, China

**Corresponding author:** Dian-Hui Tan, MD, Chief Doctor, Department of Neurosurgery, The First Affiliated Hospital of Shantou University Medical College, No. 57 Changping Road, Shantou 515041, Guangdong Province, China. [tandianhui@163.com](mailto:tandianhui@163.com)

### Abstract

#### BACKGROUND

Intracranial aneurysms (IAs) pose significant health risks, attributable to their potential for sudden rupture, which can result in severe outcomes such as stroke and death. Despite extensive research, the variability of aneurysm behavior, with some remaining stable for years while others rupture unexpectedly, remains poorly understood.

#### AIM

To employ bibliometric analysis to map the research landscape concerning risk factors associated with IAs rupture.

#### METHODS

A systematic literature review of publications from 2004 to 2023 was conducted, analyzing 3804 documents from the Web of Science Core Collection database, with a focus on full-text articles and reviews in English. The analysis encompassed citation and co-citation networks, keyword bursts, and temporal trends to delineate the evolution of research themes and collaboration patterns. Advanced software tools, CiteSpace and VOSviewer, were utilized for comprehensive data visualization and trend analysis.

#### RESULTS

Analysis uncovered a total of 3804 publications on IA rupture risk factors between 2006 and 2023. Research interest surged after 2013, peaking in 2023. The United States led with 28.97% of publications, garnering 37706 citations. Notable United States-China collaborations were observed. Capital Medical University produced 184 publications, while Utrecht University boasted a citation average of 69.62 per publication. "World Neurosurgery" published the most papers, contrasting with "Stroke", the most cited journal. The PHASES score from "Lancet Neurology" emerged as a vital rupture risk prediction tool. Early research favored endovascular therapy, transitioning to magnetic resonance imaging and flow diverters.

*"Subarachnoid hemorrhage"* stood out as a recurrent keyword.

## CONCLUSION

This study assesses global IA research trends and highlights crucial gaps, guiding future investigations to improve preventive and therapeutic approaches.

**Key Words:** Bibliometric; VOSviewer; CiteSpace; Intracranial aneurysm; Risk factor

©The Author(s) 2024. Published by Baishideng Publishing Group Inc. All rights reserved.

**Core Tip:** This bibliometric analysis provides a comprehensive overview of research on risk factors associated with intracranial aneurysms (IAs) rupture. Highlighting global trends and collaborations, it identifies key publications, influential journals, and evolving research themes. Notably, the study emphasizes the increasing research interest post-2013 and the pivotal role of tools like the PHASES score in predicting rupture risks. By synthesizing two decades of data, this analysis offers valuable insights into the dynamic landscape of IAs studies, guiding future investigations and enhancing preventive and therapeutic strategies.

**Citation:** Chen JC, Luo C, Li Y, Tan DH. Knowledge domain and emerging trends in the rupture risk of intracranial aneurysms research from 2004 to 2023. *World J Clin Cases* 2024; 12(23): 5382-5403

**URL:** <https://www.wjgnet.com/2307-8960/full/v12/i23/5382.htm>

DOI: <https://dx.doi.org/10.12998/wjcc.v12.i23.5382>

## INTRODUCTION

Unruptured intracranial aneurysms (UIAs) are localized, pathological dilations of the intracranial arterial wall that pose a significant risk of rupture[1]. The prevalence of UIAs is notably elevated, as evidenced by a comprehensive systematic review and meta-analysis spanning 21 countries, 83 study populations, and 94912 UIA patients. Within a cohort of asymptomatic adults aged 50 years, the collective prevalence of UIA was approximately 3.2% (95% confidence interval: 1.9%-5.2%)[2]. Given the grave implications of aneurysmal subarachnoid hemorrhage, a severe complication of UIAs with a mortality rate of 67%, and a substantial proportion of survivors who are left disabled[3,4], it is imperative for clinicians to discern the risk of rupture. The evolving landscape of our understanding of the risk factors associated with UIAs underscores the need for continued investigation. Past studies have indicated the dichotomous behavior of aneurysms, with some exhibiting rapid enlargement and rupture within a condensed timeframe while others remaining stable over prolonged periods[2]. The exploration of risk factors contributing to aneurysm rupture has been a focal point of numerous studies[4-8].

Various systematic methodologies exist for comprehensively mapping an academic domain, with bibliometric analysis emerging as the predominant approach due to advancements in mathematics and computation[9]. Bibliometrics not only allows for qualitative and quantitative evaluation of author contributions, organizational collaborations, country affiliations, and journal impact but also facilitates the assessment of emerging trends and developments in academic research, a task beyond the scope of traditional reviews, meta-analyses, and experimental studies[9-12]. Consequently, bibliometrics plays an increasingly crucial role in trend analysis and guideline development, making bibliometrics a valuable tool for assessing and surveying studies related to the risk factors for IA rupture. In this study, CiteSpace and VOSviewer, two prominent bibliometric software tools, were used to delineate the knowledge base and emerging trends within studies related to the risk factors for IA rupture from key perspectives[13,14]. These perspectives encompass quantifying information on rupture risk factors for IAs, including individual impacts and collaborative efforts based on annual publications, journals, co-cited publications, countries, authors, and co-cited authors. Additionally, the study identifies the most cited articles through co-citation analyses to evaluate the foundational knowledge in this area. Furthermore, this research aims to uncover the evolution of knowledge structures and key areas of interest through keyword and co-cited reference burst analyses. Subsequently, this study sought to determine the research content and potential future development directions in this field by analyzing the top 50 articles' journals, co-cited journals, countries, and keywords.

## MATERIALS AND METHODS

### Literature search

The bibliographic classification accuracy of the Web of Science Core Collection (WoSCC) surpasses that of any other database, rendering it the optimal choice for bibliographic analysis. Hence, we opted to conduct our search within this database. On March 12, 2024, we searched the WoS for articles spanning from 2004 to December 31, 2023, pertaining to the risk factors for IA rupture. The search query employed was as follows: (((((((((((((((((((((((((((((((((((((((TS =

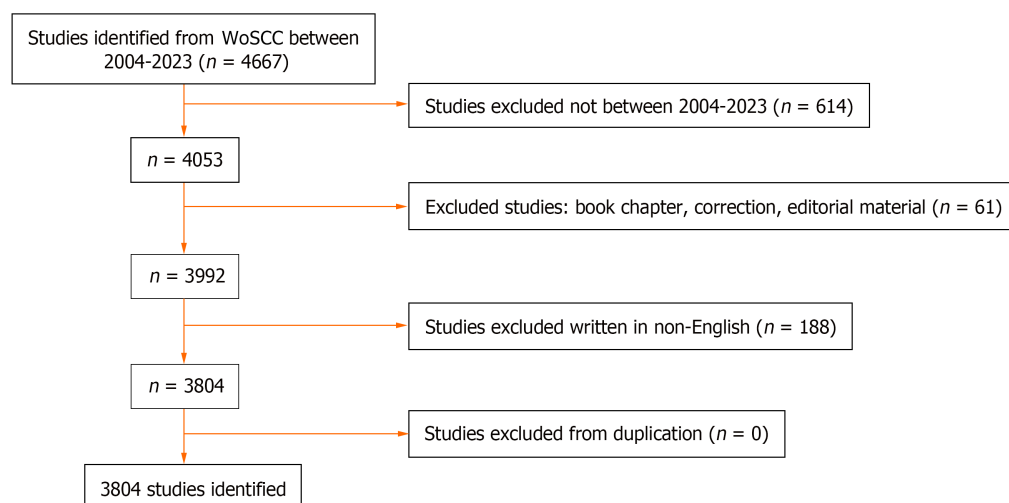


**Figure 1** Flowchart of study identification and selection. WoSCC: Web of Science Core Collection.

(intracranial aneurysm)) OR TS = (Intracranial Aneurysm)) OR TS = (Aneurysms, Intracranial)) OR TS = (Intracranial Aneurysms)) OR TS = (Aneurysm, Intracranial)) OR TS = (Aneurysm, Anterior Communicating Artery)) OR TS = (Anterior Communicating Artery Aneurysm)) OR TS = (Aneurysm, Basilar Artery)) OR TS = (Aneurysms, Basilar Artery)) OR TS = (Artery Aneurysm, Basilar)) OR TS = (Artery Aneurysms, Basilar)) OR TS = (Basilar Artery Aneurysms)) OR TS = (Basilar Artery Aneurysm)) OR TS = (Aneurysm, Middle Cerebral Artery)) OR TS = (Middle Cerebral Artery Aneurysm)) OR TS = (Aneurysm, Posterior Cerebral Artery)) OR TS = (Posterior Cerebral Artery Aneurysm)) OR TS = (Berry Aneurysm)) OR TS = (Aneurysm, Berry)) OR TS = (Aneurysms, Berry)) OR TS = (Berry Aneurysms)) OR TS = (Brain Aneurysm)) OR TS = (Aneurysm, Brain)) OR TS = (Aneurysms, Brain)) OR TS = (Brain Aneurysms)) OR TS = (Cerebral Aneurysm)) OR TS = (Aneurysms, Cerebral)) OR TS = (Cerebral Aneurysms)) OR TS = (Aneurysm, Cerebral)) OR TS = (Giant Intracranial Aneurysm)) OR TS = (Aneurysm, Giant Intracranial)) OR TS = (Giant Intracranial Aneurysms)) OR TS = (Intracranial Aneurysm, Giant)) OR TS = (Intracranial Aneurysms, Giant)) OR TS = (Mycotic Aneurysm, Intracranial)) OR TS = (Aneurysm, Intracranial Mycotic)) OR TS = (Aneurysms, Intracranial Mycotic)) OR TS = (Intracranial Mycotic Aneurysm)) OR TS = (Intracranial Mycotic Aneurysms)) OR TS = (Mycotic Aneurysms, Intracranial)) OR TS = (Aneurysm, Anterior Cerebral Artery)) OR TS = (Anterior Cerebral Artery Aneurysm)) OR TS = (Aneurysm, Posterior Communicating Artery)) OR TS = (Posterior Communicating Artery Aneurysm) AND TS = (Risk Factor). The literature screening for this study was based on the following inclusion criteria: (1) Full-text publications related to risk factors for the rupture of IAs; (2) Articles and review manuscripts written in English; and (3) Publications dated between January 1, 2004, and December 31, 2023. The exclusion criteria were as follows: (1) Irrelevant to the topic of risk factors for the rupture of IAs; and (2) Conference abstracts, news articles, brief reports, or similar formats. A plain text version of the selected papers was exported (Figure 1).

## Analysis

The annual publications, national trends, and proportions of papers were analyzed and visualized using GraphPad Prism v8.0.2. Additionally, CiteSpace (6.2.4R 64-bit Advanced Edition) and VOSviewer (version 1.6.18) were employed for further analysis of the data, facilitating the visualization of scientific knowledge maps. VOSviewer version 1.6.17, created by van Eck and Waltman *et al*[13], is a Java-based free software designed for analyzing large volumes of literature data and displaying them in map format. To visualize the research outcomes of a specific field by drawing a co-citation network map, Professor Chao-Mei Chen developed CiteSpace (version 6.2.4R) software[15]. This software envisions using an experimental framework to explore new concepts and evaluate existing technologies. It enables users to gain a better understanding of knowledge domains, research frontiers, and trends, thereby predicting future research advancements [16,17].

## RESULTS

### Overall distribution

The results indicate that from January 1, 2006, to December 31, 2023, there were a total of 3804 literature entries on risk factors for the rupture of IAs in the WoSCC database, comprising 3346 articles (94.31%) and 458 reviews (5.69%). These publications span 96 countries and regions, involve 3061 institutions, and include contributions from 14902 authors.

Since 2004, the annual publication output has shown a gradual increase (Figure 2). We divided this trend into three phases: A slow growth period from 2004 to 2009 (Figure 2) with an annual publication count of less than 100, indicating a lack of attention from researchers in the field; a gradual increase in publications from 2010 to 2012, signifying increased interest from researchers; and a rapid surge in publications after 2013, reaching a peak in 2023, indicating widespread attention to the field since 2013.

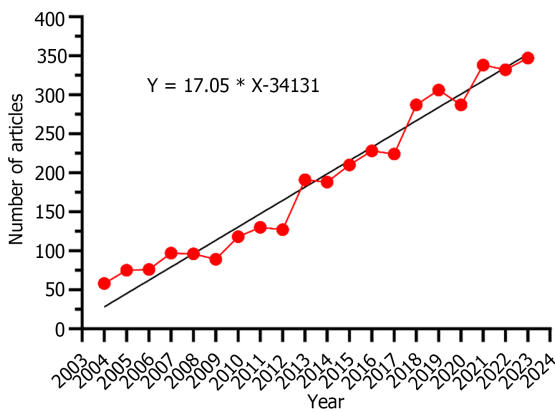


Figure 2 The annual trend publications related to risk factors for the rupture of intracranial aneurysms from 2004 to 2023.

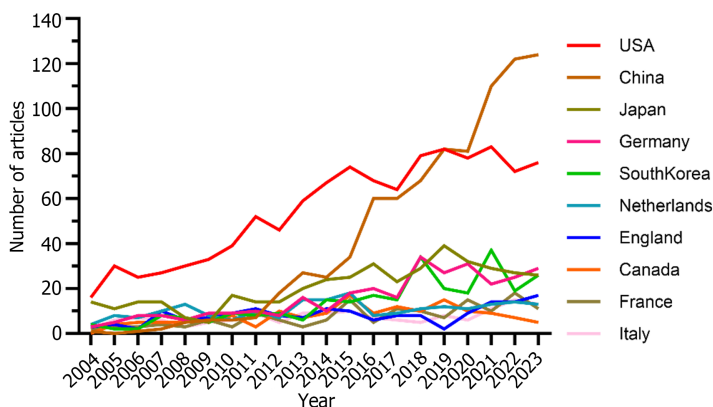


Figure 3 Number of articles by publication in countries.

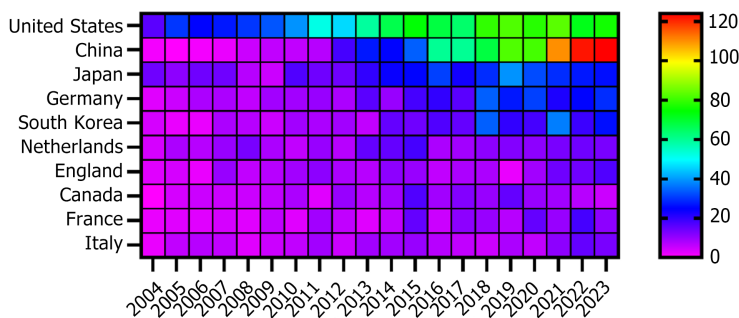


Figure 4 Publication output heatmap by countries.

### Countries/regions and institutions analysis

Research on the risk factors for IA rupture has been conducted in 96 countries and regions. Figures 3 and 4 illustrate the annual publication output of the top 10 countries in the past decade. The top 5 countries in this field are the United States, China, Japan, Germany, and South Korea. The United States accounts for 28.97% of the total publication output, significantly surpassing other nations.

Among the top ten countries/regions in terms of publication output, the United States's papers were cited 37706 times (Table 1), significantly exceeding all other countries/regions. Its citation-to-publication ratio (34.22) ranks 6<sup>th</sup> among all countries, indicating generally high-quality publications. China ranks 2<sup>nd</sup> in publication output (847 papers) and 5<sup>th</sup> in citation count (8992 times), with a citation-to-publication ratio of 10.62. The collaboration network, as depicted in Figure 5A, shows close collaboration between the most prolific producers, the United States and China. The United States collaborates closely with Germany, France, and Italy, among others, while China's collaborations are more pronounced with Japan, South Korea, and the Netherlands. The United States not only leads in publication output and citation frequency but also exhibits a centrality of 0.32, signifying its position as a leading nation in the field.

**Table 1 The top 10 countries/regions and institutions involved in risk factors for the rupture of intracranial aneurysms research**

Rank	Country/region	Article counts	Centrality	Percentage (%)	Citation	Citation per publication
1	United States	1102	0.32	28.97	37706	34.22
2	China	847	0.12	22.27	8992	10.62
3	Japan	416	0.08	10.94	10264	24.67
4	Germany	314	0.1	8.25	9871	31.44
5	South Korea	275	0.04	7.23	3546	12.89
6	Netherlands	213	0.03	5.60	13789	64.74
7	England	169	0.11	4.44	6994	41.38
8	Canada	157	0.08	4.13	7488	47.69
9	France	151	0.14	3.97	6985	46.26
10	Italy	149	0.05	3.92	5599	37.58

**Table 2 The top 10 institutions of intracranial aneurysms rupture risk factors research**

Rank	Institution	Country	Number of studies	Total citations	Average citation
1	Capital Medical University	China	184	1920	10.43
2	Utrecht University	Netherlands	149	10373	69.62
3	Mayo Clinic	United States	134	6645	49.59
4	Harvard University	United States	128	3299	25.77
5	University of California System	United States	101	3257	32.25
6	Harvard Medical School	United States	101	2778	27.50
7	University of Helsinki	Finland	95	5978	62.93
8	Beijing Neurosurgical Institute	China	85	1070	12.59
9	Helsinki University Central Hospital	Finland	78	4080	52.31
10	University of Toronto	Canada	70	4338	61.97

A total of 3061 institutions have systematically published articles on risk factors for IA rupture. Among the top ten institutions in terms of publication output, 4 are from the United States, 2 are from China, 2 are from Finland, 1 is from the Netherlands, and 1 is from Canada (Table 2, Figure 5B). Capital Medical University has the greatest number of publications (184 papers, 1920 citations, averaging 10.43 citations per paper). Utrecht University (149 papers, 10373 citations, averaging 69.62 citations per paper) ranks second, followed by Mayo Clinic (134 papers, 6645 citations, averaging 49.59 citations per paper) in third place and Harvard University (128 papers, 3299 citations, averaging 25.77 citations per paper) in fourth place.

### Journals and co-cited academic journals

Tables 3 and 4 present the top 10 journals with the highest publication output and most citations. “World Neurosurgery” (320 papers, 8.41%) is the journal with the highest number of publications in this field, followed by “Journal of Neurosurgery” (218 papers, 5.73%), “Stroke” (172 papers, 4.52%), and “Neurosurgery” (158 papers, 4.15%). Among the top 10 journals by publication output, “Cell Death & Disease” has the highest impact factor (IF) of 9.0. Approximately 90% of the journals are classified as Q1 or Q2 (Figure 6A).

The impact of a journal is determined by the frequency of its co-citation, indicating whether the journal has made a significant impact on the scientific community. According to Figure 6B and Table 4, the most co-cited journal was “Stroke” (3230 citations), followed by “J Neurosurg” (2756 citations) and “Neurosurgery” (2674 citations). Among the top 10 most co-cited journals, “Lancet” has been cited 1827 times, with the highest IF among the top 10 journals (168.9). In the co-cited journals, 90% of the journals are in the Q1/Q2 categories.

The distribution of academic publications by topic is displayed through a double-map overlay (Figure 7). The colored trajectories represent citation connections, with citing journals on the left and cited journals on the right. Based on the results, we identified 7 main colored citation paths. For example, research published in molecular/biology/immunology journals is primarily cited by research published in molecular/biology/genetics journals. Similarly, research published in medicine/medical/clinical journals is mainly cited by research published in molecular/biology/genetics, health/nursing/medicine, and psychology/education/social journals. Additionally, research published in neurology/sports/

Table 3 The top 10 journals of intracranial aneurysms rupture risk factors research

Rank	Journal	Article counts	Percentage (%)	IF	Quartile in category
1	World Neurosurgery	320	8.41	2.0	Q4
2	Journal of Neurosurgery	218	5.73	5.6	Q1
3	Stroke	172	4.52	5.2	Q2
4	Neurosurgery	158	4.15	4.7	Q2
5	Acta Neurochirurgica	123	3.23	9.0	Q1
6	Frontiers in Neurology	113	2.97	3.7	Q2
7	Journal of Neurointerventional Surgery	102	2.68	3.8	Q1
8	American Journal of Neuroradiology	87	2.29	3.3	Q2
9	Journal of Clinical Neuroscience	80	2.10	4.2	Q2
10	Clinical Neurology and Neurosurgery	66	1.74	4.8	Q1

IF: Impact factor.

Table 4 The top 10 co-cited journals related with rupture risk factors of intracranial aneurysms research

Rank	Cited Journal	Co-citation	IF (2022)	Quartile in category
1	Stroke	3230	11.2	Q1
2	J Neurosurg	2756	13.3	Q1
3	Neurosurgery	2674	3.7	Q2
4	Am J Neuroradiol	1864	4.8	Q1
5	Lancet	1827	64.5	Q4
6	Neurology	1525	11.5	Q1
7	New Engl J Med	1509	8.0	Q1
8	World Neurosurg	1375	254.7	Q1
9	Acta Neurochir	1339	64.8	Q1
10	Lancet Neurol	1215	4.8	Q2

IF: Impact factor.

ophthalmology journals is primarily cited by research published in molecular/biology/genetics, health/nursing/medicine, and psychology/education/social journals.

Authors and co-cited authors

Among all authors who have published literature related to rupture risk factors for IAs, Table 5 lists the top 10 authors with the most publications. The top 10 authors have collectively published 397 papers, accounting for 9.65% of all papers in this field. Rinkel Gabriel JE has the greatest number of research papers, with 73 publications, followed by Xin-Jian Yang (47 papers), Koivisto Timo (40 papers), and Jaaskelainen Juha E (37 papers). Further analysis revealed that among the top ten authors, 4 were from China, 3 were from the Netherlands, 2 were from Finland, and 1 was from the United States. CiteSpace visualizes the network between authors (Figure 8).

Figure 9A and Table 5 display the top 10 authors with the most co-citations and citations, respectively. A total of 54 authors have been cited more than 20 times, indicating that their research has a strong reputation and strong influence. The largest nodes are associated with the authors who have the most co-citations, including Wiebers D (795 citations), Juvela S (766 citations), and Vlak MHM (536 citations).

Co-cited references

Based on the top 10 co-cited articles (Table 6), one of them included “Development of the PHASES score for prediction of risk of rupture of IAs: A pooled analysis of six prospective cohort studies” from Lancet Neurology. The primary author of this article is Jacoba P Greving. He found that the PHASES score serves as a readily applicable tool for predicting the rupture risk of asymptomatic IAs[5]. Within the temporal scope spanning from 2004 to 2023, represented in annual time

**Table 5 The top 10 authors and co-cited authors related with rupture risk factors of intracranial aneurysms research**

Rank	Author	Count	Location	Co-cited author	Citation
1	Rinkel Gabriel JE	73	Netherlands	Wiebers D	795
2	Xin-Jian Yang	47	China	Juvela S	766
3	Koivisto Timo	40	Finland	Vlak Mhm	536
4	Jaaskelainen Juha E	37	Finland	Rinkel Gje	429
5	Du Rose	36	United States	Morita A	428
6	Shuo Wang	36	China	Greving JP	357
7	You-Xiang Li	34	China	Chalouhi N	354
8	Hernesniemi Juha	32	China	Brinjikji W	353
9	Ruigrok Ynte M	32	Netherlands	Schievink WI	335
10	Algra Ale	30	Netherlands	Inagawa T	333

**Table 6 The top 10 co-cited references related to rupture risk factors of intracranial aneurysms research**

Rank	Title	Journal	Author(s)	Total citations
1	Development of the PHASES score for prediction of risk of rupture of intracranial aneurysms: a pooled analysis of six prospective cohort studies	<i>Lancet Neurology</i>	Greving JP	150
2	The natural course of unruptured cerebral aneurysms in a Japanese cohort	<i>New England Journal of Medicine</i>	Morita A	135
3	Prevalence of unruptured intracranial aneurysms, with emphasis on sex, age, comorbidity, country, and time period: a systematic review and meta-analysis	<i>Lancet Neurology</i>	Vlak MHM	110
4	Guidelines for the management of patients with unruptured intracranial aneurysms a guideline for healthcare professionals From the American Heart Association/ American Stroke Association	<i>Stroke</i>	Thompson BG	100
5	Natural history of unruptured intracranial aneurysms: probability of and risk factors for aneurysm rupture (reprinted from <i>Journal of Neurosurgery</i> , vol 93, pg 379-387, 2000)	<i>Journal of Neurosurgery</i>	Juvela S	83
6	High WSS or low WSS? Complex interactions of hemodynamics with intracranial aneurysm initiation, growth, and rupture: Toward a unifying hypothesis	<i>American Journal of Neuroradiology</i>	Meng H	78
7	Guidelines for the management of aneurysmal subarachnoid hemorrhage a guideline for healthcare professionals From the American Heart Association/ American Stroke Association	<i>Stroke</i>	Connolly ES	78
8	Worldwide incidence of aneurysmal subarachnoid hemorrhage according to region, time period, blood pressure, and smoking prevalence in the population a systematic review and meta-analysis	<i>Jama Neurology</i>	Etminan N	73
9	Natural history of unruptured intracranial aneurysms a long-term follow-up study	<i>Stroke</i>	Juvela S	72
10	Risk factors for growth of intracranial aneurysms: A systematic review and meta-analysis	<i>American Journal of Neuroradiology</i>	Brinjikji W	70

slices, the co-citation network of references comprises 678 nodes and 2377 links (Figure 9B). Ranked second is “The natural course of unruptured cerebral aneurysms in a Japanese cohort” published in the *New England Journal of Medicine*. The authors of this article are UCAS Japan Investigators. Their study demonstrated that the natural progression of unruptured cerebral aneurysms is influenced by factors such as aneurysm size, location, and morphology[18].

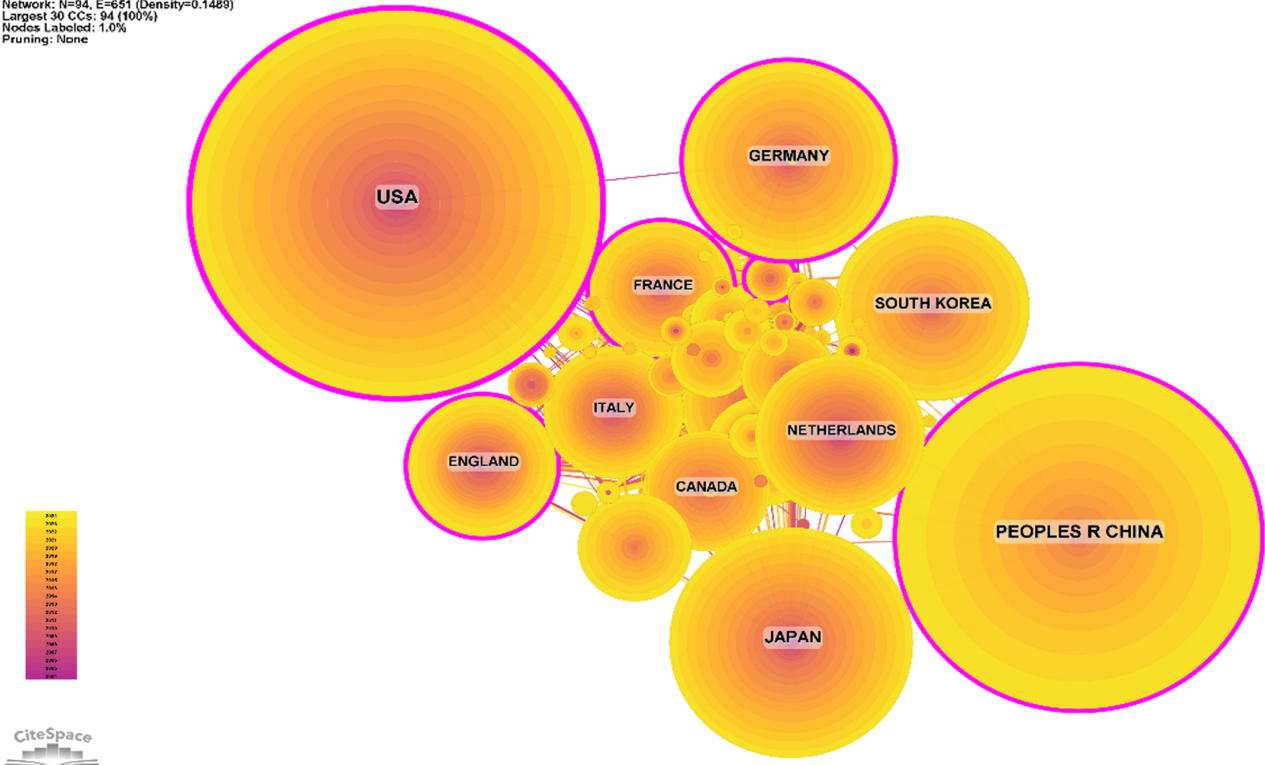
We conducted co-citation reference clustering and temporal clustering analysis (Figures 10 and 11). Our findings revealed that endovascular therapy (cluster 1), polymorphisms (cluster 8), and patent foramen ovale (cluster 10) were early research hotspots. In the mid-term, microarray analysis (cluster 2), wall shear stress (cluster 4), hydrocephalus (cluster 7), vertebral artery (cluster 11), patent foramen ovale (cluster 12), subarachnoid hemorrhage (cluster 14), and HDAC inhibitors (cluster 13) emerged as prominent research areas. Magnetic resonance imaging (cluster 0), risk factor (cluster 3), flow diverter (cluster 5), radiosurgery (cluster 6), aneurysmal subarachnoid hemorrhage (cluster 9), and the ellipticity index (cluster 13) represent the current hot topics and trends in this field.

### Keywords and references with citation burstness

By analyzing keywords, we can swiftly grasp the status and developmental trajectory of a particular field. Based on the co-occurrence of keywords in VOSviewer, the most prominent term was “subarachnoid hemorrhage” (1286 occurrences),

A

CiteSpace, v. 6.2.R4 (64-bit) Advanced  
April 1, 2024 at 4:49:46 PM CST  
WoS: D:\bibliometric\riskfactor\output  
Timespan: 2004-2024 (Slice Length=1)  
Selection Criteria: g-index (k=25), LRF=3.0, L/N=10, LBY=5, e=1.0  
Network: N=94, E=651 (Density=0.1489)  
Largest 30 CCs: 94 (100%)  
Nodes Labeled: 1.0%  
Pruning: None



B

CiteSpace, v. 6.2.R4 (64-bit) Advanced  
April 1, 2024 at 5:07:27 PM CST  
WoS: D:\bibliometric\riskfactor\output  
Timespan: 2004-2023 (Slice Length=1)  
Selection Criteria: g-index (k=25), LRF=3.0, L/N=10, LBY=5, e=1.0  
Network: N=506, E=3270 (Density=0.0256)  
Largest 30 CCs: 453 (89%)  
Nodes Labeled: 1.0%  
Pruning: None

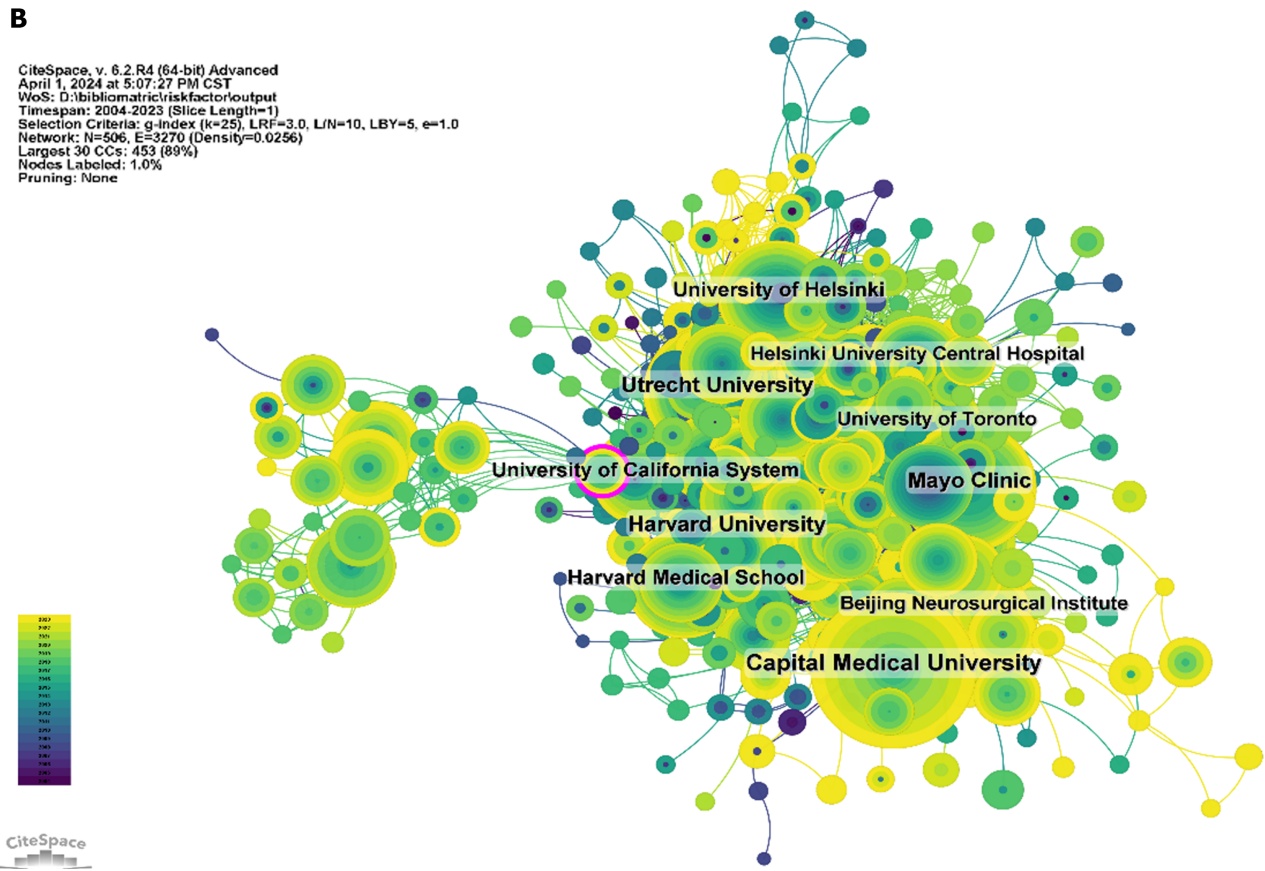


**Figure 5** Co-occurrence map of nations/regions and organizations in risk factors for the rupture of intracranial aneurysms studies. A: Co-occurrence map of nations/regions in risk factors for the rupture of intracranial aneurysms studies; B: Co-occurrence map of organizations in risk factors for the rupture of intracranial aneurysms studies.

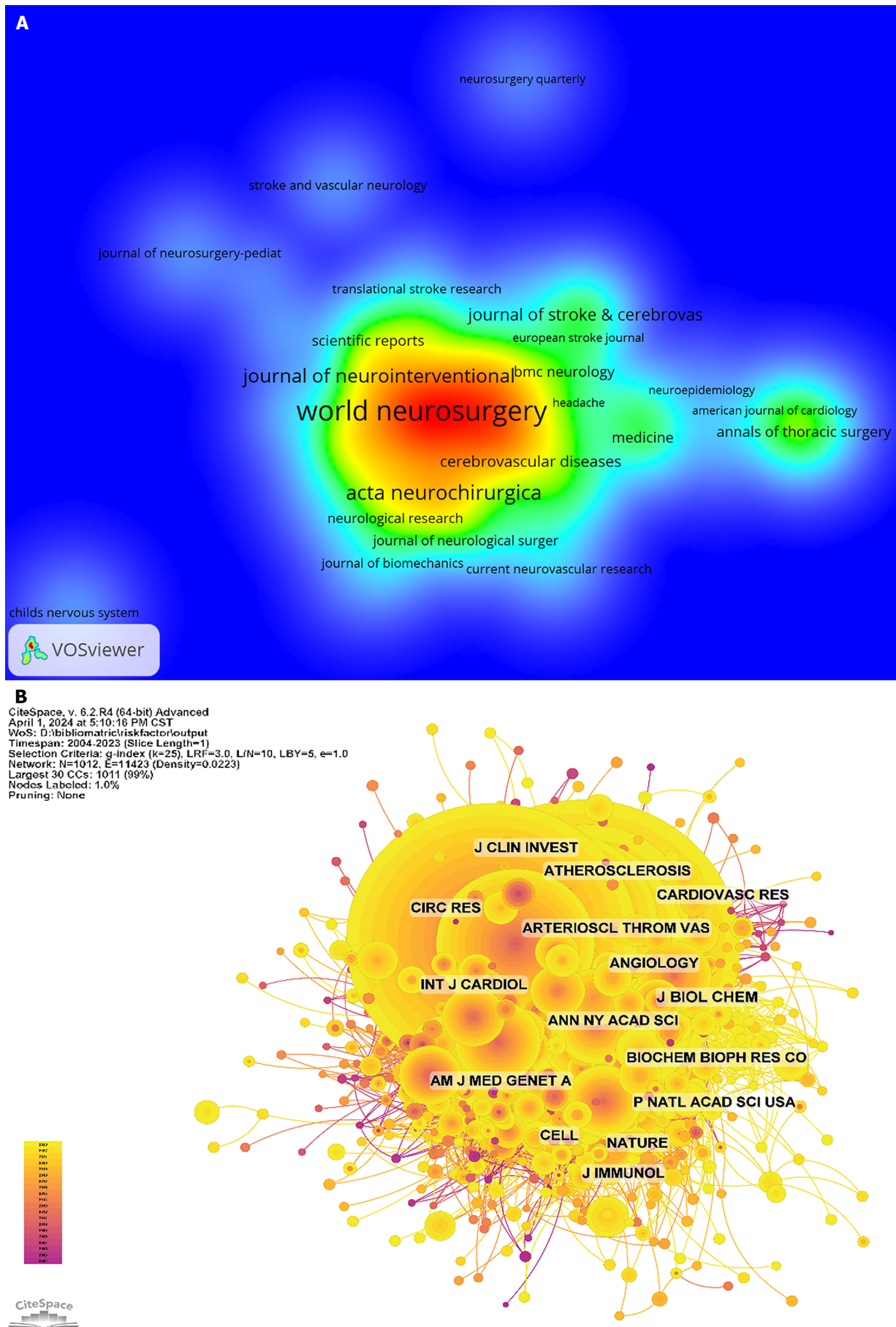
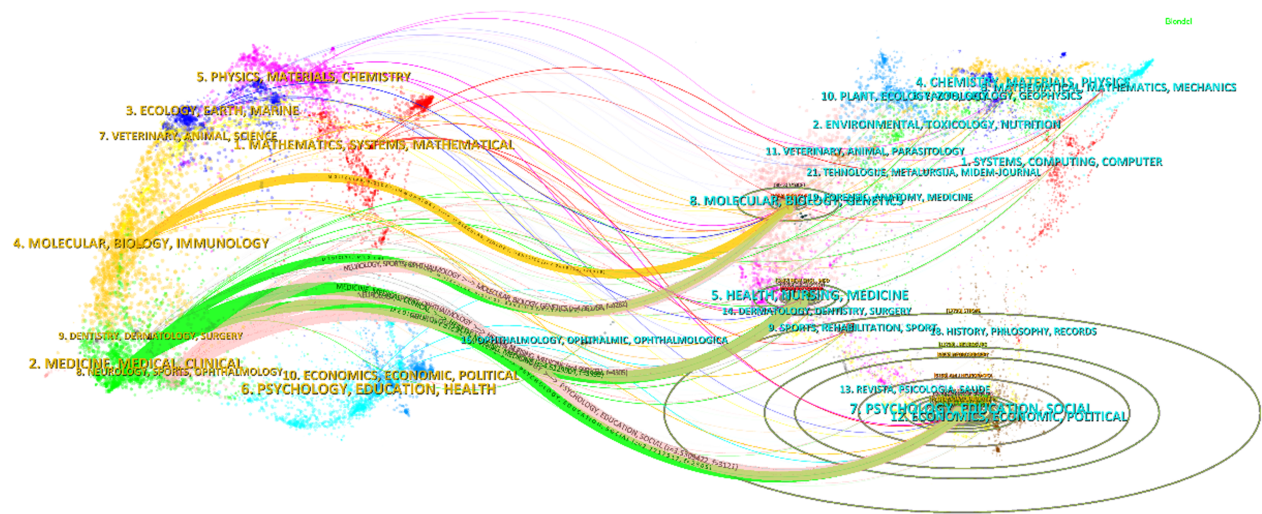
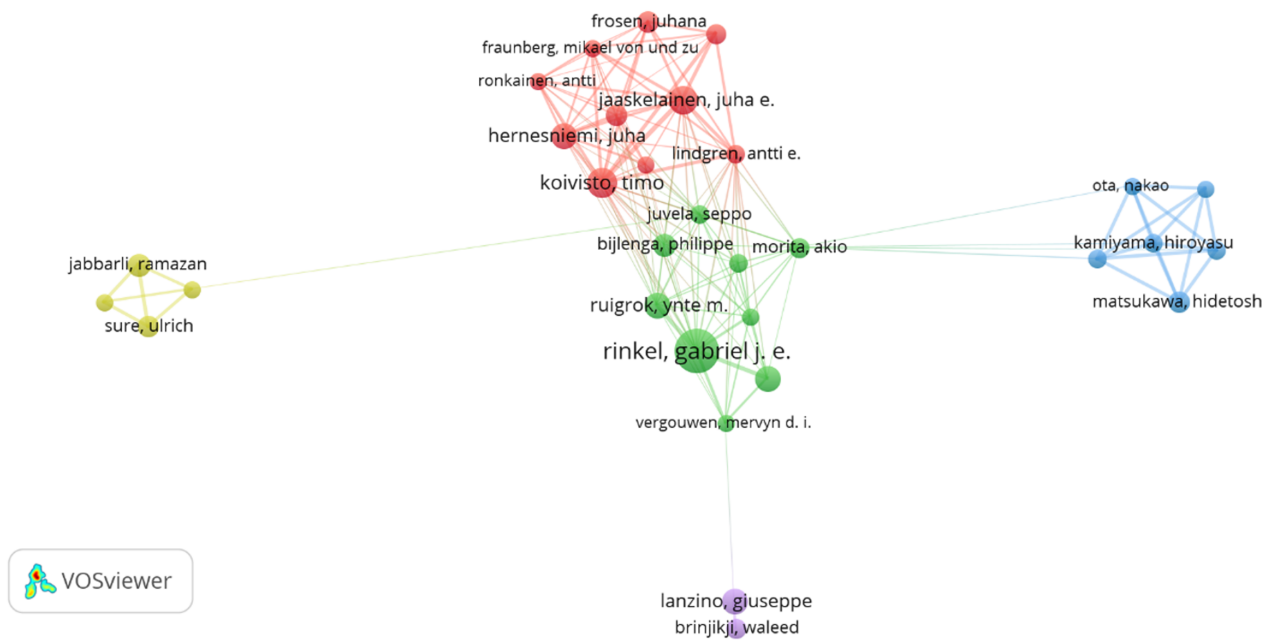


Figure 6 Density map of journals and co-cited journals in risk factors for the rupture of intracranial aneurysms research. A: Density map of

journals in risk factors for the rupture of intracranial aneurysms research; B: Density map of co-cited journals in risk factors for the rupture of intracranial aneurysms research.



**Figure 7** The dual-map overlay of periodicals associated with risk factors for the rupture of intracranial aneurysms research. The citing journals are on the left, the cited journals are on the right, and the line path represents the citation relationship.



**Figure 8** The network map of co-authors in rupture risk factors of intracranial aneurysms research.

followed by “rupture” (594), “management” (563), “natural history” (475), and “stroke” (458) (Table 7, Figures 12 and 13). After filtering out irrelevant keywords, we constructed a network comprising 170 keywords that appeared at least 33 times, yielding 5 distinct clusters. The first cluster (in red) encompasses 45 keywords, including “rupture”, “natural history”, “prediction”, “flow”, “morphology”, “aspect ratio”, “geometry”, “location”, “artery”, “CT angiography”, “geometry”, “magnetic resonance imaging”, “MRI”, “score”, “shape”, “hemodynamics”, “cohort”, and “parameters”. The second cluster (in green) comprised 39 keywords, such as “endovascular treatment”, “safety”, “follow-up”, “morbidity”, “surgery”, “therapy”, “embolization”, “recurrence”, “clipping”, “long term”, “stent”, “neurosurgery”, “efficacy”, “occlusion”, “trial”, “flow diversion”, and “recanalization”. The third cluster (in blue) included 36 keywords, such as “subarachnoid hemorrhage”, “association”, “population”, “region”, “age”, “case fatality”, “cigarette smoking”, “disease”, “emphasis”, “epidemiology”, “gender”, “genetics”, “hypertension”, “meta-analysis”, “population”, “sex”, and “time”. The fourth cluster (in yellow) consisted of 27 keywords, such as “brain”, “aneurysms”, “children”, “diagnosis”, “dissection”, “events”, “headache”, “hemorrhage”, “ischemic stroke”, “prevention”, “repair”, “replacement”, and

**Table 7** The top 20 keywords concerning rupture risk factors of intracranial aneurysms research

Rank	Keyword	Counts
1	Subarachnoid hemorrhage	1286
2	Rupture	594
3	Management	563
4	Natural-history	475
5	Stroke	458
6	Endovascular treatment	422
7	Surgery	281
8	Complications	263
9	Prevalence	240
10	Hemodynamics	222
11	Embolization	220
12	Mortality	220
13	Growth	216
14	Outcome	203
15	Aneurysms	200
16	Coiling	199
17	Angiography	195
18	Vasospasm	189
19	Age	179
20	Follow-up	171

“vertebral artery”. The fifth cluster (in purple) contains 23 keywords, including “blood”, “cerebral infarction”, “outcome”, “impact”, “predictors”, “scale”, “vasospasm”, “infarction”, “prognosis”, “delayed cerebral ischemia”, “infarction”, “rebleeding”, “vasospasm”, “quality of life”, “hydrocephalus”, and “symptomatic vasospasm”. We generated a volcano plot using CiteSpace to visually depict the evolution of research hotspots over time (Figures 14 and 15).

Through CiteSpace, we identified the 50 most reliable citation bursts in the field of rupture risk factors for IAs. The most highly cited reference (with a burst rate of 51.74) is the article titled “The natural course of unruptured cerebral aneurysms in a Japanese cohort” published in the *New England Journal of Medicine*, with the first author being The UCAS Japan Investigators. Out of the 50 references, 47 were published between 2004 and 2023, indicating that these papers have been frequently cited over the past two decades. Importantly, 8 of these papers are currently experiencing a peak in citations (as shown in Figure 16), suggesting that the rupture risk factors for IAs will continue to be a subject of interest in the future. Among the 844 most prominent burst keywords in this field, we have specifically focused on the top 50 keywords with the most intense bursts (as depicted in Figure 17). These keywords represent the current research hotspots in the field and indicate potential directions for future studies.

## DISCUSSION

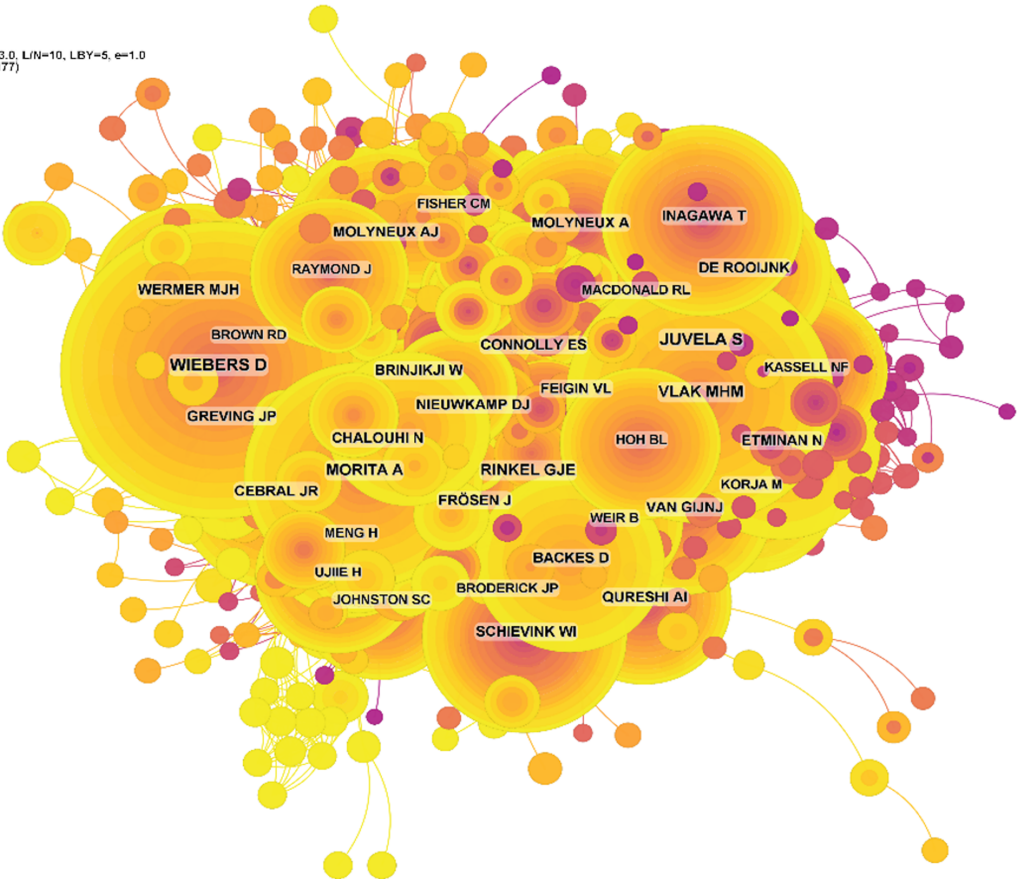
### General information

In this investigation, a bibliometric analysis was performed on publications pertaining to risk factors associated with IA rupture over the past two decades. The aim was to discern prominent areas of focus and emerging trends in this research domain. Our findings reveal a notable surge in the volume of publications concerning risk factors for IA rupture, particularly since 2012, with a pinnacle observed in 2023. This upward trajectory underscores the sustained relevance and continued interest of researchers in this field for the foreseeable future.

Our analysis revealed that the United States plays a pivotal role in research on risk factors for IA rupture, with significant contributions from China, Japan, Germany, and South Korea. Approximately 28.97% of all publications originated from researchers in the United States. Notably, the United States exhibited dominance in publication output, total citations, and international collaborations based on our findings. The notable performance of the Netherlands and Canada in total citations underscores the quality of research activities in these nations. In terms of international cooperation, the United States, Italy, and Germany were identified as closely collaborating with other countries, while

A

CiteSpace, v. 5.2.R4 (64-bit) Advanced  
April 1, 2024 at 5:18:47 PM CST  
WoS: D:\bibliometric\riskfactor\output  
Timespan: 2004-2023 (Slice Length=1)  
Selection Criteria: g-index (k=25), LRF=3.0, L/N=10, LBY=5, e=1.0  
Network: N=1010, E=9033 (Density=0.0177)  
Largest 30 CCs: 1006 (99%)  
Nodes Labeled: 1.0%  
Pruning: None



B

CiteSpace, v. 5.2.R4 (64-bit) Advanced  
April 1, 2024 at 5:37:12 PM CST  
WoS: D:\bibliometric\riskfactor\output  
Timespan: 2004-2023 (Slice Length=1)  
Selection Criteria: g-index (k=25), LRF=3.0, L/N=10, LBY=5, e=1.0  
Network: N=1301, E=6185 (Density=0.0073)  
Largest 30 CCs: 1236 (95%)  
Nodes Labeled: 1.0%  
Pruning: None

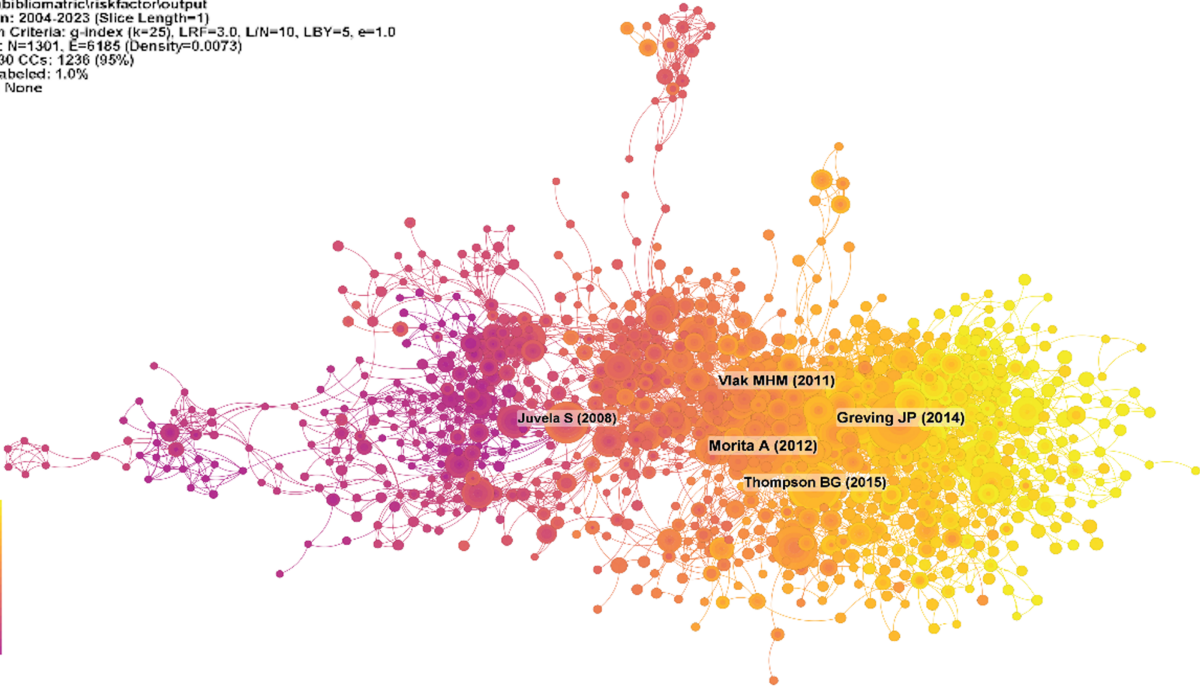


**Figure 9** Density map of co-cited authors and co-cited references in rupture risk factors of intracranial aneurysms research. A: Density map of co-cited authors in rupture risk factors of intracranial aneurysms research; B: Density map of co-cited references in rupture risk factors of intracranial aneurysms research.

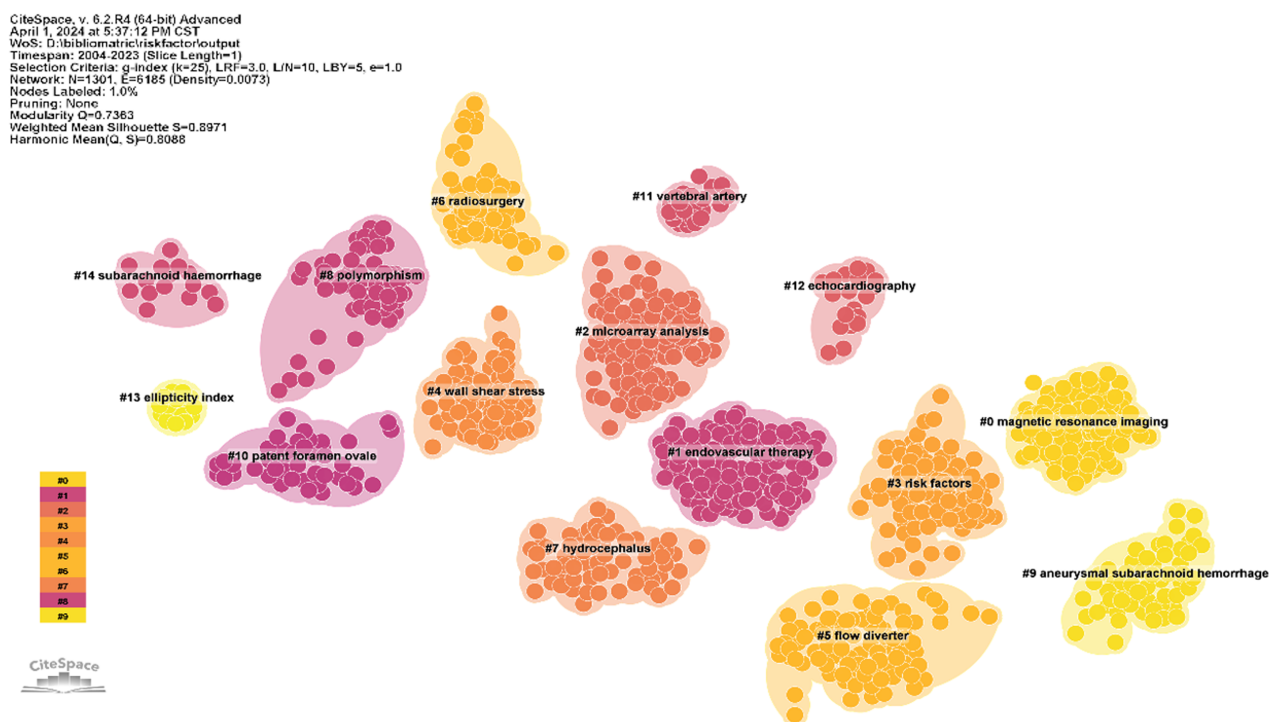


Figure 10 Co-citation Clustered network of the rupture risk factors for intracranial aneurysms research.

China, Japan, South Korea, and the Netherlands engaged in collaboration to a lesser extent, potentially impacting their citation rankings. Strengthening international collaboration in China, Japan, South Korea, and the Netherlands is essential for enhancing the dissemination of high-quality publications.

Among the top 10 institutions with the greatest impact, 40% were located in the United States. Notably, Capital Medical University in China had the highest volume of publications but was ranked ninth in overall citations. This suggests that the institution should focus on enhancing research quality and fostering increased collaboration and knowledge exchange. Among the authors, Gabriel JE, Xin-Jian Yang, Timo Koivisto, and Juha E. Jaaskelainen stood out for their significant contributions to advancing the understanding of risk factors associated with the rupture of IAs. Furthermore, works by Wiebers D, Juvela S, and Vlak MHM received the highest average number of citations, underscoring the caliber of their research contributions in this domain. Our analysis revealed that several journals are actively publishing research on the risk factors for IA rupture. Noteworthy publications in this area appeared in *World Neurosurgery*, *Journal of Neurosurgery*, *Stroke*, and *Neurosurgery*, indicating that these journals are primary outlets for disseminating research findings in this field.

### Knowledge base

Co-cited references indicate the frequency with which two publications are jointly cited by other works, serving as a knowledge repository within a specific field[19]. In this scientometric analysis, the top 10 co-cited references were examined to delineate the foundational knowledge base concerning risk factors for IA rupture. The study by Greving *et al* [5] was the most frequently cited publication in 2014, garnering 150 co-citations. This article elucidates the utility of the PHASES score in predicting the risk of IA rupture by considering factors such as age, hypertension, aneurysm size, and location, highlighting variations in rupture risk among diverse populations. The second most highly cited publication, the *New England Journal of Medicine*, was authored by UCAS Japan Investigator[18]. This study demonstrated that the natural progression of unruptured cerebral aneurysms varies based on factors such as the size, location, and shape of the aneurysm. In 2011, Vlak *et al*[2] published the third co-cited paper in *Lancet Neurology*. This study revealed that the increased incidence of subarachnoid hemorrhage in Finland and Japan could not be solely attributed to a greater incidence of UIAs, indicating an elevated risk of rupture in these populations. *Stroke* published the fourth co-cited prospective study by Thompson *et al*[20]. The objective of this guideline is to offer thorough and evidence-based recommendations for the management of patients with UIAs. A holistic approach involving both risk factor prevention and management may be essential to decrease the prevalence of unruptured aneurysms and their potential as a precursor for subarachnoid hemorrhage in the majority of cases. The fifth co-cited publication was published in the *Journal of Neurosurgery* by Juvela *et al*[21]. The study highlighted that cigarette smoking, the size of the UIA, and age (inversely) are significant factors that influence the risk of subsequent aneurysm rupture. The sixth co-cited study was published in 2014 by Meng *et al*[22]. This study suggested that low wall shear stress and a high oscillatory shear index play a role in activating an inflammatory cell-mediated pathway that could contribute to the formation and rupture of large atherosclerotic aneurysms. Conversely, high wall shear stress combined with a positive wall shear stress gradient is linked to a mural cell-mediated pathway, which may lead to the expansion and rupture of small or secondary bleb aneurysms. The seventh most commonly co-cited paper was published by Connolly *et al*[23] in *Stroke*. The guidelines concluded that,

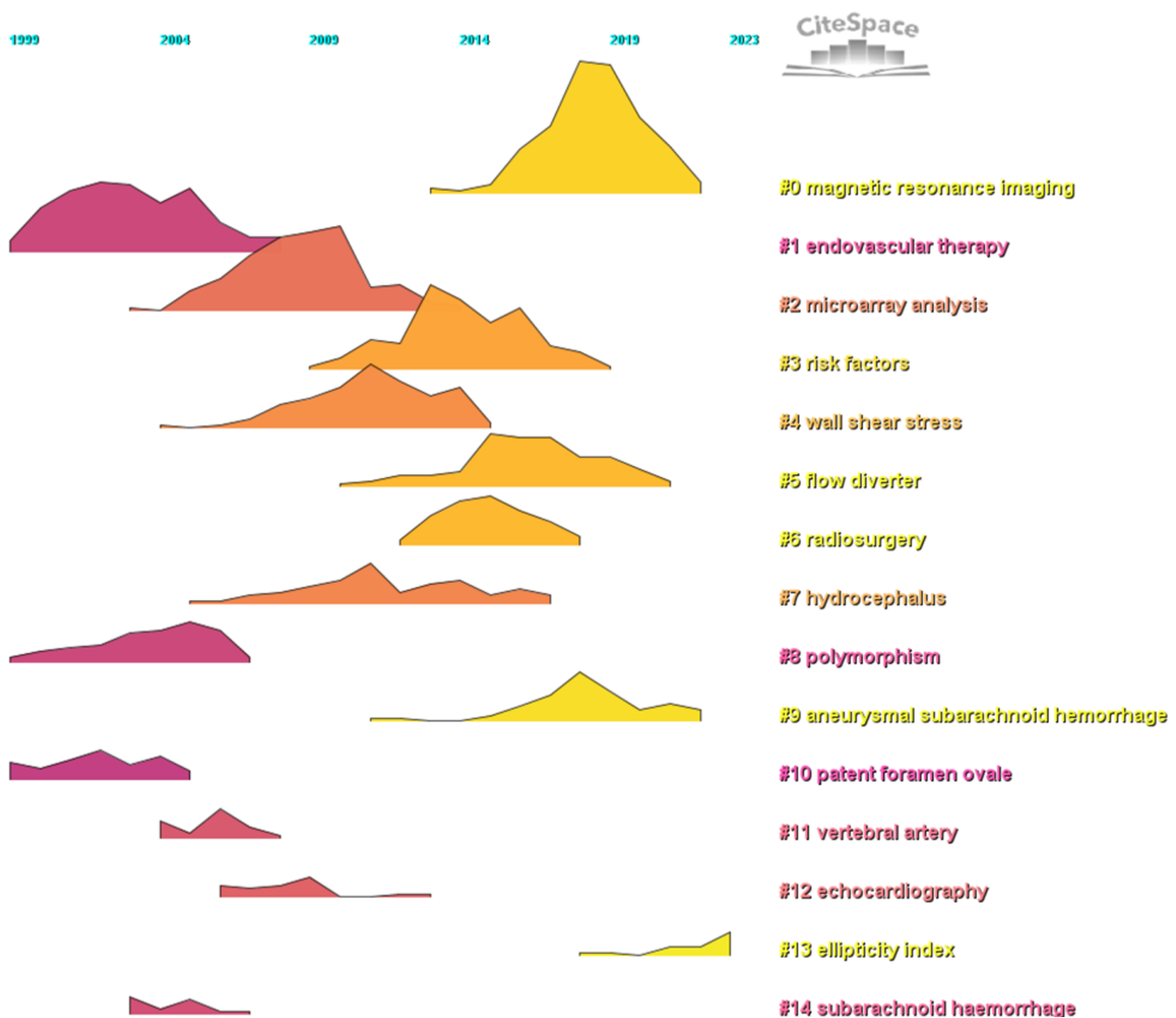
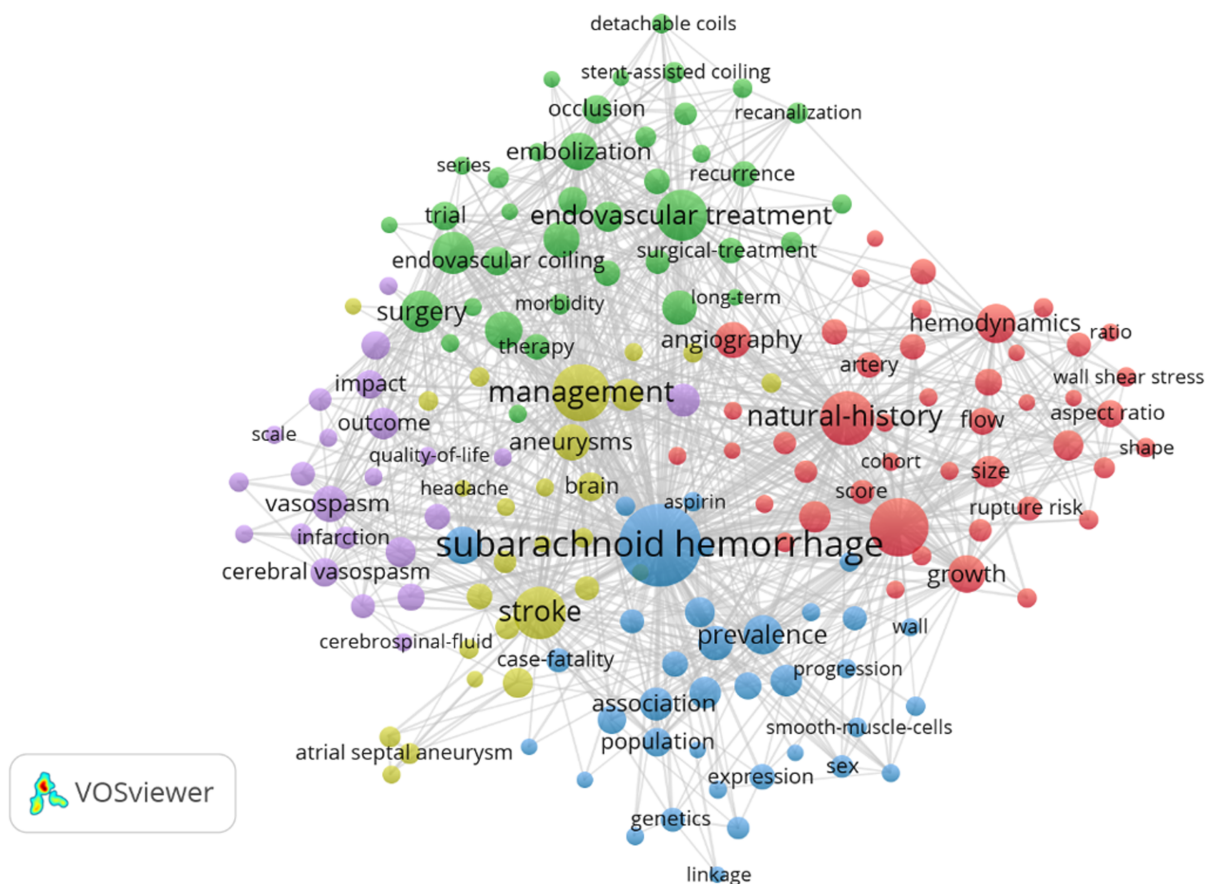


Figure 11 Volcano map of the co-citation related to the rupture risk factors for intracranial aneurysms.

beyond the size and location of the aneurysm and the patient's age and health status, it may be appropriate to take into account the morphological and hemodynamic features of the aneurysm when assessing the risk of aneurysm rupture. In 2019, the eighth most commonly co-cited paper was published by Etminan *et al*[24] in *JAMA Neurology*. In their systematic review and meta-analysis, the researchers found that the global incidence of subarachnoid hemorrhage and its decline exhibit significant regional variations, closely mirroring the reduction in blood pressure and smoking rates. Identifying the factors contributing to these regional differences and implementing strategies to further reduce blood pressure and smoking prevalence could lead to a reduction in the overall burden of subarachnoid hemorrhage. Juvela *et al*[25] investigated the long-term natural history of UIAs and risk factors predictive of subsequent rupture and published the ninth co-cited paper. Cigarette smoking, patient age (inversely), and the size and location of the UIA appear to be risk factors for aneurysm rupture. However, the risk of bleeding tends to decrease with very long-term follow-up. The article published in the *American Journal of Neuroradiology* in 2016, which received the last co-citations, presented observational evidence highlighting various clinical and anatomic risk factors for aneurysm growth. These factors included age over 50 years, female sex, smoking history, and nonsaccular shape. These findings should be taken into account when advising patients about the natural progression of UIA[26]. In general, the top 10 co-citations primarily focused on clinical, morphological, and hemodynamic risk factors, as well as the development of a simple and practical scoring system to assess the risk of rupture factors for IAs. These foundational topics have significantly contributed to advancements in this field of study.

### Emerging topics

Keywords play a crucial role in reflecting the prevailing research themes and trajectories within a specific domain. Table 7 highlights the prominence of the top 20 keywords, each appearing more than 170 times, which encapsulates the pivotal areas of investigation concerning the risk factors associated with IA rupture. Noteworthy keywords include subarachnoid hemorrhage, rupture, management, natural history, stroke, endovascular treatment, surgery, complications, prevalence, and hemodynamics. These keywords collectively paint a comprehensive picture of the landscape surrounding risk factors for IA rupture. Specifically, they underscore: (1) The critical association between IA rupture and subarachnoid



**Figure 12 The co-occurrence network and clusters of keywords related to rupture risk factors of intracranial aneurysms research.**

hemorrhage, a significant contributor to stroke[27-30]; (2) The intrinsic link between the natural history of IAs and their propensity for rupture[27,29,31]; (3) The increasing interest in hemodynamic parameters concerning IAs in recent studies [32-35]; and (4) The pivotal role of understanding risk factors for IA rupture in enhancing management and treatment strategies aimed at averting complications, encompassing both surgical and endovascular interventions[23,36-38].

The keyword density map serves as a visual representation, offering a more intuitive depiction of the prevalent keywords within this field (Figure 13). Through network clustering analysis, the keywords are categorized into five clusters, effectively delineating the research focus and breadth of this domain. As illustrated in Figure 12, these clusters are as follows: Cluster 1 (red) predominantly explores the natural history and hemodynamic risk factors associated with IA rupture. Cluster 2 (green) centers on endovascular and surgical interventions for IA treatment. Cluster 3 (blue) includes 2 epidemiological and genetic risk factors pertinent to IAs. Cluster 4 (yellow) focuses on the complications arising from IA rupture. Cluster 5 (purple) is dedicated to investigating the impact and prognosis of IA rupture. These five clusters represent the research focus and scope of IA rupture risk factor research to some extent. In addition, from this ranking, we can see that IA rupture research on natural history and hemodynamic risk factors has become a critical research focus. Only by gaining a profound understanding of the pivotal factors contributing to IA rupture can we fundamentally discern effective therapeutic modalities for the management of IAs, thereby mitigating the occurrence of rupture-related complications, reducing disability rates, and lowering mortality rates. The timeline viewer (Figure 14) for keywords enables us to discern the temporal progression of topics within this domain, facilitating an exploration of the evolutionary trajectory of this field.

References experiencing intense citation bursts denote a sudden surge in citations for specific documents within a defined timeframe. This phenomenon aids in identifying emerging topics and research areas that have garnered significant attention within a particular field[12]. This study identified the most impactful citation bursts and curated the top 50 among them (Figure 16). The paper (strength: 51.74) with the strongest citation burstness was a large, prospective cohort study published by UCAS Japan Investigators[18] in the *New England Journal of Medicine* in 2012. This study in Japan from 2001 to 2004 examined 6697 UIAs, 91% of which were incidentally discovered, predominantly in the middle cerebral and internal carotid arteries. Research has shown that the risk of aneurysm rupture increases with size, with larger aneurysms and those in the posterior and anterior communicating arteries being more likely to rupture. Overall, the study highlighted the diverse natural history of UIAs based on size, location, and shape. Currently, 8 (16%) of the top 50 papers are still in a state of citation burst, and the citation burst of 7 papers has lasted for at least 3 years. These 7 papers represent the latest research topics related to rupture risk factors for IAs. According to the ranking by burst strength (from high to low), paper No. 1 (strength: 51.47) is mentioned above. The second-ranked paper (strength: 45.31) was published by Vlak *et al*[2] in *Lancet Neurology* in 2011. Researchers have shown that the prevalence of UIAs is greater in patients with autosomal dominant polycystic kidney disease or a positive family history of IAs or subarachnoid

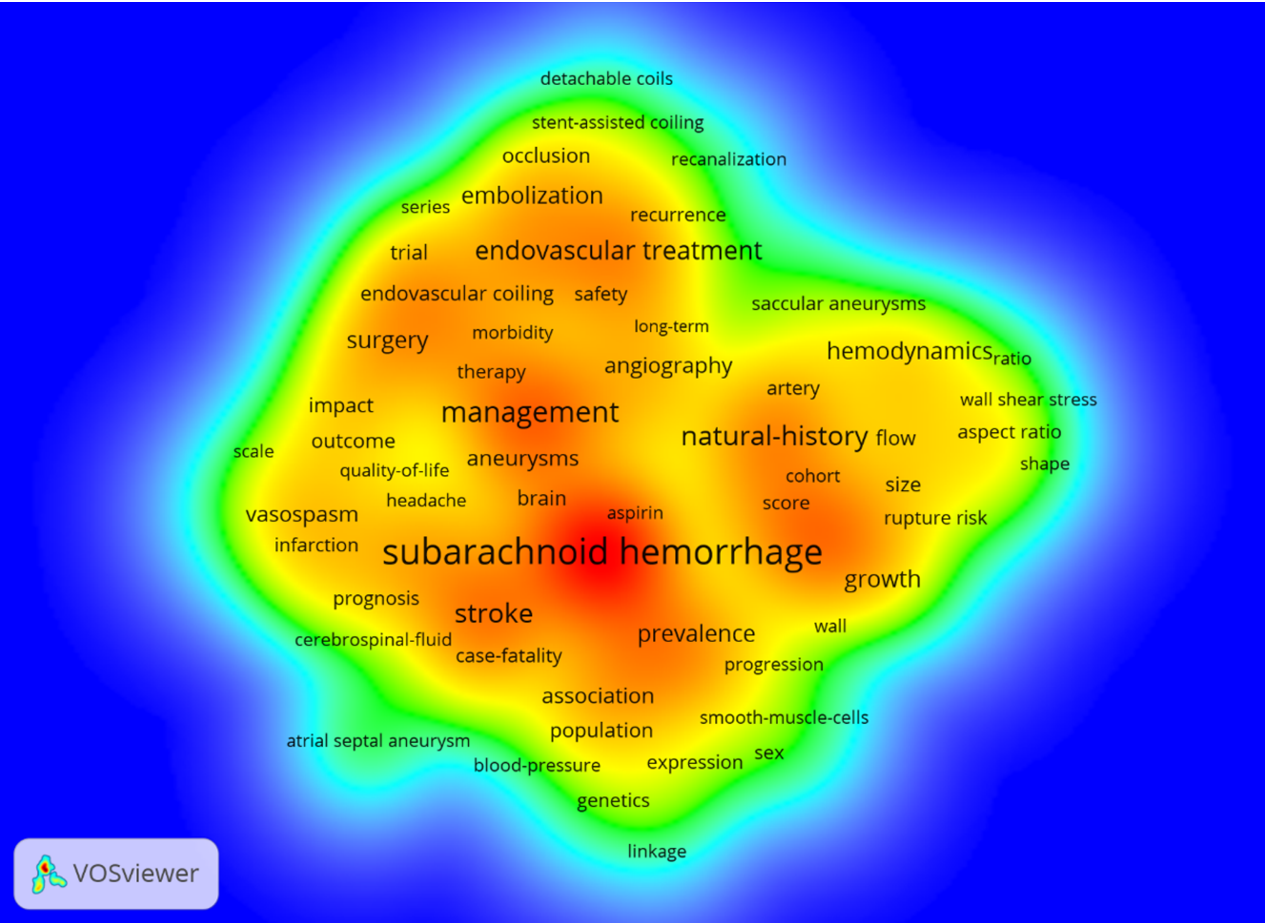


Figure 13 Density map of keywords in rupture risk factors of intracranial aneurysms research.

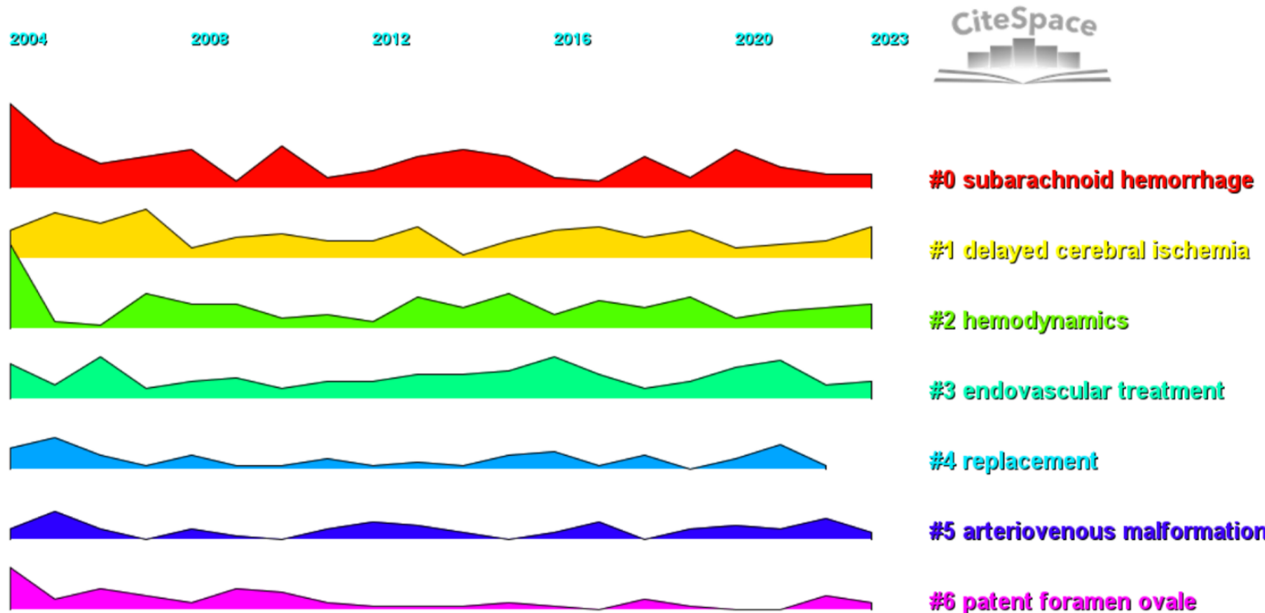


Figure 14 CiteSpace visualization keywords volcano map of timeline viewer related to the rupture risk factors for intracranial aneurysms.

CiteSpace, v. 6.2.R4 (64-bit) Advanced  
 April 1, 2024 at 5:44:23 PM CST  
 WoS: D:\bibliometric\riskfactor\output  
 Timespan: 2004-2023 (Slice Length=1)  
 Selection Criteria: g-index (k=25), LRF=3.0, L/N=10, LBY=5, e=1.0  
 Network: N=732, E=7722 (Density=0.0289)  
 Largest CCs: 732 (100%)  
 Nodes Labeled: 1.0%  
 Pruning: None  
 Modularity Q=0.3564  
 Weighted Mean Silhouette S=0.6809  
 Harmonic Mean(Q, S)=0.4679

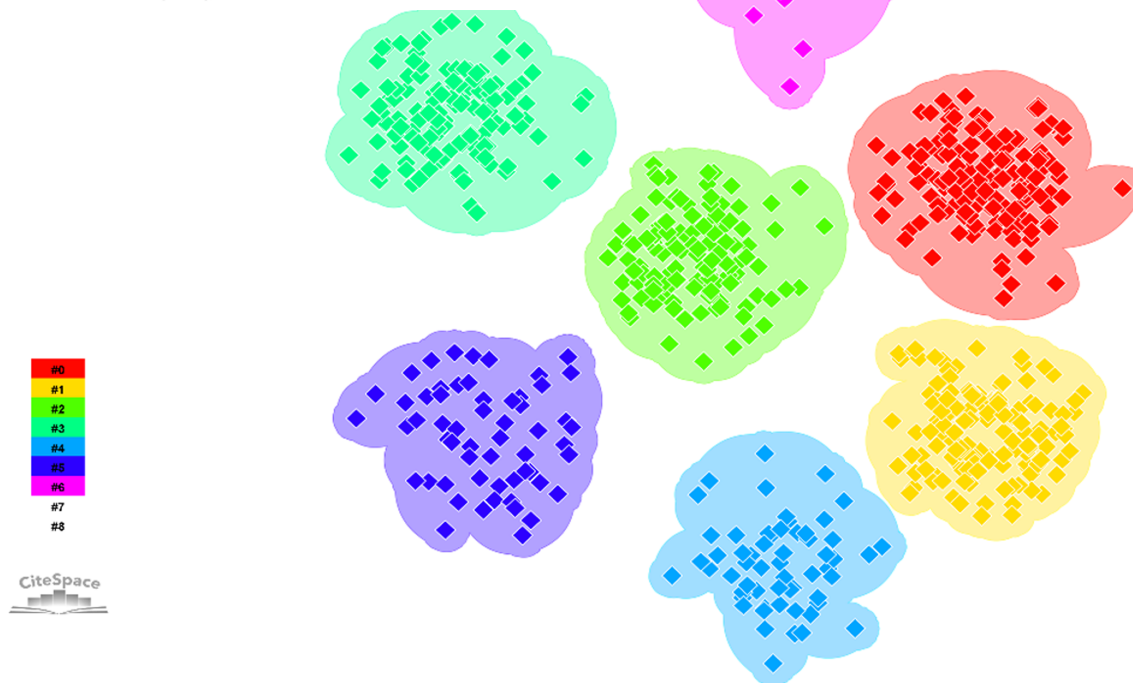


Figure 15 Keywords cluster graph of timeline viewer related to the rupture risk factors for intracranial aneurysms.

hemorrhage than in individuals without these comorbidities. In Finland and Japan, the increased incidence of subarachnoid hemorrhage cannot be solely accounted for by a higher incidence of UIAs, suggesting an elevated risk of aneurysm rupture. The third-ranked paper (strength: 43.49) was published by Greving *et al*[5] in *Lancet Neurology* in 2014. They conducted a systematic review and pooled analysis of individual patient data from 8382 participants across six prospective cohort studies focusing on subarachnoid hemorrhage as the primary outcome. The objective of this study was to identify predictors of aneurysm rupture in individuals with UIAs and to develop a risk prediction tool enabling healthcare providers to assess the 5-year risk of aneurysm rupture based on routinely evaluated patient and aneurysm features. The study concluded that the PHASES score serves as a user-friendly tool for predicting the risk of rupture in asymptomatic IAs. The fourth-ranked paper (strength: 34.43) was published by Thompson *et al*[20] in *Stroke* in 2015. The writing group members conducted systematic literature reviews spanning from January 1977 to June 2014. Additionally, they examined current evidence-based guidelines to offer thorough and evidence-supported recommendations for the management of individuals with UIAs. Finally, Juvela *et al*[21] published the article with the fifth-highest citation burst (strength: 33.43) in the *Journal of Neurosurgery* in 2000. The study revealed that cigarette smoking, the size of the UIA, and age (inversely) are crucial factors that influence the risk of future aneurysm rupture. The authors recommend surgical intervention for such unruptured aneurysms irrespective of their size and the patient's smoking habits, particularly in younger and middle-aged adults, provided that this approach is feasible and that the patient's comorbidities are not contraindicated. For older patients with small aneurysms, smoking cessation could be considered a viable alternative to surgery. The citation burstness analysis showed that exploring the different risk factors for IA rupture (such as age, smoking status, and hemodynamic parameters) and advocating for proactive surgical interventions (including both surgical procedures and endovascular treatments) are essential for mitigating the potential risk of IA rupture.

### Limitations

First, the data were exclusively sourced from the WoSCC, as opposed to conducting searches across additional databases such as Embase or Scopus. While the WoSCC serves as a widely utilized and extensive online database within the realm of scientometrics[39-41], it is plausible that numerous papers pertaining to this subject have been published in journals that are not encompassed within the Web of Science. Second, the present scientometric instruments encounter significant challenges in concurrently analyzing data from multiple databases. Subsequently, all data were extracted using scientometric tools rather than being manually curated by authors in meta-analyses or systematic review overviews[41-43]. Third, the exclusion of non-English publications meant that seminal articles published in languages other than English were not considered, leading to a limited number of articles being omitted from the analysis. Finally, potential biases may

Top 50 references with the strongest citation bursts

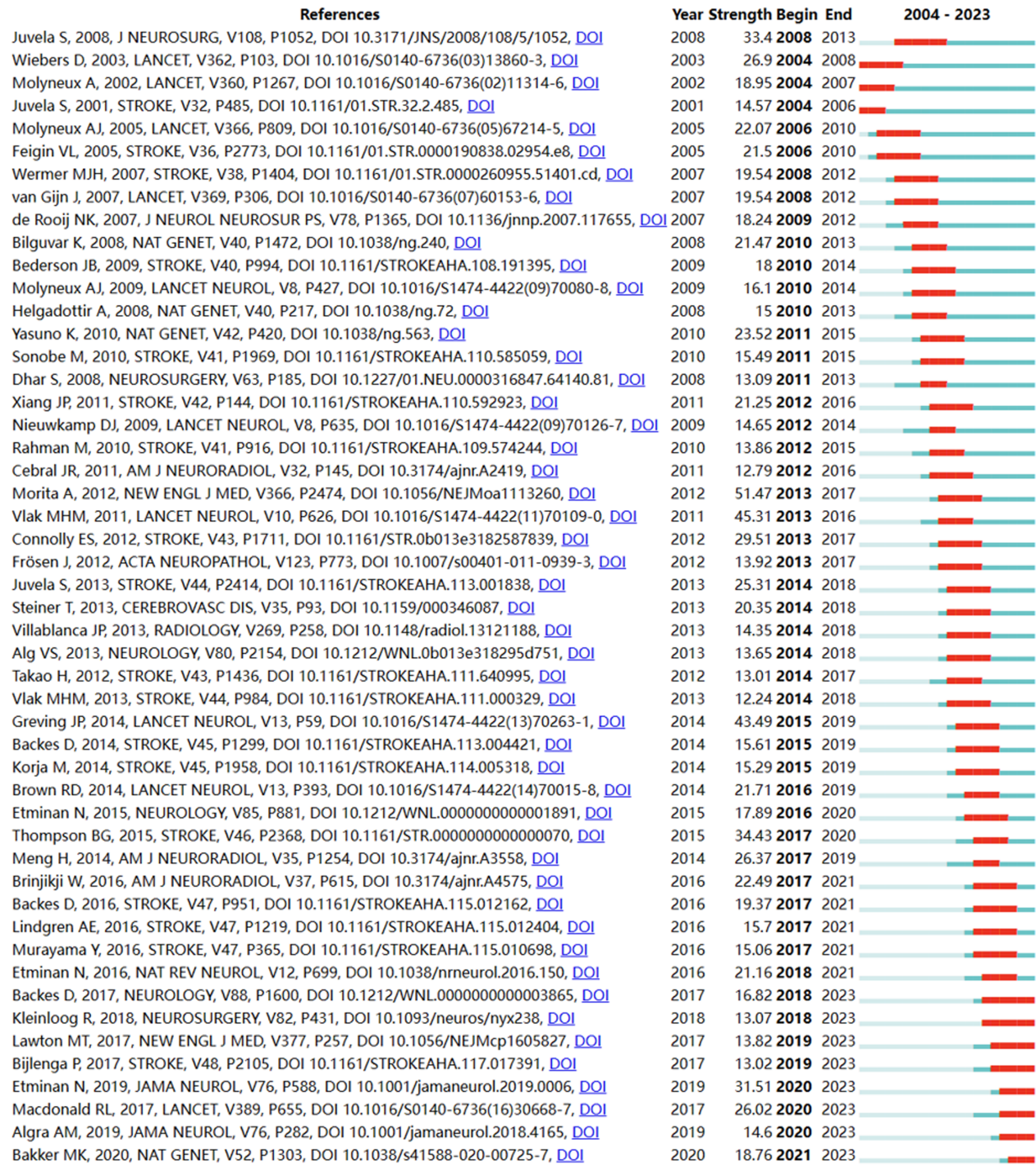


Figure 16 Representative burst references with the top 50 strongest citation.

be inherent in our findings. For instance, the likelihood of author homonymy remains a concern, as these tools may not accurately discern such nuances. These issues could be addressed in the future through advancements in machine learning, natural language processing, and data science[44]. Nonetheless, our findings are largely congruent with the conclusions drawn from the most recent traditional literature reviews while simultaneously providing scholars with more objective data, knowledge, and insights.

CONCLUSION

We used CiteSpace and VOSviewer to analyze the knowledge base and research hotspots on rupture risk factors for IA publications in the past decade. The United States contributed the most to IA risk factor-related research, and the Capital Medical University produced the most publications. *Worldwide, Neurosurgery* and *Stroke* were the most significant journals

### Top 50 keywords with the strongest citation burs

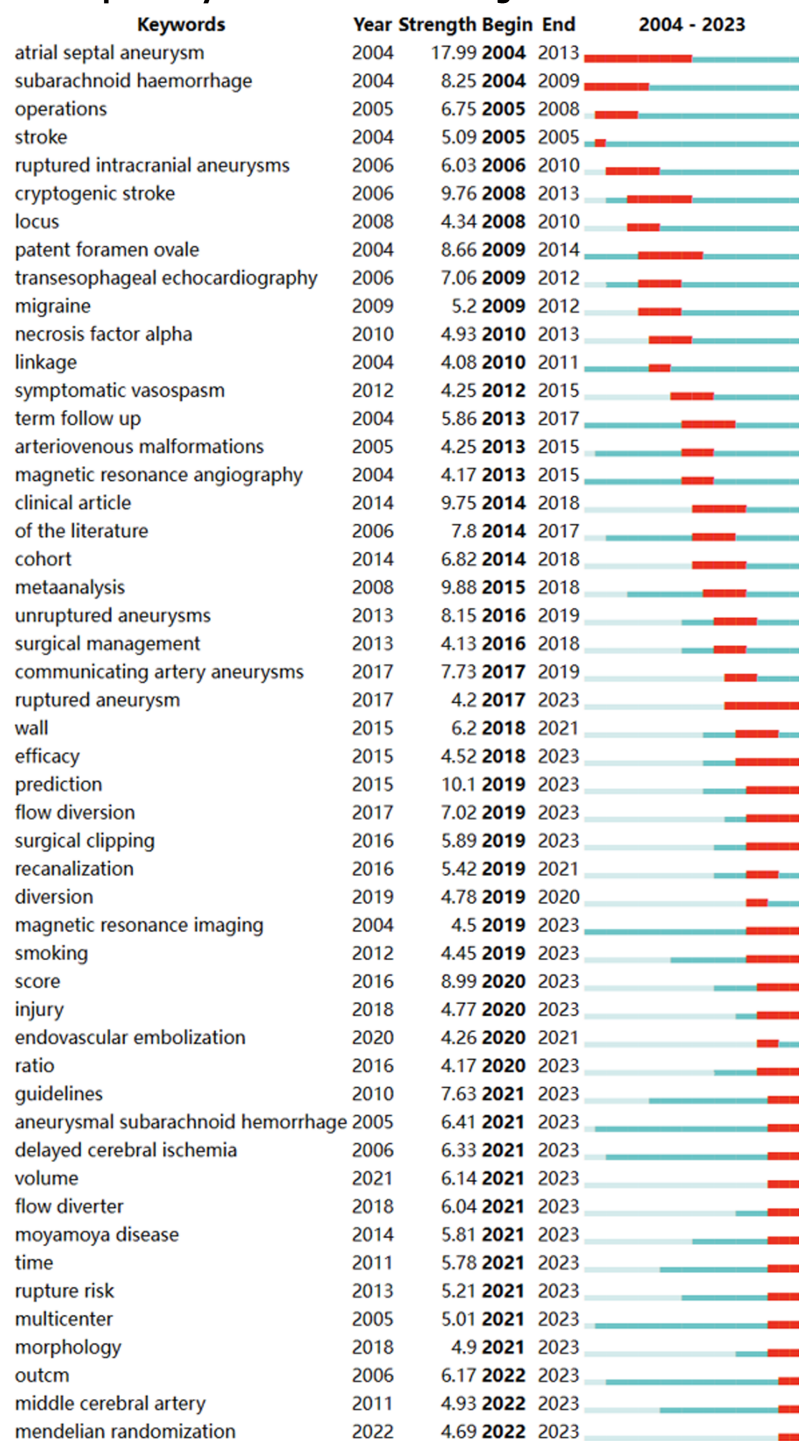


Figure 17 Representative burst keywords among top 50 references with the strongest citation bursts.

for determining the risk factors for IA rupture. Rinkel Gabriel JE and Wiebers D may have an important influence on this field because they published numerous articles and were co-cited in several more publications. Exploring the hemodynamic features and emphasizing the importance of preventing IA rupture were recent topics of interest in this research. This scientometric review offers a comprehensive understanding of drug-induced liver injury-related publications from 2004 to 2023, which could serve as a reference for researchers in this field. As investigators discover more information on rupture risk factors for IAs, we look forward to more targeted treatments and preventive measures to reduce the burden of IAs.

## FOOTNOTES

**Author contributions:** Chen JC contributed to the writing - original draft and investigation; Luo C participated in the formal analysis; Luo C and Li Y took part in the methodology; Tan DH contributed to the writing - review & editing and conceptualization.

**Supported by** Guangdong Provincial Medical Science and Technology Research Fund Project, No. A2024525.

**Conflict-of-interest statement:** All the authors report no relevant conflicts of interest for this article.

**PRISMA 2009 Checklist statement:** The authors have read the PRISMA 2009 Checklist, and the manuscript was prepared and revised according to the PRISMA 2009 Checklist.

**Open-Access:** This article is an open-access article that was selected by an in-house editor and fully peer-reviewed by external reviewers. It is distributed in accordance with the Creative Commons Attribution NonCommercial (CC BY-NC 4.0) license, which permits others to distribute, remix, adapt, build upon this work non-commercially, and license their derivative works on different terms, provided the original work is properly cited and the use is non-commercial. See: <https://creativecommons.org/licenses/by-nc/4.0/>

**Country of origin:** China

**ORCID number:** Jun-Chen Chen 0000-0001-9922-1986; Cheng Luo 0000-0002-1762-1159; Yong Li 0000-0002-6640-883X; Dian-Hui Tan 0000-0002-5624-3170.

**S-Editor:** Wang JJ

**L-Editor:** A

**P-Editor:** Cai YX

## REFERENCES

- 1 van Gijn J, Kerr RS, Rinkel GJ. Subarachnoid haemorrhage. *Lancet* 2007; **369**: 306-318 [PMID: 17258671 DOI: 10.1016/S0140-6736(07)60153-6]
- 2 Vlak MH, Algra A, Brandenburg R, Rinkel GJ. Prevalence of unruptured intracranial aneurysms, with emphasis on sex, age, comorbidity, country, and time period: a systematic review and meta-analysis. *Lancet Neurol* 2011; **10**: 626-636 [PMID: 21641282 DOI: 10.1016/S1474-4422(11)70109-0]
- 3 Nieuwkamp DJ, Setz LE, Algra A, Linn FH, de Rooij NK, Rinkel GJ. Changes in case fatality of aneurysmal subarachnoid haemorrhage over time, according to age, sex, and region: a meta-analysis. *Lancet Neurol* 2009; **8**: 635-642 [PMID: 19501022 DOI: 10.1016/S1474-4422(09)70126-7]
- 4 Kleinloog R, de Mul N, Verweij BH, Post JA, Rinkel GJE, Ruigrok YM. Risk Factors for Intracranial Aneurysm Rupture: A Systematic Review. *Neurosurgery* 2018; **82**: 431-440 [PMID: 28498930 DOI: 10.1093/neuros/nyx238]
- 5 Greving JP, Wermer MJ, Brown RD Jr, Morita A, Juvela S, Yonekura M, Ishibashi T, Torner JC, Nakayama T, Rinkel GJ, Algra A. Development of the PHASES score for prediction of risk of rupture of intracranial aneurysms: a pooled analysis of six prospective cohort studies. *Lancet Neurol* 2014; **13**: 59-66 [PMID: 24290159 DOI: 10.1016/S1474-4422(13)70263-1]
- 6 Han P, Jin D, Wei W, Song C, Leng X, Liu L, Yu J, Li X. The prognostic effects of hemodynamic parameters on rupture of intracranial aneurysm: A systematic review and meta-analysis. *Int J Surg* 2021; **86**: 15-23 [PMID: 33444872 DOI: 10.1016/j.ijssu.2020.12.012]
- 7 Shu Z, Chen S, Wang W, Qiu Y, Yu Y, Lyu N, Wang C. Machine Learning Algorithms for Rupture Risk Assessment of Intracranial Aneurysms: A Diagnostic Meta-Analysis. *World Neurosurg* 2022; **165**: e137-e147 [PMID: 35690311 DOI: 10.1016/j.wneu.2022.05.117]
- 8 Guo Y, Guo XM, Zhao K, Yang MF. Aspirin and growth, rupture of unruptured intracranial aneurysms: A systematic review and meta-analysis. *Clin Neurol Neurosurg* 2021; **209**: 106949 [PMID: 34562772 DOI: 10.1016/j.clineuro.2021.106949]
- 9 Bebis G, Levy D, Rockne R, Lima EABDF, Benos PV. Editorial: Advances in Mathematical and Computational Oncology. *Front Physiol* 2022; **13**: 889198 [PMID: 35464082 DOI: 10.3389/fphys.2022.889198]
- 10 Osareh F. Bibliometrics, Citation Analysis and Co-Citation Analysis: A Review of Literature I. *Libri* 1996; **46**: 149-158 [DOI: 10.1515/libr.1996.46.3.149]
- 11 Ellegaard O, Wallin JA. The bibliometric analysis of scholarly production: How great is the impact? *Scientometrics* 2015; **105**: 1809-1831 [PMID: 26594073 DOI: 10.1007/s11192-015-1645-z]
- 12 Chen C. Science Mapping: A Systematic Review of the Literature. *J Data Inf Sci* 2017; **2**: 1-40 [DOI: 10.1515/jdis-2017-0006]
- 13 van Eck NJ, Waltman L. Software survey: VOSviewer, a computer program for bibliometric mapping. *Scientometrics* 2010; **84**: 523-538 [PMID: 20585380 DOI: 10.1007/s11192-009-0146-3]
- 14 Synnæstvedt MB. Enriching knowledge domain visualizations: analysis of a record linkage and information fusion approach to citation data. *AMIA Annu Symp Proc* 2007; **2007**: 711-715 [PMID: 18693929]
- 15 Chen C. Searching for intellectual turning points: progressive knowledge domain visualization. *Proc Natl Acad Sci U S A* 2004; **101** Suppl 1: 5303-5310 [PMID: 14724295 DOI: 10.1073/pnas.0307513100]
- 16 Chen C, Song M. Visualizing a field of research: A methodology of systematic scientometric reviews. *PLoS One* 2019; **14**: e0223994 [PMID: 31671124 DOI: 10.1371/journal.pone.0223994]
- 17 Chen C, Leydesdorff L. Patterns of connections and movements in dual-map overlays: A new method of publication portfolio analysis. *J Asso Inf Sci Tech* 2014; **65**: 334-351 [DOI: 10.1002/asi.22968]
- 18 UCAS Japan Investigators, Morita A, Kirino T, Hashi K, Aoki N, Fukuhara S, Hashimoto N, Nakayama T, Sakai M, Teramoto A, Tominari S, Yoshimoto T. The natural course of unruptured cerebral aneurysms in a Japanese cohort. *N Engl J Med* 2012; **366**: 2474-2482 [PMID: 22444444]

- 22738097 DOI: [10.1056/NEJMoa1113260](https://doi.org/10.1056/NEJMoa1113260)]
- 19 **Chen C.** CiteSpace II: Detecting and visualizing emerging trends and transient patterns in scientific literature. *J Am Soc Inf Sci Tec* 2006; **57**: 359-377 [DOI: [10.1002/asi.20317](https://doi.org/10.1002/asi.20317)]
  - 20 **Thompson BG**, Brown RD Jr, Amin-Hanjani S, Broderick JP, Cockroft KM, Connolly ES Jr, Duckwiler GR, Harris CC, Howard VJ, Johnston SC, Meyers PM, Molyneux A, Ogilvy CS, Ringer AJ, Torner J; American Heart Association Stroke Council, Council on Cardiovascular and Stroke Nursing, and Council on Epidemiology and Prevention; American Heart Association; American Stroke Association. Guidelines for the Management of Patients With Unruptured Intracranial Aneurysms: A Guideline for Healthcare Professionals From the American Heart Association/American Stroke Association. *Stroke* 2015; **46**: 2368-2400 [PMID: [26089327](https://pubmed.ncbi.nlm.nih.gov/26089327/) DOI: [10.1161/STR.0000000000000070](https://doi.org/10.1161/STR.0000000000000070)]
  - 21 **Juvela S**, Porras M, Poussa K. Natural history of unruptured intracranial aneurysms: probability of and risk factors for aneurysm rupture. *J Neurosurg* 2000; **93**: 379-387 [PMID: [10969934](https://pubmed.ncbi.nlm.nih.gov/10969934/) DOI: [10.3171/jns.2000.93.3.0379](https://doi.org/10.3171/jns.2000.93.3.0379)]
  - 22 **Meng H**, Tutino VM, Xiang J, Siddiqui A. High WSS or low WSS? Complex interactions of hemodynamics with intracranial aneurysm initiation, growth, and rupture: toward a unifying hypothesis. *AJNR Am J Neuroradiol* 2014; **35**: 1254-1262 [PMID: [23598838](https://pubmed.ncbi.nlm.nih.gov/23598838/) DOI: [10.3174/ajnr.A3558](https://doi.org/10.3174/ajnr.A3558)]
  - 23 **Connolly ES Jr**, Rabinstein AA, Carhuapoma JR, Derdeyn CP, Dion J, Higashida RT, Hoh BL, Kirkness CJ, Naidech AM, Ogilvy CS, Patel AB, Thompson BG, Vespa P; American Heart Association Stroke Council; Council on Cardiovascular Radiology and Intervention; Council on Cardiovascular Nursing; Council on Cardiovascular Surgery and Anesthesia; Council on Clinical Cardiology. Guidelines for the management of aneurysmal subarachnoid hemorrhage: a guideline for healthcare professionals from the American Heart Association/American Stroke Association. *Stroke* 2012; **43**: 1711-1737 [PMID: [22556195](https://pubmed.ncbi.nlm.nih.gov/22556195/) DOI: [10.1161/STR.0b013e3182587839](https://doi.org/10.1161/STR.0b013e3182587839)]
  - 24 **Etminan N**, Chang HS, Hackenberg K, de Rooij NK, Vergouwen MDI, Rinkel GJE, Algra A. Worldwide Incidence of Aneurysmal Subarachnoid Hemorrhage According to Region, Time Period, Blood Pressure, and Smoking Prevalence in the Population: A Systematic Review and Meta-analysis. *JAMA Neurol* 2019; **76**: 588-597 [PMID: [30659573](https://pubmed.ncbi.nlm.nih.gov/30659573/) DOI: [10.1001/jamaneurol.2019.0006](https://doi.org/10.1001/jamaneurol.2019.0006)]
  - 25 **Juvela S**, Poussa K, Lehto H, Porras M. Natural history of unruptured intracranial aneurysms: a long-term follow-up study. *Stroke* 2013; **44**: 2414-2421 [PMID: [23868274](https://pubmed.ncbi.nlm.nih.gov/23868274/) DOI: [10.1161/STROKEAHA.113.001838](https://doi.org/10.1161/STROKEAHA.113.001838)]
  - 26 **Brinjikji W**, Zhu YQ, Lanzino G, Cloft HJ, Murad MH, Wang Z, Kallmes DF. Risk Factors for Growth of Intracranial Aneurysms: A Systematic Review and Meta-Analysis. *AJNR Am J Neuroradiol* 2016; **37**: 615-620 [PMID: [26611992](https://pubmed.ncbi.nlm.nih.gov/26611992/) DOI: [10.3174/ajnr.A4575](https://doi.org/10.3174/ajnr.A4575)]
  - 27 **Ćmiel-Smorzyk K**, Ładziński P, Kaspera W. Biology, Physics and Genetics of Intracranial Aneurysm Formation: A Review. *J Neurol Surg A Cent Eur Neurosurg* 2022 [PMID: [36482003](https://pubmed.ncbi.nlm.nih.gov/36482003/) DOI: [10.1055/a-1994-8560](https://doi.org/10.1055/a-1994-8560)]
  - 28 **Medetov Y**, Babi A, Makhambetov Y, Menlibayeva K, Bex T, Kaliyev A, Akshulakov S. Risk factors for aneurysm rupture among Kazakhs: findings from a national tertiary. *BMC Neurol* 2022; **22**: 357 [PMID: [36127629](https://pubmed.ncbi.nlm.nih.gov/36127629/) DOI: [10.1186/s12883-022-02892-y](https://doi.org/10.1186/s12883-022-02892-y)]
  - 29 **Darkwah Oppong M**, Pierscianek D, Ahmadipour Y, Dinger TF, Dammann P, Wrede KH, Özkan N, Müller O, Sure U, Jabbarli R. Intraoperative Aneurysm Rupture During Microsurgical Clipping: Risk Re-evaluation in the Post-International Subarachnoid Aneurysm Trial Era. *World Neurosurg* 2018; **119**: e349-e356 [PMID: [30059784](https://pubmed.ncbi.nlm.nih.gov/30059784/) DOI: [10.1016/j.wneu.2018.07.158](https://doi.org/10.1016/j.wneu.2018.07.158)]
  - 30 **Southerland AM**, Green IE, Worrall BB. Cerebral aneurysms and cervical artery dissection: Neurological complications and genetic associations. *Handb Clin Neurol* 2021; **177**: 241-251 [PMID: [33632443](https://pubmed.ncbi.nlm.nih.gov/33632443/) DOI: [10.1016/B978-0-12-819814-8.00033-0](https://doi.org/10.1016/B978-0-12-819814-8.00033-0)]
  - 31 **Giotta Lucifero A**, Baldoncini M, Bruno N, Galzio R, Hernesniemi J, Luzzi S. Shedding the Light on the Natural History of Intracranial Aneurysms: An Updated Overview. *Medicina (Kaunas)* 2021; **57** [PMID: [34440948](https://pubmed.ncbi.nlm.nih.gov/34440948/) DOI: [10.3390/medicina57080742](https://doi.org/10.3390/medicina57080742)]
  - 32 **Perera R**, Isoda H, Ishiguro K, Mizuno T, Takehara Y, Terada M, Tanoi C, Naito T, Sakahara H, Hiramatsu H, Namba H, Izumi T, Wakabayashi T, Kosugi T, Onishi Y, Alley M, Komori Y, Ikeda M, Naganawa S. Assessing the Risk of Intracranial Aneurysm Rupture Using Morphological and Hemodynamic Biomarkers Evaluated from Magnetic Resonance Fluid Dynamics and Computational Fluid Dynamics. *Magn Reson Med Sci* 2020; **19**: 333-344 [PMID: [31956175](https://pubmed.ncbi.nlm.nih.gov/31956175/) DOI: [10.2463/mrms.mp.2019-0107](https://doi.org/10.2463/mrms.mp.2019-0107)]
  - 33 **Tian Z**, Li X, Wang C, Feng X, Sun K, Tu Y, Su H, Yang X, Duan C. Association Between Aneurysmal Hemodynamics and Rupture Risk of Unruptured Intracranial Aneurysms. *Front Neurol* 2022; **13**: 818335 [PMID: [35528737](https://pubmed.ncbi.nlm.nih.gov/35528737/) DOI: [10.3389/fneur.2022.818335](https://doi.org/10.3389/fneur.2022.818335)]
  - 34 **Kataoka H**, Yagi T, Ikeda T, Imai H, Kawamura K, Yoshida K, Nakamura M, Aoki T, Miyamoto S. Hemodynamic and Histopathological Changes in the Early Phase of the Development of an Intracranial Aneurysm. *Neurol Med Chir (Tokyo)* 2020; **60**: 319-328 [PMID: [32536660](https://pubmed.ncbi.nlm.nih.gov/32536660/) DOI: [10.2176/nmc.st.2020-0072](https://doi.org/10.2176/nmc.st.2020-0072)]
  - 35 **Shen Y**, Molenberg R, Bokkers RPH, Wei Y, Uyttenboogaart M, van Dijk JMC. The Role of Hemodynamics through the Circle of Willis in the Development of Intracranial Aneurysm: A Systematic Review of Numerical Models. *J Pers Med* 2022; **12** [PMID: [35743791](https://pubmed.ncbi.nlm.nih.gov/35743791/) DOI: [10.3390/jpm12061008](https://doi.org/10.3390/jpm12061008)]
  - 36 **Adamou A**, Alexandrou M, Roth C, Chatziioannou A, Papanagiotou P. Endovascular Treatment of Intracranial Aneurysms. *Life (Basel)* 2021; **11** [PMID: [33920264](https://pubmed.ncbi.nlm.nih.gov/33920264/) DOI: [10.3390/11e11040335](https://doi.org/10.3390/11e11040335)]
  - 37 **Olthuis SGH**, Pirson FAV, Pinckaers FME, Hinsenveld WH, Nieboer D, Ceulemans A, Knapen RRMM, Robbe MMQ, Berkhemer OA, van Walderveen MAA, Lycklama À Nijeholt GJ, Uyttenboogaart M, Schonewille WJ, van der Sluijs PM, Wolff L, van Voorst H, Postma AA, Roosendaal SD, van der Hoorn A, Emmer BJ, Krietemeijer MGM, van Doormaal PJ, Roozenbeek B, Goldhoorn RB, Staals J, de Ridder IR, van der Leij C, Coutinho JM, van der Worp HB, Lo RTH, Bokkers RPH, van Dijk EI, Boogaarts HD, Wermer MJH, van Es ACGM, van Tuijl JH, Kortman HGJ, Gons RAR, Yo LSF, Vos JA, de Laat KF, van Dijk LC, van den Wijngaard IR, Hofmeijer J, Martens JM, Brouwers PJAM, Bulut T, Remmers MJM, de Jong TEAM, den Hertog HM, van Hasselt BAAM, Rozeman AD, Elgersma OEH, van der Veen B, Sudiono DR, Lingsma HF, Roos YBWEM, Majoie CBLM, van der Lugt A, Dippel DWJ, van Zwam WH, van Oostenbrugge RJ; MR CLEAN-LATE investigators. Endovascular treatment versus no endovascular treatment after 6-24 h in patients with ischaemic stroke and collateral flow on CT angiography (MR CLEAN-LATE) in the Netherlands: a multicentre, open-label, blinded-endpoint, randomised, controlled, phase 3 trial. *Lancet* 2023; **401**: 1371-1380 [PMID: [37003289](https://pubmed.ncbi.nlm.nih.gov/37003289/) DOI: [10.1016/S0140-6736\(23\)00575-5](https://doi.org/10.1016/S0140-6736(23)00575-5)]
  - 38 **Ries T**, Groden C. Endovascular treatment of intracranial aneurysms: long-term stability, risk factors for recurrences, retreatment and follow-up. *Klin Neuroradiol* 2009; **19**: 62-72 [PMID: [19636679](https://pubmed.ncbi.nlm.nih.gov/19636679/) DOI: [10.1007/s00062-009-8032-1](https://doi.org/10.1007/s00062-009-8032-1)]
  - 39 **Miao Y**, Zhang Y, Yin L. Trends in hepatocellular carcinoma research from 2008 to 2017: a bibliometric analysis. *PeerJ* 2018; **6**: e5477 [PMID: [30128213](https://pubmed.ncbi.nlm.nih.gov/30128213/) DOI: [10.7717/peerj.5477](https://doi.org/10.7717/peerj.5477)]
  - 40 **Gao Y**, Shi S, Ma W, Chen J, Cai Y, Ge L, Li L, Wu J, Tian J. Bibliometric analysis of global research on PD-1 and PD-L1 in the field of cancer. *Int Immunopharmacol* 2019; **72**: 374-384 [PMID: [31030093](https://pubmed.ncbi.nlm.nih.gov/31030093/) DOI: [10.1016/j.intimp.2019.03.045](https://doi.org/10.1016/j.intimp.2019.03.045)]
  - 41 **Ke L**, Lu C, Shen R, Lu T, Ma B, Hua Y. Knowledge Mapping of Drug-Induced Liver Injury: A Scientometric Investigation (2010-2019). *Front Pharmacol* 2020; **11**: 842 [PMID: [32581801](https://pubmed.ncbi.nlm.nih.gov/32581801/) DOI: [10.3389/fphar.2020.00842](https://doi.org/10.3389/fphar.2020.00842)]

- 42 **Nugent SM**, Morasco BJ, O'Neil ME, Freeman M, Low A, Kondo K, Elven C, Zakher B, Motu'apuaka M, Paynter R, Kansagara D. The Effects of Cannabis Among Adults With Chronic Pain and an Overview of General Harms: A Systematic Review. *Ann Intern Med* 2017; **167**: 319-331 [PMID: [28806817](#) DOI: [10.7326/M17-0155](#)]
- 43 **Pan B**, Ge L, Xun YQ, Chen YJ, Gao CY, Han X, Zuo LQ, Shan HQ, Yang KH, Ding GW, Tian JH. Exercise training modalities in patients with type 2 diabetes mellitus: a systematic review and network meta-analysis. *Int J Behav Nutr Phys Act* 2018; **15**: 72 [PMID: [30045740](#) DOI: [10.1186/s12966-018-0703-3](#)]
- 44 **Kehl KL**, Elmarakeby H, Nishino M, Van Allen EM, Lepisto EM, Hassett MJ, Johnson BE, Schrag D. Assessment of Deep Natural Language Processing in Ascertaining Oncologic Outcomes From Radiology Reports. *JAMA Oncol* 2019; **5**: 1421-1429 [PMID: [31343664](#) DOI: [10.1001/jamaoncol.2019.1800](#)]



## Necrolytic migratory erythema caused by pancreatic hyperglycemia with emphasis on therapeutic and prognosis: A case report

Shi-Ping Zhan

**Specialty type:** Dermatology

**Provenance and peer review:**

Unsolicited article; Externally peer reviewed.

**Peer-review model:** Single blind

**Peer-review report's classification**

**Scientific Quality:** Grade C

**Novelty:** Grade B

**Creativity or Innovation:** Grade B

**Scientific Significance:** Grade B

**P-Reviewer:** Bosevski M

**Received:** April 8, 2024

**Revised:** May 10, 2024

**Accepted:** June 13, 2024

**Published online:** August 16, 2024

**Processing time:** 87 Days and 20.6 Hours



**Shi-Ping Zhan**, Department of Dermatology, General Hospital of the Yangtze River Shipping, Wuhan Brain Hospital, Wuhan 430000, Hubei Province, China

**Corresponding author:** Shi-Ping Zhan, MMed, Doctor, Department of Dermatology, General Hospital of the Yangtze River Shipping, Wuhan Brain Hospital, No. 5 Huiji Road, Jiang'an District, Wuhan 430000, Hubei Province, China. [15271841071@163.com](mailto:15271841071@163.com)

### Abstract

#### BACKGROUND

With the incidence of pancreatic diseases increasing year by year, pancreatic hyperglycemia, as one of the common complications, is gradually gaining attention for its impact on the skin health of patients.

#### CASE SUMMARY

This was the case of an elderly female with clinical manifestations of necrolytic migratory erythema, "three more and one less," diabetes mellitus, hypertension, anemia, hypoproteinemia, and other syndromes, which had been misdiagnosed as eczema. Abdominal computed tomography showed a pancreatic caudal space-occupying lesion, and the magnetic resonance scanning of the epigastric region with dynamic enhancement and diffusion-weighted imaging suggested a tumor of the pancreatic tail, which was considered to be a neuroendocrine tumor or cystadenoma. The patient was referred to a more equipped hospital for laparoscopic pancreatic tail resection. Post-surgery diagnosis revealed a neuroendocrine tumor in the tail of the pancreas. To date, the patient's general condition is good, and she is still under close follow-up.

#### CONCLUSION

Necrolytic migratory erythema can be induced by endocrine system tumors or endocrine metabolic abnormalities, with complex clinical manifestations, difficult diagnosis, and easy misdiagnosis by dermatologists. The initial treatment principles in dermatology include symptomatic supportive therapy and effective drugs to relieve skin lesions. After clarifying the etiology of glucagonoma, comprehensive treatment in collaboration with endocrinologists, general surgeons, and oncologists can help provide individualized treatment for patients and improve their prognosis.

**Key Words:** Glucagonoma; Necrolytic loosening of wandering erythema; Treatment; Prognosis

**Core Tip:** This report presented a case of necrolytic migratory erythema, a rare skin condition triggered by pancreatic hyperglycemia. Here, we highlighted the diagnostic challenges, therapeutic strategies, and prognostic considerations in the management of this complex disease.

**Citation:** Zhan SP. Necrolytic migratory erythema caused by pancreatic hyperglycemia with emphasis on therapeutic and prognosis: A case report. *World J Clin Cases* 2024; 12(23): 5404-5409

**URL:** <https://www.wjgnet.com/2307-8960/full/v12/i23/5404.htm>

**DOI:** <https://dx.doi.org/10.12998/wjcc.v12.i23.5404>

## INTRODUCTION

The core presentation of necrolytic migratory erythema (NME) is intermittent episodes of erythema, plaques, and papules with hyperpigmentation, most often circumscribed[1]. It can be triggered by various diseases, such as enteropathic acral dermatitis, and skin disorders such as severe drug rash, pancreatic glucagonoma (GCGN), hepatitis B, and cholangiocarcinoma. NME is the first and specific skin lesion manifestation of GCGN (a tumor of pancreatic islet A cells), with an incidence of 68%-90%[2]. Both are known as GCGN syndrome, which is extremely rare clinically, with an incidence of about 1/2000000000 people[3]. Therefore, the pathophysiology of this disease is poorly understood, and misdiagnosis is frequent despite the specific symptoms of NME, perioral inflammation/linguitis, diabetes mellitus, and anemia.

Most patients diagnosed with GCGN having NME have distant metastases and poor prognosis, with a median survival of 3-7 years[4]. Therefore, it is crucial to enhance the clinical understanding of GCGN and NME, to screen and diagnose the disease at an early stage, to accept surgical treatment before distant metastasis, and to improve the prognosis of the patients. This study presents a case of GCGN with NME admitted to the Department of Dermatology of Wuhan Brain Hospital, Yangtze River Shipping General Hospital to elucidate the key points of diagnosis, treatment, and prognosis and to deepen the understanding of this disease.

## CASE PRESENTATION

### Chief complaints

A 77-year-old female was admitted to the Department of Dermatology of our hospital on April 26, 2022 for erythema of the trunk and limbs and dandruff with itching for half a year.

### History of present illness

Six months prior, the patient had migratory erythema with itching without any obvious triggers, which was concentrated in the lower limbs, buttocks, shoulders, back, waist, and abdomen but did not yet involve the face. It was initially characterized by irregular erythema, with some of the erythema bulging around to form a ring or a map and showed dark red pigmentation after scratching, ulceration, scabbing, and healing. She was administered topical medication (*e.g.*, a medication to treat the skin) by local hospitals. She had been treated with topical medication (specific name and dosage unknown) in a local hospital for eczema. The rash was reduced, but the lesions were still recurring after discontinuation of the medication. Thus, she consulted the Department of Dermatology of our hospital.

### History of past illness

The patient's medical history revealed that she had hypertension for > 40 years that was controlled by oral antihypertensive drugs. She was diagnosed with type 2 diabetes mellitus 5 years prior to admission that was controlled by oral metformin, control. The admission diagnosis was eczema, type 2 diabetes, and hypertension grade 3 (very high risk).

### Personal and family history

The patient denied any family history of malignant tumors.

### Physical examination

Vital signs included: Temperature of 36.3 °C; pulse 90 beats/minute; respiration 19/minute; and blood pressure 113/78 mmHg. Physical examination revealed clear, automatic position, neck soft, jugular vein was not furious, the hepatic jugular venous reflux sign was negative, normal respiratory sounds of the lungs, no dry and wet rales, the heart boundary was not big, heart rhythm was neat, and no murmur. The abdomen was soft, the liver and spleen were not palpable under the ribs, there was no percussion pain in either kidney, and there was mildly depressed edema below both knees.

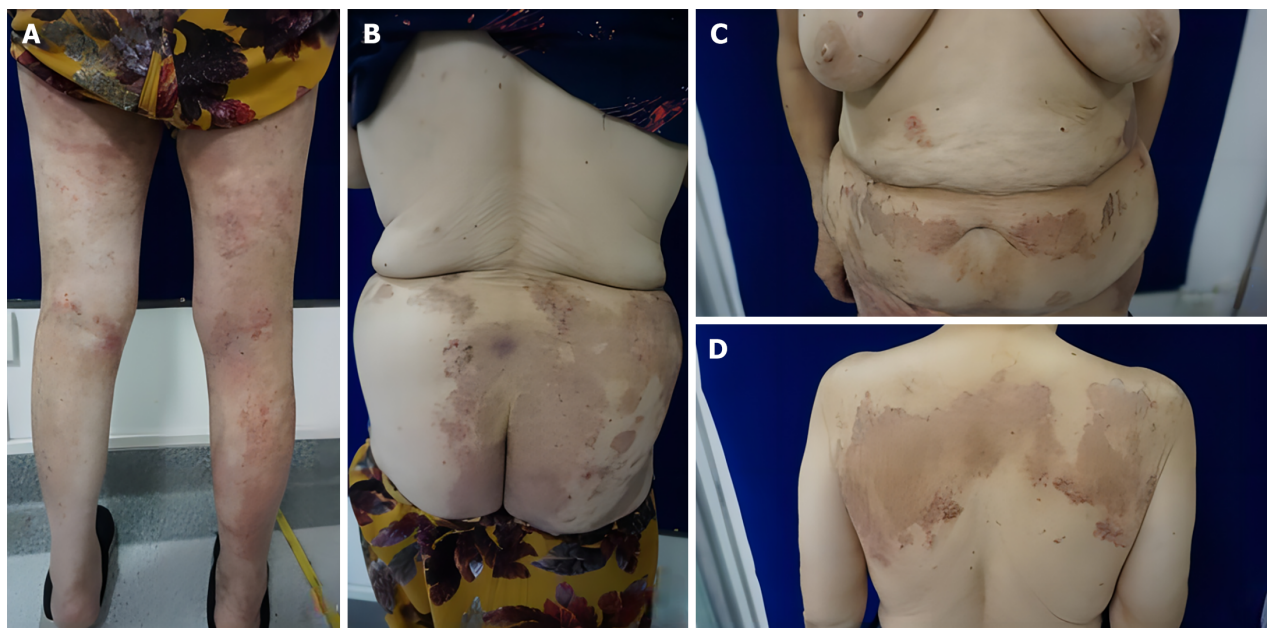


**Figure 1** Clinical manifestations of the skin lesions at different sites. A: Bilateral lower limbs; B: Buttocks; C: Lumbar abdomen; D: Back of the shoulder.

The back of the shoulders, waist and abdomen, buttocks, and limbs had large patches of dark erythema, in the form of rings and maps, raised around the erythema. They had clear boundaries, on which were scattered dander and dark red scabs. The lower limbs had erythema based on dense scratches and scabs, no obvious ulceration or oozing, no blisters, nodules, *etc*, and some of the erythema centers faded, leaving hyperpigmentation (Figure 1).

### Laboratory examinations

Random blood glucose was 9.9 mmol/L, and blood ketones were 0.1 mmol/L. Routine blood examination revealed: Lymphocyte percentage 15.70% (down); lymphocyte count  $0.80 \times 10^9/L$  (down); erythrocytes  $3.17 \times 10^{12}/L$  (down); hemoglobin concentration 95 g/L (down); erythrocyte pressure 30.0% (down); and average hemoglobin concentration 315.00 g/L (down). The fasting blood glucose was 7.27 mmol/L (up). Diabetes test revealed: C-peptide 14.97 ng/mL (up); and serum insulin 108.40  $\mu U/mL$  (up). Electrolytes were: Potassium 3.49 mmol/L (down). Lipid profile results were: Triglycerides 1.72 mmol/L (up); and high-density lipoprotein cholesterol 0.83 mmol/L (down). The renal function profile showed: Uric acid 404  $\mu mol/L$  (up); and glomerular filtration rate 79 mL/min (down). Six liver functions were: Total protein 61.40 g/L (down); albumin 37.80 g/L (down); and aspartate aminotransferase 12.30 U/L (down). Coagulation function, an immunity three, heart attack three, glycated hemoglobin, and calcitonin showed no significant abnormalities. C-reactive protein was 18.4 mg/L (up), D-dimer was 1.53 mg/L (up), and B-type natriuretic peptide was 415.6 pg/mL (up). Blood sedimentation and urinary and fecal routines revealed no significant abnormalities.

### Imaging examinations

Electrocardiogram revealed sinus rhythm and atrial premature beats. Chest computed tomography (CT) scanning revealed thickening of the tail of the pancreatic body and uneven density, leading to the possibility of pancreatic body tail occupancy. Fungal microscopy (buttocks, calves, and back dermatomes) were all negative. Epigastric magnetic resonance imaging (MRI) with dynamic enhancement and diffusion-weighted imaging (DWI) revealed a pancreatic tail mass of low-signal T1WI, low T2WI iso-low mixed signals, of approximately 2.77 cm  $\times$  2.86 cm, having clear borders. The DWI was a high signal, and the apparent diffusion coefficient map was a low signal. Pancreatic tail tumor was visualized (Figure 2; possible neuroendocrine tumor or cystadenoma).

## FINAL DIAGNOSIS

Combined with the patient's medical history, the final diagnosis was NME.

## TREATMENT

Antihistamine, antiallergic, and local physical therapy were administered during hospitalization. When the patient's skin lesions improved significantly, she was discharged from the hospital and transferred to a higher-level hospital. Carbohydrate antigen 125 was 6.2 U/mL (normal value: 0.1-27.0 U/mL), and neuron-specific enolase was 14.63  $\mu g/L$  (normal value:  $< 16.3 \mu g/L$ ). Laparoscopic resection of the pancreatic tail lesion was performed after stabilization of the

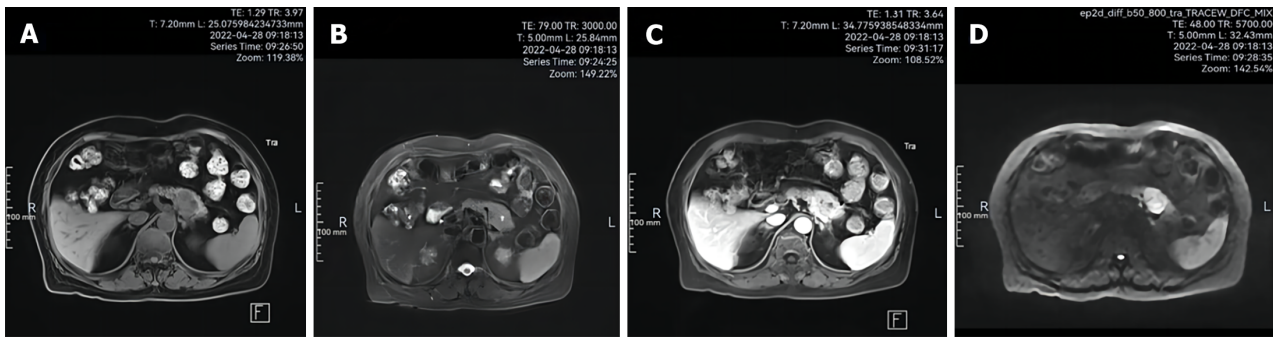


**Figure 2** Magnetic resonance sweep + dynamic enhancement + diffusion-weighted imaging of epigastric pain. A: T1-weighted image; B: T2-weighted image; C: Magnetic resonance enhanced image; D: Diffusion-weighted imaging.

condition, and postoperative pancreatic pathology was performed. The macroscopic view revealed a pancreatic tissue of 10.8 cm × 5.5 cm × 2.7 cm, and there was a 3.5 cm × 3.5 cm × 2.7 cm pancreas 3.3 cm away from the cut edge of the pancreas. There was a 3.5 cm × 3.0 cm × 2.8 cm grayish-white mass in the pancreas, grayish-white on the cut surface, hard, and no lymph nodes were detected in the splenic hilum. Immunohistochemical staining showed tumor cells: PCK (+); CD56 (+); CgA (+); Syn (+); Ki67 (LI: 4%); β-Catenin (plasma +); BCL10 (-); and Chymotrypsin (-). This was consistent with a neuroendocrine tumor in the tail of the pancreatic body (NET, G2). One week postoperatively, the patient's rash had largely subsided, and at 2 wk postoperatively, the patient's glucagon level had decreased.

## OUTCOME AND FOLLOW-UP

At present, the patient's general condition is satisfactory, and she is under regular close follow-up.

## DISCUSSION

NME was officially named by Wilkinson in 1973, initially as a specific skin lesion of GCGN. In 1979, Mallinson referred to GCGN and its associated series of syndromes (including NME, diabetes mellitus, anemia, and perioral inflammation/tongue inflammation) as GCGN syndrome. In this study, we reported a case of an elderly female who initially presented to our dermatology department with NME and was subsequently diagnosed with GCGN with NME.

We searched the relevant literature to summarize the key points of diagnosis, treatment, and prognosis of GCGN with NME as follows. The patient was admitted to the dermatology department of our hospital because of erythema on the trunk and limbs, which was concentrated on the lower limbs, buttocks, back of the shoulders, waist, and abdomen. It was initially characterized by irregular erythema, with the surrounding elevation in the form of a ring or a map, which was scratched, ulcerated, scabbed, and healed to show a dark reddish pigmentation. She also presented with typical diabetic manifestations such as dry mouth, polydipsia, polyuria, and weight loss.

Her medical history revealed type 2 diabetes mellitus for 5 years and hypertension for more than 40 years (grade 3, very high risk). According to the laboratory results, the erythrocyte pressure volume and erythrocytes were reduced, suggesting anemia. A hemoglobin concentration of 95 g/L suggests a mild degree of anemia, while an average hemoglobin concentration of < 320 g/L suggests small-cell hypopigmented anemia. The average hemoglobin concentration was < 320 g/L, suggesting microcytic hypopigmented anemia. This type of anemia has many causes, including cancer, iron deficiency, abnormal iron metabolism, chronic bleeding, and hemorrhoids. The appearance of skin lesions after anemia is clinically common.

A potassium level of 3.49 mmol/L suggests that the body is mildly hypokalemic, which is mainly related to decreased oral intake, increased release of total immunoreactive insulin, loss of potassium in the digestive tract, frequent vomiting and diarrhea, and loss of potassium in the urine. These reasons typically do not cause skin lesions. However, diabetes and diarrhea are secondary symptoms of GCGN, which cannot be excluded as a result of diabetes or diarrhea induced by GCGN.

Liver function, total protein, albumin, and aspartate aminotransferase decreased, suggesting hepatocellular damage or malnutrition. Common causes include malignant tumors, liver disease, renal disease, nutrition, and absorption disorders. Among them, albumin, as the main carrier of electrolytes and essential amino acids, will reduce the level of fatty acids, electrolytes, and other nutrient transfer, which will lead to the depletion of epidermal proteins and necrosis and then NME.

In addition, it was also found that the patient had reduced renal function and inflammation, which may have led to the accumulation of waste, which can stimulate the skin to induce itchiness. The formation of NME and inflammation can lead to dysregulation of the immune system.

Moreover, the insulin and C-peptide release test suggested that the patient was in an early stage of type 2 diabetes mellitus, which was a non-insulin-dependent type. Her blood glucose could be effectively controlled by dietary interventions and the oral administration of metformin glucose-lowering drugs. However, because GCGN tumor cells independently secrete more glucagon to raise blood glucose, it further stimulated B cells to release insulin. Due to the antagonistic effect, the body's blood glucose rise was not obvious, and it could have also manifested as early diabetes mellitus. Therefore, clinicians often misdiagnose GCGN as type 2 diabetes mellitus. According to the diagnostic criteria of GCGN agreed upon by several scholars in the past, we must focus on monitoring the glucagon level and consider the possibility of GCGN if it is  $> 1000$  ng/L.

Further, imaging examinations are necessary to find the thickening and uneven density of the tail of the pancreatic body. In this case, further imaging examination was applied, and the thickening and uneven density of the tail of the pancreatic body was found in the chest CT scan. The possibility of pancreatic tail occupation was considered. Further improvement of the upper abdomen MRI with dynamic enhancement and DWI showed that the tail of the pancreatic body was a mass of T1WI low-signal and T2WI iso-low mixed signals. The size of the mass was about  $2.77\text{ cm} \times 2.86\text{ cm}$ , with poorly defined borders, and inhomogeneous enhancement, suggesting that it was a tumor of the tail of the pancreatic body, and a neuroendocrine tumor or cystadenoma should be considered.

Based on the clinical symptoms and medical history, physical and dermatological examinations, and laboratory and imaging evidence, a preliminary diagnosis of GCGN with NME was made at our hospital. Due to the limitations of the hospital, the patient was referred to a higher-level hospital to improve the examination after the symptomatic treatment of itching and rash symptoms was relieved to enable the patient to receive timely treatment.

The additional tumor marker test and positron emission tomography/MRI of growth inhibitory receptors were considered to be positive lesions of growth inhibitory receptors, and neuroendocrine neoplasia was considered to be a positive lesion of the neuroendocrine receptor. Receptor-positive lesions, the possibility of neuroendocrine tumors, and laparoscopic pancreatic tail lesion resection, according to the postoperative pancreatic histopathology confirmed the presence of a pancreatic mass. PCK (+), CD56 (+), CgA (+), and Syn (+) were used for immunohistochemistry. They are commonly used as markers for neuroendocrine tumors, of which CgA has the strongest specificity, and CD56 is the most sensitive but lacks specificity. The results confirmed a neuroendocrine tumor of the tail of the pancreatic body. This supports the accuracy of our initial diagnosis, combined with previous evidence in the literature[5-8].

In this article, there was a lack of dermatopathologic and glucagon test data. The diagnostic basis was slightly insufficient, and the diagnostic points of GCGN with NME were briefly described: (1) Clinical symptoms of GCGN with NME were relatively typical, including NME, diabetes mellitus, "three more and one less," diarrhea, and perioral inflammation/tongue inflammation; (2) Medical history was accompanied by diabetes; (3) Routine blood tests, liver function, renal function, blood lipids, electrolytes, blood glucose and C-peptide release test, fasting glucagon and serum tumor markers were improved, and particular attention was paid to monitoring fasting glucagon levels; (4) Imaging examination was the primary method of preoperative diagnosis, using abdominal CT and MRI to show pancreatic mass as a reliable diagnostic basis, and growth inhibitor receptor positron emission tomography/MRI imaging were used under the condition. This provided information on the expression of growth inhibitor receptors and glucose transporter protein receptors in the primary and metastatic foci of neuroendocrine tumors, which can significantly improve the detection rate and accuracy of neuroendocrine tumors; and (5) The gold standards for the diagnosis of GCGN in NME are postoperative pancreatic histopathology and immunohistochemistry.

In this case, serum tumor markers were normal, and Ki67 (LI: 4%) was  $< 5\%$ , which was of low grade. Combined with the characteristics of tumor cell heterogeneity and structure, the patient was diagnosed as having a neuroendocrine tumor of the pancreatic tail (NET, G2) according to the 2010 World Health Organization Neuroendocrine Tumor Grade Criteria. Currently, the patient has not yet developed distant metastases, and surgery was the first option to improve the prognosis. Our hospital did not have surgical conditions, so only symptomatic treatment was performed, including antihistamine, anti-allergy, and local physical therapy for the skin lesions and itching on the trunk and limbs.

The patient was transferred to a higher-level hospital when the skin lesions improved significantly because the lesion involved the spleen. Laparoscopic pancreatic tail resection and laparoscopic splenectomy were performed. Postoperatively, the patient developed a pancreatic fistula that was adequately drained, and no obvious peritoneal fluid was observed on repeat CT. Postoperatively, the patient's blood potassium level was low; oral and intravenous potassium supplementation was provided. Albumin level improved, and enteral and parenteral nutritional support was provided.

Combined with previous evidence in the literature[9-12], the treatment and prognostic points of GCGN with NME were briefly summarized: (1) Preoperative application of growth inhibitory analogs such as octreotide helped to reduce patients' glucagon levels and ameliorated skin lesion symptoms; (2) If erythema and rash were present on the abdomen that interfere with the surgical incision, an intravenous infusion of amino acids or oral zinc preparations were feasible to relieve the rash; (3) Postoperative hypoglycemic drugs were generally not required and should be administered in strict compliance with medical advice; (4) Molecularly targeted drugs have brought new hope for the treatment of metastatic GCGN. Sunitinib and everolimus have been certified by the United States Food and Drug Administration for use in the treatment of low and intermediate-grade metastatic GCGN but have not yet been introduced in China. Their exact efficacy has yet to be confirmed by more evidence-based research trials; and (5) Because this patient did not have distant metastasis, no postoperative chemotherapy was needed, but most patients have distant metastasis at the time of definitive diagnosis and need to be supplemented with necessary postoperative chemotherapy.

The main chemotherapeutic drugs are adriamycin, 5-fluorouracil, and azelnimidamide. Domestic experts generally believe that azemetidine is the most effective, with a recommended dose of  $400\text{ mg/day}$ , a 5-d course of treatment once a month for a total of 3-10 courses of treatment. After discharge from the hospital, patients should improve their nutrition, pay attention to rest, and follow up regularly. Early diagnosis and surgery before the occurrence of distant metastases are essential to improve patient prognosis. Even if distant metastases are present preoperatively, aggressive surgery and

comprehensive treatment are expected to achieve high long-term survival rates.

## CONCLUSION

NME can be induced by endocrine tumors or endocrine metabolic abnormalities, and dermatologists are prone to misdiagnosis. The initial treatment principles in dermatology include symptomatic supportive therapy and effective drugs to relieve skin lesions. After clarifying the etiology of GCGN, comprehensive treatment in collaboration with endocrinologists, general surgeons, and oncologists can help provide individualized treatment and improve patient prognosis.

## FOOTNOTES

**Author contributions:** Zhan SP designed the research study; Zhan SP performed the research; Zhan SP contributed new reagents and analytical tools; Zhan SP analyzed the data, wrote the manuscript, and read and approved the final manuscript.

**Informed consent statement:** Informed written consent was obtained from the patient for publication of this report and any accompanying images.

**Conflict-of-interest statement:** Dr. Zhan has nothing to disclose.

**CARE Checklist (2016) statement:** The authors have read the CARE Checklist (2016), and the manuscript was prepared and revised according to the CARE Checklist (2016).

**Open-Access:** This article is an open-access article that was selected by an in-house editor and fully peer-reviewed by external reviewers. It is distributed in accordance with the Creative Commons Attribution NonCommercial (CC BY-NC 4.0) license, which permits others to distribute, remix, adapt, build upon this work non-commercially, and license their derivative works on different terms, provided the original work is properly cited and the use is non-commercial. See: <https://creativecommons.org/licenses/by-nc/4.0/>

**Country of origin:** China

**ORCID number:** Shi-Ping Zhan 0009-0006-5893-8853.

**S-Editor:** Lin C

**L-Editor:** Filipodia

**P-Editor:** Chen YX

## REFERENCES

- 1 **Bosch-Amate X**, Riera-Monroig J, Iranzo Fernández P. Glucagonoma-related necrolytic migratory erythema. *Med Clin (Barc)* 2020; **155**: 418-419 [PMID: 31515063 DOI: 10.1016/j.medcli.2019.06.027]
- 2 **Cui M**, Wang R, Liao Q. Necrolytic migratory erythema: an important sign of glucagonoma. *Postgrad Med J* 2021; **97**: 199 [PMID: 32527759 DOI: 10.1136/postgradmedj-2020-137587]
- 3 **Dulcich G**, Mestas Nuñez MA, Gentile EMJ. [Migratory necrolytic erythema as a manifestation of pancreatic neuroendocrine tumor. Clinical-radiological evaluation]. *Rev Fac Cien Med Univ Nac Cordoba* 2022; **79**: 188-192 [PMID: 35700469 DOI: 10.31053/1853.0605.v79.n2.32543]
- 4 **Yacine O**, Ksontini FL, Ben Mahmoud A, Magherbi H, Fterich SF, Kacem M. Case report of a recurrent resected glucagonoma. *Ann Med Surg (Lond)* 2022; **77**: 103604 [PMID: 35638031 DOI: 10.1016/j.amsu.2022.103604]
- 5 **Aragón-Miguel R**, Prieto-Barrios M, Calleja-Algarra A, Pinilla-Martin B, Rodríguez-Peralto J, Ortiz-Romero P, Rivera-Díaz R. Image Gallery: Necrolytic migratory erythema associated with glucagonoma. *Br J Dermatol* 2019; **180**: e1 [PMID: 30604550 DOI: 10.1111/bjd.17156]
- 6 **Zhu WF**, Zheng SS. Glucagonoma syndrome with necrolytic migratory erythema as initial manifestation. *Hepatobiliary Pancreat Dis Int* 2021; **20**: 598-600 [PMID: 34544669 DOI: 10.1016/j.hbpd.2021.09.005]
- 7 **Tolliver S**, Graham J, Kaffenberger BH. A review of cutaneous manifestations within glucagonoma syndrome: necrolytic migratory erythema. *Int J Dermatol* 2018; **57**: 642-645 [PMID: 29450880 DOI: 10.1111/ijd.13947]
- 8 **Wang ZX**, Wang F, Zhao JG. Glucagonoma syndrome with severe erythematous rash: A rare case report. *Medicine (Baltimore)* 2019; **98**: e17158 [PMID: 31517863 DOI: 10.1097/MD.00000000000017158]
- 9 **Wu SL**, Bai JG, Xu J, Ma QY, Wu Z. Necrolytic migratory erythema as the first manifestation of pancreatic neuroendocrine tumor. *World J Surg Oncol* 2014; **12**: 220 [PMID: 25029913 DOI: 10.1186/1477-7819-12-220]
- 10 **Rodríguez G**, Vargas E, Abaúnza C, Cáceres S. Necrolytic migratory erythema and pancreatic glucagonoma. *Biomedica* 2016; **36**: 176-181 [PMID: 27622478 DOI: 10.7705/biomedica.v36i3.2723]
- 11 **Tseng HC**, Liu CT, Ho JC, Lin SH. Necrolytic migratory erythema and glucagonoma rising from pancreatic head. *Pancreatol* 2013; **13**: 455-457 [PMID: 23890147 DOI: 10.1016/j.pan.2013.03.011]
- 12 **Adam DN**, Cohen PD, Ghazarian D. Necrolytic migratory erythema: case report and clinical review. *J Cutan Med Surg* 2003; **7**: 333-338 [PMID: 14738101 DOI: 10.1007/s10227-002-0127-0]



## Small cell lung carcinoma with *KIF5B-RET* fusion partially responded to the 4<sup>th</sup>-line therapy with anlotinib: A case report

Rui Zhang, Yu-Ting He, Yi-Sha Liu, Hang Li, Feng Zhao

**Specialty type:** Medicine, research and experimental

**Provenance and peer review:** Unsolicited article; Externally peer reviewed.

**Peer-review model:** Single blind

**Peer-review report's classification**

**Scientific Quality:** Grade C

**Novelty:** Grade B

**Creativity or Innovation:** Grade B

**Scientific Significance:** Grade B

**P-Reviewer:** Dabla PK

**Received:** March 31, 2024

**Revised:** June 12, 2024

**Accepted:** June 25, 2024

**Published online:** August 16, 2024

**Processing time:** 96 Days and 3.3 Hours



**Rui Zhang**, Meat Processing Key Laboratory of Sichuan Province, College of Food and Biological Engineering, Chengdu University, Chengdu 610106, Sichuan Province, China

**Yu-Ting He**, School of Medicine, University of Electronic Science and Technology of China, Chengdu 610072, Sichuan Province, China

**Yi-Sha Liu**, Department of Pathology, Sichuan Provincial People's Hospital, School of Medicine, University of Electronic Science and Technology of China, Chengdu 610072, Sichuan Province, China

**Hang Li**, Department of Radiology, Sichuan Provincial People's Hospital, School of Medicine, University of Electronic Science and Technology of China, Chengdu 610072, Sichuan Province, China

**Feng Zhao**, Department of Oncology, Sichuan Provincial People's Hospital, School of Medicine, University of Electronic Science and Technology of China, Chengdu 610072, Sichuan Province, China

**Corresponding author:** Feng Zhao, MBBS, Doctor, Department of Oncology, Sichuan Provincial People's Hospital, School of Medicine, University of Electronic Science and Technology of China, No. 32 W. 1<sup>st</sup> Ring Road, Qingyang District, Chengdu 610072, Sichuan Province, China. [zhaofengzl@med.uestc.edu.cn](mailto:zhaofengzl@med.uestc.edu.cn)

### Abstract

#### BACKGROUND

Small cell lung cancer (SCLC) exhibits a pronounced tendency for metastasis and relapse, and the acquisition of resistance to chemotherapy and radiotherapy, leading to complexity in treatment outcomes. It is crucial to tackle these challenges by advancing targeted therapeutic approaches in ongoing research endeavors. Variant RET fusions have been reported in several solid tumors, but are rarely reported in SCLC.

#### CASE SUMMARY

We present the first case of a *KIF5B-RET* fusion in a 65-year-old male patient with SCLC. To date, the patient has received the 4<sup>th</sup> line chemotherapy with anlotinib for one year and has shown a sustained favorable partial response. According to the results of next generation sequencing, this SCLC patient harbors the *KIF5B-RET* fusion, suggesting that RET fusion could serve as a promising molecular target for SCLC treatment. Next-generation sequencing (NGS) plays a critical role

in comprehensively assessing the genotype and phenotype of cancer.

## CONCLUSION

NGS can provide SCLC patients with personalized and targeted therapy options, thereby improving their likelihood of survival.

**Key Words:** *KIF5B-RET* fusion; Small cell lung cancer; Anlotinib; Partial response; Next-generation sequencing; Case report

©The Author(s) 2024. Published by Baishideng Publishing Group Inc. All rights reserved.

**Core Tip:** This work describes a rare case of a *KIF5B-RET* fusion in small cell lung cancer (SCLC) and the patient's sustained partial response to the 4th line therapy with anlotinib. The study highlights the potential of RET fusions as a promising molecular target in SCLC treatment and emphasizes the importance of next-generation sequencing for personalized therapy options. The innovative arguments include the identification of a novel fusion in SCLC and the potential for targeted therapy to enhance the survival rates of SCLC patients.

**Citation:** Zhang R, He YT, Liu YS, Li H, Zhao F. Small cell lung carcinoma with *KIF5B-RET* fusion partially responded to the 4<sup>th</sup>-line therapy with anlotinib: A case report. *World J Clin Cases* 2024; 12(23): 5410-5415

**URL:** <https://www.wjgnet.com/2307-8960/full/v12/i23/5410.htm>

**DOI:** <https://dx.doi.org/10.12998/wjcc.v12.i23.5410>

## INTRODUCTION

Small cell lung cancer (SCLC) is a highly aggressive malignancy often diagnosed with metastases at the time of detection. Approximately 15% of lung cancer cases are classified as SCLC, with a 5-year survival rate less than 7%[1]. SCLC is categorized into limited-stage disease (LS-SCLC) and extensive-stage disease (ES-SCLC). ES-SCLC accounts for around 70% of SCLC patients and carries a poorer prognosis compared to LS-SCLC. Standard therapy comprising cisplatin and etoposide for ES-SCLC has endured as the 1<sup>st</sup> line chemotherapy for over 30 years. Despite the favorable initial response rates to the 1<sup>st</sup> line chemotherapy, ES-SCLC patients experience increased relapse rates, leading to an unfavorable overall prognosis primarily attributed to the rapid development of drug resistance. The integration of cancer immunotherapy and gene profiling technology has started to revolutionize the standard treatment of SCLC. The IMpower133 phase III randomized trial assessed the efficacy of atezolizumab in conjunction with carboplatin and etoposide in 403 ES-SCLC patients[2]. The data indicated a noteworthy improvement in median overall survival to 12.3 months when atezolizumab was added, compared to 10.3 months with chemotherapy alone. The Food and Drug Administration (FDA), the European Medicines Agency, and National Medical Products Administration have approved both atezolizumab and durvalumab combined with carboplatin or platinum and etoposide as standards for ES-SCLC 1<sup>st</sup> line systemic therapy[3]. Furthermore, advancements in gene profiling technologies such as next-generation sequencing (NGS) have significantly accelerated our understanding of SCLC biology. Genomic losses or dysfunctions in retinoblastoma 1 (RB1) and tumor protein P53 (TP53) are prevalent in SCLC. The discovery of RET fusions in 1%-3% of non-SCLCs (NSCLC) presents a promising therapeutic target for oncologic intervention. Despite recent therapeutic advancements, ES-SCLC remains an exceptionally aggressive and challenging disease. RET fusions result from genomic loci rearrangements involving chromosomal inversion or translocation. The most prevalent RET fusion variant in lung cancer is the *KIF5B-RET* fusion. Previously reported *KIF5B-RET* fusions in lung cancer have all been associated with NSCLC. An exceptional case reported in 2023, was a 57-year-old female patient with combined SCLC who was found to harbor a *KIF5B-RET* fusion[4]. Notably, this patient demonstrated a sustained clinical response to the 4th line therapy with selpercatinib, a tyrosine kinase inhibitor. In the present study, we report the case of a patient with ES-SCLC harboring a *KIF5B-RET* fusion. To the best of our knowledge, this represents the first case of a *KIF5B-RET* fusion in ES-SCLC. Several RET-specific inhibitors are currently applied in clinical therapy, and have shown promising outcomes in terms of prognosis[5,6]. Thus, RET fusions may serve as promising molecular targets for SCLC therapies, broadening treatment options and improving survival rates. This finding also suggests the potential necessity for RET fusion testing in patients with SCLC.

## CASE PRESENTATION

### Chief complaints

A 65-year-old male patient was diagnosed with a left lung mass present for over one month and SCLC in the left lung was confirmed more than ten days ago.

### History of present illness

The patient fell and subsequently presented to a local hospital seeking medical evaluation. Chest computed tomography (CT) revealed a mass in the upper lobe of the left lung. To pursue a comprehensive diagnosis and treatment plan, the patient sought care at our hospital.

### History of past illness

The patient was diagnosed with type 2 diabetes three years previously, with a serum glucose level of 22 mmol/L, and had not received any treatment.

### Personal and family history

The patient has smoked and consumed alcohol for 45 years. Furthermore, his mother died at the age of 85 years due to cervical carcinoma.

### Physical examination

A routine physical examination did not reveal any abnormalities.

### Laboratory examinations

Laboratory examinations indicated elevated levels of keratin 19 (2.94 ng/mL), carbohydrate antigen 125 (CA125) (37.00 U/mL), and blood glucose (10.22 mmol/L). In addition, the patient's serum levels of squamous epithelial cell carcinoma antigen, neuron-specific enolase (NSE), carcinoembryonic antigen, and carbohydrate antigen 15-3 were within normal limits. Remarkably, a NGS analysis of the primary lung biopsy specimen revealed a *KIF5B-RET* fusion, along with mutations in TP53 and RB1.

### Imaging examinations

A chest CT scan revealed a lobulated soft tissue mass shadow in the apical posterior segment of the upper lobe of the left lung, measuring approximately 55 mm × 42 mm. The mass invaded the left superior pulmonary artery and the right pleura, and displayed enlargement of mediastinal and hilar lymph nodes (Figure 1A-C), indicating metastasis within the lung and lymph nodes. Histological examination of the primary mass using hematoxylin and eosin staining revealed typical SCLC features with small cell nests (Figure 1D-F). This was further confirmed by immunohistochemistry, which showed positive results for cytokeratin CAM5.2 (Figure 1G) and CD56 (Figure 1H), a Ki67 index of approximately 80% (Figure 1I), focal positivity for synaptophysin (Figure 1J), and negativity for chromogranin A (Figure 1K), and thyroid transcription factor-1 (Figure 1L).

---

## FINAL DIAGNOSIS

ES-SCLC was diagnosed based on the patient's medical history, and laboratory and imaging examinations.

---

## TREATMENT

Despite being unable to undergo the preferred regimen of chemotherapy combined with immunotherapy (atezolizumab) due to personal reasons, the patient received six cycles of etoposide/cisplatin as the 1<sup>st</sup> line chemotherapy until October 2021 (Figure 2A). The patient experienced minimal side effects, primarily slight nausea and poor appetite. Following a partial response (PR) to chemotherapy, the patient underwent thoracic intensity-modulated radiotherapy starting on November 2021, due to residual thoracic lesions. Subsequent evaluation by chest CT scanning showed further reductions in the lung lesions and confirmed a PR. In April 2022, splenic metastatic nodules were confirmed by CT scans (Figure 2B), and the patient received 2<sup>nd</sup> line chemotherapy with docetaxel, with a PR observed (Figure 2C). However, further treatment was not pursued due to grade IV bone marrow suppression.

In August 2022, recurrence was observed with a size increment in splenic metastatic nodules and newly detected hepatic metastatic nodules (Figure 2D). The patient was treated with albumin-bound paclitaxel as 3<sup>rd</sup> line chemotherapy, resulting in a PR observed on CT scans (Figure 2E). Subsequent follow-up in February 2023 showed progression of lung, splenic, and hepatic nodules (Figure 2F), leading to the initiation of targeted therapy with anlotinib as the 4<sup>th</sup> line chemotherapy up to the present, resulting in a sustained PR (Figure 2G). The levels of serum biomarkers, such as progastrin-releasing peptide, NSE and CA125, were measured to monitor the clinical response to chemotherapy and tumor progression (Figure 2H).

---

## OUTCOME AND FOLLOW-UP

Currently, the patient is still alive, taking anlotinib, and undergoing CT scanning every two months.

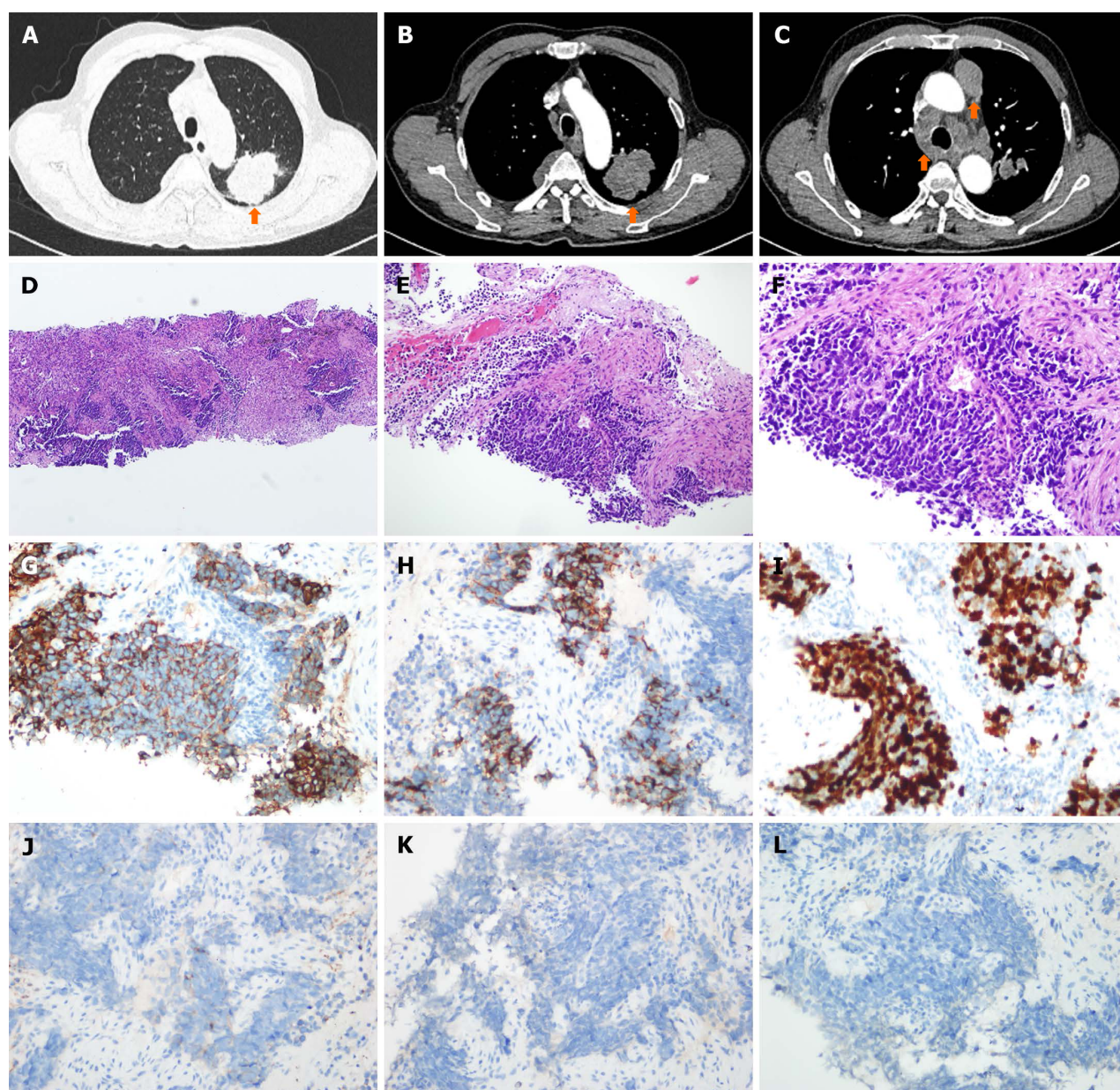


**Figure 1 Chest computed tomography and histological evaluation.** A-C: The baseline chest computed tomography assessment in May 2021 included evaluation of lung lesions, lymph node lesions, and pleural lesions; D-F: Hematoxylin and eosin staining with magnifications of 100 x, 200 x, and 400 x revealed extensive-stage disease small cell lung cancer (SCLC) classification; G-L: Immunohistochemical staining displayed cytokeratin CAM5.2, CD56, Ki67, synaptophysin, chromogranin A, and thyroid transcription factor-1 in the SCLC tumor biopsy.

## DISCUSSION

SCLC accounts for around 15% of all lung cancers and is known for its rapid tumor growth and early spread to multiple organs. Despite progress in cancer treatment, the therapeutic strategy for SCLC has stagnated, with cisplatin and etoposide being the established chemotherapy regimen for several decades. While most patients exhibit a favorable response to initial chemotherapy, recurrent disease is common, leading to a poor prognosis[7]. Current 1<sup>st</sup> line treatment continues to rely on chemotherapy, yet options remain limited for those with disease progression post-initial therapy[8]. More recent research efforts have concentrated on deciphering the molecular attributes of SCLC to tailor precise treatment approaches aimed at enhancing patient prognoses. Our patient exhibited a genomic loss of both TP53 and RB1 function, a characteristic molecular feature of SCLC. SCLC is known to be highly aggressive, attributed to genomic instability, near-universal inactivation of TP53 and RB1, rapid tumor growth, enhanced vascularity, and pronounced metastatic potential[9,10]. Notably, SCLC patients with RB1 inactivating variants demonstrate sensitivity to platinum-based chemotherapy[11]. RB1 and TP53 inactivating variants often co-occur in SCLC, with combined inactivation of these genes in murine models capable of inducing SCLC formation[12]. RET fusions, a rare oncogene in lung cancer, are detected in 1%-2% of all lung cancers and in approximately 1.6% of Chinese NSCLC cases. The predominant partners involved in RET fusions are KIF5B and CCDC6, contributing to approximately 70%-90% and 10%-25% of cases, respectively[13]. The *KIF5B-RET* fusion occurs in 1%-2% of lung adenocarcinoma cases, leading to sustained RET

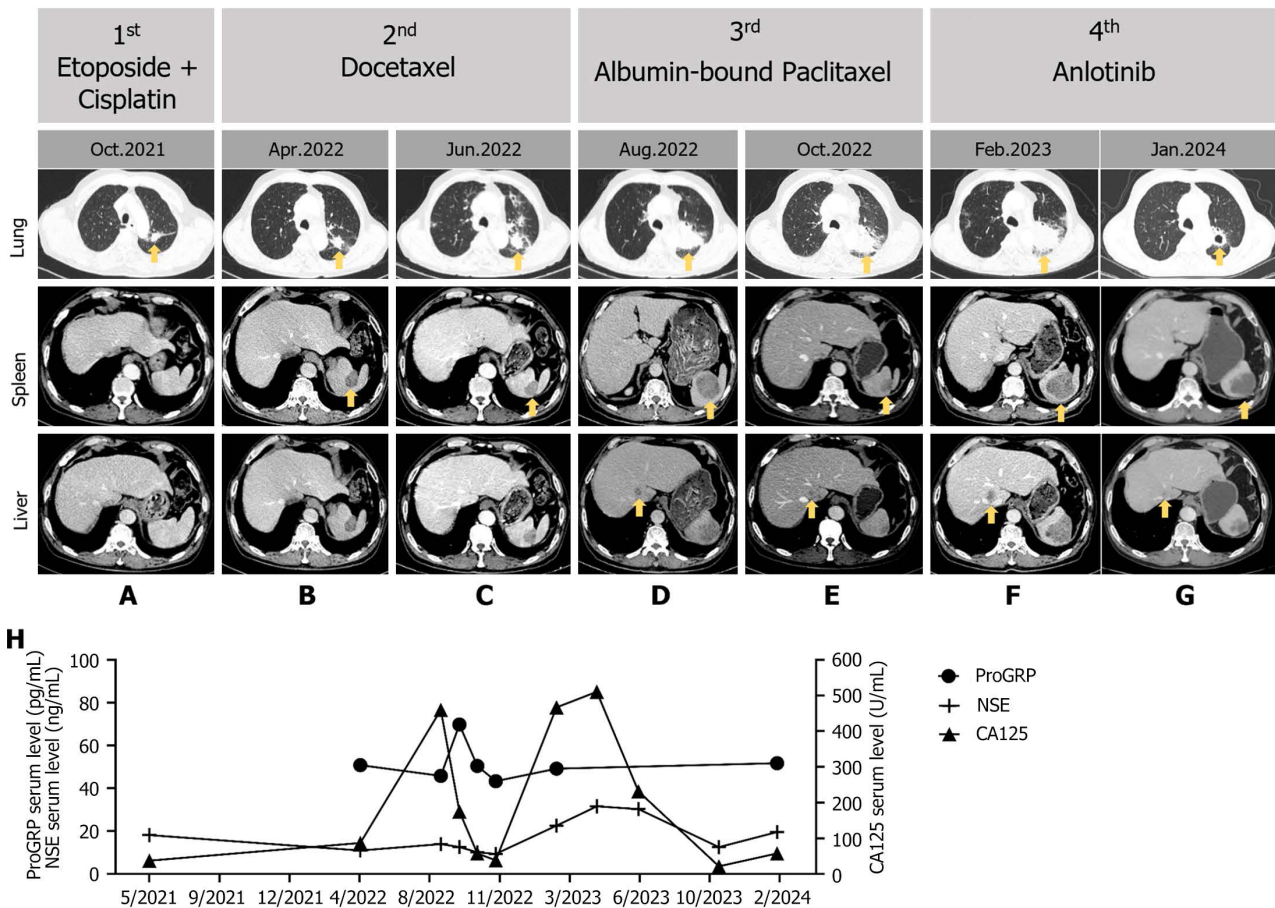


**Figure 2** Imaging evaluations and serum tumor biomarker testing during treatment. A-G: Imaging assessments of the tumor were conducted during the 1st to 4<sup>th</sup> line chemotherapy, yellow arrows were used to indicate primary tumors and metastatic lesions; H: Serum levels of progastrin-releasing peptide, neuron-specific enolase, and carbohydrate antigen 125 were measured to monitor clinical responses. NSE: Neuron-specific enolase; CA125: Carbohydrate antigen 125; ProGRP: Progastrin-releasing peptide.

activation, a key driver gene in lung adenocarcinoma. RET expression is notably elevated, being 2 to 30 times higher in *KIF5B-RET* fusion lung adenocarcinoma compared to normal lung tissue[14]. Moreover, RET expression is notably elevated in SCLC compared to lung adenocarcinoma. A subgroup of SCLC patients could potentially derive benefits from tyrosine kinase inhibitors that target RET[15]. Various multikinase inhibitors targeting RET activity, including cabozantinib and vandetanib, have also received FDA approval. Current clinical guidelines suggest selipercatinib and pralsetinib as the preferred treatment for RET-rearranged NSCLC, with cabozantinib as a recommended option. This report marks the first identification of *KIF5B-RET* fusion (*KIF5B* exon15-*RET* exon12) in a patient with ES-SCLC, showcasing the significance of fusion genes in lung cancer pathogenesis and the breakthrough potential of *KIF5B-RET* fusion discovery for targeted SCLC treatment.

## CONCLUSION

In summary, this report describes a SCLC case featuring a *KIF5B-RET* fusion. To date, the patient has received the 4<sup>th</sup> line chemotherapy with anlotinib and shown a favorable sustained PR. Given the rarity of this *KIF5B-RET* fusion in SCLC, the importance of RET fusion in SCLC patients remains unclear, underscoring the need for additional investigation. Furthermore, RET fusion represents a promising molecular target for SCLC therapies, deserving consideration in future treatment strategies.

## FOOTNOTES

**Author contributions:** Zhang R conducted the data analysis, drafted the manuscript, and made contributions to funding acquisition and software application; He YT conducted the investigation and validated the work; Liu YS conducted research and handled data visualization; Li H was responsible for data curation and visualization; Zhao F played a key role in conceptualizing the research, acquiring funding, supervising the project, and reviewing and editing the manuscript. All authors have reviewed and approved the final manuscript.

**Supported by** Meat Processing Key Laboratory of Sichuan Province, No. 22-R-16.

**Informed consent statement:** Informed written consent was obtained from the patient for publication of this report and any accompanying images.

**Conflict-of-interest statement:** The authors declare that they have no conflict of interest.

**CARE Checklist (2016) statement:** The authors have read the CARE Checklist (2016), and the manuscript was prepared and revised according to the CARE Checklist (2016).

**Open-Access:** This article is an open-access article that was selected by an in-house editor and fully peer-reviewed by external reviewers. It is distributed in accordance with the Creative Commons Attribution NonCommercial (CC BY-NC 4.0) license, which permits others to distribute, remix, adapt, build upon this work non-commercially, and license their derivative works on different terms, provided the original work is properly cited and the use is non-commercial. See: <https://creativecommons.org/licenses/by-nc/4.0/>

**Country of origin:** China

**ORCID number:** Feng Zhao 0009-0002-3741-9617.

**S-Editor:** Qu XL

**L-Editor:** A

**P-Editor:** Chen YX

## REFERENCES

- 1 **DiBonaventura MD**, Shah-Manek B, Higginbottom K, Penrod JR, Yuan Y. Adherence to recommended clinical guidelines in extensive disease small-cell lung cancer across the US, Europe, and Japan. *Ther Clin Risk Manag* 2019; **15**: 355-366 [PMID: 30881001 DOI: 10.2147/TCRM.S183216]
- 2 **Horn L**, Mansfield AS, Szczesna A, Havel L, Krzakowski M, Hochmair MJ, Huemer F, Losonczy G, Johnson ML, Nishio M, Reck M, Mok T, Lam S, Shames DS, Liu J, Ding B, Lopez-Chavez A, Kabbinavar F, Lin W, Sandler A, Liu SV; IMpower133 Study Group. First-Line Atezolizumab plus Chemotherapy in Extensive-Stage Small-Cell Lung Cancer. *N Engl J Med* 2018; **379**: 2220-2229 [PMID: 30280641 DOI: 10.1056/NEJMoa1809064]
- 3 **Gomez-Randulfe I**, Leporati R, Gupta B, Liu S, Califano R. Recent advances and future strategies in first-line treatment of ES-SCLC. *Eur J Cancer* 2024; **200**: 113581 [PMID: 38301317 DOI: 10.1016/j.ejca.2024.113581]
- 4 **Huang Y**, Dai S, Yin W, Luo F, Li Y. Sustained Clinical Response to 4th-Line Therapy with Selpercatinib in RET Fusion-Positive Combined Small Cell Lung Cancer. *Onco Targets Ther* 2023; **16**: 1015-1020 [PMID: 38050583 DOI: 10.2147/OTT.S440610]
- 5 **Curigliano G**, Subbiah V, Gainor J, Lee D, Taylor M, Zhu V, Doebele R, Lopes G, Baik C, Garralda E, Gadgil S, Kim D, Turner C, Palmer M, Miller S. Treatment with BLU-667, a potent and selective RET inhibitor, provides rapid clearance of ctDNA in patients with RET-altered non-small cell lung cancer (NSCLC) and thyroid cancer. *Annals Oncology* 2019; **30**: v790 [DOI: 10.1093/annonc/mdz268.093]
- 6 **Drilon A**, Oxnard G, Wirth L, Besse B, Gautschi O, Tan S, Loong H, Bauer T, Kim Y, Horiike A, Park K, Shah M, McCoach C, Bazhenova L, Seto T, Brose M, Pennell N, Weiss J, Matos I, Peled N, Cho B, Ohe Y, Reckamp K, Boni V, Satouchi M, Falchook G, Akerley W, Daga H, Sakamoto T, Patel J, Lakhani N, Barlesi F, Burkard M, Zhu V, Moreno Garcia V, Medioni J, Matrana M, Rolfo C, Lee D, Nechushtan H, Johnson M, Velcheti V, Nishio M, Toyozawa R, Ohashi K, Song L, Han J, Spira A, De Braud F, Staal Rohrberg K, Takeuchi S, Sakakibara J, Waqar S, Kenmotsu H, Wilson F, B. nair, Olek E, Kherani J, Ebata K, Zhu E, Nguyen M, Yang L, Huang X, Cruickshank S, Rothenberg S, Solomon B, Goto K, Subbiah V. PL02.08 Registrational Results of LIBRETTO-001: A Phase 1/2 Trial of LOXO-292 in Patients with RET Fusion-Positive Lung Cancers. *Journal of Thoracic Oncology* 2019; **14**: S6-S7 [DOI: 10.1016/j.jtho.2019.08.059]
- 7 **Scott SC**, Hann CL. Immunotherapy for small cell lung cancer: established applications and novel approaches. *Clin Adv Hematol Oncol* 2021; **19**: 654-663 [PMID: 34637432]
- 8 **Qu Z**, Liu J, Luo F, Li L, Zhu L, Zhou Q. [MDT Treatment of Small Cell Lung Cancer Complicated with Adenocarcinoma: A Case Report and Literature Review]. *Zhongguo Fei Ai Za Zhi* 2021; **24**: 808-814 [PMID: 34802214 DOI: 10.3779/j.issn.1009-3419.2021.102.37]
- 9 **Siegel RL**, Miller KD, Jemal A. Cancer statistics, 2020. *CA Cancer J Clin* 2020; **70**: 7-30 [PMID: 31912902 DOI: 10.3322/caac.21590]
- 10 **Gazdar AF**, Bunn PA, Minna JD. Small-cell lung cancer: what we know, what we need to know and the path forward. *Nat Rev Cancer* 2017; **17**: 725-737 [PMID: 29077690 DOI: 10.1038/nrc.2017.87]
- 11 **Dowlati A**, Lipka MB, McColl K, Dabir S, Behtaj M, Kresak A, Miron A, Yang M, Sharma N, Fu P, Wildey G. Clinical correlation of extensive-stage small-cell lung cancer genomics. *Ann Oncol* 2016; **27**: 642-647 [PMID: 26802149 DOI: 10.1093/annonc/mdw005]
- 12 **Semenova EA**, Nagel R, Berns A. Origins, genetic landscape, and emerging therapies of small cell lung cancer. *Genes Dev* 2015; **29**: 1447-1462 [PMID: 26220992 DOI: 10.1101/gad.263145.115]
- 13 **Sarfaty M**, Moore A, Neiman V, Dudnik E, Ilouze M, Gottfried M, Katznelson R, Nechushtan H, Sorotsky HG, Paz K, Katz A, Saute M, Wolner M, Moskovitz M, Miller V, Elvin J, Lipson D, Ali S, Gutman LS, Dvir A, Gordon N, Peled N. RET Fusion Lung Carcinoma: Response to Therapy and Clinical Features in a Case Series of 14 Patients. *Clin Lung Cancer* 2017; **18**: e223-e232 [PMID: 28082048 DOI: 10.1016/j.clcc.2016.09.003]
- 14 **Song M**. Progress in Discovery of *KIF5B-RET* Kinase Inhibitors for the Treatment of Non-Small-Cell Lung Cancer. *J Med Chem* 2015; **58**: 3672-3681 [PMID: 25625428 DOI: 10.1021/jm501464c]
- 15 **Dabir S**, Babakooi S, Kluge A, Morrow JJ, Kresak A, Yang M, MacPherson D, Wildey G, Dowlati A. RET mutation and expression in small-cell lung cancer. *J Thorac Oncol* 2014; **9**: 1316-1323 [PMID: 25122427 DOI: 10.1097/JTO.0000000000000234]



## Endobronchial metastasis secondary to renal clear cell carcinoma: A case report

Tian-Hao Xie, Yan Fu, Si-Ning Ha, Qing-Xu Meng, Qian Sun, Pan Wang

**Specialty type:** Oncology

**Provenance and peer review:**

Unsolicited article; Externally peer reviewed.

**Peer-review model:** Single blind

**Peer-review report's classification**

**Scientific Quality:** Grade C

**Novelty:** Grade B

**Creativity or Innovation:** Grade C

**Scientific Significance:** Grade B

**P-Reviewer:** Wang X, United States

**Received:** April 11, 2024

**Revised:** May 20, 2024

**Accepted:** June 11, 2024

**Published online:** August 16, 2024

**Processing time:** 85 Days and 6 Hours



**Tian-Hao Xie, Si-Ning Ha, Qing-Xu Meng, Qian Sun,** Department of General Surgery, The Affiliated Hospital of Hebei University, Baoding 071000, Hebei Province, China

**Yan Fu,** Department of Ophthalmology, Baoding First Central Hospital, Baoding 071000, Hebei Province, China

**Pan Wang,** Department of Pathology, The Affiliated Hospital of Hebei University, Baoding 071000, Hebei Province, China

**Co-corresponding authors:** Qian Sun and Pan Wang.

**Corresponding author:** Qian Sun, MD, Associate Chief Nurse, Department of General Surgery, The Affiliated Hospital of Hebei University, No. 212 East Yuhua Road, Baoding 071000, Hebei Province, China. [hdfysq@163.com](mailto:hdfysq@163.com)

### Abstract

#### BACKGROUND

Endobronchial metastases (EBMs) are tumours that metastasise from a malignant tumour outside the lungs to the central and subsegmental bronchi, and are visible under a bronchofibrescope. Most EBMs are formed by direct invasion or metastasis of intrathoracic malignant tumours, such as lung cancer, oesophageal cancer or mediastinum tumours. Renal cell carcinoma (RCC), accounting for 2% to 3% of all tumours, is a common malignant tumour of the urinary system. Renal clear cell carcinoma (RCCC) constitutes the predominant pathological subtype of RCC, comprising approximately 70% to 80% of all RCC cases. RCCC can spread and metastasise through arterial, venous and lymphatic circulation to almost all organs of the body. Moreover, lung, bone, liver, brain and local recurrence are the most common metastatic neoplasms of RCCC. However, EBM from RCCC has a low complication rate and is often misdiagnosed as primary lung cancer.

#### CASE SUMMARY

A 71-year-old male patient who had undergone radical left nephrectomy 7 years prior due to RCCC was referred to our hospital due to a 1-mo history of productive cough. The results of an enhanced chest CT scan indicated the presence of a soft tissue nodule in the upper lobe of the left lung, and flexible bronchoscopy revealed a hypervascular lesion in the bronchus of the left lung's superior lobe. Therefore, the patient underwent thoracoscopic left superior lobe wedge resection, and pathology confirmed EBM from the RCCC.

## CONCLUSION

EBM from RCCC has a low incidence and no characteristic clinical manifestations in the early stage. If a bronchial tumour is found in a patient with RCCC, the possibility of bronchial metastatic cancer should be considered.

**Key Words:** Endobronchial metastases; Clear renal cell carcinoma; Renal cell carcinoma; diagnosis; Treatment; Case report

©The Author(s) 2024. Published by Baishideng Publishing Group Inc. All rights reserved.

**Core Tip:** Endobronchial metastases (EBMs) are tumours that metastasise from a malignant tumour outside the lungs to the central and subsegmental bronchi, and are visible under a bronchofibroscope. Renal clear cell carcinoma (RCCC) is a common malignant tumour of the urinary system. EBM from RCCC has a low complication rate and is often misdiagnosed as primary lung cancer. We report a case of post-operative EBM in a patient with RCCC who underwent laparoscopic radical nephrectomy 7 years ago. This suggested that if a bronchial tumour is found in a patient with RCCC, the possibility of EBM should be considered.

**Citation:** Xie TH, Fu Y, Ha SN, Meng QX, Sun Q, Wang P. Endobronchial metastasis secondary to renal clear cell carcinoma: A case report. *World J Clin Cases* 2024; 12(23): 5416-5421

**URL:** <https://www.wjgnet.com/2307-8960/full/v12/i23/5416.htm>

**DOI:** <https://dx.doi.org/10.12998/wjcc.v12.i23.5416>

## INTRODUCTION

Renal cell carcinoma (RCC), comprising 2% to 3% of all tumours, is a common malignant neoplasm affecting the urinary system[1,2]. Renal clear cell carcinoma (RCCC), being the most prevalent pathological type of RCC, comprises approximately 70% to 80% of all RCC cases and is most frequently observed in individuals aged 50 years to 70 years. RCC can spread and metastasise through arterial, venous and lymphatic circulation to almost all organs of the body. Moreover, lung, bone, liver, brain and local recurrence are the most common metastatic neoplasms of RCC[3]. Most extrathoracic malignancies that metastasise to the lung are RCCs, but endobronchial metastasis (EBM) from RCCC has a low incidence rate[4]. Herein, we report a case of post-operative bronchial metastasis in a patient with RCCC who underwent laparoscopic radical nephrectomy 7 years ago.

## CASE PRESENTATION

### Chief complaints

A 71-year-old male patient with a 1-mo history of productive cough was referred to our outpatient department for further evaluation.

### History of present illness

Symptoms started 1-mo before presentation with recurrent productive cough. A soft tissue nodule in the upper lobe of the left lung was detected by a chest computed tomography (CT) scan, prompting hospitalisation for additional evaluation.

### History of past illness

The patient underwent laparoscopic radical resection of the left kidney 7 years ago, and post-operative pathology indicated that the grade II RCCC invaded the renal fibrous fascia, and no cancerous tissue was found in the vessels of the broken ureter or the renal portal. Post-operative recovery was successful, and Ubenimex was taken orally to enhance immunity. The patient was not re-examined after discharge.

### Personal and family history

The patient had no history of smoking, drinking, or recent travel. His medical and family history did not reveal any significant health issues.

### Physical examination

During the physical examination, both lung areas exhibited normal breathing sounds. The abdomen was soft, painless, and did not reveal any palpable masses.

### Laboratory examinations

Laboratory examinations, including routine blood, renal function, urine, and stool tests, as well as evaluations of tumour markers (carbohydrate antigen [CA] 125, CA15-3, CA19-9, CA72-4, carcinoembryonic antigen, alpha fetoprotein), did not indicate any abnormalities.

### Imaging examinations

The results of an enhanced chest CT scan indicated the presence of a soft tissue nodule in the upper lobe of the left lung, suggesting a high likelihood of peripheral lung cancer (Figure 1). Abdominal enhanced CT showed no signs of tumour recurrence or metastasis. A whole-body bone scan revealed no abnormalities.

## MULTIDISCIPLINARY EXPERT CONSULTATION

Subsequently, a hypervascular lesion was detected in the bronchus of the left lung superior lobe by flexible bronchoscopy (Figure 2). However, pathology revealed no tumour cells by bronchial brushing.

## FINAL DIAGNOSIS

Pathological examination revealed clear cell carcinoma with a maximum diameter of approximately 2.2 cm, which did not invade the visceral pleura (Figure 3). No cancer was found at the incision margin of the suture nail. Combined with the immunohistochemical results and medical history, these findings were consistent with the origin of the kidney. Immunohistochemistry revealed positivity for CD10, CAX and CK, but negativity for Melan-A, HMB-45, S-100 and CK7. The patient was diagnosed with RCCC with EBM based on the detailed microscopic findings and radiological correlation (stage IV: T1N0M1).

## TREATMENT

After consultation, the patient underwent surgery, and thoracoscopic left superior lobe wedge resection was performed under general anaesthesia.

## OUTCOME AND FOLLOW-UP

The patient recovered smoothly without severe complications, and refused radiotherapy, chemotherapy or targeted therapy. There was no recurrence or metastasis found by CT at the 6-mo follow-up.

## DISCUSSION

EBM is a tumour that metastasises from a malignant tumour outside the lungs to the central and subsegmental bronchi and is visible under a bronchofibroscope[5]. Most EBMs are formed by direct invasion or metastasis of intrathoracic malignant tumours, such as lung cancer, oesophageal cancer or mediastinum tumours. In 4% of cases where bronchoscopy is performed for suspected malignancy, extrapulmonary tumours are detected through endobronchial mucosal biopsy, and approximately 5% of these cases present with metastasis as the initial sign of the neoplasm[6]. The diagnostic modalities for EBM include CT, bronchoscopic biopsy, bronchial brushing, endobronchial ultrasound-guided transbronchial needle aspiration, surgical biopsy, X-ray and bronchoalveolar lavage.

Kiryu *et al*[5] divided EBMs into four types based on the invasion mode: Type I, direct metastasis to the airway; Type II, invasion of the airway through parenchymal lesions of the lung; Type III, mediastinal or hilar lymph node metastasis invading the airway; and Type IV, peripheral lesions growing along the proximal bronchus.

RCCC is characterised by insidious onset, high malignancy and rapid progression. Early-stage RCCC is generally asymptomatic and difficult to detect. Approximately 20%-30% of patients have metastasis at the initial diagnosis[7], and nearly 30% of patients experience recurrence and metastasis after surgery[8].

The CT imaging findings of RCCCs with lung metastasis are varied and include the following: (1) Intrapulmonary metastasis, typically characterised by single or multiple round soft tissue density nodules in the lung with clear boundaries and uniform density, which are easy to diagnose; and (2) EBM, manifested as bronchial obstruction and truncation, possibly resulting in obstructive pneumonia and atelectasis, which is rare and is often misdiagnosed as primary lung cancer. In this case, the EBM, characterised by a soft tissue density shadow and lobulated segmentation, originating from the RCCC, was located in the bronchial branch of the upper lobe of the left lung. The lesion was characterised by soft tissue density shadows and lobed segmentation. An enhanced scan revealed uneven enhancement, and the patient was misdiagnosed with peripheral lung cancer.

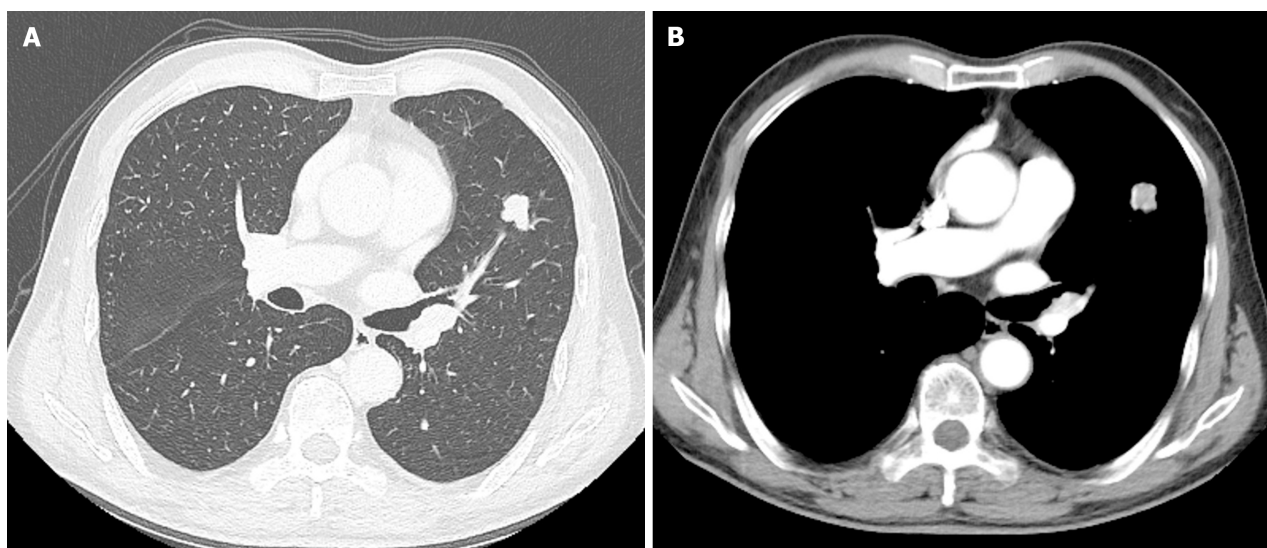


**Figure 1** A chest enhanced computed tomography scan revealing a soft tissue nodule in the upper lobe of the left lung. A: Lung window; B: Mediastinal window.

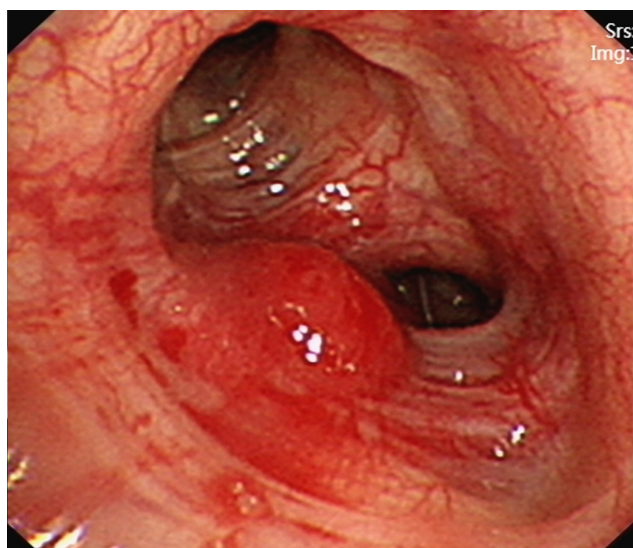


**Figure 2** Flexible bronchoscopy revealing a hypervascular lesion in the bronchus of the left superior lobe of the lung.

It has been reported that for tumours with characteristic CT findings of EBM from RCCC growth in the bronchus along the bronchial wall, bronchial tube diameter thickening resembles a glove-finger appearance. The degree of enhancement in the cortical period is significantly enhanced, and the degree of strengthening in the parenchymal period is rapidly reduced, showing a “fast-in and fast-out” phenotype[9]. Unfortunately, there were no such characteristic CT findings in this patient.

Although bronchoscopic biopsy is regarded as the most effective diagnostic tool for patients with EBM, its diagnostic accuracy in assessing EBM is comparatively low, stemming primarily from the high rate of false-negative results associated with this method[5]. In this case, bronchoscopy provided evidence of EBM, although the pathology results from the bronchial brush biopsy were negative.

The symptoms of EBM most frequently manifest as coughing and haemoptysis, subsequently accompanied by dyspnoea and wheezing[10,11]. Although these symptoms may also occur in patients with respiratory diseases, any of these symptoms in patients with extrapulmonary tumours may indicate the possibility of EBM. In addition, the proportion of asymptomatic patients is still 52%-62.5%[5,12,13]. At this time, regular chest CT and bronchoscopy after the onset of symptoms are necessary. Pathological examination and immunohistochemistry are used for the diagnosis of EBM.

Post-operative follow-up is an important part of the treatment process of RCCCs, the main purpose of which is to detect any tumour recurrence, metastasis or new tumour formation in a timely manner, in addition to monitor the preservation of renal function after surgery. The follow-up process typically involves three stages:

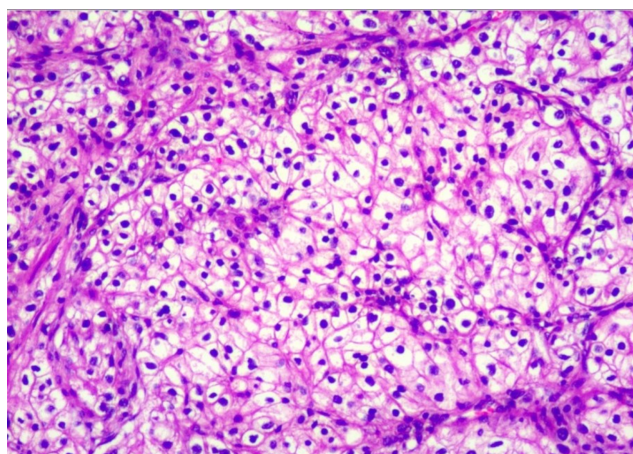


**Figure 3** Haematoxylin and eosin-stained section of the nodule biopsy showing renal clear cell carcinoma.

**Early follow-up:** This occurs within 1 to 2 wk after surgery. The focus is on assessing wound healing, determining the next steps of the treatment plan, and evaluating post-operative recovery and any complications. During this stage, the doctor may recommend necessary tests based on the patient's specific condition, such as blood tests (complete blood count, liver and kidney function tests, electrolyte levels, and erythrocyte sedimentation rate) and chest X-rays.

**Intermediate follow-up:** This occurs at 4 to 6 wk after surgery. It involves repeat blood tests, as well as additional imaging tests such as chest CT scans if abnormalities are detected on chest X-rays. Abdominal ultrasounds may also be performed, and if abnormalities are found or if the patient underwent partial nephrectomy or has advanced-stage RCCC (T3-T4), abdominal CT scans may be recommended. These scans may be repeated every 6 mo for 2 years, and the frequency may be adjusted based on the patient's condition.

**Long-term follow-up:** For patients with early-stage RCCC, follow-up visits are typically scheduled at intervals of 3 mo to 6 mo for the initial 3 years, and then annually thereafter. However, for those with advanced-stage RCCC, the follow-up schedule is more intensive, with visits every 3 mo for the first 2 years, followed by every 6 mo in the third year, and annually afterwards. During these visits, the doctor may recommend additional tests such as magnetic resonance imaging scans of the central nervous system or urine catecholamine testing, depending on the patient's specific condition and treatment.

## CONCLUSION

EBM from RCCC has a low incidence and lacks characteristic clinical manifestations in the early stage compared to that of primary lung cancer. For this type of atypical lung metastatic cancer, it is difficult to make an accurate diagnosis solely based on imaging examination, and comprehensive judgement should be made by combining medical history, physical signs, laboratory tests and other auxiliary examinations. The diagnosis ultimately depends on pathological examination and immunohistochemistry. If a bronchial tumour is found in a patient with RCCC, the possibility of bronchial metastatic cancer should be considered.

## FOOTNOTES

**Author contributions:** Xie TH and Sun Q contributed to the drafting of the manuscript and revising the final draft; Fu Y, Ha SN, and Meng QX contributed to the acquisition of data and revising the final draft; Xie TH, Sun Q, and Wang P contributed to the investigation and interpretation of the data. All authors have read and approved the manuscript. Both Sun Q and Wang P played important and indispensable roles in the investigation, data interpretation, and manuscript preparation as the co-corresponding authors. Sun Q searched the literature, and revised and submitted the early version of the manuscript with the focus on the association between endobronchial metastasis and renal clear cell carcinoma. Wang P was instrumental and responsible for re-interpretation, a comprehensive literature search, and preparation and submission of the current version of the manuscript with a new focus on the mechanisms of endobronchial metastasis. This collaboration between Sun Q and Wang P was crucial for the publication of this manuscript and other manuscripts still in preparation.

**Informed consent statement:** All study participants provided informed written consent prior to study enrolment.

**Conflict-of-interest statement:** All authors declare that they have no competing interests.

**CARE Checklist (2016) statement:** The authors have read the CARE Checklist (2016), and the manuscript was prepared and revised

according to the CARE Checklist (2016).

**Open-Access:** This article is an open-access article that was selected by an in-house editor and fully peer-reviewed by external reviewers. It is distributed in accordance with the Creative Commons Attribution NonCommercial (CC BY-NC 4.0) license, which permits others to distribute, remix, adapt, build upon this work non-commercially, and license their derivative works on different terms, provided the original work is properly cited and the use is non-commercial. See: <https://creativecommons.org/licenses/by-nc/4.0/>

**Country of origin:** China

**ORCID number:** Tian-Hao Xie 0000-0003-3993-2190; Yan Fu 0000-0001-8876-992X; Qian Sun 0000-0002-7671-577X.

**S-Editor:** Liu JH

**L-Editor:** Filipodia

**P-Editor:** Cai YX

## REFERENCES

- 1 **Motzer RJ**, Jonasch E, Agarwal N, Alva A, Baine M, Beckermann K, Carlo MI, Choueiri TK, Costello BA, Derweesh IH, Desai A, Ged Y, George S, Gore JL, Haas N, Hancock SL, Kapur P, Kyriakopoulos C, Lam ET, Lara PN, Lau C, Lewis B, Madoff DC, Manley B, Michaelson MD, Mortazavi A, Nandagopal L, Plimack ER, Ponsky L, Ramalingam S, Shuch B, Smith ZL, Sosman J, Dwyer MA, Gurski LA, Motter A. Kidney Cancer, Version 3.2022, NCCN Clinical Practice Guidelines in Oncology. *J Natl Compr Canc Netw* 2022; **20**: 71-90 [PMID: 34991070 DOI: 10.6004/jnccn.2022.0001]
- 2 **Sung H**, Ferlay J, Siegel RL, Laversanne M, Soerjomataram I, Jemal A, Bray F. Global Cancer Statistics 2020: GLOBOCAN Estimates of Incidence and Mortality Worldwide for 36 Cancers in 185 Countries. *CA Cancer J Clin* 2021; **71**: 209-249 [PMID: 33538338 DOI: 10.3322/caac.21660]
- 3 **Stephenson AJ**, Chetner MP, Rourke K, Gleave ME, Signaevsky M, Palmer B, Kuan J, Brock GB, Tanguay S. Guidelines for the surveillance of localized renal cell carcinoma based on the patterns of relapse after nephrectomy. *J Urol* 2004; **172**: 58-62 [PMID: 15201737 DOI: 10.1097/01.ju.0000132126.85812.7d]
- 4 **Doğan D**, Turan D, Özgül MA, Çetinkaya E. The role of interventional pulmonology in endobronchial metastasis of renal cell carcinoma. *Tuberk Toraks* 2019; **67**: 211-218 [PMID: 31709953 DOI: 10.5578/tt.68407]
- 5 **Kiryu T**, Hoshi H, Matsui E, Iwata H, Kokubo M, Shimokawa K, Kawaguchi S. Endotracheal/endobronchial metastases : clinicopathologic study with special reference to developmental modes. *Chest* 2001; **119**: 768-775 [PMID: 11243955 DOI: 10.1378/chest.119.3.768]
- 6 **Marchioni A**, Lasagni A, Busca A, Cavazza A, Agostini L, Migaldi M, Corradini P, Rossi G. Endobronchial metastasis: an epidemiologic and clinicopathologic study of 174 consecutive cases. *Lung Cancer* 2014; **84**: 222-228 [PMID: 24681280 DOI: 10.1016/j.lungcan.2014.03.005]
- 7 **Bukowski RM**. Natural history and therapy of metastatic renal cell carcinoma: the role of interleukin-2. *Cancer* 1997; **80**: 1198-1220 [PMID: 9317170 DOI: 10.1002/(sici)1097-0142(19971001)80:7<1198::aid-cnrc3>3.0.co;2-h]
- 8 National Comprehensive Cancer Network. Kidney cancer (v. 1. 2024) [EB/OL]. (2023-05-12) [2023-11-10]. Available from: <https://www.nccnchina.org.cn/guide/detail/406>
- 9 **Park CM**, Goo JM, Choi HJ, Choi SH, Eo H, Im JG. Endobronchial metastasis from renal cell carcinoma: CT findings in four patients. *Eur J Radiol* 2004; **51**: 155-159 [PMID: 15246521 DOI: 10.1016/S0720-048X(03)00209-2]
- 10 **Salud A**, Porcel JM, Rovirosa A, Bellmunt J. Endobronchial metastatic disease: analysis of 32 cases. *J Surg Oncol* 1996; **62**: 249-252 [PMID: 8691837 DOI: 10.1002/(SICI)1096-9098(199608)62:4<249::AID-JSO4>3.0.CO;2-6]
- 11 **Akoglu S**, Uçan ES, Celik G, Sener G, Sevinç C, Kilinç O, İtil O. Endobronchial metastases from extrathoracic malignancies. *Clin Exp Metastasis* 2005; **22**: 587-591 [PMID: 16475029 DOI: 10.1007/s10585-005-5787-x]
- 12 **Heitmiller RF**, Marasco WJ, Hruban RH, Marsh BR. Endobronchial metastasis. *J Thorac Cardiovasc Surg* 1993; **106**: 537-542 [PMID: 8361198 DOI: 10.1016/S0022-5223(19)34091-7]
- 13 **Poe RH**, Ortiz C, Israel RH, Marin MG, Qazi R, Dale RC, Greenblatt DG. Sensitivity, specificity, and predictive values of bronchoscopy in neoplasm metastatic to lung. *Chest* 1985; **88**: 84-88 [PMID: 4006560 DOI: 10.1378/chest.88.1.84]



## Fatal multiple acyl-CoA dehydrogenase deficiency caused by *ETFDH* gene mutation: A case report

Xue-Xia Li, Xiao-Nan Yang, Hu-Dan Pan, Liang Liu

**Specialty type:** Genetics and heredity

**Provenance and peer review:** Unsolicited article; Externally peer reviewed.

**Peer-review model:** Single blind

**Peer-review report's classification**

**Scientific Quality:** Grade C

**Novelty:** Grade B

**Creativity or Innovation:** Grade B

**Scientific Significance:** Grade B

**P-Reviewer:** Pisarev VM, Russia

**Received:** April 11, 2024

**Revised:** May 28, 2024

**Accepted:** June 17, 2024

**Published online:** August 16, 2024

**Processing time:** 85 Days and 1.7 Hours



**Xue-Xia Li, Xiao-Nan Yang**, State Key Laboratory of Quality Research in Chinese Medicine, Macau University of Science and Technology, Macau 999078, China

**Hu-Dan Pan, Liang Liu**, State Key Laboratory of Traditional Chinese Medicine Syndrome, The Second Affiliated Hospital of Guangzhou University of Chinese Medicine, Guangzhou 510006, Guangdong Province, China

**Co-corresponding authors:** Xue-Xia Li and Liang Liu.

**Corresponding author:** Xue-Xia Li, MD, Doctor, Department of Nephrology, Zhuhai Hospital of Integrated Chinese and Western Medicine, No. 208 Yuehua Road, Gongbei, Xiangzhou District, Zhuhai 519000, Guangdong Province, China. [sitalisa@163.com](mailto:sitalisa@163.com)

### Abstract

#### BACKGROUND

Multiple acyl-CoA dehydrogenase deficiency (MADD) is a disease of rare autosomal recessive disorder. There are three types of MADD. Type I is a neonatal-onset form with congenital anomalies. Type II is a neonatal-onset form without congenital anomalies. Type III is considered to a milder form and usually responds to riboflavin. However, late-onset form could also be fatal and not responsive to treatments.

#### CASE SUMMARY

We report a severe case of a young man with onset type III MADD induced by drugs and strenuous exercise characterized by rhabdomyolysis and liver dysfunction. Urine analysis indicated 12 out of 70 kinds of organic acids like glutaric acid-2 were detected. Serum analysis in genetic metabolic diseases revealed 24 out of 43 tested items were abnormal, revealing the elevation of several acylcarnitines and the reduction of carnitine in the patient. By next generation sequencing technology for gene sequencing related to fatty acid oxidation and carnitine cycle defects, a rare *ETFDH* gene variant was identified: NM\_004453:4:C.1448C>T(p.Pro483 Leu). The patient was diagnosed with late-onset GAI. He was not responsive to riboflavin and progressively worsened into multiple organ failure that finally led to death.

#### CONCLUSION

Type III MADD can also be fatal and not responsive to treatments.

**Key Words:** Electron transfer flavoprotein dehydrogenase mutation; Multiple acyl-CoA

dehydrogenase deficiency; Multiple organ failure; Case report

©The Author(s) 2024. Published by Baishideng Publishing Group Inc. All rights reserved.

**Core Tip:** Multiple acyl-CoA dehydrogenase deficiency (MADD) is a disease of rare autosomal recessive disorder of fatty acid, amino acid, and choline metabolism. Here, we report a severe case of a young man with onset type III MADD characterized by rhabdomyolysis and liver dysfunction. His urinary and serum analysis indicated organic acids, the elevation of several acylcarnitines and the reduction of carnitine. Eventually, we identified a rare compound heterozygous variant in the patient. Unfortunately, the patient was not responsive to riboflavin and his condition progressively worsened into multiple organ failure that finally led to death.

**Citation:** Li XX, Yang XN, Pan HD, Liu L. Fatal multiple acyl-CoA dehydrogenase deficiency caused by *ETFDH* gene mutation: A case report. *World J Clin Cases* 2024; 12(23): 5422-5430

**URL:** <https://www.wjgnet.com/2307-8960/full/v12/i23/5422.htm>

**DOI:** <https://dx.doi.org/10.12998/wjcc.v12.i23.5422>

## INTRODUCTION

Multiple acyl-CoA dehydrogenase deficiency (MADD), also called glutaric aciduria type II (GA II) (MIM:231680), is a rare autosomal recessive disorder. A defect in the alpha subunit of fatty acid mitochondrial electron transfer flavoprotein (ETFA) protein, beta subunit of fatty acid mitochondrial electron transfer flavoprotein (ETFB) protein or the electron transfer flavoprotein dehydrogenase (ETFDH) protein could lead to disorder of amino acid and choline metabolism. There are three types of MADD. Type I is a neonatal-onset form with congenital anomalies, Type II is a neonatal-onset form without congenital anomalies, and Type III is considered to a milder form and usually respond to riboflavin. Types I and II are usually considered to be more severe and sometimes fatal. The late-onset form is considered to be milder, and could be mostly responsive to treatments. Here, we report a late-onset MADD that is not responsive to riboflavin and is fatal.

## CASE PRESENTATION

### Chief complaints

Onset weakness for a month and vomiting for 5 h.

### History of present illness

The patient complained of fatigue after strenuous exercise (tug of war) a month ago. He visited a doctor in a clinic and received a febuxostat tablet for hyperuricemia and bicyclol tablet for liver injury. He suffered, vomiting, shortness of breath, chest pain and slurred speech as the disease progressed.

### History of past illness

The patient had a history of palpitation and liver dysfunction for 5 years.

### Personal and family history

The patient denied infectious diseases, genetic diseases, history of surgical trauma and blood transfusion.

### Physical examination

On admission, physical examination showed body temperature of 36.5 °C, pulse of 130 times per minute, respiration of 19 times per minute, and blood pressure [p(B)] of 16.226/10.374 kPa. The body check revealed jaundice, neck stiffness, flexor asthenia and weakness of four limbs.

### Laboratory examinations

The patient's blood glucose concentration was 2.7 mmol/L in the emergency room. Blood tests revealed an elevation of creatine kinase, alanine aminotransferase, aspartate aminotransferase on admission. His serum albumin was 37.2 U/L, serum creatinine was 80 µmol/L, and blood urea nitrogen was 6.4 mmol/L on admission, while his blood ammonia was 236 µmol/L, and ceruloplasmin was 13.1 mg/L. His urinalysis indicated occult blood in the urine. Blood clotting functions were abnormal. Blood cell analysis, index of infection, autoantibodies, tumor markers and thyroid function were normal on admission.

### Imaging examinations

Computer tomography of the patient's brain and abdomen indicated shallow cerebral sulci and severe fatty liver (Figure 1). Electrocardiograph indicated supraventricular tachycardia (SVT). The heart ultrasound and electromyography were normal.

## MULTIDISCIPLINARY EXPERT CONSULTATION

The patient was diagnosed with rhabdomyolysis, SVT, hepatic failure, acidosis, hypoglycemia and abnormal coagulation function on admission. A high dose of glucose was pumped in until his glucose level was stable. Timely fluid infusion, intravenous glutathione and glycyrhizin were used for liver protection. Intravenous ornithine aspartate and rice vinegar clysis were applied for reducing blood ammonia level. However, the patient experienced very rapid deterioration in his clinical conditions following the onset of symptoms. His liver function and myocardial enzyme levels continuously increased. On the 9<sup>th</sup> day after admission, he suffered from onset fatigue, mucocutaneous stained yellow (daily elevated serum bilirubin level over 17 mmol/L), repeated severe hypoglycemia, acidosis, hepatic encephalopathy, SVT, rhabdomyolysis, acute kidney injury, and respiratory failure (partial pressure of carbon dioxide of 10.241 kPa). He was then transferred to the intensive care unit.

His coagulation system, respiratory system, and circulatory system were collapsed, accompanied with renal and liver failure. Multiple organ failure could not be explained by the admitting diagnosis. Further, we discovered that his parents were in a consanguineous marriage. Combined with the clinical features of the patient, hereditary disease was considered. We then analyzed 70 types of organic acids in the patient's urine, among which 12 organic acids were abnormally elevated. For example, glutaric acid -2 levels were 64 times higher than normal (Table 1). We then analyzed genetic metabolic diseases in amino acid and acylcarnitine spectrum in his blood. Twenty-four out of the total 43 tested items were abnormal, revealing the elevation of several acylcarnitines and the reduction of carnitine (Table 2), inferring MADD. Furthermore, we applied next generation sequencing technology for gene sequencing related to fatty acid oxidation and carnitine cycle defects in his whole blood. Single nucleotide variation and small fragment insertion deletion variation were detected, which indicated single nucleotide variation of *ETFDH* gene with chromosomal location: Chr4:159627503; mutation information: NM.004453.4:c.1448C>T(p.Pro483Leu); Homozygous, which indicated glutaric acidemia type II (MIM:231680).

## FINAL DIAGNOSIS

The patient was diagnosed with type III (late-onset form) MADD.

## TREATMENT

Levocarnitine and riboflavin were intravenously injected at a dose of 60 mg/kg/d and 200 mg/d, respectively. Anti-infective therapy was applied for secondary infection. Unfortunately, the patient fell into a coma after the 9<sup>th</sup> day of admission. He also suffered malignant arrhythmia with a heart rate over two hundred times per minute. Esmolol and metarbamine were not effective to his heart so synchronized electrical cardioversions were applied seven times on the 11<sup>th</sup>, 12<sup>th</sup> and 13<sup>th</sup> day after his admission. The patients finally fell into a deep coma and depended on mechanical ventilation, continuous renal replacement treatment (CRRT) and artificial liver. Twenty-five days of ventilator support, eleven rounds of CRRT, two rounds of plasma exchange, three rounds of dual plasma molecular adsorption system and nine rounds of alveolar wash were applied within the twenty-five days of his coma. More than 20000 mL of plasma, 12 units of red blood cells, and some blood platelet and cryoprecipitation were used during the treatment. His liver function, kidney function and functions of other systems were improving, as demonstrated by clinical biochemistry (Figure 2).

## OUTCOME AND FOLLOW-UP

The young man finally came to after 25 days of treatment, though he was still critically ill. We transferred the patient to Yunnan according to the demand of his parents. Unfortunately, we got the message that he finally passed away in Yunnan due to malignant arrhythmia.

## DISCUSSION

MADD is also called glutaric aciduria type II (GA II) (MIM:231680). This is a rare autosomal recessive disorder caused by defects in the mitochondrial electron transport chain, which is the electron transport from flavin adenine dinucleotide-containing dehydrogenases to coenzyme Q10. Intra-mitochondrial acyl-CoA dehydrogenation causes MADD.

**Table 1 Organic acids tests in the urine**

Number	Organic acids (normal range)	
1	Lactic acid -2 (0.0-13.0)	14.2↑
2	Pyruvate-OX-2 (0.0-30.0)	91.7↑
3	2-hydroxyisovaleric acid-2 (0.0-2.0)	7.8↑
4	2-ketoisovaleric acid-OX-2 (0.0-0.3)	1.0↑
5	2-ketoisohexanoic acid-OX-2 (0.0-0.8)	1.7↑
6	Glutaric acid -2 (0.0-8.0)	516.4↑
7	Isoamyl glycine-1 (0.0-1.5)	11.3↑
8	Acetylmalonic acid-2 (0.0-7.0)	17.6↑
9	Methylsuccinic acid-2 (0.0-4.0)	5.5↑
10	Methyl fumaric acid-2 (0.0-2.5)	3.0↑
11	Glutaconic acid-2 (0.0-0.0)	2.2↑
12	Adipic acid-2 (0.0-15.0)	165↑

12 of 70 organic acids were abnormal.

**Table 2 Serum amino acid and acylcarnitine spectrum of genetic metabolic diseases**

Amino acid and acylcarnitine spectrum (normal range)		Amino acid and acylcarnitine spectrum	
Palmitoyl carnitine (C16) (0.20-3.50)	4.49↑	C8/C3 (0.01-0.40)	1.20↑
Palmitoyl carnitine (C16:1) (0.02-0.30)	2.22↑	C10/C3 (0.01-0.50)	2.70↑
Palmolive dienyln carnitine (C16:2) (0.01-0.10)	0.31↑	C12/C3 (0.01-0.35)	3.58↑
Octadecyl carnitine (C18:1) (0.20-2.80)	3.80↑	C14/C3 (0.02-0.45)	9.25↑
C3/Mot (0.02-0.30)	0.01↓	C14:1/C8:1 (0.10-6.00)	12.31↑
C3DC/C4 (0.10-1.50)	0.07↓	C16/C2 (0.01-0.20)	0.82↑
C4/C2 (0.00-0.05)	0.08↑	C16/C3 (0.10-3.50)	22.07↑
C4/C3 (0.00-0.70)	2.15↑	C18/C3 (0.05-2.00)	5.44↑
C5/C2 (0.00-0.05)	0.12↑	C16 OH/C3 (0.00-0.15)	0.22↑
C5/C3 (0.00-0.50)	3.20↑	C18 OH/C3 (0.00-0.10)	0.17↑
C5DC/C3 (0.01-0.40)	0.65↑	(C1G+C18:1)/C2 (0.03-0.40)	1.52↑
C6/C3 (0.01-0.30)	0.72↑	C0/(C1G+C18) (6.50-90.00)	1.12↓

24 out of the total 43 tested items were abnormal, revealing the elevation of several acylcarnitines and the reduction of carnitine.

There are three forms of defects. Defects in the ETFA (OMIM 231680), ETFB protein (OMIM 130410) or ETFDH proteins (OMIM 231675) could lead to disorder of amino acid and choline metabolism. ETFA (15q23-q25) encodes the alpha subunit of ETF, ETFB (19q13.3-q13.4) encodes the beta subunit of ETF, and ETFDH (4q32-q35) encoding ETF-ubiquinone oxidoreductase (ETFQO).

Thus, there are three forms of MADD. Both type I and type II are neonatal-onset forms; type I is associated with congenital anomalies, while type II is not. Types I and II are usually considered to be more severe and sometimes fatal, presenting with hypoketotic hypoglycemia, metabolic acidosis, cardiomyopathy, and hepatomegaly. Type III is a late-onset form which is considered to be milder, characterized by proximal myopathy. Episodic vomiting, encephalopathy, liver and renal impairment, and rhabdomyolysis may occur under catabolic stress[1].

ETFDH variants are the most common cause of the late-onset form[2], which[3] is considered to be more variable. There could be recurrent hypoglycemia, metabolic acidosis, vomiting, and muscle weakness during stress[4]. These atypical symptoms usually make differential diagnosis difficult. Exercise intolerance could be an atypical symptom. In our case, exercise and drugs may have induced rhabdomyolysis and liver dysfunction. Research has also indicated that a prolonged exercise test could be of diagnostic importance[5]. Intolerance for prolonged exercise in patients with anam-

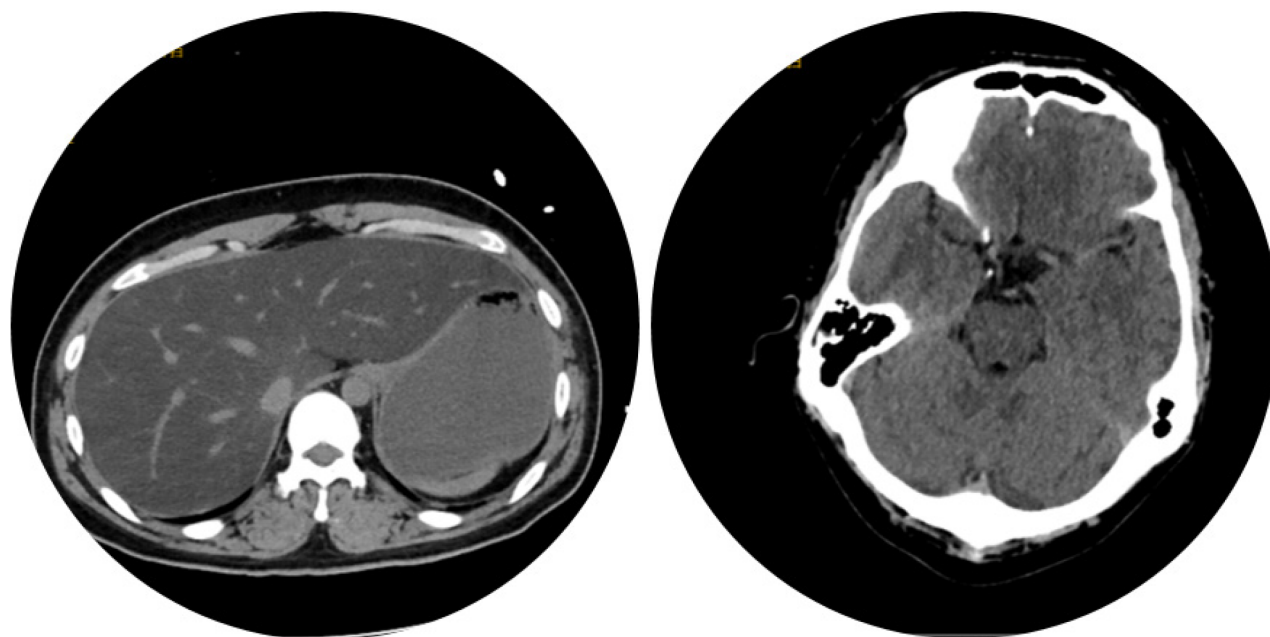


**Figure 1** Computer tomography indicated severe fatty liver and shallow cerebral sulci.

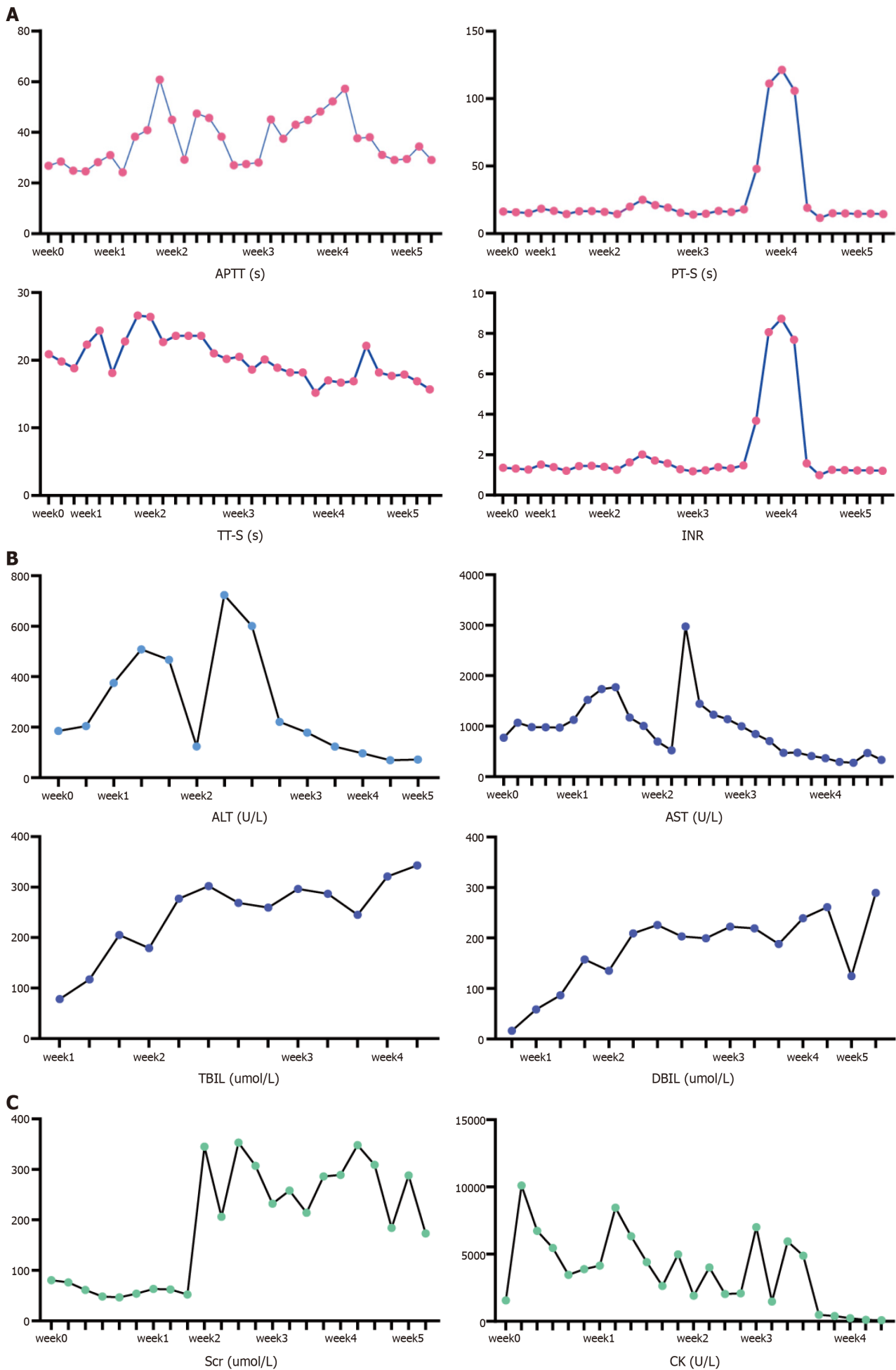
nostic signs would be an important diagnostic procedure that might replace the fasting. Medication could be another inducer. There have been reports that an anti-TB medication could increase MADD metabolic profiles[6]. Considered as a frequent missed diagnosis, late-onset of MADD should get more attention in the clinic when patients present with rhabdomyolysis with exercise or drug inducement. Our patient presented rhabdomyolysis, SVT, hepatic failure, acidosis, hypoglycemia and abnormal coagulation function that finally turned into multiple organ failure. It reminded us that late-onset MADD is also deadly; we should not only focus on prenatal diagnosis, but also pay attention to late-onset cases.

Urinary organic acid profiles could indicate MADD, which is important for the diagnosis of GAIL. The test is characterized by elevated acids, including isovaleric acid,  $\alpha$ -methylbutyrate, ethylmalonic acid, isobutyrate, glutaric acid, aliphatic dicarboxylic acids, *etc*[7,8]. Urine organic acid analysis could show these acids and their derivatives. During metabolic decompensation, lactate levels and creatine phosphokinase are typically raised. In our case, organic acids tests in the urine indicated 12 of 70 organic acids were abnormal, including lactic acid-2, pyruvate-OX-2, 2-hydroxyisovaleric acid-2, 2-ketoisovaleric acid-OX-2, *etc*. Among which, the patient's glutaric acid-2 level was over 64 times higher than the upper limit of the reference level. Adipic acid-2 level was over 11 times higher than the upper limit of the reference level. Detection of urine organic acids are effective in MADD diagnosis that could highly suggest the disease.

Serum characterization of MADD includes acylcarnitine and organic acid profiling. The biochemical test would reveal higher levels of acylglycine conjugates and dicarboxylic acids. The elevated levels of C4-C18 acylcarnitines could be also detected in the blood. All these biochemical findings might normalize during the period of stability in MADD. Acylcarnitine profile could reveal elevations of short-chain, medium-chain and long-chain acylcarnitines[9]. In our case, blood amino acid and acylcarnitine spectrum of genetic metabolic diseases revealed that 24 out of the total 43 tested items were abnormal, including the elevation of several acylcarnitines and the reduction of carnitine.

Defects in the ETFDH protein[10] account for about 90% of MADD cases. ETFDH-c.250G>A is one of the most common mutations, representing a high allelic frequency of about 80% in southern China[11]. ETFDH-c.770A>G and ETFDH-c.1227A>C are more widespread mutations in mainland China[12]. Muscle biopsy could reveal acid and lipid accumulation in skeletal muscles, reducing the activity of mitochondrial respiratory chain complexes[13,14]. In our case, we applied next generation sequencing technology for gene sequencing related to fatty acid oxidation and carnitine cycle defects in the patient's whole blood. Single nucleotide variation and small fragment insertion deletion variation were detected, which indicated single nucleotide variation of ETFDH gene with Chromosomal location: Chr4:159627503; mutation information: NM.004453.4:c.1448C>T(p.Pro483Leu). The mutation is very rare, and whether it is related to the severity of clinical symptoms could be further explored.

For treatments, type III MADD usually responds to riboflavin, with a reported response rate over 98%[1]. When riboflavin insufficient[15], MADD patients would undergo rapid degradation. Riboflavin supplementation is vital in the treatment of late-onset MADD. Research suggests that ETFDH mutations were responsible for all riboflavin-responsive GA-II patients[16]. More than 80% of patients treated with riboflavin showed a release of the disease. The treatment improved their cardiac and skeletal muscle functions. Patients receiving riboflavin treatment could also respond in urinary organic acids normalization and acylcarnitine species reductions[17]. However, there are controversies surrounding the treatment dose and course. No systematic evaluations have been reported yet. Unlike most late-onset GA-II patients, our patient did not respond to riboflavin treatment. Large amounts of riboflavin did not improve his condition, though he partially responded during the treatment. Whether the mutation was responsible for the poor outcome is worth further study.



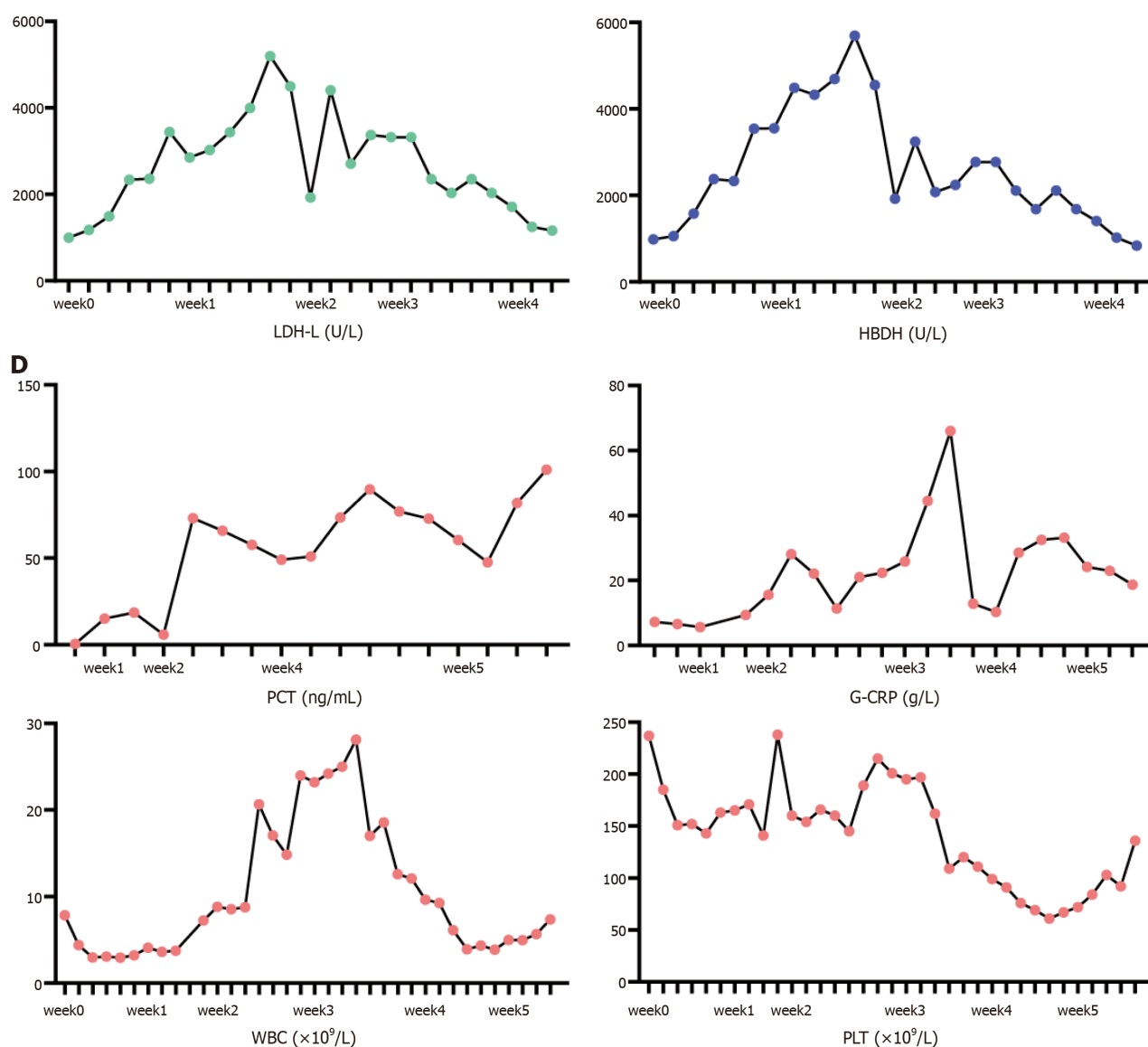


**Figure 2** Changes of clinical biochemistry after treatment. A: Coagulation system: levels of thromboplastin time (APTT), thrombin time (TT), prothrombin time (PT) and international normalized ratio (INR); B: Liver function: levels of alanine transaminase (ALT), aspartic transaminase (AST), direct bilirubin (DBIL), indirect bilirubin (IBIL); C: Kidney function and myolysis: levels of serum creatinine (Scr), creatine kinase (CK), lactate dehydrogenase (LDH-L), hydroxybutyrate dehydrogenase (HBDH); D: Infection indicators: levels of procalcitonin (PCT), high sensitive C-reactive protein (CRP), white blood cells (WBC), platelets (PLT).

In clinic, MADD should be suspected in cases with metabolic abnormalities. Patients with liver damage, kidney failure, hypoglycemia, hyperammonemia, hypoglycemia and rhabdomyolysis, *etc* would suggest GA-II. Exercise and medicine might be inducements. Early diagnosis depends on urine organic acid analysis, blood amino acid tests, serum acylcarnitine profile analysis, muscle biopsy, and genetic tests. Riboflavin supplementation is the first line medication, though it may be not effective.

## CONCLUSION

In summary, our report describes the clinical, biochemical, and molecular findings of a 21-year-old male with ETFDH-related MADD. Late onset of MADD could be with definite inducement factors like drugs and severe exercise. It could also be fatal. c.1448C>T in ETFDH were found in this young man presented with multiple organ failure, which further expands the list of mutations found in MADD patients that might be riboflavin non-responsive MADD.

## ACKNOWLEDGEMENTS

The authors are grateful to Dr. Xiao-Yong Zhang, Wan-Fang Tan and Fu-Ren Guan for entering the data.

## FOOTNOTES

**Author contributions:** Li XX analyzed the data, wrote the manuscript and revised the manuscript; Yang XN analyzed the data; Pan HD revised the manuscript; Liu L contributed to study design, paper writing and supervision.

**Informed consent statement:** Written informed consent was obtained from the patient for publication of this report and all accompanying images.

**Conflict-of-interest statement:** The authors report no relevant conflicts of interest for this article.

**CARE Checklist (2016) statement:** The authors have read the CARE Checklist (2016), and the manuscript was prepared and revised according to the CARE Checklist (2016).

**Open-Access:** This article is an open-access article that was selected by an in-house editor and fully peer-reviewed by external reviewers. It is distributed in accordance with the Creative Commons Attribution NonCommercial (CC BY-NC 4.0) license, which permits others to distribute, remix, adapt, build upon this work non-commercially, and license their derivative works on different terms, provided the original work is properly cited and the use is non-commercial. See: <https://creativecommons.org/licenses/by-nc/4.0/>

**Country of origin:** China

**ORCID number:** Xue-Xia Li 0000-0001-9827-5093.

**S-Editor:** Gong ZM

**L-Editor:** Filipodia

**P-Editor:** Wang WB

## REFERENCES

- 1 Grünert SC. Clinical and genetical heterogeneity of late-onset multiple acyl-coenzyme A dehydrogenase deficiency. *Orphanet J Rare Dis* 2014; **9**: 117 [PMID: 25200064 DOI: 10.1186/s13023-014-0117-5]
- 2 Horvath R. Update on clinical aspects and treatment of selected vitamin-responsive disorders II (riboflavin and CoQ 10). *J Inherit Metab Dis* 2012; **35**: 679-687 [PMID: 22231380 DOI: 10.1007/s10545-011-9434-1]
- 3 Olsen RK, Andresen BS, Christensen E, Bross P, Skovby F, Gregersen N. Clear relationship between ETF/ETFDH genotype and phenotype in patients with multiple acyl-CoA dehydrogenation deficiency. *Hum Mutat* 2003; **22**: 12-23 [PMID: 12815589 DOI: 10.1002/humu.10226]
- 4 Ip WC, Hammond JW, Wilcken B. Neonatal multiple acyl-CoA dehydrogenase deficiency: essentially absent fatty acid oxidation activity in proband but normal activity in parental cultured skin fibroblasts. *J Inherit Metab Dis* 1996; **19**: 379-380 [PMID: 8803790 DOI: 10.1007/BF01799277]
- 5 Takken T, Custers J, Visser G, Dorland L, Helders P, de Koning T. Prolonged exercise testing in two children with a mild Multiple Acyl-CoA-Dehydrogenase deficiency. *Nutr Metab (Lond)* 2005; **2**: 12 [PMID: 15907213 DOI: 10.1186/1743-7075-2-12]
- 6 Loots DT, Wiid IJ, Page BJ, Mienie LJ, van Helden PD. Melatonin prevents the free radical and MADD metabolic profiles induced by antituberculosis drugs in an animal model. *J Pineal Res* 2005; **38**: 100-106 [PMID: 15683464 DOI: 10.1111/j.1600-079X.2004.00176.x]
- 7 Yamada K, Kobayashi H, Bo R, Takahashi T, Purevsuren J, Hasegawa Y, Taketani T, Fukuda S, Ohkubo T, Yokota T, Watanabe M, Tsunemi T, Mizusawa H, Takuma H, Shioya A, Ishii A, Tamaoka A, Shigematsu Y, Sugie H, Yamaguchi S. Clinical, biochemical and molecular investigation of adult-onset glutaric acidemia type II: Characteristics in comparison with pediatric cases. *Brain Dev* 2016; **38**: 293-301 [PMID: 26403312 DOI: 10.1016/j.braindev.2015.08.011]
- 8 Liu J, Wu C, Gao F, Yan Q. A rare condition that mimic myopathy: Late-onset glutaric acidemia type II. *Rheumatol Immunol Res* 2023; **4**: 173-175 [PMID: 37781680 DOI: 10.2478/rir-2023-0026]
- 9 Wen B, Li D, Li W, Zhao Y, Yan C. Multiple acyl-CoA dehydrogenation deficiency as decreased acyl-carnitine profile in serum. *Neurol Sci* 2015; **36**: 853-859 [PMID: 25827849 DOI: 10.1007/s10072-015-2197-y]
- 10 Goodman SI, Binard RJ, Woontner MR, Frerman FE. Glutaric acidemia type II: gene structure and mutations of the electron transfer flavoprotein:ubiquinone oxidoreductase (ETF:QO) gene. *Mol Genet Metab* 2002; **77**: 86-90 [PMID: 12359134 DOI: 10.1016/S1096-7192(02)00138-5]
- 11 Wang ZQ, Chen XJ, Murong SX, Wang N, Wu ZY. Molecular analysis of 51 unrelated pedigrees with late-onset multiple acyl-CoA dehydrogenation deficiency (MADD) in southern China confirmed the most common ETFDH mutation and high carrier frequency of c.250G>A. *J Mol Med (Berl)* 2011; **89**: 569-576 [PMID: 21347544 DOI: 10.1007/s00109-011-0725-7]
- 12 Zhu M, Zhu X, Qi X, Weijiang D, Yu Y, Wan H, Hong D. Riboflavin-responsive multiple Acyl-CoA dehydrogenation deficiency in 13 cases, and a literature review in mainland Chinese patients. *J Hum Genet* 2014; **59**: 256-261 [PMID: 24522293 DOI: 10.1038/jhg.2014.10]
- 13 Vergani L, Barile M, Angelini C, Burlina AB, Nijtmans L, Freda MP, Brizio C, Zerbetto E, Dabbeni-Sala F. Riboflavin therapy. Biochemical heterogeneity in two adult lipid storage myopathies. *Brain* 1999; **122** ( Pt 12): 2401-2411 [PMID: 10581232 DOI: 10.1093/brain/122.12.2401]
- 14 Olsen RK, Olpin SE, Andresen BS, Miedzybrodzka ZH, Pourfarzam M, Merinero B, Frerman FE, Beresford MW, Dean JC, Cornelius N, Andersen O, Oldfors A, Holme E, Gregersen N, Turnbull DM, Morris AA. ETFDH mutations as a major cause of riboflavin-responsive multiple acyl-CoA dehydrogenation deficiency. *Brain* 2007; **130**: 2045-2054 [PMID: 17584774 DOI: 10.1093/brain/awm135]
- 15 Henriques BJ, Olsen RK, Bross P, Gomes CM. Emerging roles for riboflavin in functional rescue of mitochondrial  $\beta$ -oxidation flavoenzymes. *Curr Med Chem* 2010; **17**: 3842-3854 [PMID: 20858216 DOI: 10.2174/092986710793205462]
- 16 Law LK, Tang NL, Hui J, Fung SL, Ruiter J, Wanders RJ, Fok TF, Lam CW. Novel mutations in ETFDH gene in Chinese patients with riboflavin-responsive multiple acyl-CoA dehydrogenase deficiency. *Clin Chim Acta* 2009; **404**: 95-99 [PMID: 19265687 DOI: 10.1016/j.cca.2009.05.011]

[10.1016/j.cca.2009.02.015](https://doi.org/10.1016/j.cca.2009.02.015)

- 17 **Olsen RKJ**, Koňáriková E, Giancaspero TA, Mosegaard S, Boczonadi V, Mataković L, Veauville-Merlié A, Terrile C, Schwarzmayer T, Haack TB, Auranen M, Leone P, Galluccio M, Imbard A, Gutierrez-Rios P, Palmfeldt J, Graf E, Vianey-Saban C, Oppenheim M, Schiff M, Pichard S, Rigal O, Pyle A, Chinnery PF, Konstantopoulou V, Möslinger D, Feichtinger RG, Talim B, Topaloglu H, Coskun T, Gucer S, Botta A, Pegoraro E, Malena A, Vergani L, Mazzà D, Zollino M, Ghezzi D, Acquaviva C, Tyni T, Boneh A, Meitinger T, Strom TM, Gregersen N, Mayr JA, Horvath R, Barile M, Prokisch H. Riboflavin-Responsive and -Non-responsive Mutations in FAD Synthase Cause Multiple Acyl-CoA Dehydrogenase and Combined Respiratory-Chain Deficiency. *Am J Hum Genet* 2016; **98**: 1130-1145 [PMID: [27259049](https://pubmed.ncbi.nlm.nih.gov/27259049/) DOI: [10.1016/j.ajhg.2016.04.006](https://doi.org/10.1016/j.ajhg.2016.04.006)]



## Cushing's syndrome caused by giant Ewing's sarcoma of the kidney: A case report and review of literature

Guo-Fan Dong, Ya-Kun Hou, Qi Ma, Shuang-Yu Ma, Yu-Jie Wang, Mulati Rexiati, Wen-Guang Wang

**Specialty type:** Medicine, research and experimental

**Provenance and peer review:** Unsolicited article; Externally peer reviewed.

**Peer-review model:** Single blind

**Peer-review report's classification**

**Scientific Quality:** Grade B

**Novelty:** Grade B

**Creativity or Innovation:** Grade B

**Scientific Significance:** Grade B

**P-Reviewer:** Exbrayat JM

**Received:** April 14, 2024

**Revised:** June 6, 2024

**Accepted:** June 26, 2024

**Published online:** August 16, 2024

**Processing time:** 81 Days and 20 Hours



**Guo-Fan Dong, Ya-Kun Hou, Qi Ma, Shuang-Yu Ma, Yu-Jie Wang, Mulati Rexiati, Wen-Guang Wang,** Department of Urologic Surgery, The First Affiliated Hospital of Xinjiang Medical University, Urumqi 830000, Xinjiang Uygur Autonomous Region, China

**Co-first authors:** Guo-Fan Dong and Ya-Kun Hou.

**Corresponding author:** Wen-Guang Wang, MD, Associate Professor, Chief Doctor, Surgeon, Department of Urologic Surgery, The First Affiliated Hospital of Xinjiang Medical University, No. 137 Liyu Shan South Road, High-tech Zone, Urumqi 830000, Xinjiang Uygur Autonomous Region, China. [wwg0903@163.com](mailto:wwg0903@163.com)

### Abstract

#### BACKGROUND

Primary renal Ewing's sarcoma (ES) is extremely rare, and only two cases causing Cushing's syndrome (CS) have been reported to date. We report that the case of an 18-year-old patient is diagnosed primary renal ES with typical CS characterized by purple stripes, weight gain, and hypertension.

#### CASE SUMMARY

CS was first diagnosed by laboratory testing. A huge tumor was revealed in the kidney following an imaging examination. Moreover, brain and bone metastases were observed. After comprehensive treatment, primarily based on surgery, primary renal ES was pathologically diagnosed with a typical *EWSR1-FLI1* genetic mutation through genetic testing. Furthermore, the glucocorticoid level returned to normal. By the ninth postoperative month of follow-up, the patient was recovering well. Cushing-related symptoms had improved, and a satisfactory curative effect was achieved.

#### CONCLUSION

Primary renal ES, a rare adult malignant tumor, can cause CS and a poor prognosis.

**Key Words:** Renal; Kidney; Ewing's sarcoma; Neuroectodermal tumors; Cushing syndrome; Case report

©The Author(s) 2024. Published by Baishideng Publishing Group Inc. All rights reserved.

**Core Tip:** Primary renal Ewing's sarcoma (ES), a rare adult malignant tumor, can cause Cushing syndrome and a poor prognosis. The "gold standard" for diagnosing primary renal ES remains pathological examination, even though gene studies can aid in diagnosis and therapy planning. When treating advanced metastatic primary renal ES, a comprehensive surgical approach centered on surgery can produce specific outcomes.

**Citation:** Dong GF, Hou YK, Ma Q, Ma SY, Wang YJ, Rexiati M, Wang WG. Cushing's syndrome caused by giant Ewing's sarcoma of the kidney: A case report and review of literature. *World J Clin Cases* 2024; 12(23): 5431-5440

**URL:** <https://www.wjgnet.com/2307-8960/full/v12/i23/5431.htm>

**DOI:** <https://dx.doi.org/10.12998/wjcc.v12.i23.5431>

## INTRODUCTION

Ewing's sarcoma (ES) is a highly malignant tumor originating from the neuroectoderm and mainly occurs in children's long bones, with an incidence rate of 1 case *per* 1.5 million[1]. ES in other tissues is even rarer. Related reports of relevant cases show that, to date, there have been no more than 200 cases of renal ES[2].

Cushing's syndrome (CS) is a series of symptoms caused by excessive glucocorticoid secretion from the adrenal cortex. In general, some dispersed neuroendocrine system can secrete adrenocorticotrophic hormone (ACTH) or corticotropin releasing hormone (CRH), leading to CS, most commonly in small-cell bronchogenic carcinoma. CS is the rare symptom of primary renal ES, and only two cases have been reported. Herein, we report the case of an 18-year-old patient with typical CS and review related literature.

## CASE PRESENTATION

### Chief complaints

Weight gain and dizziness for three months.

### History of present illness

The weight of the increased by 15 kg in three months, accompanied by purple lines in the bilateral armpits, abdomen, and thigh; dizziness; fatigue; and facial pigmentation.

### History of past illness

The patient was in good physical health.

### Personal and family history

The patient had five siblings and no family history of the presentation.

### Physical examination

Physical examination revealed stable vital signs and a blood pressure, p(B) = 20.6/14.4 kpa. The patient also had a full-moon face, acne, buffalo back, obvious centripetal obesity, and relatively thin limbs. Pigmented, dark red, scattered ecchymosis could be observed on the left upper limb. Large purple stripes could be observed from the bilateral armpits, hips, and thighs to the knees (Figure 1).

### Laboratory examinations

The patient's cortisol level was examined (Table 1). An increased cortisol secretion was observed, alongside a disordered rhythm and increased adrenocorticotrophic hormone levels. Both low- and large-dose dexamethasone suppression tests were negative. The fasting blood glucose was 5.28 mmol/L, and the blood glucose level was 13.29 mmol/L 120 min after an oral glucose tolerance test (OGTT). This indicated that the patient had diabetes. His blood potassium level was 2.50 mmol/L and his blood calcium level was 2.05 mmol/L.

### Imaging examinations

A computed tomography (CT) scan revealed an 11.65 cm × 10.91 cm nonuniform enhanced occupation in the middle and lower part of the left kidney. Magnetic resonance imaging (MRI) revealed that the left temporal lobe was occupied, and the pituitary gland was normal (Figure 2). Fluorine-18 fluorodeoxyglucose (FDG) PET/CT revealed a huge mixed space occupation in the left kidney (Figure 3), unevenly high uptake of the solid component FDG, and high uptake of FDG in the left temporal pole and thoracic 3 laminae of the vertebral arch. This indicated that the left kidney had a malignant tumor, and there were brain, vertebral body, and right femur metastases (Figure 4).

**Table 1** Corticosteroid-related examination

	Blood cortisol level at 0:00 in the morning (nmol/L)	Blood cortisol level at 8:00 in the morning (nmol/L)	Blood cortisol level at 16:00 in the evening (nmol/L)	Adrenocorticotrophic hormone level (pg/mL)	24-hour urinary free cortisol level (nmol/24 h)
Reference range	101.2–535.7 (before 8:00)		79.0–477.8 (after 15:00)	7.2–63.3	11.8–485.6
Patient baseline	1293.2↑	1329.5↑	1479.1↑	96.5↑	10524.0↑
Low-dose dexamethasone suppression test		1526.6↑			
High-dose dexamethasone suppression test		1782.5↑			

**Figure 1** Physical examination. The 18-year-old patient with purple stripes on his outer thigh.

## MULTIDISCIPLINARY EXPERT CONSULTATION

After a multidisciplinary discussion in the hospital, the preoperative diagnosis was a malignant tumor of the left kidney, bone metastasis, left temporal lobe secondary malignant tumor, secondary diabetes, secondary hypertension, CS, and hypokalemia. Comprehensive treatment based on surgery was determined.

The patient underwent a Palliative nephrectomy (Figure 5). The relevant tissues were sent for pathological examination (Figure 6A), and all biochemical indicators recovered postoperatively (Table 2). On the second postoperative day, the cortisol levels were reviewed. On the third postoperative day, cortisol and ACTH levels returned to normal, and the blood potassium level recovered to 3.41 mmol/L. Primary renal ES (extraosseous ES) was confirmed by histopathological examination of the mass. No tumor accumulation was found in the perirenal fat and ureteral stump. Immunohistochemistry (Figure 6B) revealed CD99 (+), vimentin (VIM) (+), CD56 (+), synaptophysin (Syn) (less +), Ki-67 (hot spot 50% +), neuron-specific enolase (NSE) (focus +), CD34 (vascular +), AE1/AE3 (focus +), WT (-), D2-40 (-), Desmin (-), chromaffin A (CgA) (-), S-100 (-), epithelial membrane antigen (EMA) (-), and ACTH (-) (Figure 6C). Genetic test: Exactly 808 tumor-related hot spot genes (605 whole exon coding regions and 203 hot spot mutation regions) were analyzed. The mutation with clear clinical significance (primary mutation) (*NTRK1*, *NTRK1-ZPBP*) and the locus with potential clinical significance (secondary mutation) (*CHEK2* c.444 + 1G > A, *EWSR1* *EWSR1-FLI1*) were observed.

## FINAL DIAGNOSIS

The diagnosis was primary renal ES with CS.

## TREATMENT

The patient was transferred to the oncology department for postoperative radiotherapy and chemotherapy 1 month postoperatively. The chemotherapy regimen consisted of vincristine 2 mg d1 plus doxorubicin 50 mg d1-d2 plus cyclophosphamide 2 g d1. The chemotherapy cycle was 21 days. Due to the continuous increase in intracranial pressure in the patient alongside brain metastases, mannitol dehydration was ensured. Intensity-modulated radiotherapy was administered to the metastatic tumors in the left temporal lobe of the brain (3 Gy *per* fraction of 17 fractions of a total dose of 51 Gy). The patient continued chemotherapy for two courses. Owing to economic problems, chemotherapy was discon-

**Table 2 Biochemical indices after surgery**

	The second day after surgery	The third day after surgery	The fourth day after surgery
Blood cortisol level at 8:00 in the morning (nmol/L)	1649.9†	157.2	183.2
Adrenocorticotrophic hormone level (pg/mL)		20.9	27.3
K+	2.83	3.41	

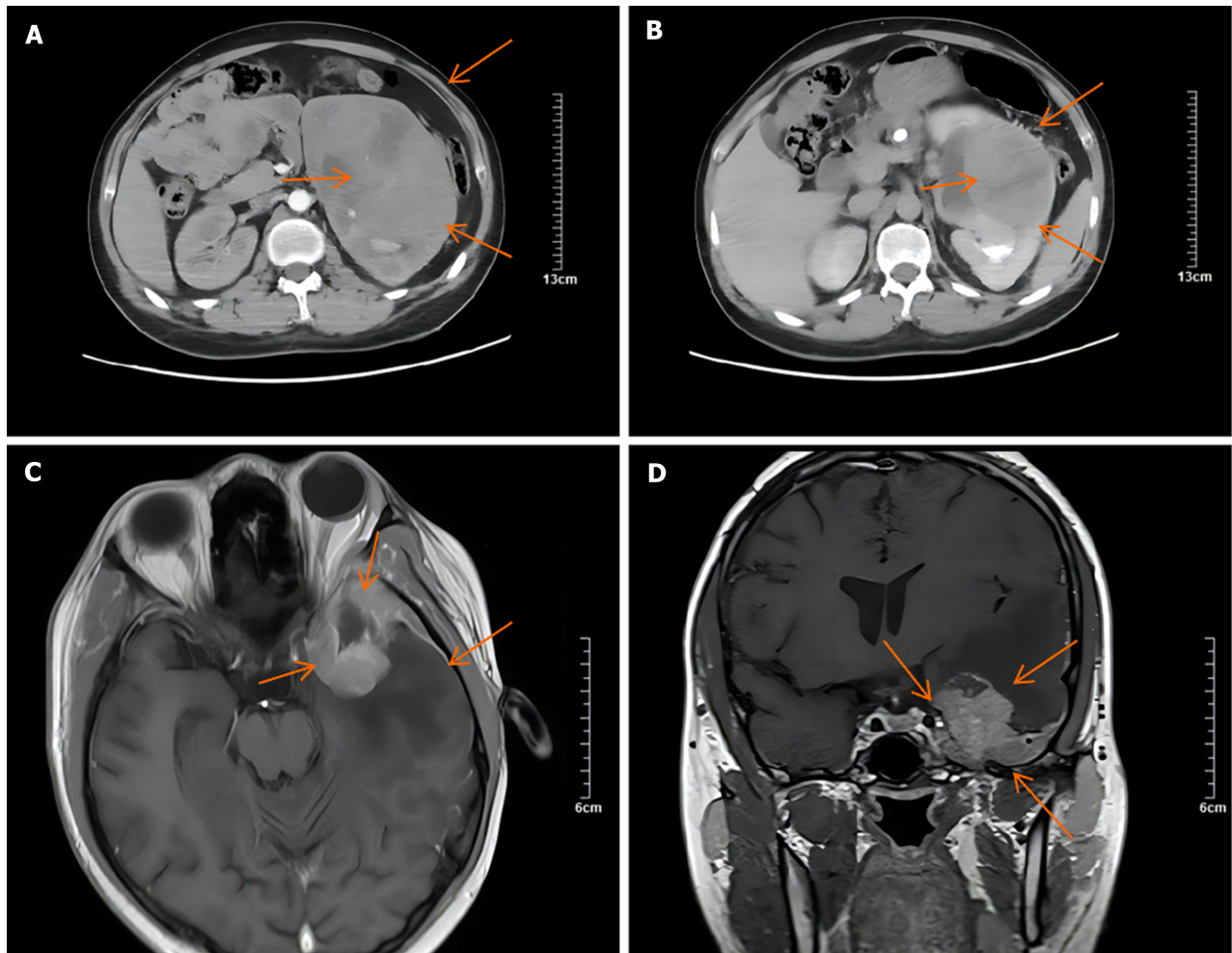


**Figure 2 Computed tomography and magnetic resonance imaging.** A and B: Corticomedullary and excretory phase axial computed tomography shows that the large tumor (11.65 cm × 10.91 cm) showed scattered irregular enhancement with large areas of necrosis; C and D: Magnetic resonance imaging coronal and axial view of the head showed mixed signals in the left temporal lobe, suggesting tumor metastasis.

tinued. The patient was followed up at 4 and 9 months after surgery.

**OUTCOME AND FOLLOW-UP**

The patient was followed up at 4 and 9 months post-surgery. Up to 9 months post-surgery, the patient was well-nourished, clear-minded, and free to move physically, with a weight loss of 2 kg. The patient reported no dizziness, nausea, vomiting, or facial acne. The purple stripes on the abdomen disappeared, and those from other body parts had reduced. The patient could perform day-to-day activities such as driving. The patient and his family were satisfied with the effectiveness of the treatment. However, the patient was eventually lost to follow-up two years after surgery

**DISCUSSION**

Primary renal ES/primary neuroectodermal tumors (PNETs) are extremely rare and highly malignant. Since Seemayer *et*

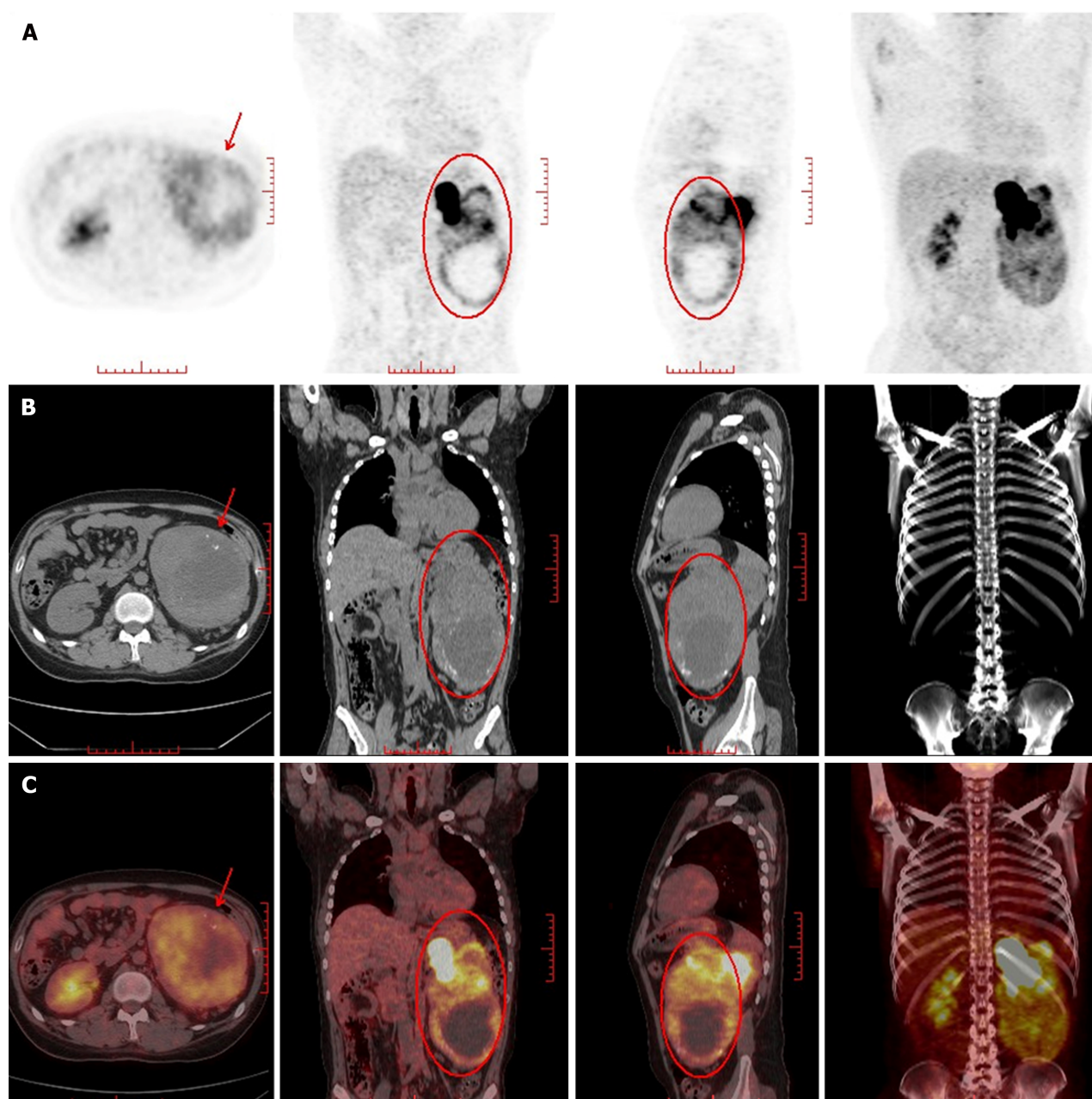


**Figure 3 Nuclear medicine image of the primary tumor.** A: Increased radioactivity in the left kidney; B: A large mass of mixed density was found in the left kidney. The large cross section of the lesion was about 11.8 cm × 9.7 cm; C: The solid component showed uneven radioactive concentration, Maximum Standardized Uptake Value 10.4, the left side of the kidney was compressed and displaced upward, and the renal calyx was dilated and hydronephrosis.

*al*[3], the first reported renal PNET was in 1975, and the number of cases reported worldwide was less than 200. The pathological type of CS caused by ectopic ACTH/CRH in Primary renal ES is rare and is usually a neuroendocrine tumor and individual nephroblastoma[4]. The most prominent feature of our case was that the primary renal ES had neuroendocrine function and secreted ectopic ACTH/CRH, which led to CS. In many reports, primary renal ES does not involve neuroendocrine function. Moreover, most of the symptoms are nonspecific, majorly involving lumbar pain. Some patients also have macroscopic or microscopic hematuria[5-7]. According to the PubMed database, only a few studies have reported the terms “Ewing's sarcoma and Cushing's syndrome” (four reports)[8-11], and even fewer studies have reported the term “Renal Ewing's sarcoma and Cushing's syndrome” (two studies)[8,12].

Renal ES is difficult to diagnose and usually does not have specific imaging manifestations. CT usually reveals large heterogeneous masses accompanied by large necrosis and uneven enhancement. As renal ES is highly malignant, approximately 57% of patients already have metastasis at the time of diagnosis[13]. Therefore, it is necessary to perform enhanced CT and bone scans to detect metastasis in patients with suspected renal ES. PET-CT is more advantageous for identifying small metastases, through which we identified many small bone metastases in our case. All the above examinations lack specificity, and the final diagnosis requires histopathological manifestations and immunophenotyping. When it is necessary to differentiate between the pathological types of tumors, such as nephroblastoma and neuroblastoma, a clear diagnosis can be made by adding the corresponding molecular pathological tests. Using immunophenotyping, the examiner can specifically judge whether the tumor produces ectopic ACTH or CRH. Histologically, the tumor cells are

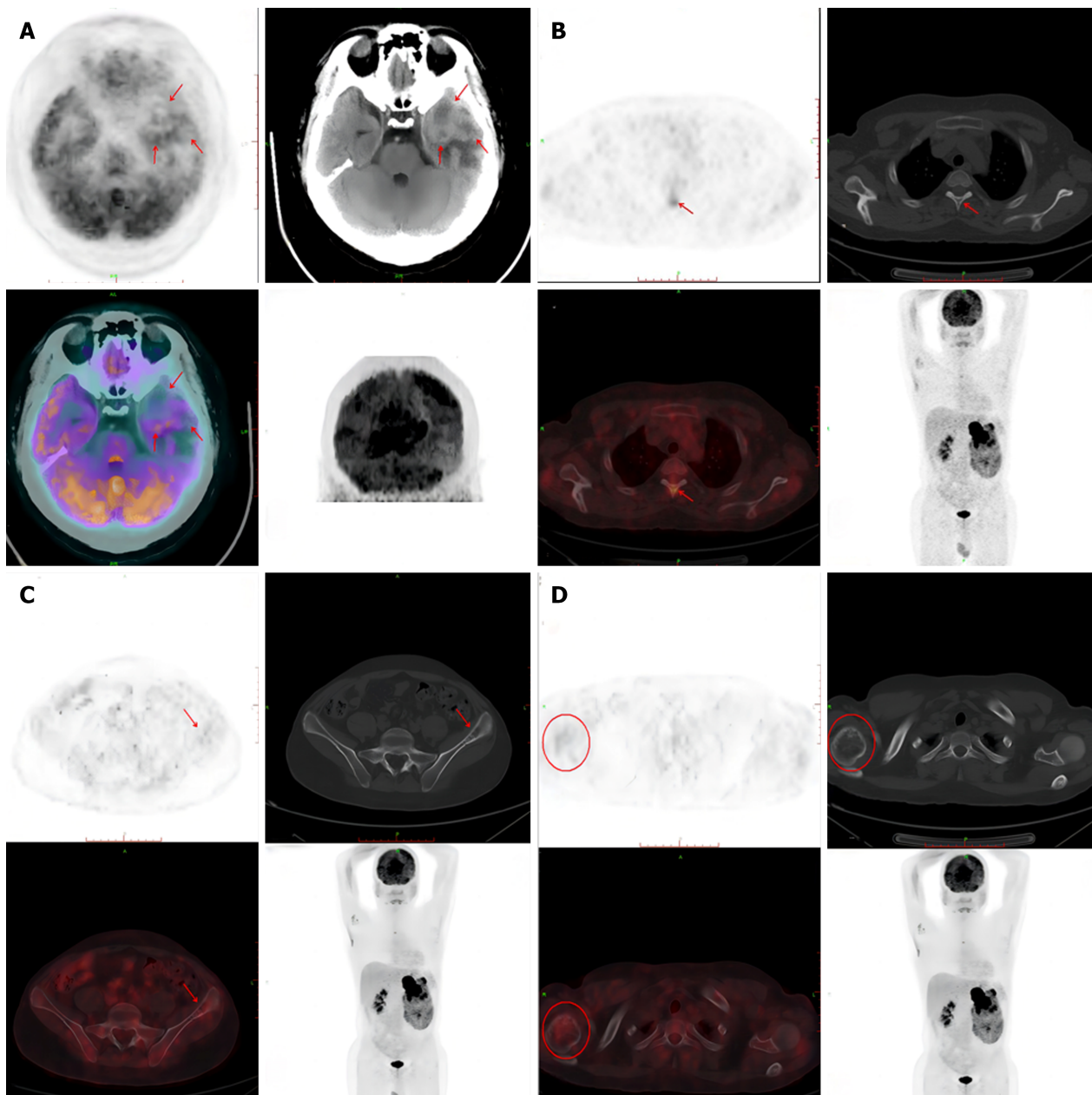


**Figure 4 Nuclear medicine image of metastatic tumors.** A: The shape of the brain was as usual, with a slightly high-density mass in the left temporal pole and a few low-density shadows in the center. The larger section was about 3.3 cm × 2.2 cm. The periphery of the lesion showed large patches of low-density edema. PET showed annular high uptake of radioactivity in the lesion, Maximum Standardized Uptake Value (SUVmax) 9.1; B: High radioactive uptake shadow was found in the thoracic third vertebral arch plate, SUVmax 5.0, and no obvious bone destruction was found in the corresponding part; C and D: Left iliac wing, right humeral head and local bone of density is decreases, and a small amount of radioactive uptake was observed in the corresponding parts. The SUVmax was 2.7.

distributed in slices or lobules under a microscope and are uniformly round and oval. The nuclei are large and hyperchromatic, and different degrees of karyokinesis are observed. The cytoplasm is clear, and some cells can be vacuolated. Homer-Wright chrysanthemums have relatively characteristic structures with varying degrees of neural differentiation[14].

Regarding immunohistochemistry, most primary renal ESs are positive for the transmembrane glycoprotein CD99, encoded by MIC2. In addition, the endocrine and neuroendocrine system markers NSE, CgA, and Syn can be positive. VIM, CD56, and hemophilia transcription integration factor 1 are also observed in some primary renal ESs. Moreover, epithelial markers, such as cytokeratin and EMA, are usually negative[14,15].

The first challenge the patient must face is the difficulty in diagnosis, where the patient first exhibits severe CS and then seeks the primary focus according to the principle of quality action before positioning. Low-dose dexamethasone failed to inhibit the secretion of cortisol, indicating that the patient had ACTH-dependent CS. The high-dose dexamethasone suppression test revealed a failure to inhibit cortisol secretion, suggesting that Cushing's disease could be excluded. Therefore, the patient may have had ectopic ACTH syndrome or ectopic CRH syndrome. Immunohistochemistry revealed negative ACTH levels. Due to the limitations of technical conditions, immunohistochemical detection of CRH could not be performed; therefore, the tumor may have produced ectopic CRH or ACTH analogs.

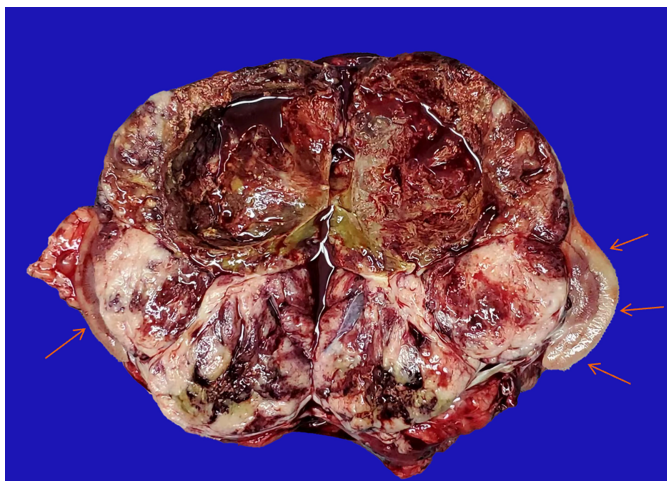


**Figure 5 Gross specimen.** A huge tumor has invaded the entire kidney (coronal cut), leaving only a small portion of normal kidney tissue (Orange arrow). The internal cystic changes of the tumor were accompanied by bleeding and necrosis.

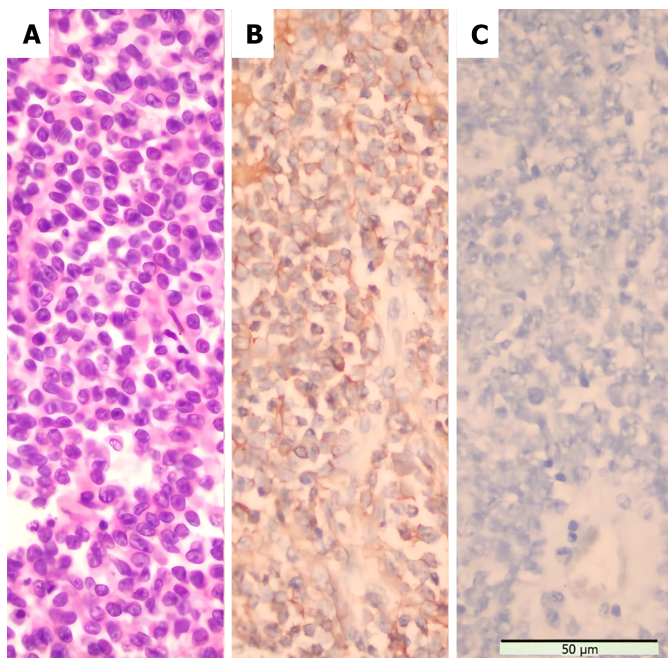


**Figure 6 Morphological features and immunostaining results of the tumor.** A: Small, round tumor cells can be seen scattered throughout the visual field Staining method: HE staining (400 ×); B: Diffuse hyperstaining of tumor cell membrane for CD99 Staining method: Polymer method (400 ×); C: No positive reaction was observed for adrenocorticotrophic hormone staining method: Polymer method (400 ×).

Only 20 cases of ectopic CRH syndrome have been reported worldwide, mostly due to medullary thyroid carcinoma (33%) and pheochromocytoma (19%), as well as carcinoid (5%) and small cell lung cancer (9.5%), which are relatively rare. If a patient produces ectopic CRH, it is generally believed that a high-dose dexamethasone suppression test can reduce the cortisol levels[16]. However, the patient showed the opposite result when high-dose dexamethasone was administered, possibly because the auxo-action of ectopic CRH on ACTH exceeded the inhibition of high-dose dexamethasone on pituitary ACTH. Only three of the 20 reported cases presented the same situation as this patient[17-19].

Pro-opiomelanocortin (POMC), the precursor of ACTH, produces ACTH, melanocyte-stimulating hormone, and other products *via* a series of processes[20]. Incorrect processing of POMC in tumor cells is likely to produce derivatives with ACTH functions. In addition, false-negative immunohistochemical reactions may be caused by the inability to store and release ACTH rapidly after production.

The relevant reports are mostly case reports owing to the low incidence of primary renal ES. Currently, there is a lack of standard treatment plans, and the treatment mainly involves exaires is combined with radiotherapy, chemotherapy, or targeted therapy. Owing to the malignant degree of primary renal ES and the large volume of the tumor, radical nephrectomy is the first choice of surgery. There is a significant correlation between chemotherapy and overall survival (OS). Neoadjuvant chemotherapy can contribute to tumor downstaging and resect ability, improving the prognosis of

patients[21-24]. In comparison, adjuvant chemotherapy can prevent tumor recurrence and metastasis[25]. However, owing to the lack of contrast tests, the existing evidence cannot determine which method is most beneficial to patients. The most commonly used treatments are VDC (vincristine + doxorubicin + decacyclophosphamide), IE (ifosfamide + etoposide), *etc.*[2,21,26]. In addition, in the EURO-E.W.I.N.G.99 experiment in Europe, the researchers used the VIDE protocol (vincristine + ifosfamide + doxorubicin + etoposide) during the induction period and the VAI protocol (vincristine + actinomycin + ifosfamide) or a large dose of busulfan/ melphalan followed by autologous stem cell transplantation according to risk stratification during the consolidation period for 24 patients with primary renal ES[18]. It is difficult to judge whether radiotherapy can benefit patients according to existing research; however, some researchers use radiotherapy to irradiate the surgical area after surgery, and reducing the residual focus significantly[21, 27].

Furthermore, there have been few reports on targeted drug treatments for primary renal ES. To date, there are only a few reports on the treatment of ES using pazopanib[28]. Zhao *et al* [29] reported a case of partial remission after the use of apatinib. The prognosis of primary renal ES was poor. In a retrospective analysis of 48 patients, the average survival time of patients with metastatic diseases was 26.14 months[30]. The Anderson Cancer Center in the United States analyzed the 4-year median event-free survival (EFS) and OS rates of 30 patients with primary renal ES in a single center with no metastasis at the time of diagnosis. These were 54% and 85%, respectively. However, the incidence rates for patients with metastasis were 35% and 47%, respectively[21]. A previous study analyzed the 3-year median EFS and OS of 22 patients with primary renal ES in EURO-E.W.I.N.G.99, diagnosed as non-metastatic. These were 78% and 92%, respectively. For patients with metastasis, these were 45% and 58%, respectively[27]. Therefore, early detection and comprehensive treatment are key to improving the prognosis.

The second challenge is treatment. Our patient had primary renal ES with CS and extensive brain and bone metastases at the time of diagnosis. Considering that the patient had severe CS and metabolic disorder, an open total left nephrectomy was performed to relieve symptoms, identify pathological types, and eradicate the tumors. Cortisol and ACTH levels returned to normal on the third day after surgery. The patient was discharged six days after the surgery. Subsequently, two courses of VDC chemotherapy were administered; the patient's symptoms improved, and the intracranial metastatic tumors were significantly reduced. However, the long-term effects require further follow-up.

At the gene level, gene mutation caused by chromosome heterotopia is the main cause of ES. The types include t (11; 22) (q24; q12), t (21; 22) (q22; q12), t (7; 22) (p22; q12), t (17; 22) (q12; q12), and t (2; 22) (q33; q12), which produce *EWS/FLI1*, *EWS/ERG*, *EWS/ETV1*, *EWS/E1AF*, and *EWS/FEV*, respectively. Approximately 85% of patients with ES exhibit *EWS/FLI1*[31], which encodes a transcription factor that promotes tumor growth by influencing gene transcription or RNA splicing. However, ES, does not affect the transcription of the CD99 gene but directly affects the expression of CD99 on the cell membrane. *EWS-FLI1* interacts with CD99 to influence the expression of CD99 through a complex post-transcriptional regulatory mechanism. CD99 is not only a marker but is also directly involved in the proliferation and metastasis of ES[32,33]. The patient harbored a typical *EWS/FLI1* mutation, which further verified the diagnosis and provided guidance for future treatments.

## CONCLUSION

In summary, primary renal ES is a rare adult malignant tumor with a poor prognosis. CS is its rare clinical manifestation. When assessing the patient, the principle of prioritization before quality must be followed in diagnosis. While gene tests are helpful for diagnosis and can guide treatment (although they are not a necessary examination method for this disease), the "gold standard" for diagnosing primary renal ES is still pathological examination. Comprehensive surgical treatment based on surgery can achieve certain effects in advanced metastatic primary renal ES.

## ACKNOWLEDGEMENTS

The authors are grateful for invaluable support and useful discussions with other members of the urology department.

## FOOTNOTES

**Author contributions:** Dong GF and Hou YK wrote the main manuscript text, contributed equally to this paper; Ma Q and Ma SY prepared the figures. Wang YJ and Rexiati M were responsible for conceptualization and supervision; Wang WG was responsible for supervision and replied to peer review. All the authors reviewed their participation in the treatment and reviewed the manuscript.

**Informed consent statement:** The use of human blood samples was in accordance with the legislation in China. Informed consent was obtained from the relatives of the patient. Written informed consent was obtained from the patient's relatives for the publication of this case report and any accompanying images.

**Conflict-of-interest statement:** We declare that there are no conflicts of interest between the authors.

**CARE Checklist (2016) statement:** The authors have read the CARE Checklist (2016), and the manuscript was prepared and revised according to the CARE Checklist (2016).

**Open-Access:** This article is an open-access article that was selected by an in-house editor and fully peer-reviewed by external reviewers. It is distributed in accordance with the Creative Commons Attribution NonCommercial (CC BY-NC 4.0) license, which permits others to distribute, remix, adapt, build upon this work non-commercially, and license their derivative works on different terms, provided the original work is properly cited and the use is non-commercial. See: <https://creativecommons.org/licenses/by-nc/4.0/>

**Country of origin:** China

**ORCID number:** Guo-Fan Dong 0000-0002-2617-4442; Wen-Guang Wang 0009-0007-9409-9388.

**S-Editor:** Liu H

**L-Editor:** A

**P-Editor:** Cai YX

## REFERENCES

- 1 **Riggi N**, Suvà ML, Stamenkovic I. Ewing's Sarcoma. *N Engl J Med* 2021; **384**: 154-164 [PMID: 33497548 DOI: 10.1056/NEJMra2028910]
- 2 **Liang L**, Song H, Ma B, Zhang Z, Zhu K, Li Q, Zhou C, Li A, Liu J, Zhang Q, Zhu S, Zhang Q. Renal Ewing's sarcoma/primitive neuroectodermal tumor (PNET): a case series of 7 patients and literature review. *Transl Androl Urol* 2021; **10**: 548-554 [PMID: 33718057 DOI: 10.21037/tau-20-1122]
- 3 **Seemayer TA**, Thelmo WL, Bolande RP, Wiglesworth FW. Peripheral neuroectodermal tumors. *Perspect Pediatr Pathol* 1975; **2**: 151-172 [PMID: 1129029]
- 4 **Arlt A**, Harbeck B, Anlauf M, Alkatout I, Klöppel G, Fölsch UR, Bewig B, Mönig H. Fatal pneumocystis jirovecii pneumonia in a case of ectopic Cushing's syndrome due to neuroendocrine carcinoma of the kidney. *Exp Clin Endocrinol Diabetes* 2008; **116**: 515-519 [PMID: 18523920 DOI: 10.1055/s-2008-1062729]
- 5 **Cochetti G**, Paladini A, de Vermandois JAR, Fatigoni S, Zanelli M, Ascani S, Mearini E. Metastatic renal Ewing's sarcoma in adult woman: Case report and review of the literature. *Open Med (Wars)* 2021; **16**: 397-409 [PMID: 33748424 DOI: 10.1515/med-2021-0207]
- 6 **Kozel ZM**, Reifsnnyder JE, Griffiths L, Gitlin JS, Kavoussi LR. Primary renal Ewing Sarcoma masquerading as Wilms in an adolescent female. *Urol Case Rep* 2020; **31**: 101187 [PMID: 32322516 DOI: 10.1016/j.eucr.2020.101187]
- 7 **Doroudinia A**, Ahmadi S, Mehrian P, Pourabdollah M. Primary Ewing sarcoma of the kidney. *BMJ Case Rep* 2019; **12** [PMID: 30696641 DOI: 10.1136/bcr-2018-227198]
- 8 **Karguppikar MB**, Oza CM, Khadilkar V, Khadilkar A. Rare case of renal Ewing sarcoma presenting as ectopic Cushing syndrome in a 12-year-old girl. *BMJ Case Rep* 2022; **15** [PMID: 35131789 DOI: 10.1136/bcr-2021-246751]
- 9 **Di Ruscio V**, Del Baldo G, De Pasquale MD, De Vito R, Miele E, Colafati GS, Deodati A, De Ioris MA, Tornesello A, Milano GM, Mastronuzzi A. Ectopic ACTH Secretion in a Child With Metastatic Ewing's Sarcoma: A Case Report. *Front Oncol* 2020; **10**: 574 [PMID: 32411598 DOI: 10.3389/fonc.2020.00574]
- 10 **Guran T**, Turan S, Ozkan B, Berrak SG, Canpolat C, Dagli T, Eren FS, Bereket A. Cushing's syndrome due to a non-adrenal ectopic adrenocorticotropin-secreting Ewing's sarcoma in a child. *J Pediatr Endocrinol Metab* 2009; **22**: 363-368 [PMID: 19554811 DOI: 10.1515/jpem.2009.22.4.363]
- 11 **Preeyasombat C**, Sirikulchayanonta V, Mahachokekeltwattana P, Sriphrapradang A, Boonpucknavig S. Cushing's syndrome caused by Ewing's sarcoma secreting corticotropin releasing factor-like peptide. *Am J Dis Child* 1992; **146**: 1103-1105 [PMID: 1325112 DOI: 10.1001/archpedi.1992.02160210105034]
- 12 **Mao W**, Xu J, Lu H, Wang Y, Zhang L, Chen M. A rare case report of renal ewing sarcoma/primitive neuroectodermal tumor with ACTH production. *BMC Urol* 2022; **22**: 103 [PMID: 35821028 DOI: 10.1186/s12894-022-01055-y]
- 13 **Ellinger J**, Bastian PJ, Hauser S, Biermann K, Müller SC. Primitive neuroectodermal tumor: rare, highly aggressive differential diagnosis in urologic malignancies. *Urology* 2006; **68**: 257-262 [PMID: 16904430 DOI: 10.1016/j.urology.2006.02.037]
- 14 **Bing Z**, Zhang P, Tomaszewski JE, MacLennan GT. Primary Ewing sarcoma/primitive neuroectodermal tumor of the kidney. *J Urol* 2009; **181**: 1341-1342 [PMID: 19157457 DOI: 10.1016/j.juro.2008.12.029]
- 15 **Risi E**, Iacovelli R, Altavilla A, Alesini D, Palazzo A, Mosillo C, Trenta P, Cortesi E. Clinical and pathological features of primary neuroectodermal tumor/Ewing sarcoma of the kidney. *Urology* 2013; **82**: 382-386 [PMID: 23800653 DOI: 10.1016/j.urology.2013.04.015]
- 16 **Wu J**, Lu AD, Zhang LP, Zuo YX, Jia YP. [Study of clinical outcome and prognosis in pediatric core binding factor-acute myeloid leukemia]. *Zhonghua Xue Ye Xue Za Zhi* 2019; **40**: 52-57 [PMID: 30704229 DOI: 10.3760/cma.j.issn.0253-2727.2019.01.010]
- 17 **Shahani S**, Nudelman RJ, Nalini R, Kim HS, Samson SL. Ectopic corticotropin-releasing hormone (CRH) syndrome from metastatic small cell carcinoma: a case report and review of the literature. *Diagn Pathol* 2010; **5**: 56 [PMID: 20807418 DOI: 10.1186/1746-1596-5-56]
- 18 **Chrisoulidou A**, Pazaitou-Panayiotou K, Georgiou E, Boudina M, Kontogeorgos G, Iakovou I, Efstratiou I, Patakiouta F, Vainas I. Ectopic Cushing's syndrome due to CRH secreting liver metastasis in a patient with medullary thyroid carcinoma. *Hormones (Athens)* 2008; **7**: 259-262 [PMID: 18694866 DOI: 10.1007/BF03401514]
- 19 **Auchus RJ**, Mastorakos G, Friedman TC, Chrousos GP. Corticotropin-releasing hormone production by a small cell carcinoma in a patient with ACTH-dependent Cushing's syndrome. *J Endocrinol Invest* 1994; **17**: 447-452 [PMID: 7930390 DOI: 10.1007/BF03347737]
- 20 **Beuschlein F**, Hammer GD. Ectopic pro-opiomelanocortin syndrome. *Endocrinol Metab Clin North Am* 2002; **31**: 191-234 [PMID: 12055989 DOI: 10.1016/s0889-8529(01)00025-1]
- 21 **Tarek N**, Said R, Andersen CR, Suki TS, Foglesong J, Herzog CE, Tannir NM, Patel S, Ratan R, Ludwig JA, Daw NC. Primary Ewing Sarcoma/Primitive Neuroectodermal Tumor of the Kidney: The MD Anderson Cancer Center Experience. *Cancers (Basel)* 2020; **12** [PMID: 33050651 DOI: 10.3390/cancers12102927]
- 22 **Perer E**, Shanberg AM, Matsunaga G, Finklestein JZ. Laparoscopic removal of extraosseous Ewing's sarcoma of the kidney in a pediatric patient. *J Laparoendosc Adv Surg Tech A* 2006; **16**: 74-76 [PMID: 16494555 DOI: 10.1089/lap.2006.16.74]

- 23 **Abolhasani M**, Salarinejad S, Moslemi MK. Ewing sarcoma/primitive neuroectodermal tumor of the kidney: A report of three cases. *Int J Surg Case Rep* 2016; **28**: 330-334 [PMID: 27776324 DOI: 10.1016/j.ijscr.2016.10.014]
- 24 **Rowe RG**, Thomas DG, Schuetze SM, Hafez KS, Lawlor ER, Chugh R. Ewing sarcoma of the kidney: case series and literature review of an often overlooked entity in the diagnosis of primary renal tumors. *Urology* 2013; **81**: 347-353 [PMID: 23374800 DOI: 10.1016/j.urology.2012.10.016]
- 25 **Ohgaki K**, Horiuchi K, Mizutani S, Sato M, Kondo Y. Primary Ewing's sarcoma/primitive neuroectodermal tumor of the kidney that responded to low-dose chemotherapy with ifosfamide, etoposide, and doxorubicin. *Int J Clin Oncol* 2010; **15**: 210-214 [PMID: 20186557 DOI: 10.1007/s10147-010-0031-3]
- 26 **Yoshihara H**, Kamiya T, Hosoya Y, Hasegawa D, Ogawa C, Asanuma H, Mizuno R, Hosoya R, Manabe A. Ewing sarcoma/primitive neuroectodermal tumor of the kidney treated with chemotherapy including ifosfamide. *Pediatr Int* 2016; **58**: 766-769 [PMID: 27324740 DOI: 10.1111/ped.12963]
- 27 **Zöllner S**, Dirksen U, Jürgens H, Ranft A. Renal Ewing tumors. *Ann Oncol* 2013; **24**: 2455-2461 [PMID: 23761687 DOI: 10.1093/annonc/mdt215]
- 28 **Attia S**, Okuno SH, Robinson SI, Webber NP, Indelicato DJ, Jones RL, Bagaria SP, Jones RL, Sherman C, Kozak KR, Cortese CM, McFarland T, Trent JC, Maki RG. Clinical Activity of Pazopanib in Metastatic Extraosseous Ewing Sarcoma. *Rare Tumors* 2015; **7**: 5992 [PMID: 26266019 DOI: 10.4081/rt.2015.5992]
- 29 **Zhao Y**, Chen Y, Cheng K, Li ZP, Zeng H, Liu JY. Renal Ewing sarcoma treated with apatinib. *Anticancer Drugs* 2018; **29**: 702-704 [PMID: 29782348 DOI: 10.1097/CAD.0000000000000630]
- 30 **Hakky TS**, Gonzalvo AA, Lockhart JL, Rodriguez AR. Primary Ewing sarcoma of the kidney: a symptomatic presentation and review of the literature. *Ther Adv Urol* 2013; **5**: 153-159 [PMID: 23730330 DOI: 10.1177/1756287212471095]
- 31 **Sorensen PH**, Lessnick SL, Lopez-Terrada D, Liu XF, Triche TJ, Denny CT. A second Ewing's sarcoma translocation, t(21;22), fuses the EWS gene to another ETS-family transcription factor, ERG. *Nat Genet* 1994; **6**: 146-151 [PMID: 8162068 DOI: 10.1038/ng0294-146]
- 32 **Ventura S**, Aryee DN, Felicetti F, De Feo A, Mancarella C, Manara MC, Picci P, Colombo MP, Kovar H, Carè A, Scotlandi K. CD99 regulates neural differentiation of Ewing sarcoma cells through miR-34a-Notch-mediated control of NF-κB signaling. *Oncogene* 2016; **35**: 3944-3954 [PMID: 26616853 DOI: 10.1038/onc.2015.463]
- 33 **Franzetti GA**, Laud-Duval K, Bellanger D, Stern MH, Sastre-Garau X, Delattre O. MiR-30a-5p connects EWS-FLI1 and CD99, two major therapeutic targets in Ewing tumor. *Oncogene* 2013; **32**: 3915-3921 [PMID: 22986530 DOI: 10.1038/onc.2012.403]



## Rare extraintestinal manifestations of ulcerative colitis treated with dual biologic therapy: A case report

Aleksandra Filipiuk, Maciej Gonciarz

**Specialty type:** Medicine, research and experimental

**Provenance and peer review:** Unsolicited article; Externally peer reviewed.

**Peer-review model:** Single blind

**Peer-review report's classification**

**Scientific Quality:** Grade C

**Novelty:** Grade B

**Creativity or Innovation:** Grade C

**Scientific Significance:** Grade C

**P-Reviewer:** Yamamoto S

**Received:** April 27, 2024

**Revised:** May 29, 2024

**Accepted:** June 20, 2024

**Published online:** August 16, 2024

**Processing time:** 68 Days and 15.9 Hours



**Aleksandra Filipiuk, Maciej Gonciarz**, Department of Gastroenterology and Internal Medicine, Military Institute of Medicine–National Research Institute in Warsaw, Warsaw 04-141, Poland

**Corresponding author:** Aleksandra Filipiuk, MD, Doctor, Department of Gastroenterology and Internal Medicine, Military Institute of Medicine–National Research Institute in Warsaw, Szaserów 128, Warsaw 04-141, Poland. [afilipiuk@wim.mil.pl](mailto:afilipiuk@wim.mil.pl)

### Abstract

#### BACKGROUND

Ulcerative colitis (UC) is an idiopathic, chronic inflammatory bowel disease (IBD) most often located in the rectum, but may involve the entire colon. Extra intestinal manifestations (EIMs) occur with varying frequency depending on the affected organ. The most common ones are musculoskeletal EIMs, affecting up to 33%-40% of IBD patients. These include, among others, inflammatory back pain, tendinitis, plantar fasciitis and arthritis. Only a few case reports in literature discuss Achilles tendinitis.

#### CASE SUMMARY

This report describes a patient with UC and Achilles tendinitis in whom after many unsuccessful attempts of treatment with sulfasalazine, mesalazine, glucocorticosteroids, infliximab and tofacitinib, a complete UC remission and resolution of Achilles tendinitis were achieved with the use of dual biologic therapy (DBT)-ustekinumab and adalimumab (ADA).

#### CONCLUSION

This case mentions rare EIMs of UC and suggests that DBT may be an alternative for patient with ulcerative colitis and EIMs.

**Key Words:** Achilles tendinitis; Dual biologic therapy; Extraintestinal manifestations; Spondyloarthropathy; Ulcerative colitis; Case report

©The Author(s) 2024. Published by Baishideng Publishing Group Inc. All rights reserved.

**Core Tip:** Achilles tendinitis is one of the rarest extra intestinal manifestations of ulcerative colitis (UC). To our best knowledge only a few case reports in literature discuss this problem. This article is a case report of a patient immobilized by Achilles tendinitis and excluded from social life by a very long-lasting exacerbation of UC. His way to recovery was full of ups and downs. We tried many lines of biological treatment with no permanent success. Only dual biologic therapy with ustekinumab and adalimumab thanks to combining two mechanisms of action brought the desired effect—a steroid free remission of UC and Achilles tendinitis.

**Citation:** Filipiuk A, Gonciarz M. Rare extraintestinal manifestations of ulcerative colitis treated with dual biologic therapy: A case report. *World J Clin Cases* 2024; 12(23): 5441-5447

**URL:** <https://www.wjgnet.com/2307-8960/full/v12/i23/5441.htm>

**DOI:** <https://dx.doi.org/10.12998/wjcc.v12.i23.5441>

## INTRODUCTION

Ulcerative colitis (UC) is an autoimmune disease localized in the large intestine. According to the literature, extra intestinal manifestations (EIMs) of UC originating from the musculoskeletal system are in the range of 33% to 40%[1-3]. In recent years significant progress has been made in understanding the pathogenesis of arthritis associated with inflammatory bowel disease (IBD) although the exact pathomechanism linking gut inflammation with arthritis and tendinitis still remains unclear. The coexistence of EIMs including musculoskeletal symptoms worsens the quality of patients' lives and usually requires separate specialized pharmacological treatment and rehabilitation. In 2007, for the first time, a study demonstrating the safety of dual biologic therapy (DBT) was published[4]. Since then, there has been some progress, especially with the introduction of small molecules such as Janus kinase inhibitors and drugs modulating the sphingosine-1-phosphate signaling pathway into the therapy of IBD.

## CASE PRESENTATION

### Chief complaints

A 47-year-old Caucasian man, tax official with UC was admitted to our department in order to qualify for a biological therapy. On admission, the patient was passing 15 loose, non-bloody stools *per day*. At that time, the patient denied the presence of EIMs, but in the past had complained of ankle and knee pain. However, during the treatment described here, after glucocorticosteroids (GCs) dose reduction patient complained of severe Achilles tendons pain, leading to patient's immobility.

### History of present illness

The patient was diagnosed with UC 22 years ago and had a long history of treatment with 5-aminosalicylic acid and GCs, but also a short ineffective course of cyclosporine complicated by transient bone marrow aplasia. On admission, the patient was taking 28 mg of methylprednisolone (MP) orally daily.

### History of past illness

The patient's past medical history revealed osteopenia, hyperlipidemia, depression and hypertension.

### Personal and family history

There was no history of ethanol or drug abuse, herbal use or depot injections. The patient was vaccinated according to the local vaccination schedule. His family history was insignificant.

### Physical examination

Physical examination revealed stable vital signs, his body mass index was 29 (height 176 cm, weight 90 kg) and heart rate was 110/min. Also, tenderness in the lower abdomen was found. The negative Otto test 3 cm ( $n > 3$  cm) and a positive Schober test 3 cm ( $n > 4.5$  cm) in physical examination indicated a reduction in mobility of the spine in the lumbar region. The Patrick's test was negative bilaterally.

### Laboratory examinations

Abnormalities in laboratory tests included increased calprotectin stool concentration-410.5 mg/kg ( $n < 50$ ) and C-reactive protein (CRP) serum concentration - 1.1 mg/dL ( $n$ : 0-0.8 mg/dL). The liver enzymes and renal parameters were within the normal range. Possible infectious triggers of the exacerbation were excluded: Serological tests for Epstein-Barr virus, cytomegalovirus as well as stool cultures for *Salmonella*, *Shigella*, *Yersinia*, *Campylobacter*, enterotoxigenic *E. coli*, and also *Clostridioides* were negative. The serum CRP concentration persisted at 1.2 mg/dL ( $n$ : 0-0.8) and the peripheral white blood cells remained within normal range. A radiological examination of the chest as well as abdominal ultrasound

examination showed no abnormalities. The rheumatoid factor, anti-cyclic citrullinated peptide antibodies and human leukocyte antigen B27 were negative.

### Imaging examinations

The first endoscopic examination during steroid therapy showed the Mayo endoscopic score of 1 with a full Mayo Score of 6. After a few lines of treatment, another endoscopic examination revealed the disease activity at Mayo 3 (Figure 1A) with a full Mayo Score of 9. Also, an ultrasound of the tendons was performed, confirming their bilateral inflammation (Figure 2). At the time, the patient was also examined for other EIMs of UC, revealing bilateral sacroiliitis and Achilles tendon enthesopathy (Figures 3 and 4). The spine X-ray showed squaring of the vertebral bodies in the area of the thoracic-lumbar junction, right-sided curvature of the spine in the Th/L section and degenerative changes of the intervertebral joints.

## FINAL DIAGNOSIS

In concordance with the Assessment of SpondyloArthritis International Society (ASAS) 2010 criteria, seronegative peripheral SpA was diagnosed as an EIM of UC[5].

## TREATMENT

Due to the moderate-severe relapse of the UC after many years of ineffective GCs therapy, the patient was qualified for biological therapy with infliximab (INF) administered intravenously at a dose of 5 mg/kg resulting in clinical improvement after induction therapy. Concurrently, MP dose reduction was initiated and when the MP dose was 20 mg *per day*, the patient complained of Achilles tendon pain for the first time in his life. The treatment with INF was continued, achieving complete steroid-free clinical remission of UC on the 6th week of the treatment. The tendon pain, however, persisted and the patient was additionally on oral non-steroidal anti-inflammatory drugs. On the 12<sup>th</sup> week of the treatment, the patient experienced an exacerbation of the UC. Physical examination revealed mild abdominal tenderness, as well as swelling and tenderness in the area of the heel attachment of the Achilles tendons bilaterally. Endoscopic examination revealed the disease activity at Mayo 3 with a full Mayo Score of 9 (significant deterioration compared to the beginning of the therapy). Consequently, it was decided to convert biological therapy to tofacitinib (TOFA) at a dose of 10 mg orally twice daily and reintroduce MP at a dose of 16 mg daily. The efficacy of TOFA was evaluated at week 8 of the treatment. The patient remained in clinical remission, and colonoscopy showed Mayo endoscopic score of 1 with a full Mayo score of 3. Unfortunately, it was not possible to completely discontinue MP, as with a dose below 6 mg, recurrence of the tendon pain was observed, yet of a much lower intensity than before. For this reason, it was decided to convert the treatment with mesalazine at a dose of 4 g to sulfasalazine at a dose of 4 g daily. At week 8 of the treatment, after clinical and endoscopic response, the dosage of TOFA was reduced to 5 mg twice a day. At week 15 of the therapy (with MP dose of 4 mg), the patient presented to the outpatient clinic with a significant increase in Achilles tendon pain (6/10 in the numerical rating scale) and also ankle, knee and shoulder joints pain. He remained in clinical remission for intestinal symptoms, sigmoidoscopy showed Mayo endoscopic score of 1 and the dose of TOFA was increased to 10 mg twice daily. At week 26 of therapy, joint symptoms and tendon pain persisted resulting in the patient requiring daily opioids. In addition, an exacerbation of intestinal symptoms has recurred. The sigmoidoscopy revealed an increase in disease activity-Mayo endoscopic score of 2, with the total Mayo score of 8, a decision was made to change treatment to ustekinumab (UST) (520 mg intravenously). Eight weeks after the induction dose, a reduction in the total Mayo score from 8 to 5 was observed, as well as a slight improvement in tendon and joint pain, with no endoscopic improvement. The patient was then placed on DBT, UST dosing was maintained 90 mg subcutaneously every 8 weeks and INF was added at a dose of 5 mg/kg intravenously, but unfortunately with the 2<sup>nd</sup> dose, the patient experienced anaphylactic shock. Consequently, we decided to combine UST with adalimumab (ADA) at an induction dose of 160 mg subcutaneously, next 80 mg after 2 weeks, and then 40 mg every 2 weeks. After steroid discontinuation the patient suffered from tendons pain again, but of lower intensity. Then, we added methotrexate (MTX) at a dose of 15 mg subcutaneously weekly to DBT.

## OUTCOME AND FOLLOW-UP

After 12 weeks of DBT combined with MTX for 2 months, the effectiveness of the treatment was evaluated. The patient has remained in steroid-free clinical remission, joint pains have subsided and tendon pain has remained minimal, requiring only rehabilitation and periodic low doses of analgesics. The colonoscopy showed full endoscopic remission for the first time-Mayo endoscopic score of 0 with total Mayo score of 0 (Figure 1B). The patient continues the treatment with UST (90 mg every 8 weeks), ADA (40 mg every 2 weeks) and MTX (15 mg every week) maintaining a steroid-free remission and no EIMs for the first time in many years. No adverse events have been observed.

The patient achieved clinical remission during anti-TNF treatment (only transiently as it later turned out), but extraintestinal symptoms were still present. The temporary reintroduction of GCs allowed the control of tendon pain and the implementation of appropriate treatment, which proved to be effective in the long term and allowed a steroid-free UC

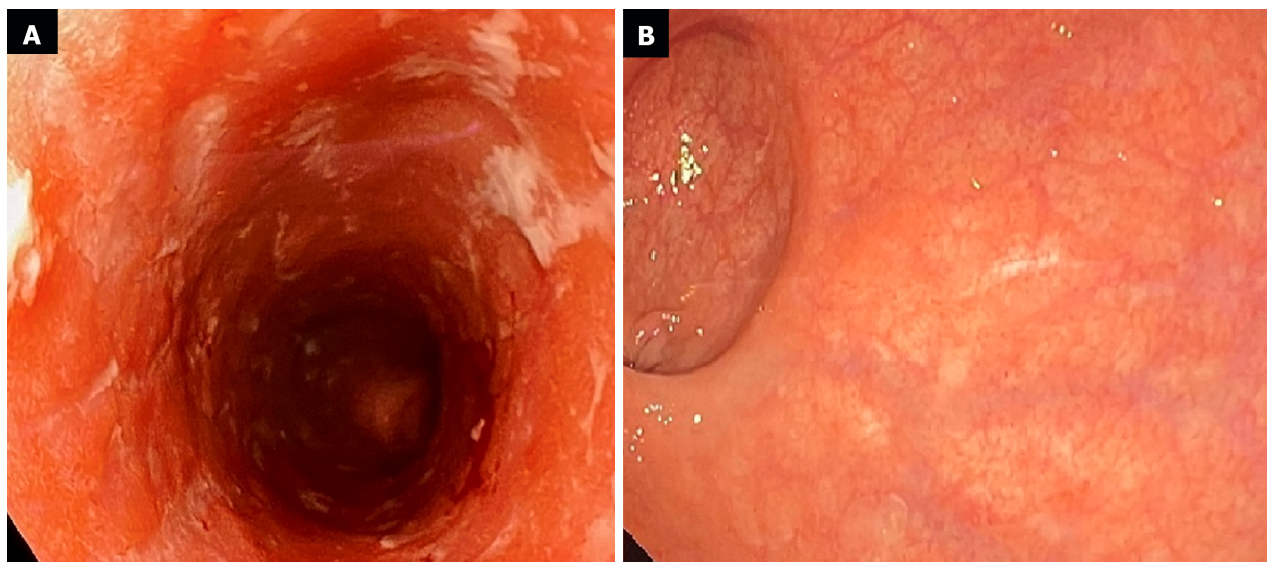


**Figure 1** The endoscopic view of the colon. A: Before starting tofacitinib (Mayo 3); B: After 12 weeks of dual biologic therapy (Mayo 0).

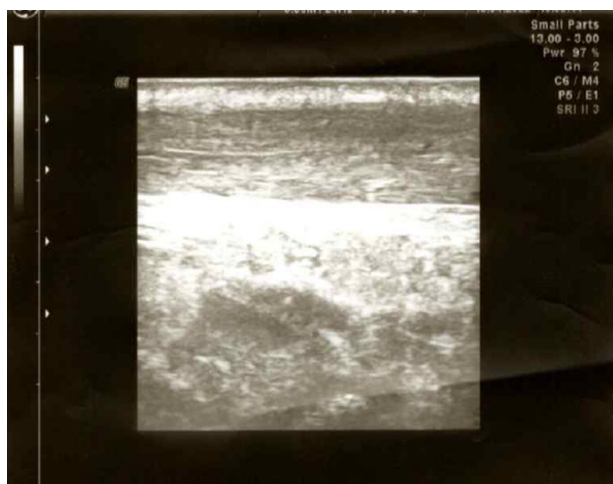


**Figure 2** Tendons ultrasound revealing tendinitis.

remission after many years. The way to remission was long and difficult, requiring multiple treatment modifications and ultimately the use of DBT.

## DISCUSSION

When analyzing the patient's disease course and treatment, attention should be paid to three key points. Firstly, the long-term and unjustified use of GCs. Secondly, the long delay in qualifying the patient for biological therapy despite the evident ineffectiveness of standard treatment. Thirdly, the lack of diagnosis of SpA despite the patient's reported symptoms in the form of ankle and knee joints pain in the past. Physicians usually correctly diagnose arthropathies in the course of IBD (although this had not been done for many years in the patient's case), however, they often forget that tendinitis is also an EIM of this group of diseases. In a study to validate a questionnaire for the detection of SpA in IBD patients, it has been shown that 102 (24.4%) patients met ASAS criteria for this diagnosis. Among these patients, enthesitis was present in 26 patients (25.5%)[6]. Despite that, case reports of patients with Achilles tendinitis are extremely rarely reported in the literature. ter Borg *et al*[7] described a case of a patient with tendinitis accompanying "pouchitis", ergo this manifestation should not be forgotten even in patients with UC after colectomy. In all described cases, tendinitis was accompanied by the exacerbation of the underlying disease and resolved with the remission of intestinal symptoms[7-10]. However, it was not sufficient in the case discussed here, and required a novel approach.

The benefits of combining two biological drugs with different mechanisms of action are being increasingly discussed in literature[11-14]. For example, Glassner *et al*[13] described retrospectively 50 patients treated with DBT using different drug combinations (the most often vedolizumab combined with UST). In the described cohort, there were 10 patients who



Figure 3 X-ray revealing Achilles enthesopathy.

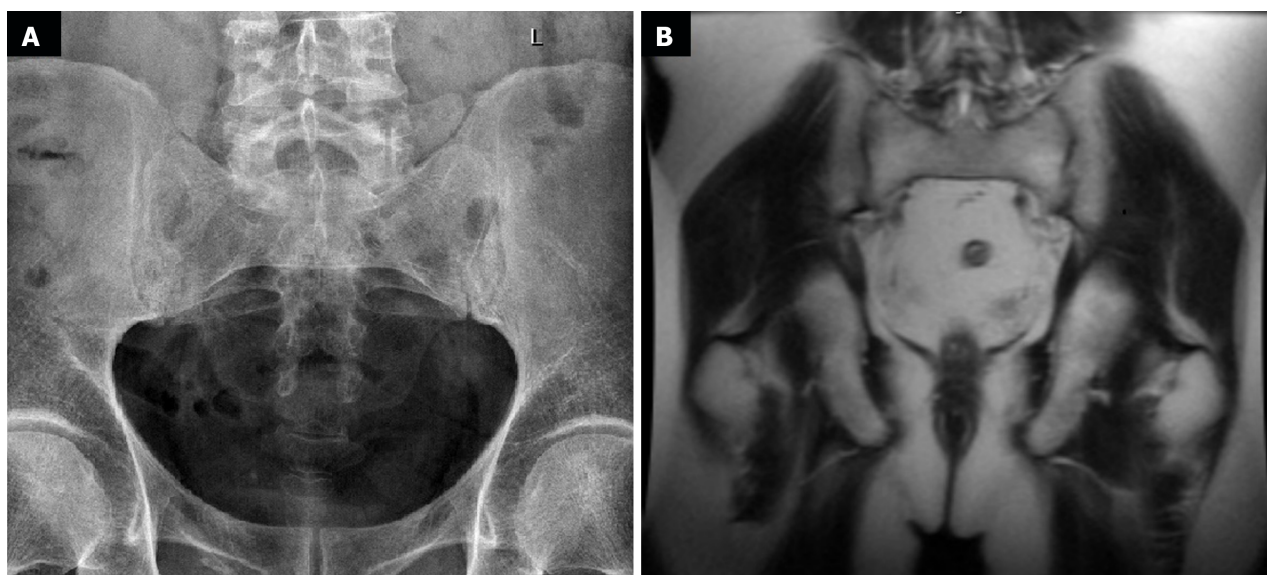


Figure 4 Images revealing bilateral sacrolitis. A: On the X-ray; B: In magnetic resonance imaging.

had concomitant rheumatological or dermatological disease, especially psoriasis and psoriatic arthritis. However, so far only one case of UC and concomitant peripheral arthropathy successfully treated with DBT (vedolizumab and UST) have been reported[15]. DBT is most widely referred to in systematic reviews, meta-analysis, retrospective studies and case series, but it is also a promising direction for clinical research. In 2023, randomized double-blind controlled phase 2 trial evaluating guselkumab plus golimumab combination therapy *vs* guselkumab or golimumab monotherapy in patients with UC was published. Both the efficacy and a good safety profile have been demonstrated for DBT. Despite the growing number of available therapies for some patients, inhibition of only one inflammatory response pathway may be

insufficient, especially in challenging IBD patients and those with accompanying EIMs resistant to treatment with a single mechanism of action drugs.

## CONCLUSION

The case of the patient with bilateral Achilles tendinitis discussed in this article represents rarely reported EIMs of UC and suggests that DBT may be an alternative for patient with UC and EIMs who did not respond for standard either first- or second-line medical therapies.

## ACKNOWLEDGEMENTS

We sincerely appreciate the work of the endoscopists and radiologists.

## FOOTNOTES

**Author contributions:** Filipiuk A, Gonciarz M contributed equally to the entire work on the article: Patient treatment planning, substantial contributions to conception and design of the case report, data gathering, or analysis and interpretation of the data, drafting the article or making critical revisions related to important intellectual content of the article, final approval of the version of the article to be published.

**Informed consent statement:** Informed consent was given by the patient.

**Conflict-of-interest statement:** We have no conflict of interest to declare.

**CARE Checklist (2016) statement:** The authors have read the CARE Checklist (2016), and the manuscript was prepared and revised according to the CARE Checklist (2016).

**Open-Access:** This article is an open-access article that was selected by an in-house editor and fully peer-reviewed by external reviewers. It is distributed in accordance with the Creative Commons Attribution NonCommercial (CC BY-NC 4.0) license, which permits others to distribute, remix, adapt, build upon this work non-commercially, and license their derivative works on different terms, provided the original work is properly cited and the use is non-commercial. See: <https://creativecommons.org/licenses/by-nc/4.0/>

**Country of origin:** Poland

**ORCID number:** Aleksandra Filipiuk 0000-0002-6700-2719; Maciej Gonciarz 0000-0003-1322-2457.

**Corresponding Author's Membership in Professional Societies:** Polish Society of Gastroenterology.

**S-Editor:** Liu H

**L-Editor:** A

**P-Editor:** Cai YX

## REFERENCES

- 1 Du L, Ha C. Epidemiology and Pathogenesis of Ulcerative Colitis. *Gastroenterol Clin North Am* 2020; **49**: 643-654 [PMID: 33121686 DOI: 10.1016/j.gtc.2020.07.005]
- 2 Malik TF, Aurelio DM. Extraintestinal Manifestations of Inflammatory Bowel Disease. 2023 Mar 6. In: StatPearls [Internet]. Treasure Island (FL): StatPearls Publishing; 2024 Jan- [PMID: 33760556]
- 3 Salvarani C, Vlachonikolis IG, van der Heijde DM, Fornaciari G, Macchioni P, Beltrami M, Olivieri I, Di Gennaro F, Politi P, Stockbrügger RW, Russel MG; European Collaborative IBD Study Group. Musculoskeletal manifestations in a population-based cohort of inflammatory bowel disease patients. *Scand J Gastroenterol* 2001; **36**: 1307-1313 [PMID: 11761022 DOI: 10.1080/003655201317097173]
- 4 Sands BE, Kozarek R, Spainhour J, Barish CF, Becker S, Goldberg L, Katz S, Goldblum R, Harrigan R, Hilton D, Hanauer SB. Safety and tolerability of concurrent natalizumab treatment for patients with Crohn's disease not in remission while receiving infliximab. *Inflamm Bowel Dis* 2007; **13**: 2-11 [PMID: 17206633 DOI: 10.1002/ibd.20014]
- 5 Braun J, van den Berg R, Baraliakos X, Boehm H, Burgos-Vargas R, Collantes-Estevez E, Dagfinrud H, Dijkmans B, Dougados M, Emery P, Geher P, Hammoudeh M, Inman RD, Jongkees M, Khan MA, Kiltz U, Kvien T, Leirisalo-Repo M, Maksymowych WP, Olivieri I, Pavelka K, Sieper J, Stanislawski-Biernat E, Wendling D, Ozgocmen S, van Drogen C, van Royen B, van der Heijde D. 2010 update of the ASAS/EULAR recommendations for the management of ankylosing spondylitis. *Ann Rheum Dis* 2011; **70**: 896-904 [PMID: 21540199 DOI: 10.1136/ard.2011.151027]
- 6 Benfaremo D, Luchetti MM, Di Carlo M, Laganà B, Picchianti-Diamanti A, Carubbi F, Pica R, Chimenti MS, Lorenzetti R, Scolieri P, Bruzzese V, Benedetti A, Ramonda R, Giacomelli R, Salaffi F, Gabrielli A; GRADES-IBD Study Group. Multicenter Validation of the

- DETAIL Questionnaire for the Screening of Spondyloarthritis in Patients With Inflammatory Bowel Diseases. *J Rheumatol* 2021; **48**: 179-187 [PMID: 32669448 DOI: 10.3899/jrheum.200364]
- 7 **ter Borg EJ**, Nadorp JH, Elbers JR. Ileal pouch arthritis: a case report. *Eur J Gastroenterol Hepatol* 1996; **8**: 957-959 [PMID: 8930558 DOI: 10.1097/00042737-199610000-00004]
  - 8 **Akbal A**, Gökmen F, Döner D, Uysal F. Are inflammatory bowel disease patients aware of Achilles tendonitis? *J Crohns Colitis* 2014; **8**: 711 [PMID: 24370390 DOI: 10.1016/j.crohns.2013.12.004]
  - 9 **Fremlin GA**, Rawlings C, Livingstone JA, Bray AP. An unusual case of bilateral pyoderma gangrenosum with Achilles tendon rupture. *Br J Dermatol* 2015; **172**: 522-526 [PMID: 25040076 DOI: 10.1111/bjd.13264]
  - 10 **Zenda T**, Araki I, Nakamiya O, Tokuumi Y, Shimada Y, Komai K, Taniuchi Y. Achilles tendinitis as a rare extraintestinal manifestation of ulcerative colitis. *Clin J Gastroenterol* 2016; **9**: 129-133 [PMID: 27059338 DOI: 10.1007/s12328-016-0645-8]
  - 11 **Buer LCT**, Høivik ML, Warren DJ, Medhus AW, Moum BA. Combining Anti-TNF- $\alpha$  and Vedolizumab in the Treatment of Inflammatory Bowel Disease: A Case Series. *Inflamm Bowel Dis* 2018; **24**: 997-1004 [PMID: 29668901 DOI: 10.1093/ibd/izx110]
  - 12 **Peter CD**, Huang YH, Tian WN. Dual biologic therapy for severe ulcerative colitis, concomitant extraintestinal manifestations and an orbital osteoma: a successful treatment. *Rev Esp Enferm Dig* 2022; **114**: 757-758 [PMID: 35770593 DOI: 10.17235/reed.2022.8964/2022]
  - 13 **Glassner K**, Oglat A, Duran A, Koduru P, Perry C, Wilhite A, Abraham BP. The use of combination biological or small molecule therapy in inflammatory bowel disease: A retrospective cohort study. *J Dig Dis* 2020; **21**: 264-271 [PMID: 32324969 DOI: 10.1111/1751-2980.12867]
  - 14 **Yang E**, Panaccione N, Whitmire N, Dulai PS, Vande Casteele N, Singh S, Boland BS, Collins A, Sandborn WJ, Panaccione R, Battat R. Efficacy and safety of simultaneous treatment with two biologic medications in refractory Crohn's disease. *Aliment Pharmacol Ther* 2020; **51**: 1031-1038 [PMID: 32329532 DOI: 10.1111/apt.15719]
  - 15 **Feagan BG**, Sands BE, Sandborn WJ, Germinaro M, Vetter M, Shao J, Sheng S, Johans J, Panés J; VEGA Study Group. Guselkumab plus golimumab combination therapy versus guselkumab or golimumab monotherapy in patients with ulcerative colitis (VEGA): a randomised, double-blind, controlled, phase 2, proof-of-concept trial. *Lancet Gastroenterol Hepatol* 2023; **8**: 307-320 [PMID: 36738762 DOI: 10.1016/S2468-1253(22)00427-7]



Published by **Baishideng Publishing Group Inc**  
7041 Koll Center Parkway, Suite 160, Pleasanton, CA 94566, USA

**Telephone:** +1-925-3991568

**E-mail:** [office@baishideng.com](mailto:office@baishideng.com)

**Help Desk:** <https://www.f6publishing.com/helpdesk>

<https://www.wjgnet.com>

